



Libraries and Learning Services

University of Auckland Research Repository, ResearchSpace

Copyright Statement

The digital copy of this thesis is protected by the Copyright Act 1994 (New Zealand).

This thesis may be consulted by you, provided you comply with the provisions of the Act and the following conditions of use:

- Any use you make of these documents or images must be for research or private study purposes only, and you may not make them available to any other person.
- Authors control the copyright of their thesis. You will recognize the author's right to be identified as the author of this thesis, and due acknowledgement will be made to the author where appropriate.
- You will obtain the author's permission before publishing any material from their thesis.

General copyright and disclaimer

In addition to the above conditions, authors give their consent for the digital copy of their work to be used subject to the conditions specified on the [Library Thesis Consent Form](#) and [Deposit Licence](#).

**Oxidation of Cylindrospermopsin and Anatoxin-a
by the Fe^{III}-B*/H₂O₂ Catalyst System**

Jishan Liu

A thesis submitted in fulfilment of the requirements for the degree of Doctor of Philosophy
in Environmental Engineering, the University of Auckland, 2018.

Abstract

Cyanotoxins released by cyanobacterial blooms into natural water reservoirs are considered hazardous contaminants, as they pose direct threats to the aquatic ecosystem and have serious effects on animals and humans. There are limitations in the current technologies for cyanotoxin degradation and removal, including the reduced degradation efficiency by natural organic matter (NOM). This thesis describes an investigation into oxidation of the cyanotoxins cylindrospermopsin (CYL) and anatoxin-a (ANA) by a green catalyst system, Fe^{III}-B* (iron (III) tetra-amido-macrocyclic ligand)/H₂O₂. Studies on cyanotoxin oxidative degradation by Fe^{III}-B*/H₂O₂ were conducted in three steps. The first step investigated cyanotoxin degradation by Fe^{III}-B*/H₂O₂ and built the degradation pathway. Next, the influence of NOM on cyanotoxin removal by the Fe^{III}-B*/H₂O₂ mediated oxidative system was explored. The third component of the research studied the potential estrogenicity of these cyanotoxins and the effects of Fe^{III}-B*/H₂O₂ oxidation on estrogenicity.

The Fe^{III}-B*/H₂O₂ catalyst system provides effective catalytic oxidative degradation of both cyanotoxins CYL and ANA, compared with the selective oxidation by general oxidants. Cyanotoxin degradation by homogeneous Fe^{III}-B*/H₂O₂ (5 μM/ 5 mM) was observed to be pH-dependent at pH ranging from 8.5 to 11.5. The maximum removal of CYL (0.24 μM) and ANA (7.1 μM) occurred at pH 8.5 and pH 9.5 respectively, while the highest rate constant was observed at pH 11.5. Significant cyanotoxin removal by heterogeneous Fe^{III}-B*, produced by immobilising dissolved Fe^{III}-B* (2.5×10⁻⁷ mole) onto functionalised silica gel (240 mg), was observed when activated by H₂O₂ at 5 mM. Intermediate products identified by high resolution mass spectrometry enabled the formulation of cyanotoxin degradation pathways. Additionally, the toxicity of cyanotoxin oxidized by Fe^{III}-B*/H₂O₂ is expected to reduce, due to the destruction of the CYL uracil ring and a conformational change in the ANA molecule.

NOM increased CYL (0.24 μM) and ANA (7.1 μM) removal when mediated by $\text{Fe}^{\text{III}}\text{-B}^*/\text{H}_2\text{O}_2$ (5 μM / 5 mM) at pH 9.5, resulting in 100 % removal (NOM \geq 10 ppm). The results for excitation-emission matrix (EEM) and UV-vis show that NOM components with aromatic ring and carboxylate group were oxidized by $\text{Fe}^{\text{III}}\text{-B}^*/\text{H}_2\text{O}_2$. For cyanotoxins treated with model NOM compounds (i.e., guaiacol and glycolic acid), increased removal was related to their cross-coupling with specific functional groups of NOM constituents. The cyanotoxins and their degradation products suggest a further lowering toxicity due to their cross-coupling with NOM.

Estrogenicity tests were conducted using the yeast estrogen screen (YES) assay. In the YES assay, CYL and ANA can act as agonists to induce the production of enzyme β -galactosidase. The ring structures of CYL and ANA display the binding affinity to estrogen receptors. The competition assay with cyanotoxins and E2 showed that CYL and ANA can perform as endocrine disruptors to modulate E2-induced estrogenicity and induce non-monotonic dose-response behaviours. In comparison to the estrogenicity of the un-oxidized cyanotoxins, the estrogenicity of CYL after oxidation was significantly different, while the estrogenicity of ANA after oxidation did not change significantly. The reduced estrogenic activity of CYL is likely due to its reduced concentration and the formation of less active degradation products. The insignificantly changed estrogenic activity of ANA is associated with its ring-structural degradation products.

This thesis has advanced the understanding of cyanotoxin oxidative degradation by the $\text{Fe}^{\text{III}}\text{-B}^*/\text{H}_2\text{O}_2$ catalyst system, and also mimicked the cyanotoxin removal in the real system by NOM addition. This thesis has also added to our knowledge of cyanotoxins as endocrine disrupting chemicals.

Dedication

This doctoral thesis is dedicated to my grandma, Yuqin Ai (1940 – 2016)

Acknowledgments

First of all, I would like to show my greatest appreciation to my supervisors A/P. Naresh Singhal, Prof. James Wright, A/P. David Greenwood, A/P. Simon Swift for their support, contribution and immense knowledge throughout this research project. Their guidance and insightful comments helped me in all the time of research and writing of this thesis.

My sincere thanks go to my friends Dr. Sandra Uy, Dr. Yantao Song, and Dr. Sandra Elizabeth Hernandez, who provided me much laboratory technical support. I would like to thank all the environmental engineering research group members for their warm encouragement in the last four years. I would also like to thank Ms Lisa Morice for her kind help with proofreading.

I would like to express my deep and sincere gratitude to my parents for their continuous and unparalleled love and encouragement through my life. Special thanks to my husband, Xin Zhang, for his unlimited love and support.

Table of Contents

Abstract.....	ii
Dedication.....	iv
Acknowledgments.....	v
Table of Contents.....	vi
List of Figures.....	x
List of Tables.....	xii
List of Schemes.....	xiii
List of Abbreviations.....	xiv
Chapter 1: Literature Review and Background.....	1
1.1 Overview of cyanotoxins.....	1
1.2 Cyanotoxins selected for this study.....	2
1.2.1 Cyindrospermopsin (CYL).....	3
1.2.2 Anatoxin-a (ANA).....	5
1.3 Previous methods used for removal of CYL and ANA from water.....	6
1.3.1 Cyanotoxin removal by conventional and physical methods.....	9
1.3.2 Cyanotoxin removal by chemical oxidants.....	9
1.3.3 Cyanotoxin removal by advanced oxidation processes.....	10
1.3.4 Cyanotoxin removal impacted by NOM.....	11
1.4 Fe ^{III} -TAML activators.....	12
1.4.1 Oxidation of Fe ^{III} -TAML by H ₂ O ₂	13
1.4.2 Overall mechanism of Fe ^{III} -TAML/H ₂ O ₂ in oxidation of pollutants.....	16
1.4.3 Application of Fe ^{III} -TAML/H ₂ O ₂ in degradation of pollutants.....	17
1.4.4 The potential of Fe ^{III} -TAML/H ₂ O ₂ in cyanotoxin treatment.....	18
1.5 Heterogeneous Fe ^{III} -TAML activators.....	19
1.5.1 Application of heterogeneous catalysts.....	20

1.5.2 Generation of heterogeneous Fe ^{III} -TAML activators	20
1.6 Estrogenic activity of CYL and ANA.....	21
1.6.1 Endocrine disrupting chemicals.....	22
1.6.2 Limitations of general technologies in quantifying estrogenic activity.....	22
1.6.3 <i>In vitro</i> assays for quantification of estrogenic activity.....	23
1.6.4 Mechanism of the yeast estrogen screen assay	24
1.7 Research gaps.....	26
1.8 Research objectives.....	26
1.9 Thesis framework.....	27
Chapter 2: Oxidative degradation of cylindrospermopsin and anatoxin-a by Fe ^{III} -B*/H ₂ O ₂ ..	30
Chapter abstract	30
2.1 Introduction.....	32
2.2 Methodology	34
2.2.1 Chemicals preparation	34
2.2.2 Heterogeneous Fe ^{III} -B* production	34
2.2.3 Coverage assessment of heterogeneous Fe ^{III} -B*	35
2.2.4 Degradation experiments	36
2.2.5 Cyanotoxin quantification by LC-MS	36
2.2.6 Solid-phase extraction procedure.....	37
2.2.7 CYL and ANA degradation analysis	38
2.3 Results and discussion	38
2.3.1 Effect of pH on cyanotoxin oxidation by homogeneous Fe ^{III} -B*/H ₂ O ₂	38
2.3.2 Cyanotoxin removal by heterogeneous Fe ^{III} -B*/H ₂ O ₂	42
2.3.3 Identification of intermediate products in the catalytic oxidation of cyanotoxin ...	45
2.4 Conclusions.....	50
Chapter 3: Oxidative removal of cylindrospermopsin and anatoxin-a by Fe ^{III} -B*/H ₂ O ₂ in the presence of natural organic matter	51

Chapter abstract	51
3.1 Introduction.....	53
3.2 Methodology	55
3.2.1 Materials and chemical preparation.....	55
3.2.2 Cyanotoxin removal in the presence of NOM or NOM surrogate	56
3.2.3 LC-MS quantification of cyanotoxin in reactions	56
3.2.4 Measurement of NOM oxidation by Fe ^{III} -B*/H ₂ O ₂	56
3.2.5 Identification of cross-coupled products.....	57
3.2.6 CYL and ANA data regression.....	59
3.3 Results and discussion	59
3.3.1 Cyanotoxin removal in the presence of NOM	59
3.3.2 Fe ^{III} -B*/H ₂ O ₂ catalysed oxidation of NOM.....	63
3.3.3 Cyanotoxin removal in the presence of NOM surrogates.....	66
3.3.4 NOM surrogate radical-mediated cross-coupling with cyanotoxin	68
3.3.5 The effect of NOM on cyanotoxin degradation products	76
3.4 Conclusions.....	77
Chapter 4: Estrogenic activity of cylindrospermopsin and anatoxin-a and their oxidative products by Fe ^{III} -B*/H ₂ O ₂	78
Chapter abstract	78
4.1 Introduction.....	80
4.2 Methodology	82
4.2.1 Reagents and materials	82
4.2.2 Yeast estrogen screen assay	82
4.2.3 Estrogenic response of cyanotoxin treated by Fe ^{III} -B*/H ₂ O ₂	84
4.2.4 Cytotoxicity of cyanotoxins on yeast cells	84
4.2.5 Data calculation and statistical analysis.....	85
4.3 Results and discussion	86

4.3.1 Cytotoxicity of cyanotoxins to yeast cells	86
4.3.2 Estrogenic activity of cyanotoxins.....	88
4.3.3 Modulation of E2 activity by cyanotoxins.....	90
4.3.4 Estrogenicity of treated cyanotoxins by Fe ^{III} -B*/H ₂ O ₂	97
4.4 Conclusions.....	105
Chapter 5: Summary, Conclusions and Recommendations for Future Work.....	106
5.1 Summary	106
5.2 Conclusions.....	108
5.2.1 Oxidative degradation of CYL and ANA by Fe ^{III} -B*/H ₂ O ₂	108
5.2.2 Oxidative removal of CYL and ANA by Fe ^{III} -B*/H ₂ O ₂ in the presence of NOM.....	110
5.2.3 Estrogenic activity of CYL and ANA and their oxidative products by Fe ^{III} -B*/H ₂ O ₂	111
5.3 Recommendations for Future Work.....	112
Appendix - Chapter 2.....	115
Appendix - Chapter 3.....	131
Appendix - Chapter 4.....	138
References.....	146

List of Figures

Figure 1. 1: The structure of Fe ^{III} -B*	12
Figure 2. 1: The structure of (a) cylindrospermopsin, (b) anatoxin-a, (c) Fe ^{III} -B* catalyst	32
Figure 2. 2: Cyanotoxins removal by homogeneous Fe ^{III} -B*/H ₂ O ₂ at different pH.....	40
Figure 2. 3: The rate constants of CYL and ANA degradation by homogeneous Fe ^{III} -B*/H ₂ O ₂ at different pH.....	42
Figure 2. 4: Cyanotoxins removal by homogeneous and heterogeneous Fe ^{III} -B*/H ₂ O ₂	43
Figure 3. 1: The structure of (a) cylindrospermopsin, (b) anatoxin-a, (c) Fe ^{III} -B* catalyst....	53
Figure 3. 2: CYL removal by Fe ^{III} -B*/H ₂ O ₂ with varying NOM.....	60
Figure 3. 3: ANA removal by Fe ^{III} -B*/H ₂ O ₂ with varying NOM.	61
Figure 3. 4: The rate constants of CYL and ANA degradation by Fe ^{III} -B*/H ₂ O ₂ in the presence of NOM.....	62
Figure 3. 5: Fluorophore signatures of NOM oxidized by Fe ^{III} -B*/H ₂ O ₂	64
Figure 3. 6: UV absorbance of NOM reacted with Fe ^{III} -B*/H ₂ O ₂	65
Figure 3. 7: The structure of (a) guaiacol and (b) glycolic acid	66
Figure 3. 8: CYL removal by Fe ^{III} -B*/H ₂ O ₂ in the presence of NOM surrogates.....	67
Figure 3. 9: ANA removal by Fe ^{III} -B*/H ₂ O ₂ in the presence of NOM surrogates.....	68
Figure 3. 10: ESI (-)-MS spectra for the cross-coupled product of CYL and glycolic acid....	70
Figure 3. 11: ESI (+)-MS spectra for the cross-coupled product of CYL and guaiacol.....	73
Figure 3. 12: GC-MS mass spectra for the cross-coupled product of ANA and guaiacol.....	75
Figure 4. 1: The structure of (a) cylindrospermopsin and (b) anatoxin-a.....	81
Figure 4. 2: Cytotoxicity of cyanotoxins on the yeast cells.....	87
Figure 4. 3: Estrogenicity induced by cyanotoxins.....	88
Figure 4. 4: Modification on E2 induced estrogenicity by CYL..	92
Figure 4. 5: Modification on E2 induced estrogenicity by ANA.....	93

Figure 4. 6: Modification on E2 induced estrogenicity by ZnCl₂.....94

Figure 4. 7: Estrogenicity of CYL treated by Fe^{III}-B*/H₂O₂... ..98

Figure 4. 8: Estrogenicity of ANA treated by Fe^{III}-B*/H₂O₂.....99

List of Tables

Table 1. 1: Technologies for CYL and ANA removal and their drawbacks	7
Table 1. 2: Half-lives for CYL (1 μ M) and ANA (1 μ M) oxidation at pH 8	10
Table 4. 1: Parameters in the YES assay.....	83
Table 4. 2: Parameters in cytotoxicity test.....	84
Table 4. 3: Proposed structures and formula from CYL mass spectra	101
Table 4. 4: Proposed structures and formula from ANA mass spectra.....	103

List of Schemes

Scheme 1. 1: Fe ^{III} -B* in solid state and in water	13
Scheme 1. 2: Stoichiometric mechanism of Fe ^{III} -TAMLs oxidation by H ₂ O ₂	14
Scheme 1. 3: A picture of pathways in the formation of a Fe(V)oxo intermediate.....	15
Scheme 1. 4: Speciation of Fe(IV)oxo complexes in water.....	15
Scheme 1. 5: Overall mechanism of Fe ^{III} -TAML/H ₂ O ₂	16
Scheme 1. 6: Hormone-induced chemiluminescence in the YES assay	25
Scheme 2. 1: Covalent attachment of quaternary nitrogen reagent to silica gel and homogeneous Fe ^{III} -B* immobilisation onto the functionalised silica gel.....	35
Scheme 2. 2: The process flow for heterogeneous Fe ^{III} -B* production	36
Scheme 2. 3: Proposed pathway for CYL oxidation by Fe ^{III} -B*/H ₂ O ₂	46
Scheme 2. 4: Proposed pathway for ANA oxidation by Fe ^{III} -B*/H ₂ O ₂	49

List of Abbreviations

ANA	Anatoxin-a
AOPs	Advanced oxidation processes
CID	Collision-induced dissociation
CYL	Cylindrospermopsin
DOC	Dissolved organic carbon
E2	17 β -estradiol
EACs	Estrogen active chemicals
EDCs	Endocrine disrupting chemicals
EEM	Excitation-emission matrix
Fe-TAML	Iron tetra-amido-macrocyclic ligand
GAC	Granular activated carbons
MSG	Modified silica gel
NOM	Natural organic matter
O ₃	Ozone
PAC	Powder activated carbons
Si-QAC	Dimethyloctadecyl [3-(trimethoxysilyl) propyl] ammonium chloride
SPE	Solid-phase extraction
UV	Ultraviolet
YES assay	Yeast estrogen screen assay

Notes: Sort abbreviations according to alphabetical order

Co-Authorship Form

This form is to accompany the submission of any PhD that contains published or unpublished co-authored work. **Please include one copy of this form for each co-authored work.** Completed forms should be included in all copies of your thesis submitted for examination and library deposit (including digital deposit), following your thesis Acknowledgements. Co-authored works may be included in a thesis if the candidate has written all or the majority of the text and had their contribution confirmed by all co-authors as not less than 65%.

Please indicate the chapter/section/pages of this thesis that are extracted from a co-authored work and give the title and publication details or details of submission of the co-authored work.

Chapter 2 is from this paper:

Oxidative degradation of cylindrospermopsin and anatoxin-a by FeIII-B*/H2O2

Nature of contribution by PhD candidate	Conducted experimental tests, analysis and wrote the text
Extent of contribution by PhD candidate (%)	85%

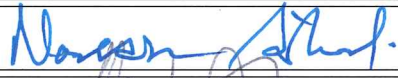
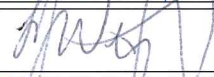
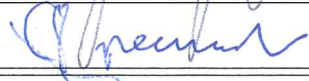
CO-AUTHORS

Name	Nature of Contribution
Naresh Singhal	Supervisor and reviewer
L. James Wright	Supervisor and reviewer
David Greenwood	Supervisor and reviewer

Certification by Co-Authors

The undersigned hereby certify that:

- ❖ the above statement correctly reflects the nature and extent of the PhD candidate's contribution to this work, and the nature of the contribution of each of the co-authors; and
- ❖ that the candidate wrote all or the majority of the text.

Name	Signature	Date
Naresh Singhal		15/8/2017
L. James Wright		12/7/17
David Greenwood		29 June 2017

Co-Authorship Form

This form is to accompany the submission of any PhD that contains published or unpublished co-authored work. **Please include one copy of this form for each co-authored work.** Completed forms should be included in all copies of your thesis submitted for examination and library deposit (including digital deposit), following your thesis Acknowledgements. Co-authored works may be included in a thesis if the candidate has written all or the majority of the text and had their contribution confirmed by all co-authors as not less than 65%.

Please indicate the chapter/section/pages of this thesis that are extracted from a co-authored work and give the title and publication details or details of submission of the co-authored work.

Chapter 3 is from this paper:

Oxidative removal of cylindrospermopsin and anatoxin-a by FeIII-B*/H2O2 in the presence of natural organic matter

Nature of contribution by PhD candidate	Conducted experimental tests, analysis and wrote the text
Extent of contribution by PhD candidate (%)	85%

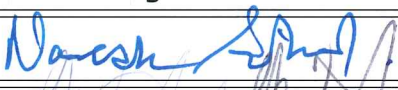

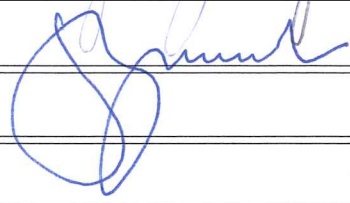
CO-AUTHORS

Name	Nature of Contribution
Naresh Singhal	Supervisor and reviewer
L. James Wright	Supervisor and reviewer
David Greenwood	Supervisor and reviewer

Certification by Co-Authors

The undersigned hereby certify that:

- ❖ the above statement correctly reflects the nature and extent of the PhD candidate's contribution to this work, and the nature of the contribution of each of the co-authors; and
- ❖ that the candidate wrote all or the majority of the text.

Name	Signature	Date
Naresh Singhal		15/8/2017
L. James Wright		12/7/17
David Greenwood		29 June 2017.

Co-Authorship Form

This form is to accompany the submission of any PhD that contains published or unpublished co-authored work. **Please include one copy of this form for each co-authored work.** Completed forms should be included in all copies of your thesis submitted for examination and library deposit (including digital deposit), following your thesis Acknowledgements. Co-authored works may be included in a thesis if the candidate has written all or the majority of the text and had their contribution confirmed by all co-authors as not less than 65%.

Please indicate the chapter/section/pages of this thesis that are extracted from a co-authored work and give the title and publication details or details of submission of the co-authored work.

Chapter 4 is from this paper:

Estrogenic activity of cylindrospermopsin and anatoxin-a and their oxidative products by FeIII-B*/H2O2

Nature of contribution by PhD candidate	Conducted experimental tests, analysis and wrote the text
---	---

Extent of contribution by PhD candidate (%)	85%
---	-----

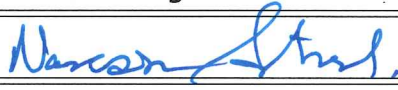

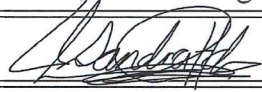
CO-AUTHORS

Name	Nature of Contribution
Naresh Singhal	Supervisor and reviewer
Simon Swift	Supervisor and reviewer
Sandra Elizabeth Hernandez	Analysis and part of writing

Certification by Co-Authors

The undersigned hereby certify that:

- ❖ the above statement correctly reflects the nature and extent of the PhD candidate's contribution to this work, and the nature of the contribution of each of the co-authors; and
- ❖ that the candidate wrote all or the majority of the text.

Name	Signature	Date
Naresh Singhal		15/8/2017
Simon Swift		24 July 2017
Sandra Elizabeth Hernandez		21 July 2017

Chapter 1: Literature Review and Background

1.1 Overview of cyanotoxins

High concentrations of elements like phosphorus and nitrogen in human, industrial and agricultural wastewater become excess nutrients for aquatic plants in natural reservoirs (Daniel J Conley et al., 2009; Hans W Paerl et al., 2008). Eutrophication, sunlight, global warming and carbon availability all promote the growth of cyanobacteria, resulting in the formation of cyanobacterial blooms (Hans W Paerl et al., 2008). Cyanobacterial blooms attract increasing attention due to their various adverse impacts, including deterioration in water quality (G. A. Codd, 2000; Graham et al., 2010), damage to ecosystems (Karl E Havens, 2008), adverse economic effects (Dodds et al., 2009) and significant hazards posed to public health (Funari et al., 2008; Hitzfeld et al., 2000; Hans W. Paerl et al., 2011). The geographical expansion of harmful cyanobacterial blooms is very evident, with their prevalence documented worldwide (Fristachi et al., 2008; Hudnell, 2008), including in Kasumigaura in Japan (K. E. Havens et al., 2001), Okeechobee in the USA (K. E. Havens et al., 2001), Taihu in China (Qin et al., 2010), and the Baltic Sea in Northern Europe (Daniel J. Conley et al., 2009).

Animal and human deaths related to cyanobacterial blooms have been traced back to the 18th century. The first scientific report of animal poisoning associated with cyanobacteria appeared in 1878 after animals died from ingesting water from a reservoir affected by a bloom (Lake Alexandrina, South Australia) (G. Codd et al., 1994). In 1979, over one hundred indigenous Australians from Northern Queensland suffered vomiting, anorexia and enlarged, tender livers, which was linked to drinking water from a reservoir heavily contaminated with a cyanobacterial bloom (Francis, 1878; Griffiths et al., 2003). Cyanobacterial poisoning was subsequently shown to be fatal to humans when, in 1996, 76 people in the northeast of Brazil died after ingesting water from a bloom contaminated reservoir (Prociv, 2004; Svrcek et al.,

2004). During cyanobacterial blooms, a wide range of cyanobacterial secondary metabolites acting as hormones, antibiotics, and toxins are released into surrounding water (W. W. Carmichael, 1992; Moore, 1996; Svrcek et al., 2004), and are responsible for the health and life threatening consequences described above.

Human and animal exposure to harmful cyanotoxins occurs through three main routes: ingestion of food such as shellfish in which cyanotoxins have accumulated; dermal contact or accidental ingestion during recreational activity in contaminated water; and drinking water from cyanotoxin-contaminated reservoirs (Merel et al., 2013). Toxic cyanobacteria have been observed worldwide in fresh and marine waters (Pelaez et al., 2010; Svrcek et al., 2004), and there have been numerous reports of poisonings and deaths caused by cyanotoxins in many countries (Bláha et al., 2009; Catherine et al., 2013; G. A. Codd, 2000).

1.2 Cyanotoxins selected for this study

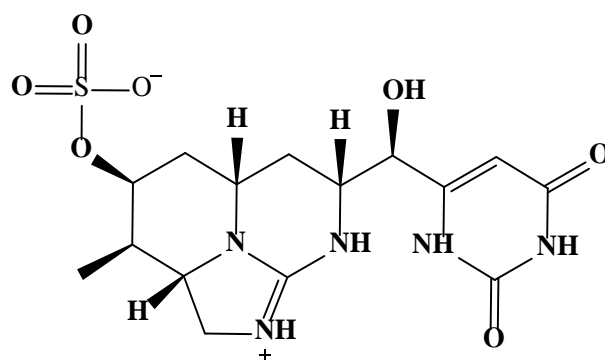
Cyanotoxins are a diverse group of compounds, produced by various cyanobacterial species (Bláha et al., 2009; Funari et al., 2008; Wiegand et al., 2005). Cyanotoxins are variously classified as cyclic peptides, alkaloids and lipopolysaccharides in terms of their chemical structures (Hitzfeld et al., 2000; Svrcek et al., 2004); they can be hepatotoxic, neurotoxic, cytotoxic, dermatotoxic or irritant in their actions (Funari et al., 2008; Wiegand et al., 2005).

To this end, one cytotoxin (cylindrospermopsin) and one neurotoxin (anatoxin-a) were selected for this study. Occurrences of cylindrospermopsin and anatoxin-a have been recorded in countries in Asia, Africa, Australia, Europe, North America and South America and both are well documented in the literature (de la Cruz et al., 2013; Delgado et al., 2012; Duy et al., 2000; A. Humpage, 2008; Kinnear, 2010; Osswald et al., 2007). Further, cylindrospermopsin and anatoxin-a are commonly associated with poisoning incidents, and examples of fatal poisoning cases have been reported in the USA (Juday et al., 1981; Puschner et al., 2008; D. Stevens et

al., 1988), Australia (Hawkins et al., 1985; Saker et al., 1999), Finland (Sivonen et al., 1990), Scotland (Edwards et al., 1992), Ireland (James et al., 1997), Brazil (Wayne W Carmichael et al., 2001), France (Gugger et al., 2005), New Zealand (Wood et al., 2007) and the Netherlands (Faassen et al., 2012). Because of their widespread distribution and high toxicity, cylindrospermopsin and anatoxin-a have attracted a high level of research focus.

1.2.1 Cylindrospermopsin (CYL)

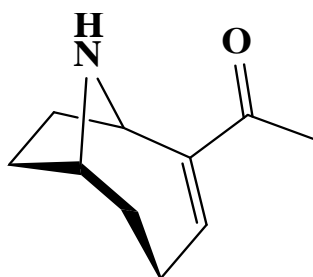
Cylindrospermopsin, known as CYL, acts as a cytotoxic alkaloid. It consists of a tricyclic guanidine moiety, hydroxymethyluracil and sulphate, and has a molecular weight of 415 (Ian R. Falconer et al., 1999; Ian R. Falconer et al., 2006; Ohtani et al., 1992). CYL is highly water soluble and relatively stable under a wide range of environmental conditions, such as temperature, pH, and sunlight (Chiswell et al., 1999). Due to its stability in aqueous solution, CYL is known as a highly recalcitrant pollutant released from cyanobacterial cells during algal blooms. Its proven toxicological characteristics include hepatotoxicity, nephrotoxicity and genotoxicity in human and animal cells (Ian R. Falconer et al., 1999; Funari et al., 2008; A. R. Humpage et al., 2005; Seawright et al., 1999; Terao et al., 1994). In addition, it is also a potential endocrine disrupter through inhibition of progesterone production (F. M. Young et al., 2008) and a potent inhibitor of protein and glutathione synthesis (Bláha et al., 2009; Runnegar et al., 1995; Terao et al., 1994).



Chemical formula	C ₁₅ H ₂₁ N ₅ O ₇ S	
Molecular weight (g/mol)	415.43	
pK _a	8.8	(Onstad et al., 2007; E. Rodríguez, Onstad, et al., 2007)
Producer genera	<i>Anabaena</i> , <i>Aphanizomenon</i> , <i>Cylindrospermopsis</i> , <i>Raphidiopsis</i> , <i>Umezakia</i>	(Bláha et al., 2009; G. A. Codd, 2000; Funari et al., 2008; Wiegand et al., 2005)
Toxin group	Cytotoxic alkaloids	(Svrcek et al., 2004)
Toxic effect	Cytotoxic, hepatotoxic, neurotoxic, genotoxic	(Svrcek et al., 2004)
Target organs	Liver, kidneys, adrenals, lung, spleen, intestine, thymus, heart	(Chorus et al., 1999; Hawkins et al., 1985)
	2.1 mg/kg(24 h), 0.2 mg/kg (6 days)	(Funari et al., 2008)
	2 mg/kg (24 h), 0.2 mg/kg (5 days)	(Ohtani et al., 1992)
Intraperitoneal LD ₅₀	4.4-6.9 mg/kg after 2-6 days	(Seawright et al., 1999)
	50-110 mg/kg (24 h), 20-65 mg/kg (7days)	(Ian R. Falconer et al., 1999)
	0.17 mg/kg (7 days)	(Duy et al., 2000)
	0.3 mg/kg (24 h), 0.18 mg/kg (7 days)	(Van Apeldoorn et al., 2007)
Oral LD ₅₀	4.4-6.9 mg/kg (2-6 days)	(Seawright et al., 1999)

1.2.2 Anatoxin-a (ANA)

Anatoxin-a (ANA) is an alkaloid neurotoxin and was the first toxin identified from a freshwater cyanobacterium (W. W. Carmichael, 1992; Wayne W. Carmichael et al., 1979). ANA is a bicyclic secondary amine with a molecular weight of 165. ANA is relatively stable in the dark, with a half-life of 5 days at pH 9 (Osswald et al., 2007; D. K. Stevens et al., 1991). Despite its instability in sunlight and at high pH, treatment technologies to address ANA are essential because ANA production may outstrip the rate of natural degradation, especially when algae blooms occur (Osswald et al., 2007). Toxicologically and pharmacologically, ANA is a potent agonist that irreversibly binds to neuronal nicotinic acetylcholine receptors, blocking both muscarinic and nicotinic activity (Bláha et al., 2009; Wayne W. Carmichael et al., 1979; Molloy et al., 1995; P. Thomas et al., 1993; Wiegand et al., 2005). As a result of the blocking of neuromuscular transmission, death occurs due to respiratory arrest caused by overstimulation of the muscles (Osswald et al., 2007).



Chemical formula	C ₁₀ H ₁₅ NO	
Molecular weight (g/mol)	165.23	
pK _a	9.4	(Duy et al., 2000; Onstad et al., 2007; E. Rodríguez, Onstad, et al., 2007)
Producer genera	<i>Anabaena</i> , <i>Aphanizomenon</i> , <i>Cylindrospermum</i> , <i>Microcystis</i> , <i>Planktothrix</i> , <i>Phormidium</i> , <i>Raphidiopsis</i> , <i>Oscillatoria</i>	(Bláha et al., 2009; G. A. Codd, 2000; Funari et al., 2008; Wiegand et al., 2005)
Toxin group	Neurotoxic alkaloids	(Svrcek et al., 2004)
Toxic effect	Neurotoxic	(Svrcek et al., 2004)
Target organs	Neuromuscular system	(Funari et al., 2008)
Intraperitoneal LD ₅₀	375 µg/kg	(Fitzgeorge et al., 1994)
	250 µg/kg	(Devlin et al., 1977)
	200-250 µg/kg	(Chorus et al., 1999; D. K. Stevens et al., 1991)
Oral LD ₅₀	200 µg/kg	(W. W. Carmichael, 1992)
Oral LD ₅₀	>5000 µg/kg	(Fitzgeorge et al., 1994)
Intranasal LD ₅₀	2000 µg/kg	(Fitzgeorge et al., 1994)

1.3 Previous methods used for removal of CYL and ANA from water

Due to the pernicious effects and the common occurrence of CYL and ANA, treatment approaches have used a range of technologies. The current treatment technologies for cylindrospermopsin and anatoxin-a can be broadly categorised into conventional methods,

physical removal, chemical oxidation, and advanced oxidation processes (de la Cruz et al., 2013; Vlad et al., 2014; J. Westrick et al., 2010). In the following section, the cyanotoxin removal efficiencies of current technologies are discussed, along with their shortcomings (Table 1.1).

Table 1. 1: Technologies for CYL and ANA removal and their drawbacks

Technologies	Efficiency & Disadvantages	Reference
Coagulation, flocculation, sedimentation, and filtration	<ul style="list-style-type: none"> • Removal efficiency dependent on chemical dosage and coagulation pH; • Regular backwashing of the filters required; • Cyanobacterial cell lysis and toxins released by inadequate washing processes; • Not very efficient in removing extracellular cyanotoxin 	(He, Zhang, et al., 2014; Hitzfeld et al., 2000; Ho et al., 2012; Newcombe et al., 2004; Song et al., 2012; J. Westrick et al., 2010)
Powder activated carbons (PAC) & Granular activated carbons (GAC)	<ul style="list-style-type: none"> • Removal efficiency dependent on PAC dosing parameter (10 µg/L toxin: > 200 mg/PAC/L) and GAC source (coal, wood > peat, coconut); • Biofilm formation 	(Hitzfeld et al., 2000; J. Westrick et al., 2010)
Membrane filtration	<ul style="list-style-type: none"> • Low removal efficiency for high concentration contaminants; • Membrane fouling 	(Dixon et al., 2010; J. A. Westrick, 2008)
Chlorine	<ul style="list-style-type: none"> • Not effective for ANA removal; • Efficiency reduced by dissolved organic carbon (DOC) matter; • Low pH required; • Disinfection by-product formation 	(de la Cruz et al., 2013; Newcombe et al., 2004; E. Rodríguez, Onstad, et al., 2007; P. Senogles et al., 2000; Zamyadi et al., 2012)

Technologies	Efficiency & Disadvantages	Reference
Chloramine & Chlorine dioxide	<ul style="list-style-type: none"> • Not effective 	(E. Rodríguez, Onstad, et al., 2007)
Permanganate	<ul style="list-style-type: none"> • Not effective for CYL removal 	(E. Rodríguez, Onstad, et al., 2007; E. Rodríguez, Sordo, et al., 2007)
Ozone (O ₃)	<ul style="list-style-type: none"> • pH-dependent; • Disinfection by-product formation 	(Onstad et al., 2007; von Gunten et al., 1994)
Ultraviolet (UV)	<ul style="list-style-type: none"> • Medium-pressure lamps not economically feasible; • Cost of low-pressure lamp implementation; • Disinfection by-product formation 	(Afzal et al., 2010; P.-J. Senogles et al., 2000; J. A. Westrick, 2008; Wolfe, 1990)
Fe ²⁺ /H ₂ O ₂	<ul style="list-style-type: none"> • High concentration of Fe^{II} (Fe^{II}/H₂O₂) required; • pH-dependent (pH 2~5) 	(Duesterberg et al., 2008; Gallard et al., 2000; Munter, 2001)
O ₃ /UV, H ₂ O ₂ /UV, O ₃ /H ₂ O ₂ /UV, UV/TiO ₂ , photo-Fenton/Fenton-like systems	<ul style="list-style-type: none"> • Difficulty in removing the photo catalysts (TiO₂); • Low energy efficiency of commercial UV lamps; • Reduced efficiency of catalysts and radiation by dissolved organic matter; • Operating costs (UV/O₃, and/or H₂O₂ system) vary widely depending on the wastewater flow rate, types, and concentration of contaminants. 	(Carneiro et al., 2014; Munter, 2001; Verma et al., 2015; J. A. Westrick, 2008; Zhang et al., 2014; C. Zhao et al., 2014)

1.3.1 Cyanotoxin removal by conventional and physical methods

Conventional water treatment processes of coagulation, flocculation, sedimentation, and filtration are effective for intracellular cyanotoxin removal, but not viable for extracellular toxin degradation (He, Zhang, et al., 2014; Newcombe et al., 2004; J. Westrick et al., 2010). Physical removal by activated carbon, sand filtration, and membrane filtration has been applied, however potential drawbacks of physical methods include the problem of residual toxins (He, Zhang, et al., 2014; Song et al., 2012), cost inefficiencies (Senogles et al., 2001; C. Zhao et al., 2014), membrane fouling (Dixon et al., 2010) and reduced effectiveness through blocking filters (Hitzfeld et al., 2000).

1.3.2 Cyanotoxin removal by chemical oxidants

A range of common oxidants (e.g., chlorine, chlorine dioxide, chloramine, potassium permanganate and ozone) has been used to inactivate cyanotoxins (de la Cruz et al., 2013; Vlad et al., 2014; J. Westrick et al., 2010; J. A. Westrick, 2008) and varying degrees of cyanotoxin degradation have been obtained (Table 1.2) (E. Rodríguez, Onstad, et al., 2007). Chlorine is able to oxidize CYL, but CYL chlorination is only effective when levels of dissolved organic carbon matter and the pH are low (P. Senogles et al., 2000). Although chlorine is an effective oxidant for CYL removal, chlorination is not a feasible option for oxidative ANA removal due to the very slow reactivity of ANA with chlorine (Newcombe et al., 2004; E. Rodríguez, Onstad, et al., 2007; E. Rodríguez, Sordo, et al., 2007). In addition, two chlorine-based processes (i.e., chloramine and chlorine dioxide) have been shown to be ineffective for CYL and ANA oxidation (E. Rodríguez, Onstad, et al., 2007). Permanganate is a feasible option for ANA degradation, but not applicable for CYL removal because of a low rate constant for CYL oxidation by permanganate and a high dose requirement (E. Rodríguez, Onstad, et al., 2007; E. Rodríguez, Sordo, et al., 2007). Ozone, a common oxidant, has been suggested as feasible for

the oxidation of CYL and ANA (Onstad et al., 2007), but the ozonation effectiveness strongly depends on the characteristics of water (e.g., DOC concentration) (Rositano et al., 2001). The formation of disinfection by-products is also associated with oxidants (E. Rodríguez, Onstad, et al., 2007; E. Rodríguez, Sordo, et al., 2007), since trihalomethanes produced by chlorination (Zamyadi et al., 2012) and bromate formed during ozonation (von Gunten et al., 1994), all pose major health hazards.

Table 1. 2: Half-lives for CYL (1 μ M) and ANA (1 μ M) oxidation at pH 8

Oxidant	CYL	ANA
Chlorine (0 – 4 ppm)	1.7 min	> 14 h
Chloramine	NA	NA
Chlorine dioxide	14.4 h	NA
Permanganate (0 – 1.5 ppm)	4.2 d	4.8 s
Ozone (0 – 2 ppm)	0.10 s	0.52 s

1.3.3 Cyanotoxin removal by advanced oxidation processes

Advanced oxidation processes (AOPs) consist of non-photochemical (i.e., O_3/H_2O_2 , O_3 /catalyst and Fe^{2+}/H_2O_2) and photochemical methods (i.e., O_3/UV , H_2O_2/UV , $O_3/H_2O_2/UV$, UV/TiO_2 and photo-Fenton/Fenton-like systems). Ultraviolet (UV) systems are being increasingly applied in water treatment (Würtele et al., 2011), however effective cyanotoxin oxidation by UV requires the assistance of oxidizing agents such as ozone or H_2O_2 or catalyst (e.g., TiO_2) (Afzal et al., 2010; L. Chen et al., 2015; Fotiou et al., 2015; P.-J. Senogles et al., 2000). There are some potential shortcomings associated with the used of photochemical methods, including the requirement for specific low pressure lamps (Afzal et al., 2010; Munter, 2001; P.-J. Senogles et al., 2000; Wolfe, 1990), the high cost of using artificial sources of radiation (Carneiro et al., 2014), the potential formation of disinfection by-products by UV (Wolfe, 1990), difficulty in removing the photo catalysts after treatment (Carneiro et al., 2014).

Further, other essential shortcomings of AOPs include the requirement for high Fe^{II} (Fe^{II}/H₂O₂) concentrations (Munter, 2001) and acidic solution (Duesterberg et al., 2008; Gallard et al., 2000), and the reduced efficiency of catalysts and radiation caused by dissolved organic matter (Munter, 2001; Verma et al., 2015; Zhang et al., 2014; C. Zhao et al., 2014).

1.3.4 Cyanotoxin removal impacted by NOM

Natural organic matter (NOM) is ubiquitous in natural waters and can reduce cyanotoxin removal efficiency through multiple mechanisms. NOM is reported to compete with micro-pollutants for adsorption sites on activated carbon, thereby adversely impacting its adsorption capacity for cyanobacterial metabolites (Ho et al., 2011; Newcombe et al., 1997; Pelekani et al., 1999). NOM is also known to be responsible for generating negative fouling on membranes used in filtration processes, which decreases permeate flux and increases membrane operation and maintenance costs during long-term water treatment (Her et al., 2008; Jarusutthirak et al., 2007; Teixeira et al., 2013). Because NOM acts as a radical scavenger and a UV-vis blocker, the presence of NOM can also reduce the effectiveness of photocatalysis in cyanotoxin removal (He, de la Cruz, et al., 2014; Zhang et al., 2014; C. Zhao et al., 2014). Furthermore, NOM can also consume chlorine and so decrease the effectiveness of cyanotoxin removal by chlorine oxidation (P. Senogles et al., 2000). Notably, NOM provides precursors during the formation of disinfection by-products such as trihalomethanes and haloacetic acids, which are associated with adverse human health effects (Bond et al., 2009; de la Cruz et al., 2013; Lamsal et al., 2011; Sadiq et al., 2004; Sarathy et al., 2010). As a consequence, NOM creates challenges for transferring these technologies to real world water treatment plants.

Each of the above technologies comes with particular advantages for cyanotoxin removal or degradation, but also limitations. For the purposes of reviewing cyanotoxin treatments, high effectiveness, low operational costs and minimum levels of disinfection by-product formation

are shown to be essential factors in evaluating the efficiency of a method. In terms of meeting these criteria, green chemistry catalysts which can effectively mimic peroxidase enzymes are an encouraging development in relation to the current study's aim of achieving rapid removal of cyanotoxins with no toxic product formation.

1.4 Fe^{III}-TAML activators

A green technology for efficiently purifying water has been widely promoted and commercially utilized in recent years. The Fe^{III}-TAML activators are designed to simulate cytochrome P450 enzymes (Terrence J. Collins, 2002; Terrence J. Collins et al., 1989), containing a central ferric ion coordinated to the cavity of a tetra-anionic tetra-amido-macrocylic-ligand (Ghosh et al., 2008). Fe^{III}-TAML activators are synthesized either in chloro or in aqua forms (Ghosh et al., 2003), such as Fe^{III}-B* as shown in Figure 1.1 (W. Chadwick Ellis et al., 2009). Fe^{III}-TAML activators oxidized by H₂O₂ and other peroxides can oxidize a wide range of substrates via peroxidase-like activity (Ryabov et al., 2009) and can also catalytically decompose H₂O₂ into dioxygen in the absence of other reducing agents via a catalase-like reaction (Ghosh et al., 2008).

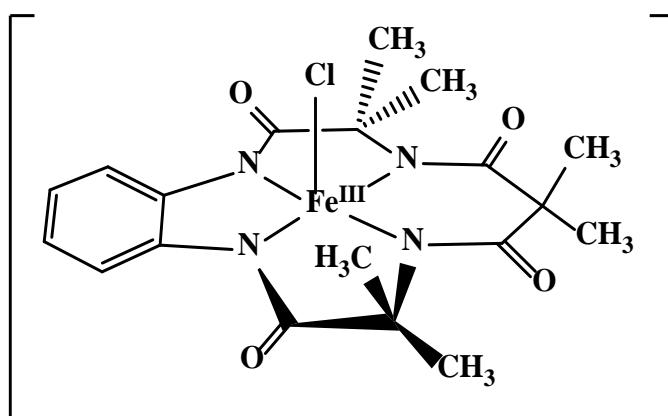
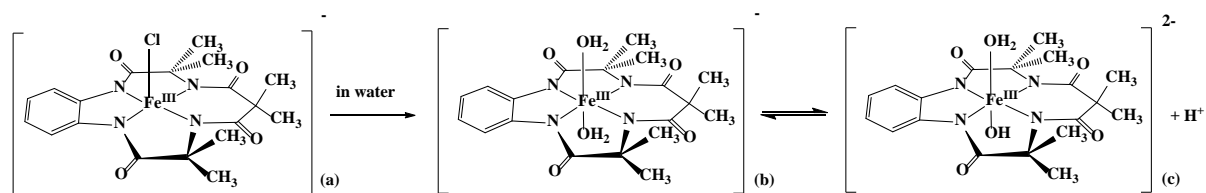


Figure 1. 1: The structure of Fe^{III}-B*

1.4.1 Oxidation of Fe^{III}-TAML by H₂O₂

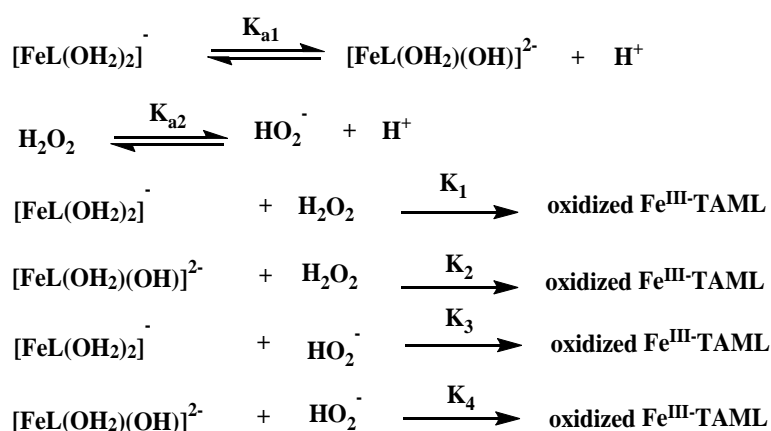
In solid phase, Fe^{III}-TAML activators perform as five-coordinated square-pyramidal complexes (Scheme 1.1a). The base amide Fe-N bonds are short and the macrocyclic ligands pose a high degree of planarity (Ryabov et al., 2009). Once dissolved into water, the chloro ligands of Fe^{III}-TAML activators undergo rapid hydrolysis (Ghosh et al., 2003; Ryabov et al., 2009), meantime, Fe^{III}-TAML activators are transformed into six-coordinated species with two axial ligands by binding another water molecule, affording one negative charge (Scheme 1.1b) and two negative charges (Scheme 1.1c) (Banerjee et al., 2009; W Chadwick Ellis et al., 2010; Popescu et al., 2008; Ryabov et al., 2009). The species shown in Scheme 1.1b, commonly represented as [FeL(H₂O)₂]⁻, can produce species [FeL(OH)(H₂O)]²⁻ in Scheme 1.1c via losing a proton, where L represents the ligand of TAML.



Scheme 1. 1: Fe^{III}-B* in solid state and in water

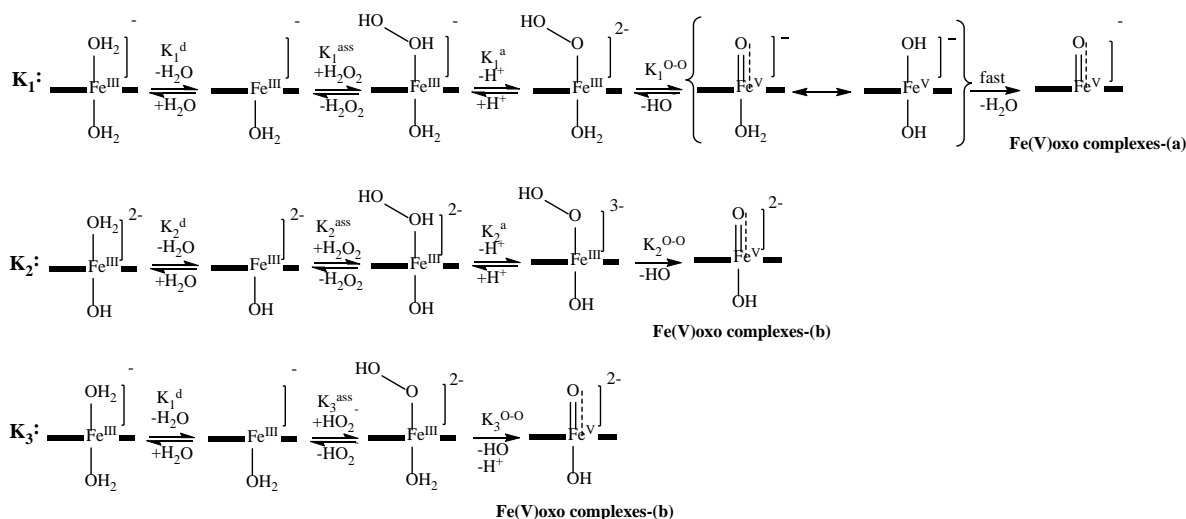
The di-aqua [FeL(H₂O)₂]⁻ complexes and aqua/hydroxo [FeL(OH)(H₂O)]²⁻ complexes are likely to interact pairwise with H₂O₂ or HO₂⁻ species following the pathways indicated by Scheme 1.2 (Ghosh et al., 2008; Popescu et al., 2008; Popescu et al., 2010). All these pathways contribute to the formation of oxidized Fe^{III}-TAML, which further oxidizes the substrate. Since oxidized Fe^{III}-TAML reacts with substrate very quickly, the reactions between Fe^{III}-TAML and H₂O₂ are formally irreversible (Ghosh et al., 2008). Comparing the rates of oxidized Fe^{III}-TAML production, H₂O₂ oxidizes the electron rich [FeL(OH)(H₂O)]²⁻ species much faster than the [FeL(H₂O)₂]⁻ species, resulting in K₂ >> K₁; singly deprotonated [FeL(OH)(H₂O)]²⁻ reacts rapidly with H₂O₂ but slowly with HO₂⁻, resulting in K₂ > K₄; furthermore, the K₂ and K₃

pathways are assumed to be kinetically indistinguishable (Ghosh et al., 2008; Popescu et al., 2008). Because of the pK_a values of Fe^{III}-TAML activators (pH 9.3 ~ 10.5) (W Chadwick Ellis et al., 2010; Ghosh et al., 2003; Popescu et al., 2010) and H₂O₂ (pH 11.2 ~ 11.6) (Jones, 1999), the reaction rate by Fe^{III}-TAML/H₂O₂ increases when increasing pH; as pH is increased further, the reaction rate starts to decrease due to HO₂⁻ species. Therefore, a bell-shaped pH profile for Fe^{III}-TAML activated by H₂O₂ is observed, with an optimum rate occurring around pH 10 (Ghosh et al., 2008; Popescu et al., 2008; Popescu et al., 2010).



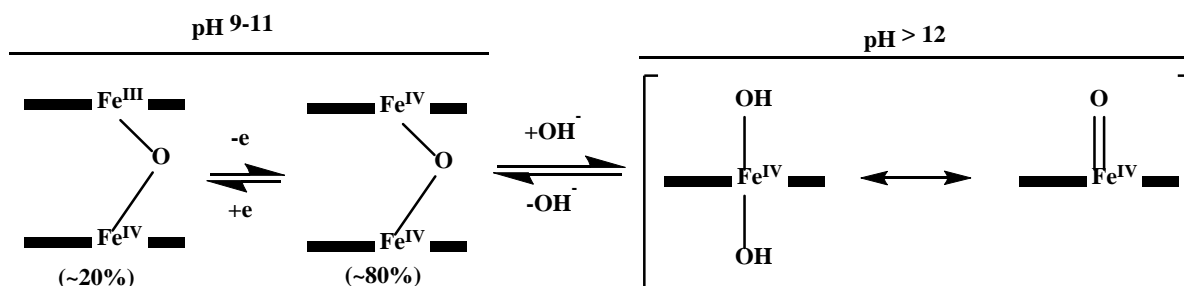
Scheme 1. 2: Stoichiometric mechanism of Fe^{III}-TAMLs oxidation by H₂O₂

The routes in Scheme 1.3 further describe the underlying sequence of events occurring in the conversion of Fe^{III}-TAML activators to oxidized Fe^{III}-TAML, namely Fe(III) species transforming to the final Fe(V)oxo complexes (Ghosh et al., 2008; Popescu et al., 2010). Fe(V)oxo complexes-(a) have been only observed in non-aqueous solvents, but not yet detected in water (Ghosh et al., 2008; Popescu et al., 2010); Fe(V)oxo complexes-(b) are proposed as hypothetical species based on a mechanistic theory of the pH-dependent rate of interaction between Fe(III) and H₂O₂ (Ghosh et al., 2008). Fe(V) species have not been observed in water because of their rapid conversion into Fe(IV) species (Chanda et al., 2008; Popescu et al., 2010).



Scheme 1. 3: A more extensive picture of K₁, K₂ and K₃ pathways in the formation of a Fe(V)oxo intermediate

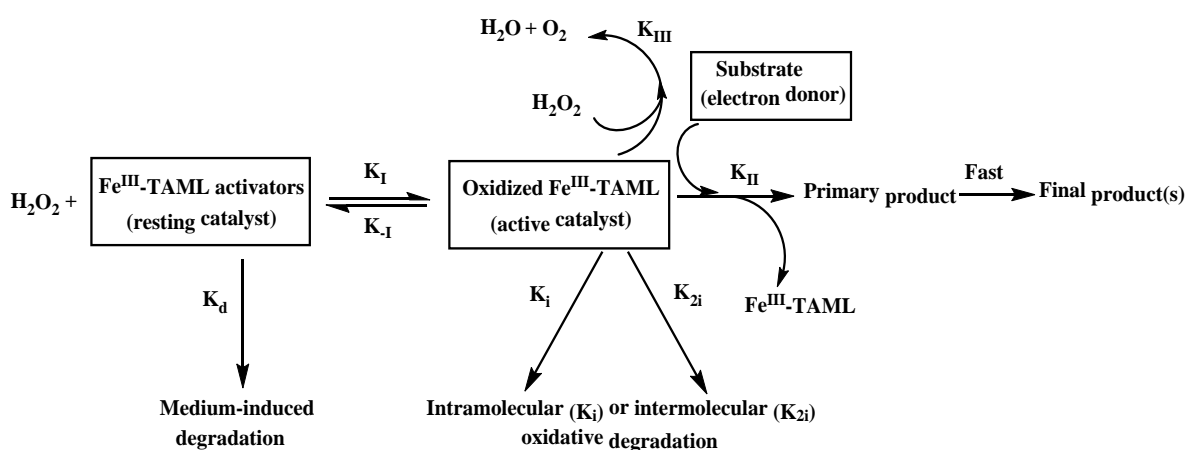
It has been proposed that the intermediates shown in Scheme 1.4 are generated by the rapid comproportionation of Fe(III) and Fe(V) species, or formed by Fe(V)oxo complexes-(a) or Fe(V)oxo complexes-(b) via a catalase type reduction (Ghosh et al., 2008). Further, only Fe(IV) complexes are observed when Fe(III) complexes react with excess H₂O₂ in water with no substrate present (Ghosh et al., 2008). Because both Fe(V) complexes and Fe(IV) species are suggested to be involved in catalysis (Ghosh et al., 2008; Ryabov et al., 2009), the term “oxidized Fe^{III}-TAML” in Scheme 1.2 refers to Fe(V) as well as Fe(IV) species.



Scheme 1. 4: Speciation of Fe(IV)oxo complexes in water

1.4.2 Overall mechanism of Fe^{III}-TAML/H₂O₂ in oxidation of pollutants

Scheme 1.5 demonstrates the steps when Fe^{III}-TAMLs are activated by H₂O₂, and substrate is oxidized by the oxidized Fe^{III}-TAML (Banerjee et al., 2009; Chanda, Ryabov, et al., 2006; Terrence J Collins, 2011; W Chadwick Ellis et al., 2010; Ghosh et al., 2008; Ryabov et al., 2009). Fe^{III}-TAML activators firstly interact with H₂O₂ to produce oxidized Fe^{III}-TAML (K_I) via pathways aforementioned in Scheme 1.2. In the following step, oxidized Fe^{III}-TAML reacts with substrate in a peroxidase-like activity (K_{II}), or decomposes H₂O₂ in a catalase-like manner (K_{III}) (Chanda, Ryabov, et al., 2006; Ghosh et al., 2008), but the exact nature of the reactive species associated with both activities is uncertain (Ghosh et al., 2008). Although catalase-like chemistry is assumed to be wasteful of H₂O₂ in the competition for oxidized TAML, this activity is suppressed in the presence of electron donors and proven to be negligible. As a consequence, peroxidase-like chemistry (K_{II}) dominates the overall reaction and economically oxidizes substrates (Ghosh et al., 2008). However, catalase-like activity (K_{III}) may be significant when Fe^{III}-TAMLs do not attack “hard-to-oxidize” substrates (Terrence J Collins, 2011), or electron donors are absent (Ghosh et al., 2008).



Scheme 1. 5: Overall mechanism of peroxidase-like activities and catalase-like activities by Fe^{III}-TAML/H₂O₂

Furthermore, Fe^{III}-TAML activators in the resting state can be consumed by medium-induced degradation (K_d); and oxidized TAML can suicide through intramolecular (K_i) and intermolecular (K_{2i}) inactivation (Chanda, Ryabov, et al., 2006). The medium-induced hydrolytic degradation (K_d) and intermolecular inactivation (K_{2i}) are kinetically insignificant because hydrolysis (K_d) performs reversibly at pH 8 to 11 (Ghosh et al., 2003), and intermolecular inactivation (K_{2i}) is negligible at low catalyst concentrations (10^{-6} to 10^{-8} M) (Chanda, Ryabov, et al., 2006). According to the mass-balance equation for catalyst (Chanda, Ryabov, et al., 2006), $[Fe^{III}]_{total} = [Fe^{III}\text{-TAML activators}] + [oxidized Fe^{III}\text{-TAML}]$, intramolecular (K_i) inactivation is seen as the main pathway for losing Fe^{III}-TAML catalysts.

1.4.3 Application of Fe^{III}-TAML/H₂O₂ in degradation of pollutants

As shown in the literature reviewed, Fe^{III}-TAML/H₂O₂ has made remarkable progress in purifying numerous recalcitrant organic pollutants from water and destroying recalcitrant pathogens (Terrence J Collins, 2011). Plenty of textile dyes discharged in textile dyeing effluents from manufacturing industries presents a serious environmental issue by causing non-aesthetic discolouration of water, limiting the use of water and reducing the efficiency of microbiological wastewater treatment (Hunger, 2005). The anaerobic conditions resulting and aerobic treatment required to decolourise and detoxify textile dyes stress biological treatment plants (Easton, 1995; Gottlieb et al., 2003). In addition to the current technologies for decolourisation of textile dyes (Forgacs et al., 2004), Fe^{III}-TAML/H₂O₂ performs efficiently in destroying azo dye Orange II (Chahbane et al., 2007), safranin O (Chanda, Ryabov, et al., 2006), and pinacyanol chloride (Chanda, Ryabov, et al., 2006; Mitchell et al., 2010). The potential harm and negative impacts of organophosphorus triesters are causing global concern (Barr et al., 2004; Casida et al., 2004; Tamura et al., 2001). In conventional methods, toxic by-products and waste are produced by the degradation and detoxification of organophosphorus triesters (Amitai et al., 1998; Furuta et al., 2004; Kazankov et al., 2000; Kuo et al., 2000; Neverov et al., 2004; Noyori

et al., 2003). Total degradation of three types of organophosphorus triesters has been achieved by Fe^{III}-TAML/H₂O₂ in both a rapid and environmentally friendly manner (Chanda, Khetan, et al., 2006). Another significant achievement of Fe^{III}-TAML/H₂O₂ is its efficient degradation of endocrine disrupting chemicals (EDCs). Natural estrogens (e.g., 17β-E₂ and E₁) and excreted artificial estrogens (e.g., EE₂) increase the estrogenic activity in surface water (Ying et al., 2002) and cause reproductive impairments in living organisms (Fowler et al., 2012; Palace et al., 2002; Rose et al., 2002). However, the removal of EDCs by municipal wastewater treatment plants is incomplete; concentrations of 17β-E₂ and EE₂ in treated effluents have been shown to be higher than their corresponding predicted-no-effect-concentrations (Hashimoto et al., 2007; W. Young et al., 2002). Rapid degradation of natural and synthetic reproductive hormones, including 17α-E₂, 17β-E₂, E₃, E₁, and EE₂ is indicated for Fe^{III}-TAML/H₂O₂ (J. L. Chen et al., 2012; Shappell et al., 2008). As well as degrading textile dyes, organophosphorus triesters, and EDCs, Fe^{III}-TAML/H₂O₂ has been used to destroy persistent chlorinated pollutants (Gupta et al., 2002), oxidize the sulfur components of diesel fuel (Mondal et al., 2006), and deactivate spores of *Bacillus atrophaeus* (Banerjee et al., 2006).

1.4.4 The potential of Fe^{III}-TAML/H₂O₂ in cyanotoxin treatment

Fe^{III}-TAMLs have been designed and developed based on the least toxic transition metal (Terrence J Collins, 2011), produced as small molecules with low molecular weight (W Chadwick Ellis et al., 2010; Ghosh et al., 2008). It has been suggested that Fe^{III}-TAML/H₂O₂ is benign in practice due to its non-endocrine disrupting activity (W Chadwick Ellis et al., 2010), and is environmentally friendly because it self-decomposes (Terrence J Collins, 2011; W Chadwick Ellis et al., 2010). At room temperature and under ambient conditions (Terrence J Collins, 2011; W. Chadwick Ellis et al., 2009), Fe^{III}-TAML/H₂O₂ is generally able to effectively oxidize pollutants over a broad pH range (pH 6 ~ 12.4) (Ghosh et al., 2008), and even at low μM to nM catalyst concentrations (W. Chadwick Ellis et al., 2009). Unlike other

oxidative catalysts which require non-aqueous conditions (Marques, 2007; Meunier, 2000a, 2000b), Fe^{III} -TAML/ H_2O_2 can be applied in aqueous solution. The application of Fe^{III} -TAML/ H_2O_2 has achieved high degradation efficiency of recalcitrant pollutants while producing less toxic products (Chahbane et al., 2007; Gupta et al., 2002; Shappell et al., 2008). To this end, Fe^{III} -TAML/ H_2O_2 is assumed to be an attractive alternative for the catalytic oxidative purification of cyanotoxin-contaminated water. In order to reduce the potential adverse impact on health and environment by fluorine atoms (Terrence J Collins, 2011; W. Chadwick Ellis et al., 2009), Fe^{III} -B*, a F-free Fe^{III} -TAML activator has been selected from the first generation of Fe^{III} -TAML activators for CYL and ANA degradation in this work.

1.5 Heterogeneous Fe^{III} -TAML activators

Because Fe^{III} -TAML activators and reactants are in the same phase, Fe^{III} -TAML/ H_2O_2 is considered as homogeneous, termed homogeneous Fe^{III} -TAML/ H_2O_2 . Homogeneous catalysts are highly selective and provide accessibility to all catalytically active sites; however, homogeneous catalysts are associated with corrosion, toxicity, difficulty with dosage handling, high costs and issues of separation in treatment systems (X. S. Zhao et al., 2006). To overcome these limitations, heterogeneous catalysts, used in a different phase to the reactants and the medium, are seen as an alternative; they are commonly generated by immobilising active components onto a solid support (Ross, 2011; X. S. Zhao et al., 2006). It has been recognized for decades that heterogeneous catalysts would be preferable due to their potential for easy separation and recovery from reactants/products/catalysts, and subsequent regeneration; easy handling; and the associated possibility of reuse (J. M. Thomas et al., 1999). Significantly, replacing homogeneous catalysts with solid catalysts has long been seen as the ultimate goal in catalysis science and engineering (X. S. Zhao et al., 2006).

1.5.1 Application of heterogeneous catalysts

In these environmentally conscious and economically pressured times, the production of various heterogeneous catalysts from their homogeneous state is being studied. Enzymes in their native form have been used in food industries for centuries, and also applied more recently in the pharmaceutical and chemical industries (Katchalski-Katzir et al., 2000). Enzyme immobilisation enables the easy separation of enzymes from the reaction mixture, dramatically lowering expenditure on enzymes and achieving recyclability of catalysts (Tischer et al., 1999). Due to their advantages over homogeneous enzymes, immobilised enzymes are in common usage and the range of applications for these enzymes is steadily increasing (Katchalski-Katzir, 1993). Similarly, applications of immobilised metal catalysts (del Pozo et al., 2011; Hu et al., 2005; Matsumoto et al., 2008; Sabater et al., 2014; Sotiriou-Leventis et al., 2008), organic catalysts (Cozzi, 2006; Severeys et al., 2001) and photochemical catalysts (Y. Liu et al., 2005; Puma et al., 2008; Shephard et al., 2002) have also been widely reported.

1.5.2 Generation of heterogeneous Fe^{III}-TAML activators

Fe^{III}-TAML researchers are making a concerted effort to improve and diversify Fe^{III}-TAML/H₂O₂, with the aim of meeting the needs of an ever-growing market. Motivated by a growing awareness of the clear advantages and popularity of immobilised catalysts, much attention has been directed to the development of heterogeneous Fe^{III}-TAMLs to replace homogeneous ones. The development of a heterogeneous Fe^{III}-TAML/H₂O₂ catalyst system could potentially be applied in different reaction phases, such as liquid/solid systems. Heterogeneous Fe^{III}-TAML activators may further extend the application of the Fe^{III}-TAML/H₂O₂ catalyst system, such as continuous large scale water treatment by lowering the dosage required.

Depending on the form of interaction between catalysts and solid support, the basic methods of catalyst immobilisation can be categorised as covalent bonding, electrostatic interaction, adsorption and encapsulation (Alaerts et al., 2008; X. S. Zhao et al., 2006). Solid material with a high surface area is able to disperse and stabilize the catalysts, and expose as many as possible active sites to the reaction medium (John M Thomas, 1988). Among the solid support materials reviewed, silica is suggested as an outstanding substrate with pronounced advantages for the immobilisation of homogeneous catalysts. Silica possesses a wide range of pore sizes and supplies a large surface area with plenty of available and well-defined silanol groups, all of which are all important for immobilising catalysts via adsorption, ion exchange and covalent binding (Jal et al., 2004; Ross, 2011; X. S. Zhao et al., 2006). In addition to their binding reaction, silanol groups on the surface can be modified with a range of reagents to form functionalised silanol groups, which are then able to anchor homogeneous catalysts by catalytic or ion-exchange reactions to synthesize heterogeneous catalysts (Jal et al., 2004; G. Lu et al., 2004; Price et al., 2000).

1.6 Estrogenic activity of CYL and ANA

In addition to the hepatotoxicity, neurotoxicity, and cytotoxicity of cyanotoxins (Funari et al., 2008; Wiegand et al., 2005), there are indications cyanotoxins may also be endocrine disruptors. Extracts of cyanobacteria are reported to be estrogenic in *in vitro* assays using the human breast carcinoma cell line MVLN (Jonas et al., 2015; Štěpánková et al., 2011; Sychrová et al., 2012). Besides, two cyclic peptide cyanotoxins, microcystin-LR and nodularin-R are reported to generate weak estrogenic potency in cultured mammalian cells (Oziol et al., 2010); moreover, the endocrine disrupting effect of microcystin-LR is also observed in an *in vivo* assay (Rogers et al., 2011). Hence, CYL and ANA are also suspected to induce estrogenic activity. Being typical alkaloids cyanotoxins are formed at all stages of cyanobacterial growth (Svrcek et al.,

2004), the potential estrogenicity of CYL and ANA would similarly lead to chronic and hazardous consequences to aquatic life.

1.6.1 Endocrine disrupting chemicals

Endocrine disrupting compounds (EDCs) are chemicals which elicit negative effects on the endocrine systems of humans and animal by mimicking the activity of endogenous estrogens and androgens (Campbell et al., 2006; Gillesby et al., 1998). To date, a wide range of natural and synthetic pharmaceuticals, pesticides, industrial chemicals and heavy metals have been identified as having the ability to mimic or induce estrogen-like responses in the endocrine system (Campbell et al., 2006; Denier et al., 2009; Giesy et al., 2002; Söffker et al., 2012). EDCs are able to functionalise at low nanomolar to micromolar concentrations (De Coster et al., 2012; Vandenberg et al., 2012), causing permanent and irreversible impacts on reproductive behaviours and fertility (Colborn et al., 1993; Fenton, 2006; Nash et al., 2004).

1.6.2 Limitations of general technologies in quantifying estrogenic activity

In the early days, CYL extracts were mostly detected by bioassays (de la Cruz et al., 2013; Hawkins et al., 1985). The evolution of liquid chromatography mass spectrometry techniques and commercial use of CYL standards have promoted the development of chromatographic techniques for detecting CYL levels (de la Cruz et al., 2013) and there are now a range of techniques available for detection and quantification of CYL. CYL detection is achieved by microscopy, molecular and chromatographic methods, bioassays and immunoassays (de la Cruz et al., 2013; Moreira et al., 2013), including *in vivo* mouse assays (Hawkins et al., 1985), an *in vitro* cell line assay (Gutiérrez-Praena et al., 2012), a cell-free protein synthesis inhibition assay (S. M. Froscio et al., 2008), enzyme-linked immunosorbent assays (ELISA) (Ballot et al., 2010) and liquid chromatography tandem mass spectrometry (Gallo et al., 2009; Guzmán-Guillén et al., 2015). The quantification methods for ANA, which encompass biological

methods as well as chromatographic methods, perform well for ANA monitoring and investigation (Osswald et al., 2007). Specifically, bioassays for ANA include an *in vivo* mouse assay (Devlin et al., 1977) and a brine shrimp bioassay (Lahti et al., 1995). Chromatographic methods mainly consist of gas chromatography coupled with mass spectrometry (Dagnino et al., 2005; Ghassempour et al., 2005; V. Rodríguez et al., 2006), high performance liquid chromatography (Al-Sammak et al., 2013; James et al., 1998) and liquid chromatography tandem mass spectrometry (Bogialli et al., 2006; Faassen et al., 2012; Furey et al., 2003). However, the estrogenic effects cannot be ascertained by these chromatographic methods; meanwhile, detection of estrogenic activity of cyanotoxins by *in vivo* bioassays can be masked due to the high toxicity (Jonas et al., 2015). Additionally, *in vivo* bioassays are costly and time-consuming (Beresford et al., 2000).

1.6.3 *In vitro* assays for quantification of estrogenic activity

Compounds mimicking the activity of endogenous estrogens are classified as estrogenic compounds and estrogen-like compounds (Gillesby et al., 1998). While estrogenic substances produce effects which are mediated through estrogen receptors, the effects produced by estrogen-like substances are not mediated by estrogen receptors (Gillesby et al., 1998). Modelling the mechanisms of action of endogenous estrogens, a number of *in vitro* estrogenicity assays are available for detecting EDCs, including estrogen receptor competitive ligand binding assays, recombinant receptor/reporter gene assays, cell proliferation assays, post-confluent cell accumulation, endogenous protein expression, quantitative reverse transcriptase-polymerase chain reaction and yeast-based assays (Bistan et al., 2011; Gillesby et al., 1998; Leusch et al., 2010). In previous studies, recombinant cells transfected with an estrogen receptor-regulated luciferase gene were used to detect signalling from cyanobacterial extracts and cyanotoxins which initiate effects mediated through estrogen receptors (Jonas et al., 2015; Oziol et al., 2010; Štěpánková et al., 2011; Sychrová et al., 2012). Compounds

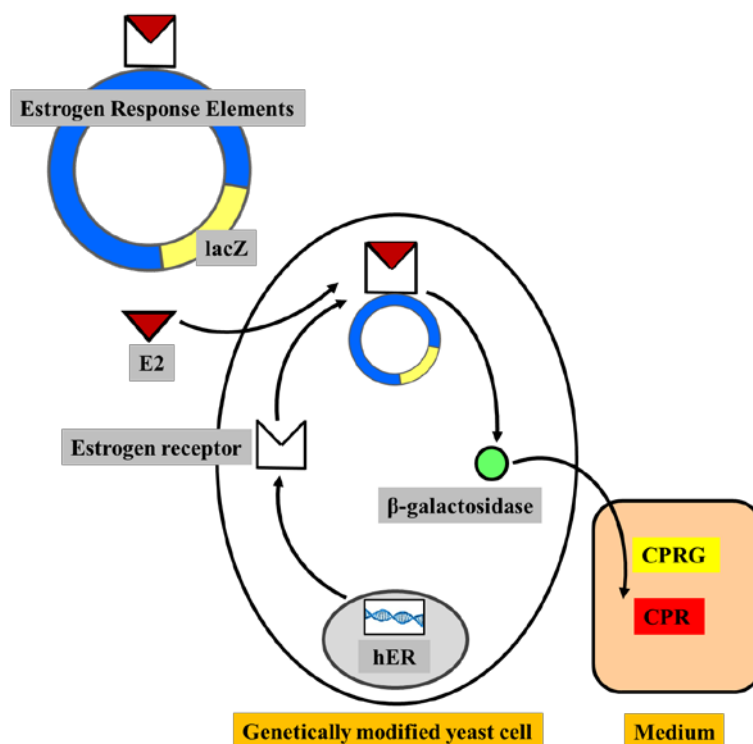
produced by cyanobacteria were consequently classified as estrogenic substances, due to their receptor-mediated effects. Further, reporter gene-based assays are suggested as the preferred assays for detecting the estrogenic potency of cyanotoxins.

However, the significant disadvantages of mammalian cell assays should be considered. The long periods required for cell growth and necessary sterility of samples make this a relatively costly method in terms of the time-consuming techniques and equipment required to avoid potential contamination, and the deviation in results produced by different types of hormone receptors (Balsiger et al., 2010). Instead, another reporter gene assay, the *in vitro* yeast estrogen screen (YES) assay is recommended. The YES assay is widely used now because of its short incubation time, high resistance to environmental samples, low operational costs, capacity to rapidly screen a large number of samples simultaneously, and the simplicity of the procedure (Balsiger et al., 2010). The YES assay has been applied to measure the estrogenic activity of individual chemicals (Routledge et al., 1996; Segner et al., 2003), samples from wastewater (Aerni et al., 2004; Balsiger et al., 2010; Thorpe et al., 2006) and sewage (Rutishauser et al., 2004), and surface water samples (Murk et al., 2002).

1.6.4 Mechanism of the yeast estrogen screen assay

The yeast cell-based assay uses genetically modified yeast strains engineered with the human estrogen receptor gene and expression plasmids which carry a reporter gene (Routledge et al., 1996). The reaction mechanism processes are described by Scheme 1.6 (McLachlan et al., 1996): 1) estrogen enters the yeast cells; 2) when activated by estrogen, the recombinant human estrogen receptor gene encodes more estrogen receptors; 3) estrogen binds to these estrogen receptors; 4) the estrogen and receptor complex then binds to the estrogen response elements; 5) the linked *lacZ* gene is transcribed producing the enzyme β -galactosidase (β -gal); 6) the enzyme β -gal is liberated into the media; and 7) causes a colour reaction that converts

chlorophenol red- β -*d*-galactopyranoside (CPRG) into chlorophenol red (CPR); 8) the intensity of the colorimetric response is quantified as estrogenic activity (Campbell et al., 2006; De Boever et al., 2001; McLachlan et al., 1996).



Scheme 1. 6: Hormone-induced chemiluminescence in the YES assay

Despite its reputation as a reliable detection tool, some studies have reported that the YES assay measured estrogenicity of a variety of samples differed from the values predicted by the concentration addition model, and differed to the estrogenicity calculated by chemical analysis (Beck et al., 2006; Thorpe et al., 2006). Such deviations likely result from the chemical disruption of the activation of estrogen response elements (Thorpe et al., 2006), the presence of anti-estrogenic compounds and/or unknown compounds with estrogenicity (Beck et al., 2006; Nakada et al., 2004; Pauwels et al., 2008; Peck et al., 2004), the influence of estrogen receptor antagonists (Snyder et al., 2001), the considerable impact of weak estrogens (Rajapakse et al., 2001), the salinity of samples (Kase et al., 2008), various alterations in

methodology (Beresford et al., 2000), and also non-estrogenic toxicants (Frische et al., 2009). When binding to the human estrogen receptor α (ER α), nonsteroidal compounds are likely to mimic the natural estrogen 17 β -estradiol (De Boever et al., 2001), thereby modulating natural estrogenic activity.

1.7 Research gaps

Shortcomings have been observed in current technologies for cyanotoxin removal and degradation, however treatment of cyanotoxins by Fe^{III}-B*/H₂O₂, a high activity catalyst system, has not been described in the literature.

While NOM has shown negative impacts on cyanotoxin removal, the characteristics of NOM involved in CYL and ANA degradation by Fe^{III}-B*/H₂O₂ remain unknown.

Although there are some indications of endocrine disrupting effects of cyanotoxins, information on the estrogenicity induced by CYL and ANA is limited. Furthermore, information on changes in estrogenicity following CYL and ANA treatment by a powerful oxidant is lacking in the current scientific literature.

1.8 Research objectives

The overarching objectives of this research are to investigate the degradation of CYL and ANA by Fe^{III}-B*/H₂O₂, explore the influence of NOM on cyanotoxin degradation, and assess the estrogenic activity of cyanotoxins. The study has been designed in sequential steps, with the aim of extending knowledge toward the implementation of Fe^{III}-B*/H₂O₂ in water treatment plants and bridging the knowledge gap around cyanotoxin related endocrine-disrupting effects. The specific research objectives and steps are to:

1. Investigate the catalytic oxidative degradation of cyanotoxins CYL and ANA by Fe^{III}-B*/H₂O₂

2. Explore the influence of NOM on cyanotoxin degradation by $\text{Fe}^{\text{III}}\text{-B}^*/\text{H}_2\text{O}_2$
3. Assess the estrogenic activity of these cyanotoxins and the estrogenic response of their degradation products

1.9 Thesis framework

As this thesis consists of three manuscripts to be submitted for publication, repetition of some materials has been unavoidable. Details of each chapter are presented below:

Chapter 1

Chapter 1 discusses global cyanobacterial blooms and associated adverse impacts from various perspectives. The serious consequences are seen in the poisonings and deaths in humans and animals associated with cyanotoxins and reported globally over decades. The chapter explains the rationale for selecting CYL and ANA as the target compounds and outlines the primary characteristics of these cyanotoxins. The chapter then presents a brief review of the available treatment methods for cyanotoxins, describing the challenges of current cyanotoxin treatment options and the negative influence of NOM on treatment efficiency. Details are provided for the sequence of reactions contributing to the action of $\text{Fe}^{\text{III}}\text{-TAML}/\text{H}_2\text{O}_2$, and the factors that make $\text{Fe}^{\text{III}}\text{-TAML}/\text{H}_2\text{O}_2$ an attractive alternative for cyanotoxin degradation. The chapter draws attention to the limited knowledge about the estrogenic activity of cyanotoxins, and highlights the possibility that CYL and ANA act as endocrine disrupting chemicals. The yeast estrogen screen assay is introduced as a currently available technique for detecting the estrogenic activity of cyanotoxins.

Chapter 2

Catalytic degradation of cyanotoxins by $\text{Fe}^{\text{III}}\text{-B}^*/\text{H}_2\text{O}_2$ is discussed in Chapter 2, and the degradation of CYL and ANA at varying pH levels is evaluated. The next section of Chapter 2

summarises the production of heterogeneous $\text{Fe}^{\text{III}}\text{-B}^*$ and provides an assessment of the coverage ratio of heterogeneous $\text{Fe}^{\text{III}}\text{-B}^*$. Heterogeneous $\text{Fe}^{\text{III}}\text{-B}^*$ catalysts are produced by immobilising homogeneous $\text{Fe}^{\text{III}}\text{-B}^*$ onto functionalised silica gel. The coverage ratio of heterogeneous $\text{Fe}^{\text{III}}\text{-B}^*$ is then assessed by monitoring the reduction in dye absorbance. The efficiency of cyanotoxin removal by heterogeneous $\text{Fe}^{\text{III}}\text{-B}^*/\text{H}_2\text{O}_2$ is monitored and compared to homogeneous $\text{Fe}^{\text{III}}\text{-B}^*/\text{H}_2\text{O}_2$. Degradation products and corresponding degradation pathways are identified based on the analysis of chromatograms and mass spectra. The changes in toxicity following the transformation of CYL and ANA by a powerful oxidant are discussed, in light of the structural destruction and conformational changes.

Chapter 3

In Chapter 3, the influence of dissolved NOM (0 ~ 30 ppm) on cyanotoxin degradation by $\text{Fe}^{\text{III}}\text{-B}^*/\text{H}_2\text{O}_2$ is investigated. NOM oxidation by $\text{Fe}^{\text{III}}\text{-B}^*/\text{H}_2\text{O}_2$ is monitored by excitation–emission matrix (EEM) and ultraviolet spectrometry. Changes in the fluorophore signature and UV/Vis absorbance indicate the potential NOM components oxidised by $\text{Fe}^{\text{III}}\text{-B}^*/\text{H}_2\text{O}_2$. The radical-mediated cross-coupling reactions between the NOM compounds and cyanotoxin by $\text{Fe}^{\text{III}}\text{-B}^*/\text{H}_2\text{O}_2$ likely increase cyanotoxin removal. Guaiacol and glycolic acid are used as NOM surrogates in cyanotoxin degradation to further illustrate the interaction between cyanotoxin and NOM constituents. Radical-mediated cross-coupling pathways between NOM surrogates and cyanotoxin are proposed based on the radicals generated via one-electron oxidation by $\text{Fe}^{\text{III}}\text{-B}^*/\text{H}_2\text{O}_2$. The changes in toxicity of cyanotoxins and their degradation products complexing with NOM are discussed as due to the conformational changes of the uracil moiety of CYL and the molecular structure of ANA.

Chapter 4

Chapter 4 presents the first study on the evaluation of potential estrogenic activity of CYL and ANA employing the yeast estrogen screen (YES) assay. The intensity of the colorimetric response by CYL and ANA is quantified and the curves representing the % β -galactosidase responses of cyanotoxin are plotted by a four-parameter-log(agonist) vs response-curve equation. The logEC₅₀ values induced by the cyanotoxins are compared to the logEC₅₀ values induced by E2 and ZnCl₂, which are used as endogenous hormone and endocrine disrupting chemical respectively. The binding affinity of CYL and ANA to the estrogen receptor is associated with their ring structures and toxicological properties. Cyanotoxin modulation of E2-induced estrogenicity are observed in the competition assay. Their agonistic and/or antagonistic modulation of E2-induced estrogenicity are discussed. The estrogenicity of CYL and ANA treated by Fe^{III}-B*/H₂O₂ is explored, with the aim of extending knowledge of changes in cyanotoxin-induced estrogenicity following treatment. Because estrogenic potency is correlated with ring structures, the destruction of parent cyanotoxin and the formation of various products are discussed in relation to this changed estrogenicity. The reduced level of estrogenicity in the treated cyanotoxins is correlated with the reduced cyanotoxin levels and also with the degradation products, which may affect the estrogenicity measurement by acting as exogenous ligands.

Chapter 5

This chapter summarises the findings of this work and their significance to cyanotoxin treatment research. It concludes with a series of overall recommendations and highlights directions for further work, which should improve the performance of Fe^{III}-B*/H₂O₂ in real life applications.

Chapter 2: Oxidative degradation of cylindrospermopsin and anatoxin-a by Fe^{III}-B*/H₂O₂

Manuscript to be submitted to Water Research journal

Chapter abstract

Cylindrospermopsin (CYL) and anatoxin-a (ANA) are alkaloid-like potent cyanotoxins produced during cyanobacterial blooms. Their high toxicity and widespread distribution have raised concerns over the safety of impacted drinking water sources. Current physical and chemical oxidation technologies are not always effective in treating CYL and ANA contaminated water. The novel catalyst iron tetra-amido-macrocyclic ligand (Fe^{III}-TAML, designated as Fe^{III}-B*) activates H₂O₂, and is known to degrade a range of recalcitrant pollutants. We explore the oxidative degradation of CYL and ANA by Fe^{III}-B* in a homogeneous formulation and a heterogeneous formulation produced by anchoring dissolved Fe^{III}-B* onto functionalised silica gel. Cyanotoxin oxidation by homogeneous Fe^{III}-B*/H₂O₂ (5 μM/ 5 mM) was conducted at 25 °C at pH ranging between 8.5 and 11.5 over 120 min. The apparent first order rate constants increased for higher pH, reaching a maximum at pH 11.5 for both compounds. The decrease in oxidation efficiency at pH 10.5 and 11.5 is explained by activator self-decomposition. In view of the opposing effect of high pH on the rate constant and the removal efficiency, a lower pH of 9.5 was used to assess the degradation of both compounds by heterogeneous Fe^{III}-B*/H₂O₂. At pH 9.5, homogeneous Fe^{III}-B*/H₂O₂ (2.5×10⁻⁷ mole /5 mM) decreased the concentration of CYL (0.24 μM) by 87 % and ANA (7.1 μM) by 96 %, while heterogeneous Fe^{III}-B*/H₂O₂ (2.5×10⁻⁷ mole of Fe^{III}-B* loaded on 240 mg of functionalised silica gel in 5 mM H₂O₂) lowered the concentration of CYL by 93 % and ANA by 88 %. The mechanisms of cyanotoxin removal by heterogeneous formulation were solid adsorption and catalytic oxidative degradation. When identical moles of Fe^{III}-B* and H₂O₂

were used in the heterogeneous formulation, heterogeneous $\text{Fe}^{\text{III}}\text{-B}^*/\text{H}_2\text{O}_2$ showed similar efficiency in cyanotoxin removal as homogeneous $\text{Fe}^{\text{III}}\text{-B}^*/\text{H}_2\text{O}_2$ and so extended the application of the $\text{Fe}^{\text{III}}\text{-B}^*/\text{H}_2\text{O}_2$ catalyst system. High resolution mass spectrometry analysis of the intermediate products of homogeneous CYL and ANA oxidation showed that CYL transformation involved hydroxylation, sulphate elimination, uracil ring modification, and tricyclic ring destruction, while ANA transformation involved epoxidation and deamination. These intermediates suggest that the transformations lowered cyanotoxin toxicity from the oxidation of the uracil ring of CYL and the formation of non-toxic epoxy-ANA. Both the homogeneous and heterogeneous formulations of $\text{Fe}^{\text{III}}\text{-B}^*/\text{H}_2\text{O}_2$ were shown to transform CYL and ANA, and the intermediates identified indicate the toxicity of the mixture decreased.

2.1 Introduction

Cyanobacterial blooms impact water quality by releasing compounds which taint the smell and taste of water (Ian R Falconer, 1999; Graham et al., 2010). Of greater concern, cyanobacterial blooms produce secondary metabolites such as cyanotoxins which can pose a threat to human and animal health (Van Apeldoorn et al., 2007). Animal deaths from cyanotoxin ingestion have been recorded as far back as 1878 at Lake Alexandrina in South Australia (G. Codd et al., 1994). Since then, other incidences of animal poisoning and deaths from cyanotoxins have been reported in many countries (Bláha et al., 2009; Catherine et al., 2013; G. A. Codd, 2000; Svrcek et al., 2004). Cylindrospermopsin (CYL, Figure 2.1a) and anatoxin-a (ANA, Figure 2.1b) are members of the cyanotoxin family and have received a lot of attention because of their high toxicity and widespread distribution (A. Humpage, 2008; Kinnear, 2010; Pelaez et al., 2010).

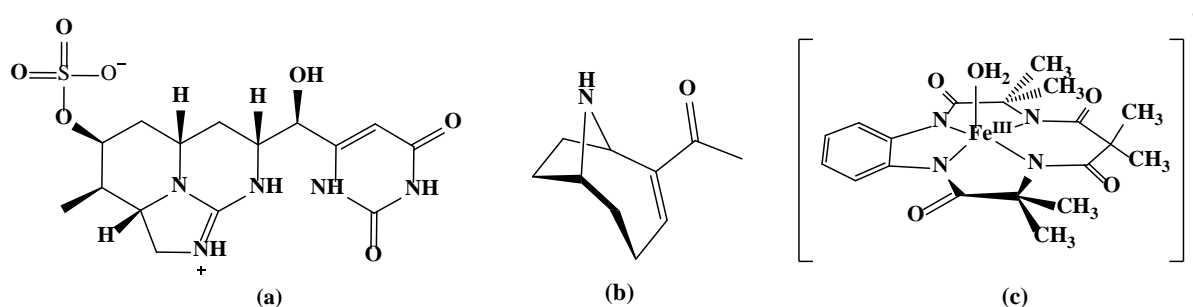


Figure 2. 1: The structure of (a) cylindrospermopsin, (b) anatoxin-a, (c) Fe^{III}-B* catalyst

Traditional methods (e.g., coagulation and flocculation), physical removal, chemical oxidation and advanced oxidation processes (AOPs) have been used to treat CYL and ANA (de la Cruz et al., 2013; Vlad et al., 2014; J. Westrick et al., 2010). Sedimentation is effective for the removal of intracellular cyanotoxins, but not for extracellular cyanotoxins (He, Zhang, et al., 2014; Newcombe et al., 2004; J. Westrick et al., 2010). Effective physical removal of cyanotoxins requires a high dose of activated carbon and repeat treatments (Hitzfeld et al., 2000). Cyanotoxin degradation by oxidizing agents has shown varying degrees of efficiency

(E. Rodríguez, Onstad, et al., 2007). Chlorine and permanganate cannot effectively remove both CYL and ANA (Newcombe et al., 2004; E. Rodríguez, Onstad, et al., 2007; E. Rodríguez, Sordo, et al., 2007; P. Senogles et al., 2000). CYL and ANA removal by ozonation has been reported (Onstad et al., 2007; E. Rodríguez, Onstad, et al., 2007), but the effectiveness of this treatment is strongly dependent on the DOC concentration of water (Rositano et al., 2001). The criteria for gauging the effectiveness of cyanotoxin treatment are suggested as removal efficiency, operational costs, and levels of detoxification achieved. The iron (III) tetra-amido-macrocyclic ligand (Fe^{III} -TAML, designated as Fe^{III} -B*, as shown in Figure 2.1c), an activator of H_2O_2 , is expected to achieve efficient and economic oxidation and detoxification of CYL and ANA. The Fe^{III} -B*/ H_2O_2 oxidation system has been shown to rapidly oxidize various contaminants (Chahbane et al., 2007; Chanda, Ryabov, et al., 2006; J. L. Chen et al., 2012; Mitchell et al., 2010; Shappell et al., 2008) without producing toxic by-products (Chahbane et al., 2007; Gupta et al., 2002). Fe^{III} -TAML/ H_2O_2 can act efficiently at low μM concentrations (W. Chadwick Ellis et al., 2009) and over a broad pH range (pH 6 ~ 12.4) (Ghosh et al., 2008). Many catalysts are typically applied homogeneously by dissolving them in solution. An alternative procedure is to use the catalyst in heterogeneous form as a solid catalyst (X. S. Zhao et al., 2006), for example by immobilising the catalyst onto solid surfaces (Sabater et al., 2014). Since the half-life of homogeneous Fe^{III} -TAML is short (Chanda, Ryabov, et al., 2006), heterogeneous Fe^{III} -TAML activators may make continuous large scale water treatment possible by lowering the dosage required. Several types of catalyst have been immobilised on solid surfaces, e.g., biological catalysts (Katchalski-Katzir et al., 2000; Tischer et al., 1999), metal catalysts (del Pozo et al., 2011; Hu et al., 2005; Matsumoto et al., 2008; Sabater et al., 2014; Severeys et al., 2001; Sotiriou-Leventis et al., 2008) and photochemical catalysts (Y. Liu et al., 2005; Puma et al., 2008; Shephard et al., 2002). Silica gel is one of the most

commonly used as the immobilisation substrates (Jal et al., 2004; G. Lu et al., 2004; Price et al., 2000; Ross, 2011).

The aims of this work are to investigate the oxidative degradation of CYL and ANA by homogeneous and heterogeneous $\text{Fe}^{\text{III}}\text{-B}^*/\text{H}_2\text{O}_2$ under different pH conditions, identify the intermediate products of transformation, propose the transformation pathways and assess the detoxification of cyanotoxins by $\text{Fe}^{\text{III}}\text{-B}^*/\text{H}_2\text{O}_2$.

2.2 Methodology

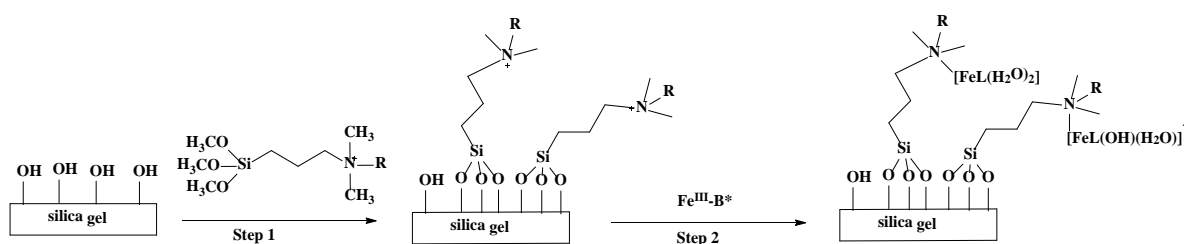
2.2.1 Chemicals preparation

Cylindrospermopsin from Sapphire Bioscience Pty. Ltd. and (\pm)-anatoxin-a fumarate from Abcam Australia Pty. Ltd. were used as received. $\text{Fe}^{\text{III}}\text{-B}^*$ was supplied by the School of Chemical Sciences, University of Auckland. H_2O_2 (30 %) was purchased from Thermo Fisher Scientific. Silica gel (200 – 400 mesh) and dimethyloctadecyl [3-(trimethoxysilyl) propyl] ammonium chloride (Si-QAC) solution (42 wt. % in methanol) were purchased from Sigma Aldrich. The solvents were HPLC grade from Merck Millipore. Water (18.2 M Ω .cm resistivity) was purified by a Milli-Q filtration system (Millipore). All operations with cyanotoxins were undertaken in a chemical fume hood adhering to the proper precautions for handling hazardous chemical.

2.2.2 Heterogeneous $\text{Fe}^{\text{III}}\text{-B}^*$ production

The method (Scheme 2.1) for generating heterogeneous $\text{Fe}^{\text{III}}\text{-B}^*$ consisted of two steps. Firstly, the silica gel was functionalised (Isquith et al., 1972; NIKAWA et al., 2005; Walters et al., 1973), and then $\text{Fe}^{\text{III}}\text{-B}^*$ was anchored onto the modified solid surface via electrostatic interaction (McMorn et al., 2004; Sakpal et al., 2012; Shimizu et al., 1997). In Step 1, 5 g silica gel was reacted with 70 mL of 10 % (v/v) diluted Si-QAC solution for 2 hrs at 60 °C under

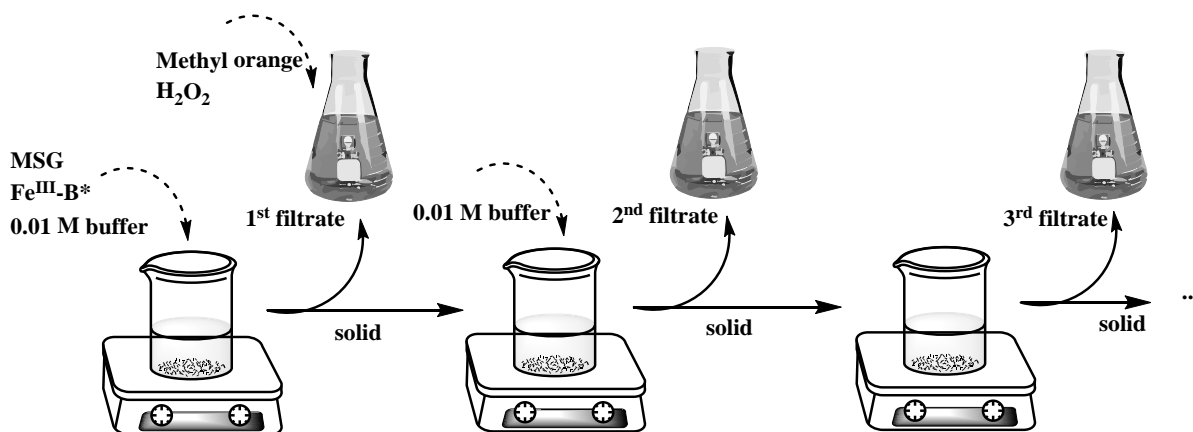
stirring (300 rpm). The reacted silica gel was recovered by washing it thoroughly with water (3×50 mL) and acetone (3×50 mL) and then dried in a vacuum oven at $110\text{ }^{\circ}\text{C}$ overnight. The functionalised modified silica gel was harvested the following day. In Step 2, 2.5×10^{-7} mole, 1.25×10^{-6} mole and 2.5×10^{-6} mole $\text{Fe}^{\text{III}}\text{-B}^*$ in pH 9.5 0.01 M $\text{Na}_2\text{CO}_3/\text{NaHCO}_3$ buffer was stirred with 240 mg modified silica gel at 300 rpm. Heterogeneous $\text{Fe}^{\text{III}}\text{-B}^*$ was harvested by filtration after 15 min.



Scheme 2. 1: Covalent attachment of quaternary nitrogen reagent to silica gel and homogeneous $\text{Fe}^{\text{III}}\text{-B}^*$ immobilisation onto the functionalised silica gel

2.2.3 Coverage assessment of heterogeneous $\text{Fe}^{\text{III}}\text{-B}^*$

The coverage ratio of $\text{Fe}^{\text{III}}\text{-B}^*$ on the solid support was quantified by determining the residual $\text{Fe}^{\text{III}}\text{-B}^*$ in the filtrate by monitoring the drop in absorbance of methyl orange. Due to the equilibrium between absorption and desorption, repeated sets of re-suspension and filtration were conducted to obtain a stable coating of $\text{Fe}^{\text{III}}\text{-B}^*$ with optimized coverage. The total released $\text{Fe}^{\text{III}}\text{-B}^*$ was calculated by adding up the $\text{Fe}^{\text{III}}\text{-B}^*$ left in each filtrate. In Scheme 2.2, filtrate from each cycle was mixed with $45\text{ }\mu\text{M}$ methyl orange and pH 9.5 0.01 M $\text{Na}_2\text{CO}_3/\text{NaHCO}_3$ buffer to reach 100 mL. Dye bleaching was initiated by adding 1 mM H_2O_2 into each bulk solution and the absorbance ($\lambda = 464.5\text{ nm}$) recorded at set intervals. The amount of $\text{Fe}^{\text{III}}\text{-B}^*$ in the filtrate was converted by calibrating the initial bleaching rate by standard $\text{Fe}^{\text{III}}\text{-B}^*$. The coverage ratio of heterogeneous $\text{Fe}^{\text{III}}\text{-B}^*$ was converted by the total released $\text{Fe}^{\text{III}}\text{-B}^*$ (mole) and silica gel (mg).



Scheme 2. 2: The process flow for heterogeneous Fe^{III}-B* production

2.2.4 Degradation experiments

The initial reaction conditions were: 0.24 μM CYL or 7.1 μM ANA in the 0.01 M $\text{Na}_2\text{CO}_3/\text{NaHCO}_3$ buffer, 5 μM homogeneous Fe^{III}-B* or heterogeneous Fe^{III}-B* (2.5×10^{-7} mole homogeneous Fe^{III}-B* on 240 mg modified silica gel), and 5 mM H_2O_2 . Because the pK_a of Fe^{III}-TAML is in the range 9.4 – 10.5 (Ghosh et al., 2003), CYL's pK_a is 8.8 and ANA's pK_a is 9.4 (Onstad et al., 2007), the degradation of cyanotoxin by the homogeneous Fe^{III}-B*/ H_2O_2 catalyst system was studied at pH 8.5 to 11.5. Reactions were carried out in glassware covered with aluminium foil paper and shaken at 600 rpm in a mechanical shaker at 25 °C. Samples were taken at intervals and the residual H_2O_2 quenched by catalase, which was 60 times the concentration capable of destroying 5 mM H_2O_2 in 1 min. Samples were then filtered through 0.2 μm RC syringe filters (Phenomenex NZ Ltd) and applied to LC-MS for cyanotoxin quantification.

2.2.5 Cyanotoxin quantification by LC-MS

Cyanotoxin quantification was conducted by LC-MS (Shimadzu Series model LC-MS 2020, Japan). The separation method was modified from Faassen et al. (2012). Compounds were separated on a Waters Atlantis T3 column (3 μm , 3.0 \times 150 mm) at 0.2 mL/min flow rate under

30 °C column. Milli-Q water/0.1 % formic acid (v/v) as mobile phase A and methanol/0.1 % formic acid (v/v) as mobile phase B were used for both cyanotoxins. The gradient elution program for CYL was 1 min: 5 % B, 8 – 12 min: 50 % B, and 16 min: 0 % B, with a linear increase between the isocratic periods. The gradient elution program for ANA was 0.01 min: 20 % B, 3 – 5 min: 90 % B, and 10 min: 20 % B, with a linear increase between the isocratic periods. CYL was monitored at m/z 416 and ANA was monitored at m/z 166 in positive ion mode (SIM). The concentration of cyanotoxin was determined based on a standard curve obtained by plotting pure cyanotoxin against the peak area of the LC-MS curve.

2.2.6 Solid-phase extraction procedure

Degradation samples were concentrated by the solid-phase extraction (SPE) and analysed by Q-Exactive tandem mass spectrometry (LC-MS/MS). The CYL-SPE method was modified from Metcalf et al. (2002) and Foss et al. (2013) with the application of Hypersep Hypercab SPE cartridges (Thermo Fisher Scientific, NZ Ltd.): 1) cartridges were conditioned with two column volumes of methanol and rinsed with two column volumes of water; 2) samples were loaded onto cartridges at a flow rate of 1 – 2 mL/min; 3) cartridges were washed with one column volume of water and fully air-dried prior to elution; and 4) CYL was eluted with 95 % methanol/ 5 % formic acid (v/v). The ANA-SPE using Strata-X-CW polymeric weak cation SPE cartridges (Phenomenex Australia Pty Ltd.) was conducted as follows: 1) one column volume of methanol followed by one column volume of water was applied to condition the cartridges; 2) samples were loaded after adjustment to pH 6 ~ 7; 3) one column volume of water followed by one column volume of methanol was used to wash the cartridges; and 4) samples were eluted with 5 % formic acid in methanol. For all SPE samples, the eluate was evaporated to dryness in a speed vacuum concentrator (Savant SPD131DDA, ThermoFisher) and then reconstituted in methanol for analysis.

2.2.7 CYL and ANA degradation analysis

The apparent-first-order rate constants for CYL and ANA degradation by $\text{Fe}^{\text{III}}\text{-B}^*/\text{H}_2\text{O}_2$ were obtained using the following first-order decay relationship (Jho et al., 2012):

$$C = (1 - C_{res})e^{-kt} + C_{res} \quad \text{Eq.2.1}$$

where C represents C_t/C_0 that CYL or ANA concentration at time t (min) normalized to its initial concentration (C_0), C_{res} represents the residual CYL or ANA concentration normalized with respect to its initial concentration (C_0), and k indicates the apparent first-order rate constant (min^{-1}).

2.3 Results and discussion

2.3.1 Effect of pH on cyanotoxin oxidation by homogeneous $\text{Fe}^{\text{III}}\text{-B}^*/\text{H}_2\text{O}_2$

We explored the effect of changes in pH on the rates at which CYL and ANA is oxidized by homogeneous $\text{Fe}^{\text{III}}\text{-B}^*/\text{H}_2\text{O}_2$, because the rate of the $\text{Fe}^{\text{III}}\text{-TAML}/\text{H}_2\text{O}_2$ catalyst system oxidation of substrate is known to be strongly dependent on the pH of the solution (Chanda, Ryabov, et al., 2006; Ghosh et al., 2008). As seen from the degradation of CYL by $\text{Fe}^{\text{III}}\text{-B}^*/\text{H}_2\text{O}_2$ in Figure 2.2a, CYL oxidation showed a rapid decline in the first 20 min, followed by a slower removal and then finally entered into a fairly steady state up until the end of the experiment at 120 min. As shown by the degradation rates at varying pH, CYL oxidation by $\text{Fe}^{\text{III}}\text{-B}^*/\text{H}_2\text{O}_2$ is highly pH dependent. Treatment at pH 8.5 reduced the parent compound by 37 % after 5 min and 85 % after 30 min. Beyond the 30 min reaction time, there was no further significant reduction in residual CYL concentration. Increasing the pH to 9.0 resulted in slightly reduced removal (13 % CYL residual at 120 min). As pH was further increased to 9.5, no significant difference was observed for residual CYL. When pH was increased to 10.5 and 11.5, CYL was removed rapidly in the first 5 min, decreasing by 44 % and 53 % respectively.

However, the rapid rate of removal decreased by the 10th min and then plateaued, resulting in 77 % removal at pH 10.5 after 2 hrs and 70 % at pH 11.5. The results for ANA removal by Fe^{III}-B*/H₂O₂ indicated a fast initial drop in concentration for all levels of pH, but the changes thereafter varied by pH (Figure 2.2b). At pH 8.5, ANA removal increased gradually to 75 % ANA removal by 120 min. ANA removal then increased with increasing pH up to 9.5, with 87 % ANA oxidation at pH 9.0 and 96 % ANA oxidation at pH 9.5. However, the efficiency of Fe^{III}-B*/H₂O₂ then decreased as pH was further increased to 10.5 (81 % ANA removal) and 11.5 (67 % ANA removal). For both cyanotoxins, removal by degradation occurred rapidly at the beginning, which can be associated with high oxidized Fe^{III}-B* concentrations. After this point, the decreasing rates of degradation correlated with either the consumption of oxidized Fe^{III}-B* (ANA degradation) or removal of the reactant (CYL degradation).

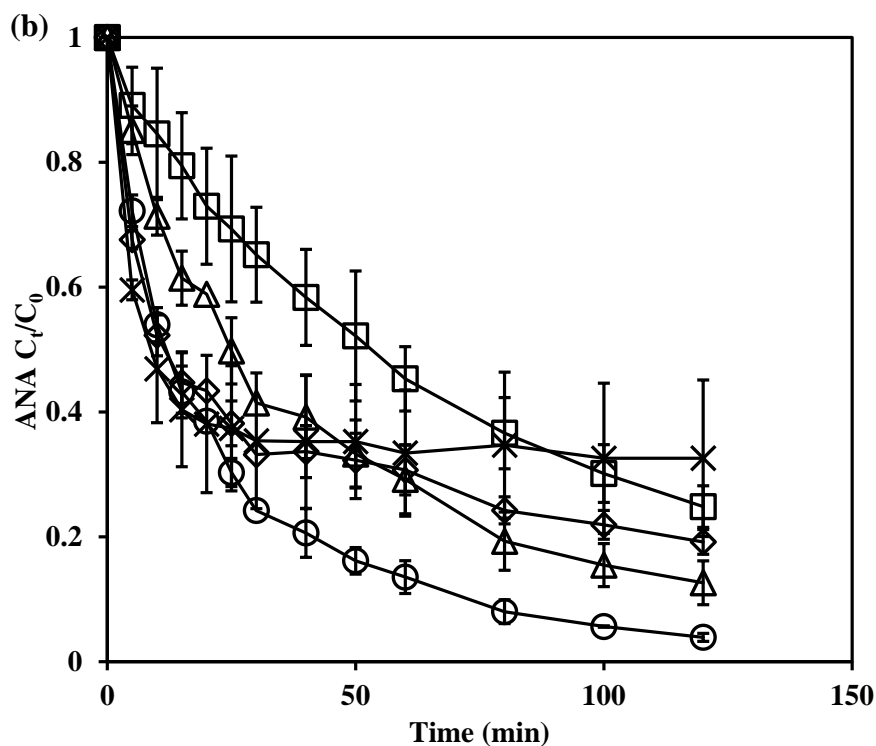
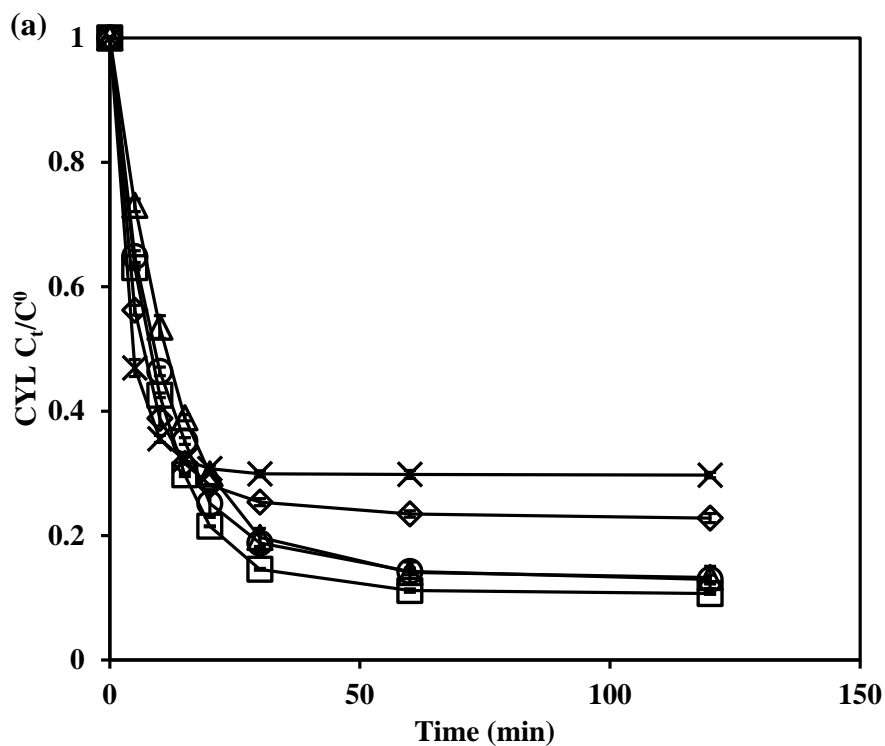


Figure 2. 2: Cyanotoxins removal by homogeneous $\text{Fe}^{\text{III}}\text{-B}^*/\text{H}_2\text{O}_2$ at different pH. (a) CYL ($0.24 \mu\text{M}$) and (b) ANA ($7.1 \mu\text{M}$) removal by $\text{Fe}^{\text{III}}\text{-B}^*/\text{H}_2\text{O}_2$ ($5 \mu\text{M}/5 \text{mM}$) at pH 8.5 (\square), 9.0 (Δ), 9.5 (\circ), 10.5 (\diamond) and 11.5 (\times) (0.01M) (mean \pm standard deviation of three independent runs).

The cyanotoxin decay kinetics are well described by the model in Eq.2.1, with a corresponding regression for high R^2 ranging from 0.96 to 1.00 observed (Appendix Figure A2.1). Figure 2.3 shows that the modelling rate constants increased from low pH 8.5 and peaked at pH 11.5. The climbing curve from pH 8.5 to 11.5 is consistent with the bell-shaped pH profiles demonstrated previously (Popescu et al., 2010), and the peaking value at pH 11.5 implied the highest point of reactivity of $\text{Fe}^{\text{III}}\text{-B}^*$ toward H_2O_2 . Contrary to previous findings of the reduced performance of the catalyst system due to the substrate's reversible binding (Kundu et al., 2015; Mitchell et al., 2010), the influence of charged cyanotoxin at pH 10.5 and 11.5 (above the pK_a value of cyanotoxin) on $\text{Fe}^{\text{III}}\text{-B}^*$ reactivity was negligible, because the observations agreed with the literature that pH from 10 to 11 is known to be the pH at which oxidized $\text{Fe}^{\text{III}}\text{-B}^*$ species are formed at the fastest rate (W Chadwick Ellis et al., 2010; Ghosh et al., 2008). Removal rates were consistent with the rate constants in that higher pH resulted in higher removal rates for CYL (0 ~ 15 min) and for ANA (0 ~ 20 min). However, pH 10.5 and 11.5 led to lower removal rates when the reaction continued further, which was unexpected for $\text{Fe}^{\text{III}}\text{-B}^*/\text{H}_2\text{O}_2$. The significant amount of oxidizing species produced around pH 10 ~ 11 (Ghosh et al., 2008; Popescu et al., 2008) can lead to rapid degradation at the initial decay phase. $\text{Fe}^{\text{III}}\text{-B}^*$ self-decomposition was also expected due to the large amount of oxidized $\text{Fe}^{\text{III}}\text{-B}^*$ species produced. Due to the self-destruction of $\text{Fe}^{\text{III}}\text{-B}^*$ at pH 11 (25 °C) and its corresponding half-lives of 3.4 min (Chanda, Ryabov, et al., 2006), we propose the self-consumption of $\text{Fe}^{\text{III}}\text{-B}^*$ as one reason for the reduced removal rates under high reactivity.

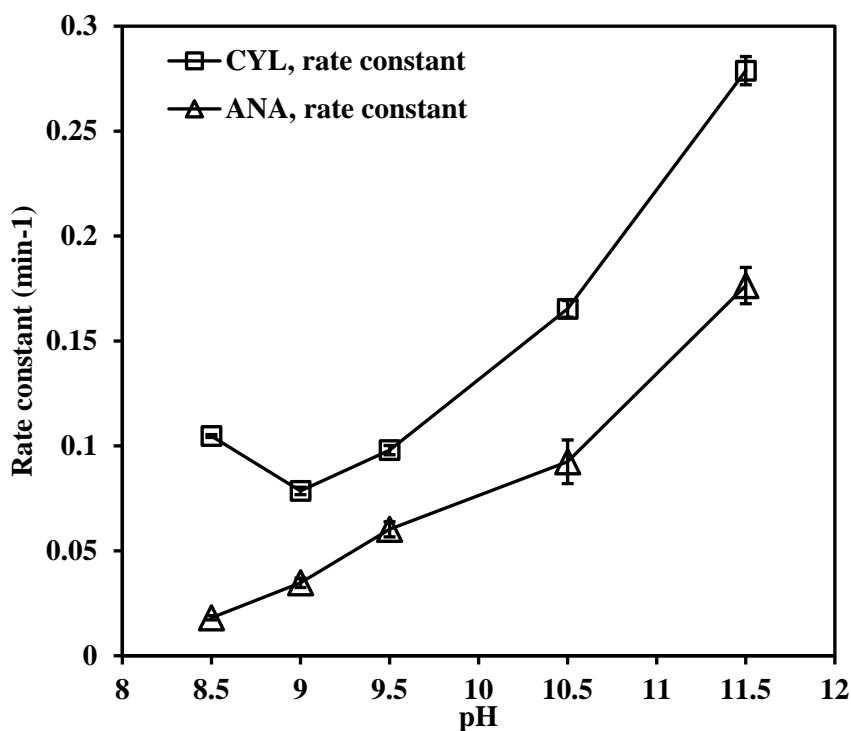


Figure 2. 3: The rate constants of CYL and ANA degradation by homogeneous Fe^{III}-B*/H₂O₂ at different pH

2.3.2 Cyanotoxin removal by heterogeneous Fe^{III}-B*/H₂O₂

A pH of 9.5 was applied in the cyanotoxin catalytic studies by heterogeneous Fe^{III}-B*/H₂O₂, based on the maximum rate of cyanotoxin loss and feasible rate constants for homogeneous Fe^{III}-B*/H₂O₂. Information from the assessment of heterogeneous Fe^{III}-B* coverage ratio is provided in Appendix Figure A2.2. CYL and ANA degradation by homogeneous Fe^{III}-B* and heterogeneous Fe^{III}-B*, with and without H₂O₂, is shown in Figure 2.4a and Figure 2.4b, and the modelled data for degradation by heterogeneous Fe^{III}-B*/H₂O₂ shown in Appendix Figure A2.3.

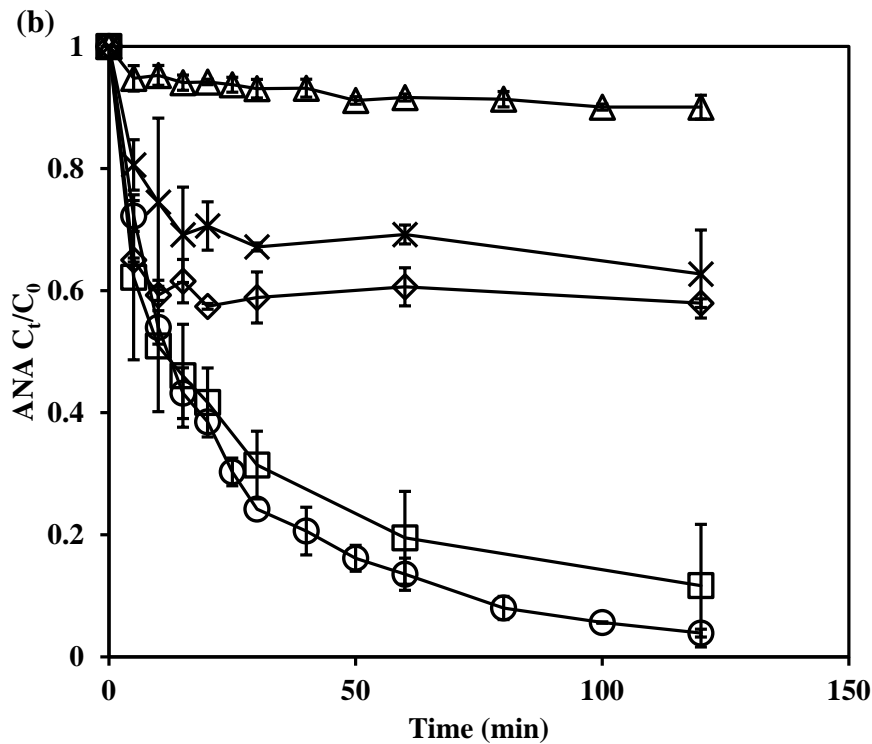
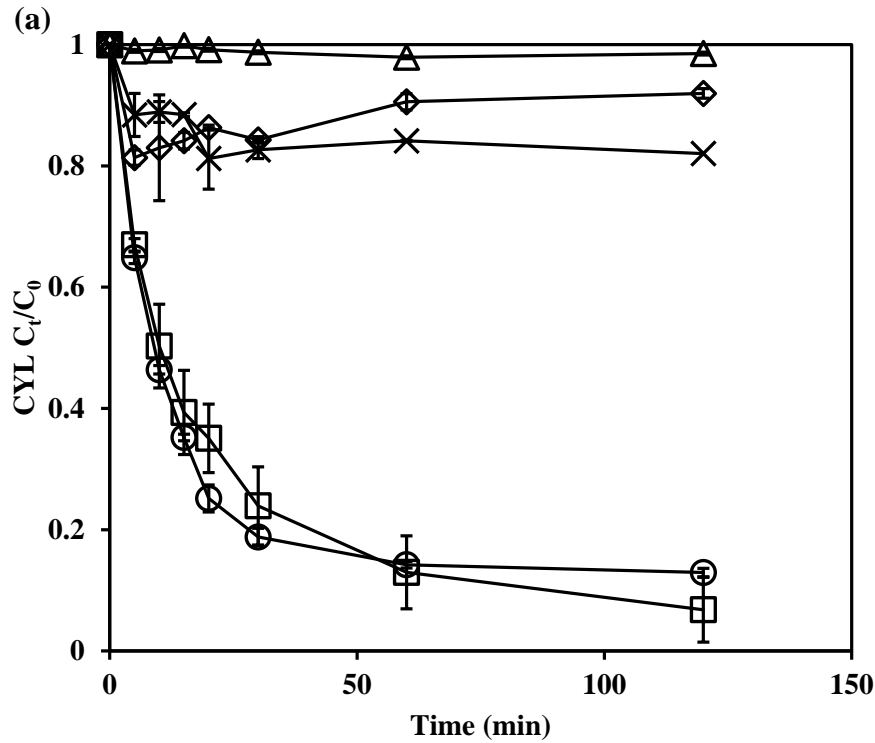


Figure 2. 4: Cyanotoxins removal by homogeneous and heterogeneous $Fe^{III}-B^*/H_2O_2$ at pH 9.5. (a) CYL ($0.24 \mu M$) and (b) ANA ($7.1 \mu M$) removal by modified silica gel (240 mg) (x), homogeneous $Fe^{III}-B^*$ (2.5×10^{-7} mole) (Δ), heterogeneous $Fe^{III}-B^*$ (2.5×10^{-7} mole $Fe^{III}-B^*$ on 240 mg MSG) (\diamond), homogeneous $Fe^{III}-B^*/H_2O_2$ (2.5×10^{-7} mole / 5 mM) (\circ) and heterogeneous $Fe^{III}-B^*/H_2O_2$ (2.5×10^{-7} mole $Fe^{III}-B^*$ on 240 mg MSG / 5 mM) (\square) at pH 9.5 (0.01 M) (mean \pm standard deviation of three independent runs).

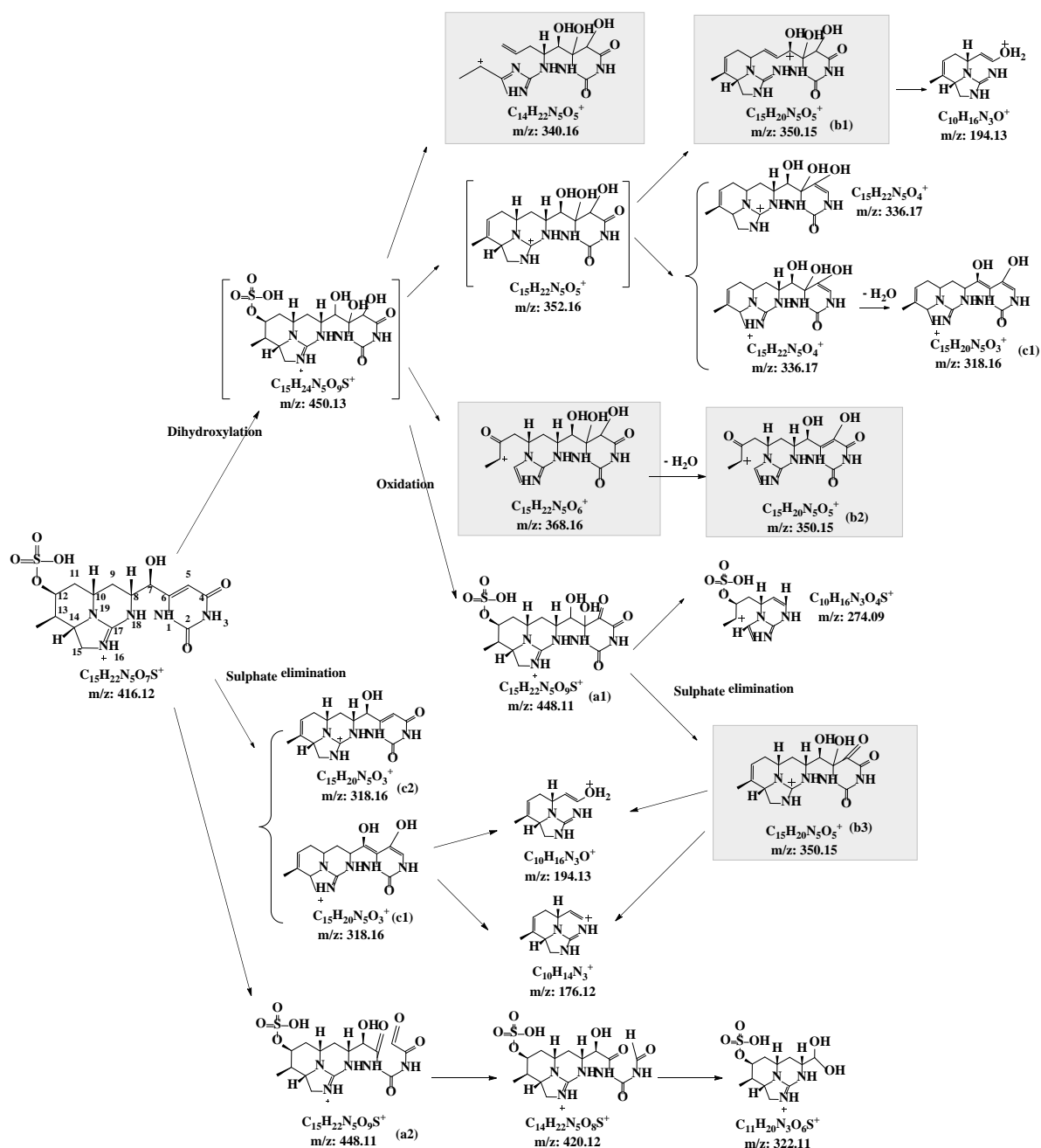
Figure 2.4a shows CYL removal by the modified silica gel (MSG) and heterogeneous Fe^{III}-B*, likely due to electrostatic adsorption on the solid material. CYL is a zwitterionic compound, containing a positively charged guanidine moiety and a negatively charged sulphate group at neutral pH (Meriluoto et al., 2008; Walker, 2014). At pH 9.5, the negatively charged CYL (pK_a = 8.8) molecules (Walker, 2014; Zhang et al., 2014) were attracted to the positively charged MSG, but barely attached to the equivalently charged heterogeneous Fe^{III}-B*, leading to a higher CYL adsorption percentage by MSG (18 % removal) and lower adsorption by heterogeneous Fe^{III}-B* (8 % removal). When H₂O₂ was applied, CYL removal efficiency increased from 87 % for homogeneous Fe^{III}-B*/H₂O₂ to 93 % for heterogeneous Fe^{III}-B*/H₂O₂ over 2 hrs of treatment.

ANA (pK_a = 9.36) molecules can show both neutral and positive charges (Meriluoto et al., 2008) in pH 9.5 solution. With its lower molecular weight and simple chemical structure, ANA molecules can more readily traverse the chains on MSG and heterogeneous Fe^{III}-B*, resulting in respective adsorptions of 37 % and 42 % for MSG and heterogeneous Fe^{III}-B*. In addition, some silanol groups remain available on the surface of silica gel after polymeric treatment. The negatively charged silanol groups (pK_a = 7.1) (Tanabe et al., 1990) are thought to take part in electrostatic interactions with ANA, leading to a further adsorption of ANA. When H₂O₂ was added, both the homogeneous and heterogeneous Fe^{III}-B* induced significant oxidation of the cyanotoxins, removing 96 % and 88 % of ANA respectively (Figure 2.4b).

The removal efficiency of cyanotoxin by heterogeneous Fe^{III}-B*/H₂O₂ is facilitated by catalytic oxidative degradation and solid adsorption, and so the removal rate constants can be jointly affected by these mechanisms. Nevertheless, the homogeneous and heterogeneous formulations of Fe^{III}-B* activated by H₂O₂ showed effective catalytic oxidative degradation of both cyanotoxins.

2.3.3 Identification of intermediate products in the catalytic oxidation of cyanotoxin

The characterisation and interpretation of collision-induced dissociation (CID) CYL product ions based on the MS¹ mass spectrum (Appendix Figure A2.4a), with assistance from Mass Frontier, are shown in Appendix Table A2.1. According to the product ions from the MS² mass spectra (Appendix Figure A2.4b-d), a CID fragmentation series of CYL oxidized by Fe^{III}-B*/H₂O₂ is proposed for Scheme 2.3. Some of the products identified for CYL have previously been reported from its photocatalysis, including the following charged species: *m/z* 448 (L. Chen et al., 2015; Fotiou et al., 2015; He, de la Cruz, et al., 2014; He, Zhang, et al., 2014; Song et al., 2012; Zhang et al., 2015), *m/z* 420 (He, de la Cruz, et al., 2014) and *m/z* 322 (He, de la Cruz, et al., 2014; He, Zhang, et al., 2014; Zhang et al., 2015). It was noteworthy that product ions *m/z* 322, 420 and 448 were detected at low intensity in the MS¹ mass spectrum. In Scheme 2.3, shaded product ions *m/z* 368, 350 and 340 were observed with significant intensity in the MS² mass spectra (Appendix Figure A2.4c, Figure A2.4d), but were absent in the MS¹ mass spectrum (Appendix Figure A2.4a), which was likely due to their instability.



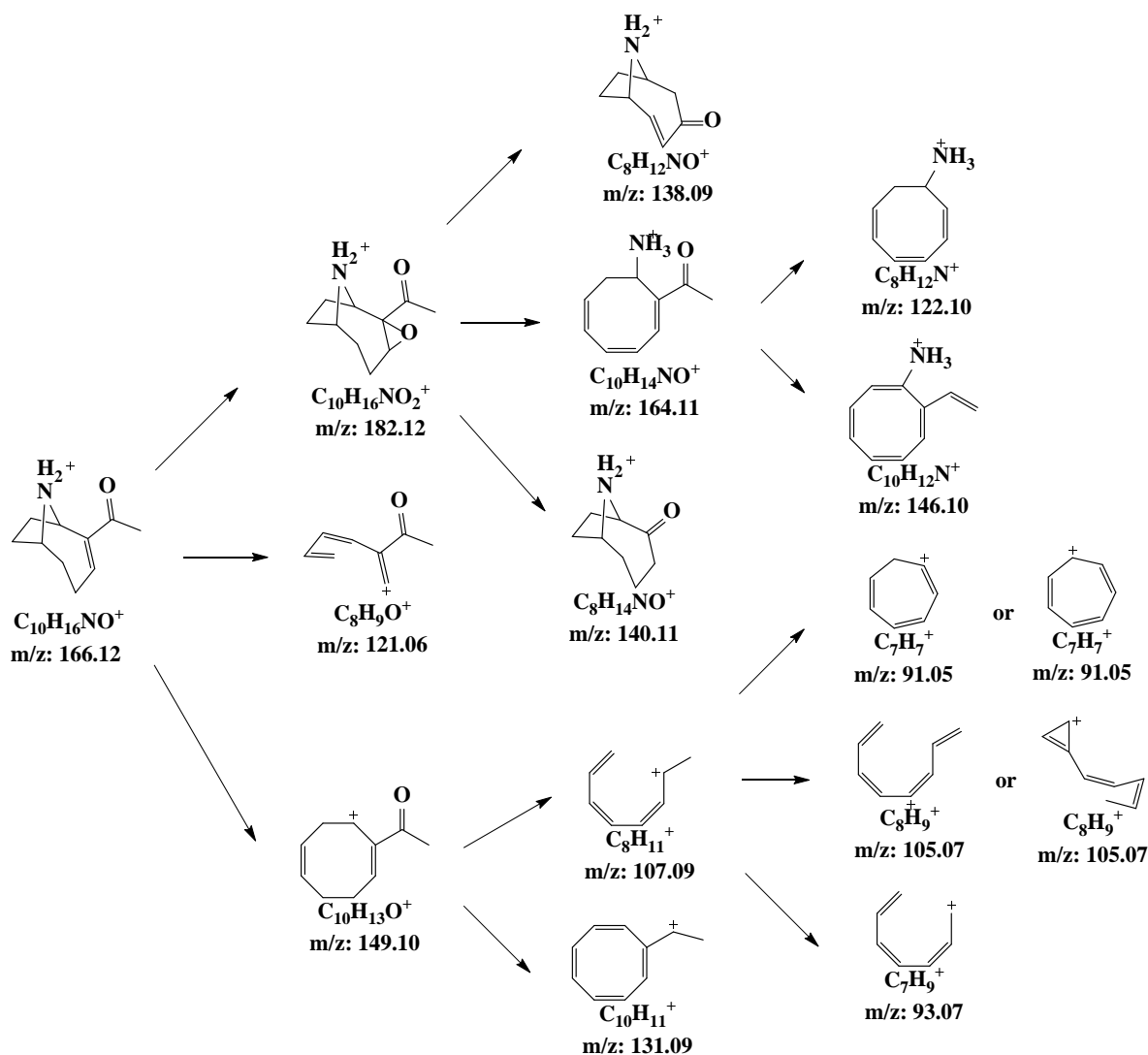
Scheme 2. 3: Proposed pathway for CYL oxidation by Fe^{III} -B*/ H_2O_2 . Ionic species were recovered from SPE eluate and observed in the MS^1 mass spectrum. Bracketed structures were not observed but were hypothesized to be present theoretically. Shaded composition were absent in MS^1 mass spectrum but seen in the tandem mass spectra as key ions, so were included in CID fragmentations analysis.

The unsaturated double bond on the uracil ring is a reactive site for mono-hydroxylation or dihydroxylation (Fotiou et al., 2015; He, de la Cruz, et al., 2014). Di-hydroxylated CYL m/z 450 has been proposed in the literature (L. Chen et al., 2015; Fotiou et al., 2015; He, Zhang, et al.,

2014; Song et al., 2012). Although the prevalent di-hydroxylated species (Song et al., 2012) was not seen, a series of ionic products including m/z 448 (a1) (L. Chen et al., 2015; Fotiou et al., 2015), 368 and 340 (He, de la Cruz, et al., 2014) were observed. Their transformations from m/z 450 have been described previously. Accordingly, di-hydroxylated CYL m/z 450 is most likely involved in the transformation pathways for CYL oxidation by $\text{Fe}^{\text{III}}\text{-B}^*/\text{H}_2\text{O}_2$. Products are generated from CYL essentially through hydroxylation, sulphate elimination, uracil ring modification and tricyclic ring destruction. Sulphate elimination has been reported in a photochemical transformation (Shah et al., 2013) and products from ring-opening of the tricyclic alkaloid described previously (Fotiou et al., 2015; He, Zhang, et al., 2014; Zhang et al., 2015). The MS^2 spectrum targeting m/z 416 (Appendix Figure A2.4b) indicates m/z 336 was likely transformed through sulphate elimination and hydroxylation from a possible product ion m/z 352, which did not produce a clear mass spectrum. Further dehydration of m/z 336 may explain the appearance of m/z 318 (c1). m/z 318 (c2) but a different structure can also be suggested, both product ions at m/z 318 being further degraded to m/z 194 and m/z 176 through hydrogen abstraction at C8 and uracil moiety removal. The MS^2 spectrum targeting m/z 448 (Appendix Figure A2.4c) indicates that uracil ring elimination with bond cleavage from product m/z 448 (a1) contributed to the formation of product m/z 274. Different formulations of products m/z 350 (b1), m/z 350 (b2) and m/z 350 (b3) are proposed via various transformation routes, including hydrogen abstraction at C8 from the hypothesized product m/z 352, one water molecule eliminated from product m/z 368 and sulphate removal from product m/z 448 (a1). Products m/z 420 and m/z 318 were observed in Appendix Figure A2.4d. A C5=C6 bond cleavage of m/z 448 (a2) produced m/z 420, which was then further transformed to product m/z 322 via fragmentation of C6-C7 (He, de la Cruz, et al., 2014).

The CID product ions of ANA interpreted from the MS^1 mass spectrum (Appendix Figure A2.5a), with assistance from Mass Frontier, are listed in Appendix Table A2.2. The proposed

CID fragmentation schema of ANA oxidized by $\text{Fe}^{\text{III}}\text{-B}^*/\text{H}_2\text{O}_2$ in Scheme 2.4 mainly consists of two routes: degradation from ANA epoxidation and degradation from ANA deamination. Previous studies (Draisci et al., 2001; James et al., 2005; James et al., 1998) have reported that ANA can convert to dihydro-ANA (m/z 168) and epoxy-ANA (m/z 182). While the peak representing dihydro-ANA m/z 168 was not observed in the mass spectra, epoxy-ANA m/z 182 was observed with significant intensity (Appendix Figure A2.5c). The fragment ion m/z 182 is therefore revealed as the preferred attack reaction of ANA mediated by $\text{Fe}^{\text{III}}\text{-B}^*/\text{H}_2\text{O}_2$ catalysis. The mass spectra indicate that one water molecule was removed initially from epoxy-ANA m/z 182 to form fragment m/z 164. Another water molecule was then removed from m/z 164 to form m/z 146. The fragment m/z 138 can be generated from epoxy-ANA m/z 182 by losing CH_3CHO . All the fragments generated from m/z 182, including m/z 164, 146, 140, 138 and 122, were identified as nitrogen-containing products by virtue of their even charge. Another fragment identified with high mass accuracy is m/z 149, the result of the parent ANA m/z 166 losing ammonia (Appendix Figure A2.5b). The MS^2 spectrum (Appendix Figure A2.5d) indicates a series of fragments (m/z 131, 107, 105, 93 and 91) yielded from m/z 149. This route has been detailed previously (Furey et al., 2003). Although m/z 149 and m/z 131 were described as product ions from precursor m/z 166, we suggest m/z 149 and its corresponding products are actually ANA oxidation products from the action of $\text{Fe}^{\text{III}}\text{-B}^*/\text{H}_2\text{O}_2$.



Scheme 2. 4: Proposed pathway for ANA oxidation by $\text{Fe}^{\text{III}}\text{-B}^*/\text{H}_2\text{O}_2$. Ionic species were recovered from SPE eluate and observed in the MS^1 mass spectrum.

The uracil moiety has been reported to be responsible for the toxicity of CYL (Banker et al., 2001). Consequently, destruction of the uracil ring by hydrogenation or hydroxylation to the double bond C5=C6, ring-opening, or bond cleavage should lead to a reduction in the toxicity of CYL. Given the majority of degradation products involve the modified uracil ring, $\text{Fe}^{\text{III}}\text{-B}^*/\text{H}_2\text{O}_2$ is expected to reduce CYL toxicity. Although the toxicity of product m/z 149 and its corresponding products is not clear, ANA toxicity is most likely reduced by $\text{Fe}^{\text{III}}\text{-B}^*/\text{H}_2\text{O}_2$ because the non-toxic epoxy-ANA (m/z 182) (James et al., 1998) and its corresponding products account for the major ANA reaction products.

2.4 Conclusions

Green chemistry $\text{Fe}^{\text{III}}\text{-B}^*$ coordinated with H_2O_2 was applied in cyanotoxin degradation at different pH values to determine pH-dependent efficiencies. Heterogeneous $\text{Fe}^{\text{III}}\text{-B}^*$ was developed by immobilising dissolved homogeneous $\text{Fe}^{\text{III}}\text{-B}^*$ onto a functionalised silica surface. The removal efficiency of heterogeneous $\text{Fe}^{\text{III}}\text{-B}^*/\text{H}_2\text{O}_2$ compared to homogeneous $\text{Fe}^{\text{III}}\text{-B}^*/\text{H}_2\text{O}_2$ highlights the potential of heterogeneous $\text{Fe}^{\text{III}}\text{-B}^*/\text{H}_2\text{O}_2$ as a bioremediation catalyst. CYL and ANA oxidative degradation products were elucidated using Q-Exactive tandem mass spectrometry and Mass Frontier. CYL product ions are thought to be generated by hydroxylation, sulphate group elimination and tricyclic guanidine moiety opening. The degradation products of ANA consisted of epoxidized products, deaminated products and linear products. Toxicity of CYL and ANA are expected to be reduced by $\text{Fe}^{\text{III}}\text{-B}^*/\text{H}_2\text{O}_2$ due to the uracil ring destruction of CYL and formation of non-toxic epoxidized ANA respectively. Our study has provided a better understanding of CYL and ANA oxidative degradation by $\text{Fe}^{\text{III}}\text{-B}^*/\text{H}_2\text{O}_2$, and underscores the potential of heterogeneous $\text{Fe}^{\text{III}}\text{-B}^*/\text{H}_2\text{O}_2$ for use in large scale water treatment.

Chapter 3: Oxidative removal of cylindrospermopsin and anatoxin-a by Fe^{III}-B*/H₂O₂ in the presence of natural organic matter

Manuscript to be submitted to Water Research journal

Chapter abstract

Natural organic matter (NOM) is known to negatively impact cyanotoxin degradation/removal by currently used technologies. Efficient oxidative degradation of cylindrospermopsin (CYL) and anatoxin-a (ANA) was obtained in Chapter 2 by the iron tetra-amido-macrocyclic ligand (Fe^{III}-B*)/H₂O₂, but the influence of NOM on the oxidative removal of CYL and ANA by Fe^{III}-B*/H₂O₂ is not clear. We explored the influence of NOM ranging from 0 to 30 ppm on the oxidative removal of CYL (0.24 μM) and ANA (7.1 μM) by Fe^{III}-B*/H₂O₂ (5 μM/ 5 mM) at pH 9.5 in a 2-hour reaction. Increasing NOM concentration from 0 ppm to 30 ppm improved CYL removal from 87 % to 100 % and ANA removal from 96 % to 100 % with higher rate constants. The decreased fluorescence intensity found by EEM showed that the humic and fulvic-like regions were oxidized by Fe^{III}-B*/H₂O₂. Further, the transformed chromophores identified in UV-vis indicated that the NOM oxidation was associated with aromatic compounds and carboxylate compounds. NOM surrogates and high resolution mass spectrometry were used to demonstrate that enzyme-catalysed oxidative coupling occurred between CYL and NOM components with aromatic and carboxylate moieties, and ANA and NOM constituents with aromatic rings. Radical-mediated cross-coupling pathways for NOM interaction with CYL and ANA were proposed based on Fe^{III}-B* mediated one-electron oxidation. It is suggested the toxicity of cyanotoxin cross-coupling with NOM will reduce through CYL toxic moiety inhibition and ANA conformational changes. This study has developed an understanding of the fate of CYL and ANA oxidation by Fe^{III}-B*/H₂O₂ when

NOM is present. The results indicate that cyanotoxin catalytic oxidative degradation and NOM radical-mediated cross-coupling can significantly enhance overall cyanotoxin removal.

3.1 Introduction

The occurrence of cyanobacterial blooms in water reservoirs has induced deterioration in water quality globally, with serious impacts on public health and ecosystems (de la Cruz et al., 2013; Hitzfeld et al., 2000; Mohamed, 2008; Hans W. Paerl et al., 2011; Smith, 2003; Walker, 2014). During cyanobacterial blooms, cyanotoxins and other cyanobacterial secondary metabolites are released into the surrounding water (W. W. Carmichael, 1992; Fristachi et al., 2008; Svrcek et al., 2004). Cylindrospermopsin (CYL, Figure 3.1a) and anatoxin-a (ANA, Figure 3.1b) are frequently studied cyanotoxin species (Catherine et al., 2013; de la Cruz et al., 2013; Osswald et al., 2007). CYL and ANA are fatal to animals and humans, with poisonings and death reported worldwide (Wayne W Carmichael et al., 2001; Faassen et al., 2012; Griffiths et al., 2003; Gugger et al., 2005; Wood et al., 2007). Because of their wide distribution and highly pernicious effects, CYL and ANA are categorized as hazardous impact contaminants and included on recent Contaminant Candidate Lists (CCL 3 & 4) (EPA, 2008; Hudnell, 2010).

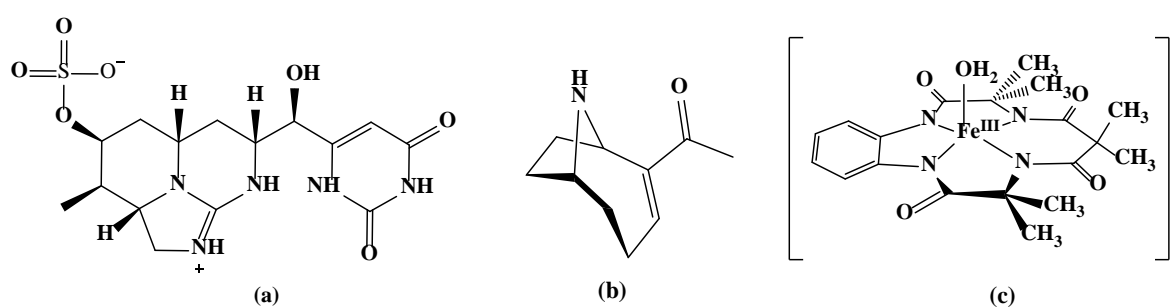


Figure 3. 1: The structure of (a) cylindrospermopsin, (b) anatoxin-a, (c) Fe^{III}-B* catalyst

An environmentally friendly catalyst system (Terrence J. Collins, 2002; Terrence J Collins, 2011), the iron (III) tetra-amido-macrocyclic ligand (Fe^{III}-TAML, designated as Fe^{III}-B* and shown in Figure 3.1c) (W. Chadwick Ellis et al., 2009) activators/H₂O₂, has attracted a high level of research focus due to its efficient oxidation of recalcitrant pollutants (Banerjee et al., 2006; Chahbane et al., 2007; Chanda, Khetan, et al., 2006; Gupta et al., 2002; Mitchell et al.,

2010; Mondal et al., 2006; Shappell et al., 2008). In our previous study on the catalytic oxidative degradation of cyanotoxin (Chapter 2), cyanotoxin oxidation was achieved by Fe^{III}-B*/H₂O₂ over a broad pH range, with 70 % ~ 89 % CYL (0.24 μM) and 67 % ~ 96 % ANA (7.1 μM) removed by Fe^{III}-B*/H₂O₂ (5 μM/ 5 mM) at pH values from 8.5 to 11.5. Further, the toxicity of cyanotoxin was expected to reduce by CYL uracil ring destruction and non-toxic epoxidized ANA formation. Consequently, Fe^{III}-B*/H₂O₂ is suggested as a promising oxidation system for cyanotoxin degradation.

NOM is ubiquitous in environmental systems. It is broadly categorised into hydrophilic NOM and hydrophobic NOM, and both types of NOM can be fractionalized into neutral, acidic and basic components (Matilainen et al., 2011; Nkambule et al., 2009). Hydrophobic acids account for the largest fraction. Hydrophobic acids are also described as humic substances and comprise humic acid, fulvic acid and humin (Matilainen et al., 2010; Schnitzer, 1978). NOM molecules contain multiple amines, carboxylic acids and phenols with varying structural functionalities (Świetlik et al., 2004).

NOM has been previously reported to reduce cyanotoxin removal through multiple mechanisms, including occupying the adsorption sites of activated carbon (Ho et al., 2011; Newcombe et al., 1997; Pelekani et al., 1999), generating membrane fouling (Her et al., 2008; Jarusutthirak et al., 2007; Teixeira et al., 2013), performing as a radical scavenger and UV-vis blocker (He, de la Cruz, et al., 2014; Zhang et al., 2014; C. Zhao et al., 2014), and competing for chlorine (P. Senogles et al., 2000). On the other hand, NOM has been shown to participate as a substrate in enzyme-mediated oxidative reactions, resulting in self-coupled products (Berry et al., 1985; Cozzolino et al., 2002; J. Lu et al., 2009; Piccolo et al., 2000; Weber et al., 2005). NOM is also widely assumed to act as an enzyme co-substrate leading to radical-mediated cross-coupling with micro-pollutants (Feng et al., 2013; J. Lu et al., 2009; Mao et al., 2010; Sun, Huang, et al., 2016; Sun, Luo, et al., 2016). Free NOM radicals containing aniline

and/or with phenolic functionalities are suggested to non-selectively couple with the targeted compound radicals to form cross-coupling species (Feng et al., 2013; J. Lu et al., 2009; Mao et al., 2010; Sun, Huang, et al., 2016), where the radicals are generated via one-electron oxidation mediated by an enzyme (Berry et al., 1985; Feng et al., 2013; Mao et al., 2010; Weber et al., 2005). One-electron oxidation of substrates and radical-mediated cross-coupling have also been reported for $\text{Fe}^{\text{III}}\text{-B}^*/\text{H}_2\text{O}_2$ (Ghosh et al., 2008; Onundi, 2015). However, information on NOM oxidation by $\text{Fe}^{\text{III}}\text{-B}^*/\text{H}_2\text{O}_2$ and the influence of NOM on the degradation of cyanotoxins mediated by $\text{Fe}^{\text{III}}\text{-B}^*/\text{H}_2\text{O}_2$ is limited. Further, due to the diverse functionalities and structural properties of NOM, the characteristics of NOM radicals involved in radical-radical covalent coupling reactions with cyanotoxins remain unknown. A comprehensive understanding of the influence of NOM on cyanotoxin removal by $\text{Fe}^{\text{III}}\text{-B}^*/\text{H}_2\text{O}_2$ is essential to confirm the potential of $\text{Fe}^{\text{III}}\text{-B}^*/\text{H}_2\text{O}_2$ for application in actual water treatment plants.

In this study, we investigate the influence of NOM on the catalytic oxidative degradation of cyanotoxin by $\text{Fe}^{\text{III}}\text{-B}^*/\text{H}_2\text{O}_2$, study NOM oxidation by $\text{Fe}^{\text{III}}\text{-B}^*/\text{H}_2\text{O}_2$, and explore the potential cross-coupling between cyanotoxin and NOM in $\text{Fe}^{\text{III}}\text{-B}^*$ -mediated oxidative reactions.

3.2 Methodology

3.2.1 Materials and chemical preparation

Cylindrospermopsin from Sapphire Bioscience Pty. Ltd. and (\pm)-anatoxin-a fumarate from Abcam Australia Pty. Ltd. were used as received. $\text{Fe}^{\text{III}}\text{-B}^*$ was supplied by the School of Chemical Sciences, University of Auckland. Natural organic matter (Suwannee River, Code 2R101N) was purchased from the International Humic Substances Society, USA. Catalase, guaiacol and glycolic acid were purchased from Sigma Aldrich, H_2O_2 (30 % v/v) from Thermo Fisher Scientific, and HPLC grade solvents from Merck Millipore. Water (18.2 M Ω .cm

resistivity) was purified by a Milli-Q filtration system (Millipore). Operations with cyanotoxins were undertaken in a chemical fume hood using proper hazard chemical handling measures.

3.2.2 Cyanotoxin removal in the presence of NOM or NOM surrogate

The initial reaction conditions were: 0.24 μM CYL or 7.1 μM ANA in the pH 9.5 0.01 M $\text{Na}_2\text{CO}_3/\text{NaHCO}_3$ buffer, 5 μM $\text{Fe}^{\text{III}}\text{-B}^*$, 5 mM H_2O_2 , and 0 ~ 30 ppm NOM or NOM surrogate (used at the same molar concentration as the designated cyanotoxin). Reactants were placed in a mechanical shaker at 600 rpm. Samples were taken at intervals and treated with catalase at 60 times the concentration capable of destroying 5 mM H_2O_2 in 1 min. Samples were filtered through 0.2 μm RC syringe filters (Phenomenex NZ Ltd) and then applied to LC-MS.

3.2.3 LC-MS quantification of cyanotoxin in reactions

Cyanotoxin was quantified by LC-MS (Shimadzu Series model LC-MS 2020, Japan) using a method modified from Faassen et al. (2012). Compounds were separated on a Waters Atlantis T3 column (3 μm , 3.0 mm \times 150 mm) at 0.2 mL/min flow rate and 30 $^\circ\text{C}$ column temperature. Mobile phase A (Milli-Q water/0.1 % formic acid) and mobile phase B (methanol/0.1 % formic acid) were used for both cyanotoxins. The gradient elution program for CYL was 1 min: 5 % B, 8 – 12 min: 50 % B, and 16 min: 0 % B, with a linear increase between the isocratic periods. The gradient elution program for ANA was 0.01 min: 20 % B, 3 – 5 min: 90 % B, and 10 min: 20 % B, with a linear increase between the isocratic periods. CYL 416 m/z and ANA 166 m/z were monitored in positive ion mode mass spectrometry. The concentration of cyanotoxin in samples was determined based on standard curves obtained by plotting pure cyanotoxin against the peak area of the LC-MS curves.

3.2.4 Measurement of NOM oxidation by $\text{Fe}^{\text{III}}\text{-B}^*/\text{H}_2\text{O}_2$

The fluorescence spectroscopic measurement of NOM samples was conducted using an aqualog-UV-C spectrofluorometer (Horiba Scientific, Japan) equipped with a xenon lamp as

the excitation source. Scans were normalized using a quinine sulphate blank and standard. The sample was placed in a square quartz cuvette cell (10 mm path length), which was rinsed with Milli-Q water prior to each analysis. Fluorescence spectra were collected in EEMs by scanning at excitation wavelengths from 240 nm to 600 nm in 3-nm steps, and emission wavelengths from 200 nm to 600 nm in 3-nm steps. An EEM of Milli-Q water was subtracted from each sample EEM to eliminate Raman scatter peaks. Using Aqualog Software, the fluorescence spectra of NOM sample were processed by the inner filter effect and Rayleigh mask. Three-dimensional contour plots were generated by plotting fluorescence intensity as a function of emission (X-axis) and excitation (Y-axis) wavelengths.

Ultraviolet-visible spectrophotometry (Shimadzu UV-vis 2700) was used to monitor the absorbance of NOM components before and after catalytic oxidation by $\text{Fe}^{\text{III}}\text{-B}^*/\text{H}_2\text{O}_2$. A reaction containing NOM, buffer, and $\text{Fe}^{\text{III}}\text{-B}^*$ was initiated by adding H_2O_2 . After 2 hrs reaction, the absorbance of the sample was recorded by transferring the sample to a quartz cell and monitoring by wavelength scanning from 190 to 600 nm.

3.2.5 Identification of cross-coupled products

3.2.5.1 Solid-phase extraction (SPE) procedure

The CYL-SPE using Hypersep Hypercab SPE cartridges (Thermo Fisher Scientific, NZ Ltd.) (Foss et al., 2013; Metcalf et al., 2002) was conducted as follows: 1) cartridges were conditioned with two column volumes of methanol and rinsed with two column volumes of water; 2) samples were loaded onto cartridges (1 – 2 mL/min); 3) cartridges were washed with one column volume of water and fully air-dried prior to elution; and 4) CYL was eluted using 5 % formic acid in methanol. The ANA-SPE using Strata-X-CW polymeric weak cation SPE cartridges (Phenomenex Australia Pty Ltd.) was conducted as follows: 1) cartridges were conditioned with one column volume of methanol and one column volume of water; 2) samples

(pH 6 ~ 7) were loaded onto cartridges; 3) cartridges were washed with one column volume of water and one column volume of methanol; and 4) samples were eluted using 5 % formic acid in methanol. For all SPE samples, the eluate was evaporated to dryness in a speed vacuum concentrator (Savant SPD131DDA, ThermoFisher) and reconstituted in methanol for analysis.

3.2.5.2 Samples of glycolic acid cross-coupling with CYL

The cross-coupled product of CYL and glycolic acid was identified using LC-MS/MS (Shimadzu Series model 8040, Japan) and a Gemini 3 μ C18 10A column (100 mm \times 2.0 mm, Phenomenex). The mobile phases A (water/0.1 % formic acid) and B (methanol/0.1 % formic acid) were applied under the gradient elution program 0.01 min: 10 % B, 3 – 6 min: 90 % B, 11 min: 50 % B, and 15 – 16min: 10 % B, with a linear increase between the isocratic periods. CYL m/z 416 was monitored by positive multiple reaction monitoring (MRM) and glycolic acid m/z 75 was monitored in negative ion mode (SIM).

3.2.5.3 Samples of guaiacol cross-coupling with CYL

The cross-coupled product of CYL and guaiacol was detected using LC-MS/MS (Shimadzu Series model 8040, Japan) and a Waters Atlantis T3 column (3 μ m, 3.0 mm \times 150 mm). The mobile phases A (water/0.1 % formic acid) and B (methanol/0.1 % formic acid) were applied under the following gradient elution program 0.01 min: 10 % B, 3 – 6 min: 90 % B, and 8 min: 10 % B, with a linear increase between the isocratic periods. CYL m/z 416 was monitored by positive multiple reaction monitoring (MRM).

3.2.5.4 Samples of guaiacol cross-coupling with ANA

The cross-coupled product of ANA and guaiacol identification was conducted using GC-MS (GCMS-QP2010S, Shimadzu). ANA derivatization with methyl chloroformate was conducted following a method modified from V. Rodríguez et al. (2006). The ANA sample was treated with methyl chloroformate (1.95 g/L), then ultrasonicated for 10 min and left overnight at room

temperature. The following day, solid-phase micro-extraction was performed by dipping a PDMS fibre (50/ 30 μm DVB-CAR-PDMS) into the sample for 20 min while it was being stirred with a magnetic bar. After the extraction, the PDMS fibre was inserted into the GC-MS injector port for 30 min desorption under a gradient temperature program 0 – 10 min: 50 to 150 $^{\circ}\text{C}$, and 10 – 20 min: 150 to 300 $^{\circ}\text{C}$.

3.2.6 CYL and ANA data regression

First-order rate constants for cyanotoxin removal by $\text{Fe}^{\text{III}}\text{-B}^*/\text{H}_2\text{O}_2$ in the presence of NOM were modelled using the following first-order decay relationship (Jho et al., 2012):

$$C = (1 - C_{res})e^{-kt} + C_{res} \quad \text{Eq.3.1}$$

where C represents C_t/C_0 that CYL or ANA concentration at time t (min) normalized to its initial concentration (C_0), C_{res} represents the residual CYL or ANA concentration normalized with respect to its initial concentration (C_0), and k indicates the apparent first-order rate constant (min^{-1}).

3.3 Results and discussion

3.3.1 Cyanotoxin removal in the presence of NOM

Figure 3.2 and Figure 3.3 indicate cyanotoxin removal by NOM under different parameter conditions. For both cyanotoxins, a small percentage of cyanotoxin removal was detected upon the addition of NOM without initiating catalysis. This observation was most likely the result of cyanotoxin-NOM complexation caused by non-covalent interactions, such as electrostatic interactions, hydrophobic interactions, hydrogen bonding, π - π interactions and van der Waals force (Kubicki et al., 1999; Moreno-Castilla, 2004). Further, the observation signified the possibility of NOM complexing with cyanotoxin under ambient conditions in natural waters. The cyanotoxin quantification showed a slight fluctuation, which may also be caused by weak

intermolecular non-covalent interactions. Compared to the slight physical adsorption by NOM, significant cyanotoxin removal was obtained when the catalytic oxidation was initiated with H_2O_2 . Figure 3.2 shows that CYL removal efficiency was enhanced by 0.5 ppm and 3.5 ppm NOM by the 5th min. At the end of the reaction, CYL removal improved from 87 % with 0 ppm NOM to 91 % for 0.5 ppm NOM and 92 % for 3.5 ppm NOM. As the NOM dose was further increased to 10 ppm and then 30 ppm, CYL was totally removed in 2 hrs by 10 ppm NOM, and in 1 hr by 30 ppm. Figure 3.3 shows nearly 100 % ANA removal by 0.6 ppm NOM in 2 hrs. Removal efficiency was further increased by 10 ppm and 30 ppm NOM that 100 % ANA removal was achieved in 1 hr at an increased rate.

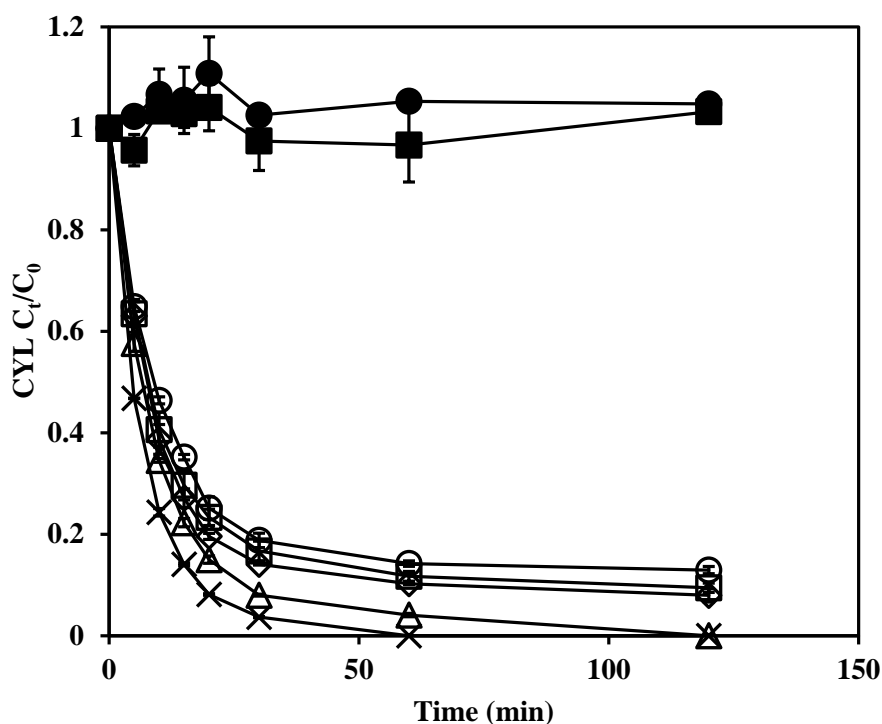


Figure 3. 2: CYL removal by $Fe^{III}\text{-B}^*/H_2O_2$ with varying NOM. CYL ($0.24 \mu\text{M}$) removal by $Fe^{III}\text{-B}^*/H_2O_2$ ($5 \mu\text{M}/5 \text{mM}$) with 0 ppm (\circ), 0.5 ppm (\square), 3.5 ppm (\diamond), 10 ppm (Δ) and 30 ppm (\times) NOM at pH 9.5 (0.01 M). \bullet represents sample of CYL and NOM (3.5 ppm). \blacksquare represents sample of CYL, NOM (3.5 ppm) and $Fe^{III}\text{-B}^*$ ($5 \mu\text{M}$) (mean \pm standard deviation of three independent runs).

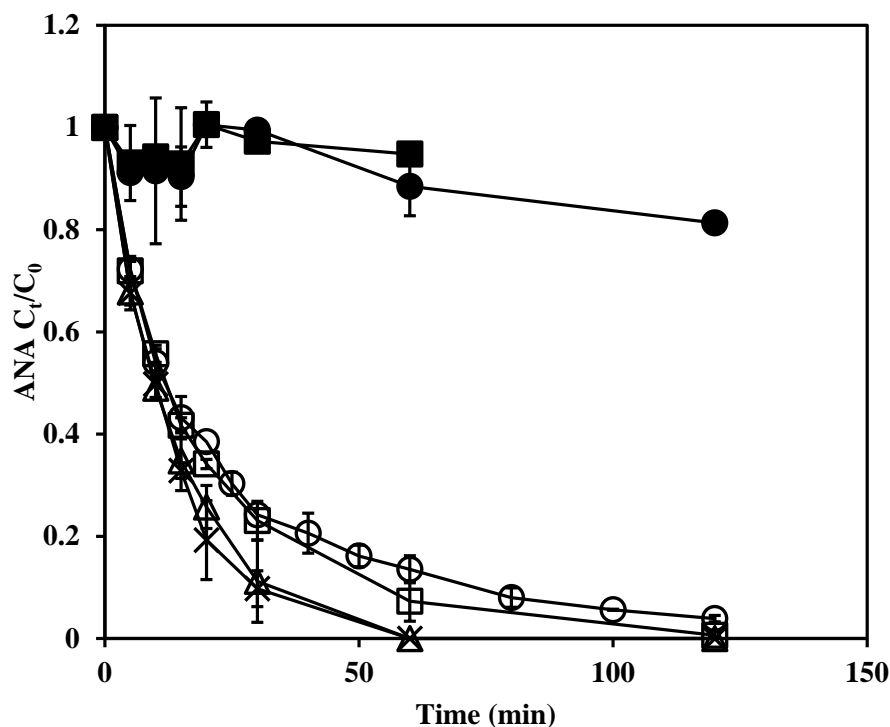


Figure 3. 3: ANA removal by Fe^{III}-B*/H₂O₂ with varying NOM. ANA (7.1 μM) removal by Fe^{III}-B*/H₂O₂ (5 μM/ 5 mM) with 0 ppm (○), 0.6 ppm (□), 10 ppm (△) and 30 ppm (×) ppm NOM at pH 9.5 (0.01 M). ● represents sample of ANA and NOM (30 ppm). ■ represents sample of ANA, NOM (30 ppm) and Fe^{III}-B* (5 μM) (mean ± standard deviation of three independent runs).

In our previous chapter, the kinetics of cyanotoxin decay by Fe^{III}-B*/H₂O₂ at pH ranging from 8.5 to 11.5 were described by the model in Eq.2.1. The data of cyanotoxin removal with NOM fitted well to the model in Eq.3.1, such that the corresponding regression results were observed with high R² (Appendix Figure A3.1). The increase in rate constants from low NOM to high NOM levels shown in Figure 3.4 are consistent with cyanotoxin removal efficiency, such that the highest concentration of NOM (30 ppm) contributed to complete cyanotoxin removal at the fastest rate. NOM is suggested to be responsible for the increased cyanotoxin removals and the increased rate constants.

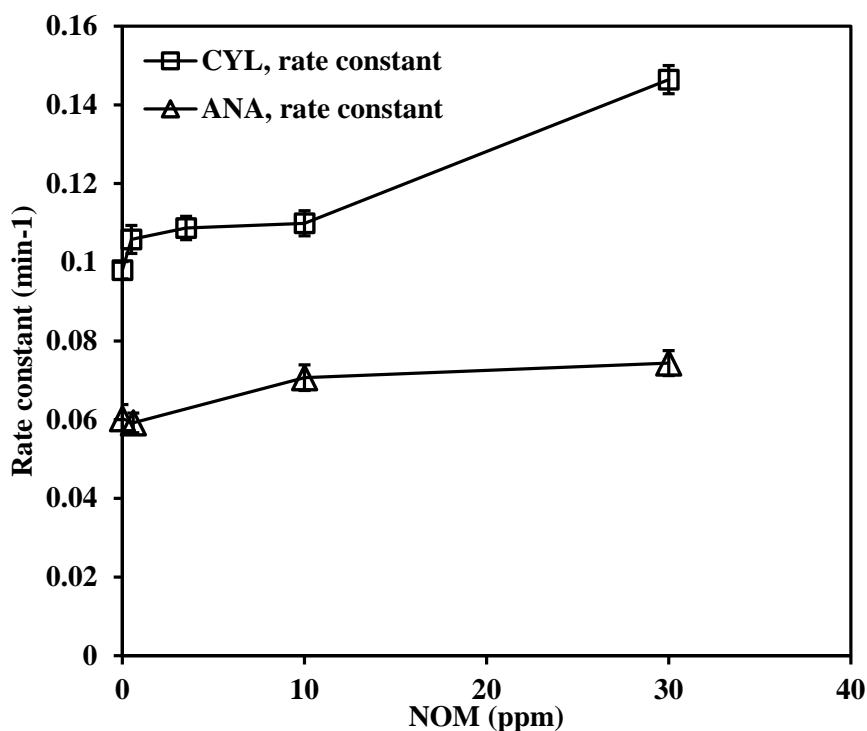
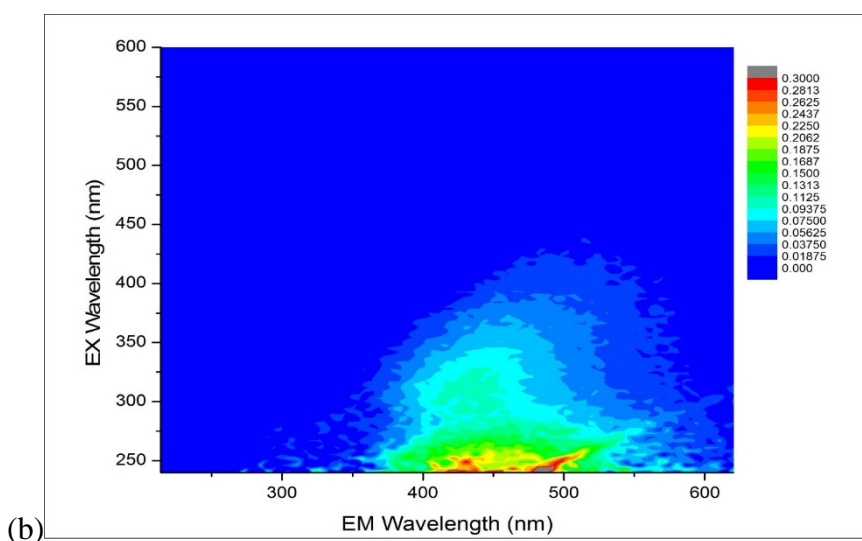
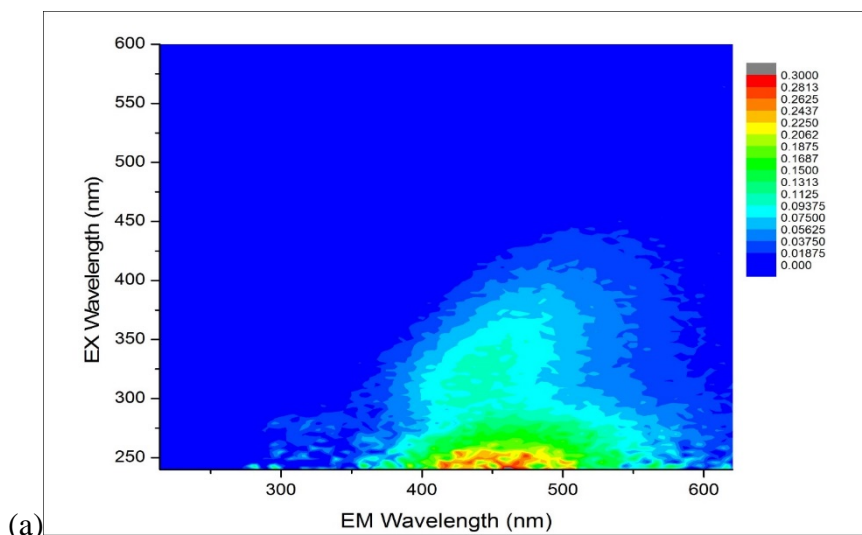


Figure 3. 4: The rate constants of CYL and ANA degradation by Fe^{III}-B*/H₂O₂ in the presence of NOM

Based on the oxidation of humic substance by Fe^{III}-TAML described previously (Beach et al., 2009), the influence of the oxidized NOM on cyanotoxin removal was considered. However, the contribution from oxidized NOM was negligible due to its insignificant effect on cyanotoxin removal (Appendix Figure A3.2). Accordingly, the intermolecular interactions between NOM components and cyanotoxin are proposed as one possibility for the increased cyanotoxin removal. It has been demonstrated previously that NOM can serve as substrate for the enzyme and cross-couple with target compounds (Feng et al., 2013; J. Lu et al., 2009; Mao et al., 2010; Sun, Huang, et al., 2016), so the interaction between NOM and cyanotoxin is further confirmed as cross-coupling of NOM radicals with cyanotoxin radicals. To characterize the NOM constituents participating in the oxidative cross-coupling with cyanotoxin, NOM oxidized by Fe^{III}-B*/H₂O₂ was monitored in the absence of cyanotoxin.

3.3.2 Fe^{III}-B*/H₂O₂ catalysed oxidation of NOM

Figure 3.5a-d are the EEM fluorescence spectra of 3.5 ppm and 30 ppm NOM treated by Fe^{III}-B*/H₂O₂. The enhanced intensities of the fluorophore signatures for 30 ppm NOM (Figure 3.5c) compared to 3.5 ppm NOM (Figure 3.5a) indicate the presence of rich humic acid and fulvic acid fractions in NOM (Matilainen et al., 2011). The transformed fluorophore signatures of both fractions by H₂O₂ (Figure 3.5b and Figure 3.5d) imply that the components of NOM made up of humic acid and fulvic acid fractions can be mediated by Fe^{III}-B*/H₂O₂. Further, the significantly changed fluorophore signatures of humic-like matter show a greater potential to be oxidized than fulvic-like matter.



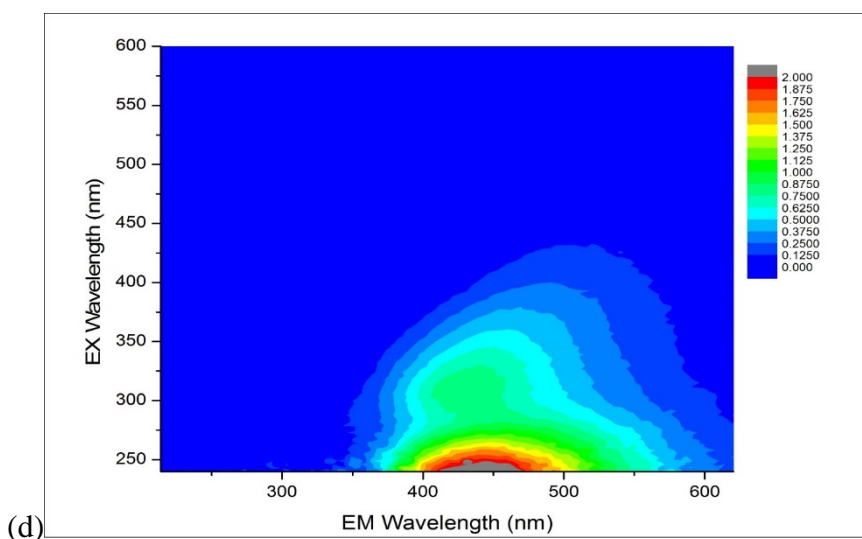
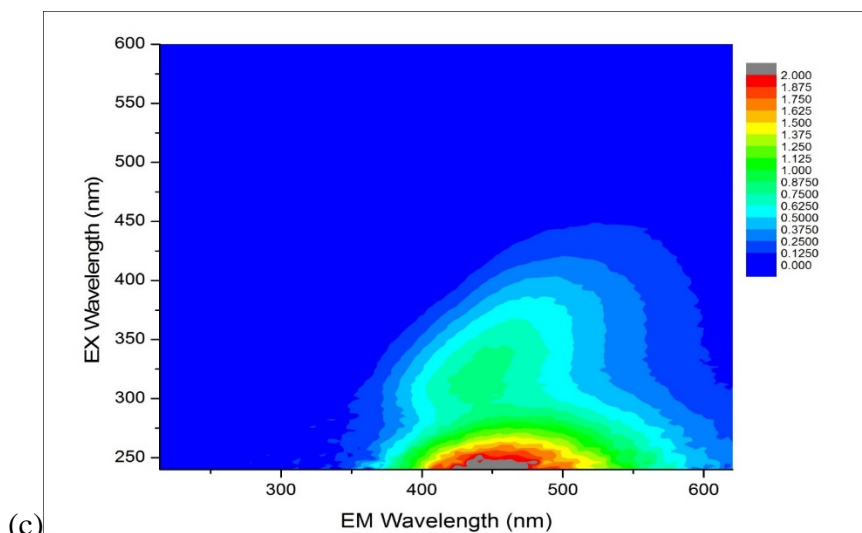


Figure 3. 5: Fluorophore signatures of NOM oxidized by $\text{Fe}^{\text{III}}\text{-B}^*/\text{H}_2\text{O}_2$. (a) NOM (3.5 ppm) with $\text{Fe}^{\text{III}}\text{-B}^*$ (5 μM) at pH 9.5 (0.01 M); (b) NOM (3.5 ppm) oxidized by $\text{Fe}^{\text{III}}\text{-B}^*/\text{H}_2\text{O}_2$ (5 $\mu\text{M}/$ 5 mM) at pH 9.5 (0.01 M); (c) NOM (30 ppm) with $\text{Fe}^{\text{III}}\text{-B}^*$ (5 μM) at pH 9.5 (0.01 M); (d) NOM (30 ppm) oxidized by $\text{Fe}^{\text{III}}\text{-B}^*/\text{H}_2\text{O}_2$ (5 $\mu\text{M}/$ 5 mM) at pH 9.5 (0.01 M). Ex 270 – 280/Em 310 – 320 for tyrosine-like and protein-like materials, Ex 270 – 285/Em 340 – 360 for tryptophan-like and protein-like matter, Ex 320 – 350/Em 400 – 450 for fulvic-like matter, Ex 310 – 320/Em 380 – 420 and Ex 330 – 390/Em 420 – 500 for humic-like matter (Matilainen et al., 2011).

Figure 3.6 illustrates the changes in absorbance spectra of NOM samples treated by $\text{Fe}^{\text{III}}\text{-B}^*/\text{H}_2\text{O}_2$. The intensity of NOM absorbance was increased with NOM increasing from 0.6 ppm to 30 ppm. With catalysis initiated by H_2O_2 , the absorbance was observed to decrease at wavelengths from 220 to 500 nm. Different wavelength absorbance of NOM is associated with different chromophores, so the changed absorbance correlates with changes to structural characteristics of NOM components (Matilainen et al., 2011), such as the transformation of aromaticity (S. Liu et al., 2010). Specifically, spectral changes at 220 nm have been associated with changes to carboxylic and aromatic fractions, absorbance changes around 254 nm as well as 320 nm are considered to be changes to aromatic components, and absorbance of NOM at 472 nm is associated with long-range resonance conjugation of electrons (Korshin et al., 2009; Onundi, 2015). Further, NOM with aromatic rings is generally thought to have high reactivity in peroxidase catalyzed reactions (Cozzolino et al., 2002; Weber et al., 2005).

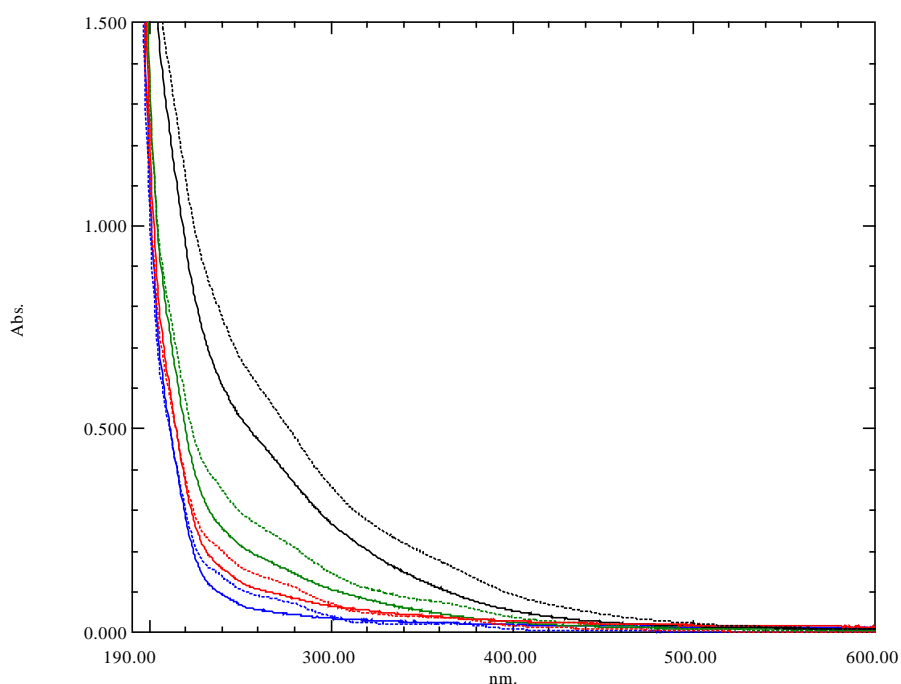


Figure 3. 6: UV absorbance of NOM reacted with $\text{Fe}^{\text{III}}\text{-B}^*/\text{H}_2\text{O}_2$. NOM (0.6, 3.5, 10 and 30 ppm) reacted with $\text{Fe}^{\text{III}}\text{-B}^*$ (5 μM) (dashed line) or with $\text{Fe}^{\text{III}}\text{-B}^*/\text{H}_2\text{O}_2$ (5 μM / 5 mM) (solid line) at pH 9.5 (0.01 M). NOM was measured after 2 hrs reaction as initiated by H_2O_2 .

The results for EEM fluorophore signatures and UV/Vis absorbance by oxidation showed that NOM components with aromatic and carboxylate groups from humic-like and fulvic-like fractions were oxidized by $\text{Fe}^{\text{III}}\text{-B}^*/\text{H}_2\text{O}_2$, implying their potential to cross-couple with cyanotoxins. This finding was supported by a study on enzyme-catalysed oxidative coupling of humic substances (Piccolo et al., 2000), which illustrated that phenolic and benzene carboxylic acids may participate in the oxidative coupling reactions. We conducted further experiments to characterize the cross-coupling of cyanotoxins using NOM surrogates. Reviews of possible NOM surrogates (Bialk et al., 2005; Campinas et al., 2006; Devitt et al., 1998; Zularisam et al., 2011) suggest guaiacol (Figure 3.7a) as a representative with a phenolic moiety (Bialk et al., 2005; J. Lu et al., 2009) for humic acid, and glycolic acid (Figure 3.7b) as a surrogate which mimics the carboxylate moiety of fulvic acid.

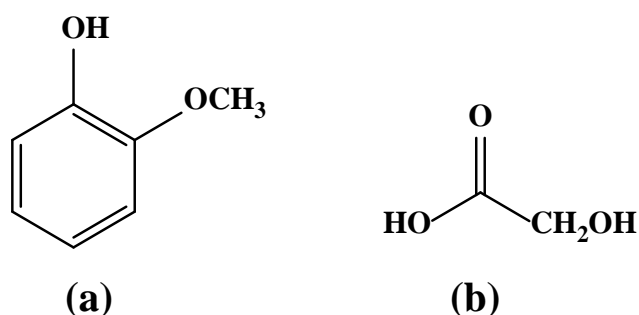


Figure 3. 7: The structure of (a) guaiacol and (b) glycolic acid

3.3.3 Cyanotoxin removal in the presence of NOM surrogates

NOM surrogates showed an insignificant effect on CYL removal in the absence of $\text{Fe}^{\text{III}}\text{-B}^*/\text{H}_2\text{O}_2$ (Figure 3.8). The 87 % CYL removal by 0 ppm NOM and 89 % CYL removal by 0.05 ppm NOM were consistent with our previous finding that the addition of NOM improved cyanotoxin removal rate when mediated by $\text{Fe}^{\text{III}}\text{-B}^*/\text{H}_2\text{O}_2$. Addition of guaiacol and glycolic acid both resulted in 100 % CYL removal over 2 hrs of reaction, with significant removal seen by the 5th min. The complete CYL removal by guaiacol and glycolic acid was likely caused by

NOM surrogate radical-mediated cross-coupling. Based on the functional groups of surrogates, NOM radicals with aromatic ring and carboxylate moiety are suggested as facilitating cross-coupling with CYL molecules in the catalytic oxidation by $\text{Fe}^{\text{III}}\text{-B}^*/\text{H}_2\text{O}_2$.

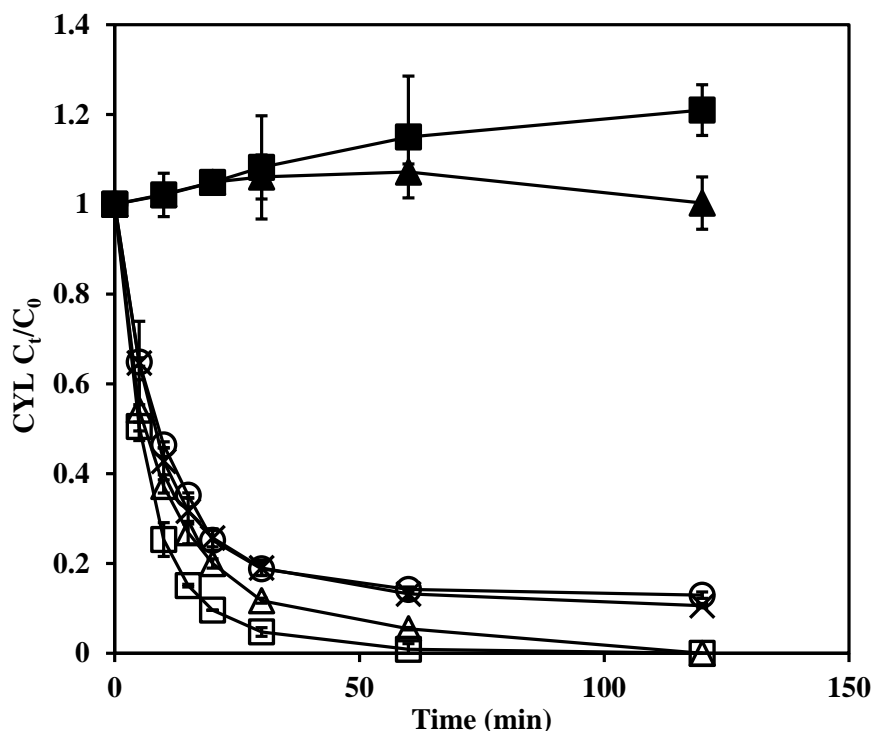


Figure 3. 8: CYL removal by $\text{Fe}^{\text{III}}\text{-B}^*/\text{H}_2\text{O}_2$ in the presence of NOM surrogates. CYL ($0.24 \mu\text{M}$) removal alone (\circ), CYL ($0.24 \mu\text{M}$) removal with NOM (0.05 ppm) (\times), with guaiacol ($0.24 \mu\text{M}$) (Δ), with glycolic acid ($0.24 \mu\text{M}$) (\square) by $\text{Fe}^{\text{III}}\text{-B}^*/\text{H}_2\text{O}_2$ ($5 \mu\text{M}/5 \text{ mM}$) at pH 9.5 (0.01 M). \blacktriangle represents sample of CYL and guaiacol. \blacksquare represents sample of CYL and glycolic acid (mean \pm standard deviation of three independent runs).

Figure 3.9 indicates increased ANA removal by NOM and guaiacol, and decreased removal by glycolic acid. There was 100 % ANA removal by 0.6 ppm NOM and guaiacol, and 85 % ANA removal by glycolic acid. As previously mentioned, guaiacol and glycolic acid radicals can favour the cross-coupling with CYL, however a similar mechanism for glycolic acid did not occur in ANA. Glycolic acid radicals would not be able to obtain electrons from ANA molecules, likely due to the relatively low level of activity of ANA towards glycolic acid radicals. Instead, glycolic acid may compete with ANA for $\text{Fe}^{\text{III}}\text{-B}^*$ activators. In contrast to

the amount of Fe^{III}-B* available in the CYL reaction, where the molar ratio was 21 (Fe^{III}-B*): 21000 (H₂O₂): 1 (CYL): 1 (glycolic acid), less Fe^{III}-B* was available for ANA oxidation when glycolic acid was consumed when the molar ratio was 0.7 (Fe^{III}-B*): 700 (H₂O₂): 1 (ANA): 1 (glycolic acid). As a result, guaiacol can contribute to ANA removal by cross-coupling with ANA when mediated by Fe^{III}-B*/H₂O₂, but glycolic acid was more likely to inhibit ANA removal by competing for oxidized Fe^{III}-B*.

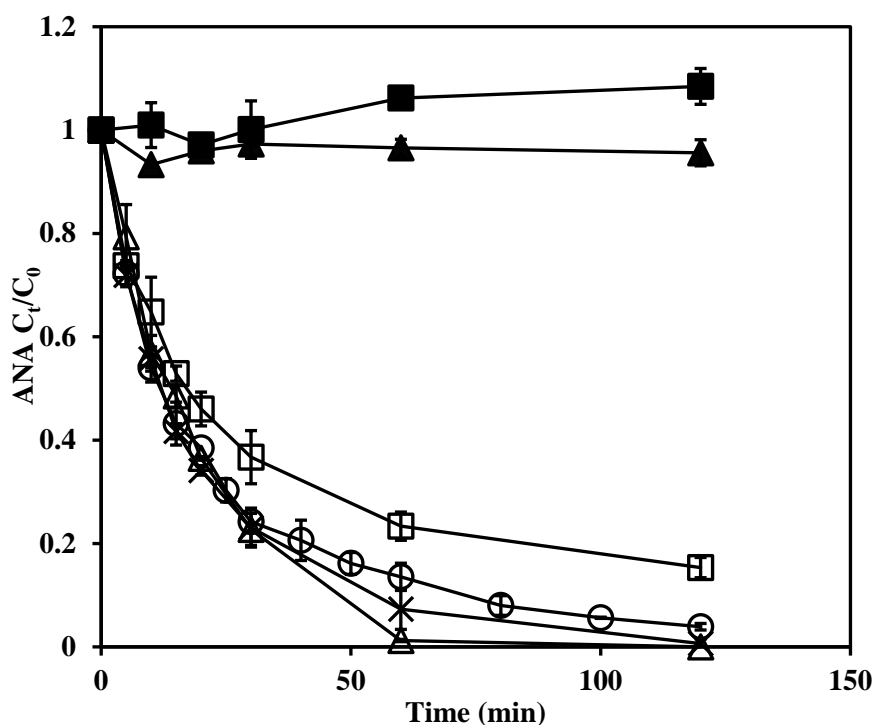


Figure 3. 9: ANA removal by Fe^{III}-B*/H₂O₂ in the presence of NOM surrogates. ANA (7.1 μM) removal alone (○), ANA (7.1 μM) removal with NOM (0.6 ppm) (×), with guaiacol (7.1 μM) (△), with glycolic acid (7.1 μM) (□) by Fe^{III}-B*/H₂O₂ (5 μM/ 5 mM) at pH 9.5 (0.01 M). ▲ represents sample of ANA and guaiacol. ■ represents sample of ANA and glycolic acid (mean ± standard deviation of three independent runs).

3.3.4 NOM surrogate radical-mediated cross-coupling with cyanotoxin

Samples of CYL and glycolic acid were analysed using negative ESI-MS, due to the acid deprotonation. The MS spectra in Figure 3.10 show the appearance of a product ion *m/z* 503, which was observed clearly in the spectrum for CYL and glycolic acid (Figure 3.10b), but was

absent in the spectrum of glycolic acid only (Figure 3.10a). Accordingly, the product ion m/z 503 likely formed from CYL cross-coupling with glycolic acid. Glycolic acid can transform to carboxylic acid by hydrolysis under alkaline conditions (Gao et al., 1998), which then further generates carboxylate ions due to deprotonation. The unsaturated double bond on the uracil ring of CYL acts as a reactive site (Fotiou et al., 2015; He, de la Cruz, et al., 2014), and the secondary C5 has a higher affinity to hydroxyl radical addition than the tertiary carbocation at C6 (L. Chen et al., 2015; Fotiou et al., 2015). Consequently, the carboxylate ions joining to the secondary C5 of the uracil group of CYL would result in the formation of the cross-coupled product (MW = 502), which would then be transformed into product ion m/z 503 by hydrogenation. Despite the proposed product having a molecular weight of 502, we would be unlikely to see it in the mass spectrum due to its rapid transformation. Figure 3.10c illustrates the proposed cross-coupling pathway of CYL and glycolic acid.

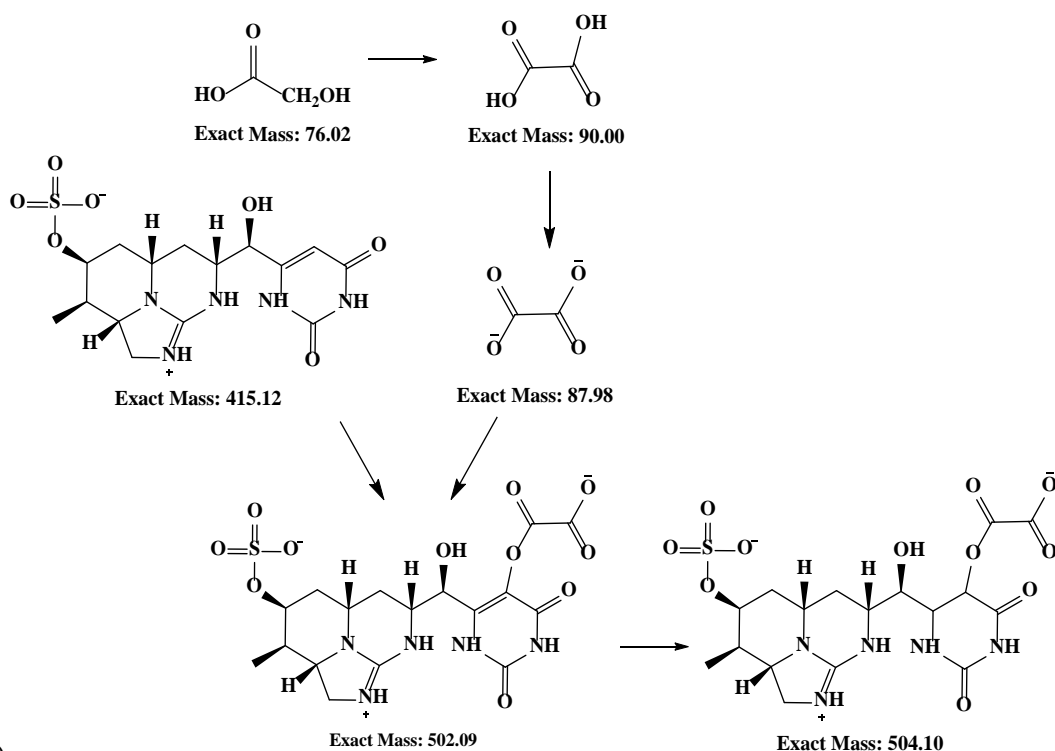
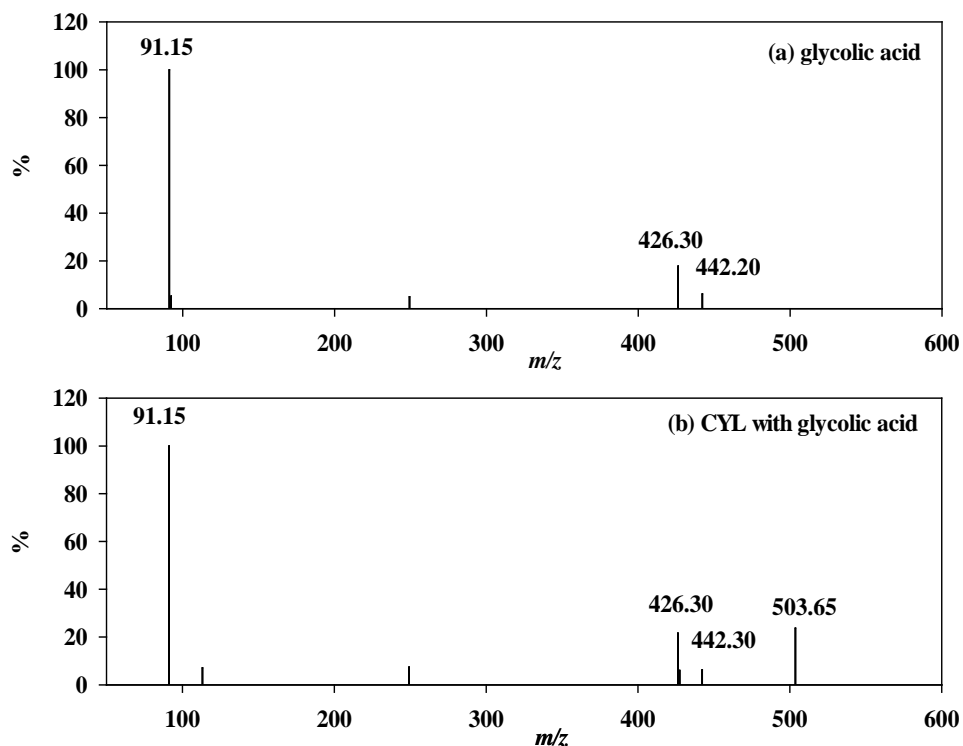


Figure 3. 10: High resolution ESI (-)-MS spectra from LC-Quadrupole-MS/MS for the cross-coupled product of CYL and glycolic acid. (a) Glycolic acid as control and (b) CYL treated with glycolic acid as a NOM surrogate (SPE extract after 2 hrs reaction of compounds by Fe^{III}-B*/H₂O₂ (5 μM/ 5 mM) at pH 9.5); (c) proposed reaction pathway of CYL cross-coupling with glycolic acid.

When we characterized guaiacol by chromatographic methods, guaiacol standard (0.088 ppm) produced a clear signal in the gas chromatographic profile (Appendix Figure A3.3), while guaiacol standard (1.129×10^3 ppm) indicated low signal intensities in the positive mode liquid chromatographic profile (Appendix Figure A3.4). As well as targeting the guaiacol parent ion at m/z 147, $[M+Na]^+$, two ions at m/z 146 and 145 were observed with significant intensity (Appendix Figure A3.4). These ions formed by guaiacol ionization would likely reduce the intensity level of self-coupled products and cross-coupled products when identifying them in the LC-MS mass spectra. Further, it has been reported in the literature that the coupled products by NOM can be significantly retained by 0.45 μm pore size membrane (Mao et al., 2010; Sun, Huang, et al., 2016; Weber et al., 2005), implying that syringe filters likely bind these products. This level of product retention can also be achieved by exclusion or adsorption during the SPE procedure. Guaiacol ionization as well as the exclusion of coupled products resulted in a cumulating reduction in the intensity of coupled products in the mass spectra. Next we explore the potential cross-coupled products of guaiacol with CYL using LC-MS/MS. To optimize the intensity of guaiacol, the cross-coupled products of guaiacol with ANA were explored using GC-MS. In addition, we speculate on one possible pathway by which cyanotoxin cross-couples with guaiacol.

Samples of CYL and guaiacol were analysed using positive ESI-MS. MS spectra are presented in Figure 3.11. The product ions including m/z 245, 367 and 611 were seen when guaiacol was mediated by $\text{Fe}^{\text{III}}\text{-B}^*/\text{H}_2\text{O}_2$ (Figure 3.11a). These product ions can be formed by guaiacol self-coupling with its multiple units (J. Lu et al., 2009). A product ion m/z 660 was present in the spectrum of CYL and guaiacol (Figure 3.11b), but absent in the spectrum of guaiacol alone (Figure 3.11a). Self-coupled guaiacol has been reported to subsequently undergo cross-coupling reactions with the substrate (Simmons et al., 1989; Thorn et al., 1996). Hence, the product ion m/z 660 likely corresponds to a product from CYL cross-coupling with the self-

coupled guaiacol. The cross-coupling most likely occurred as a result of self-coupled guaiacol attacking at the secondary C5 of uracil ring of CYL (Figure 3.11c).

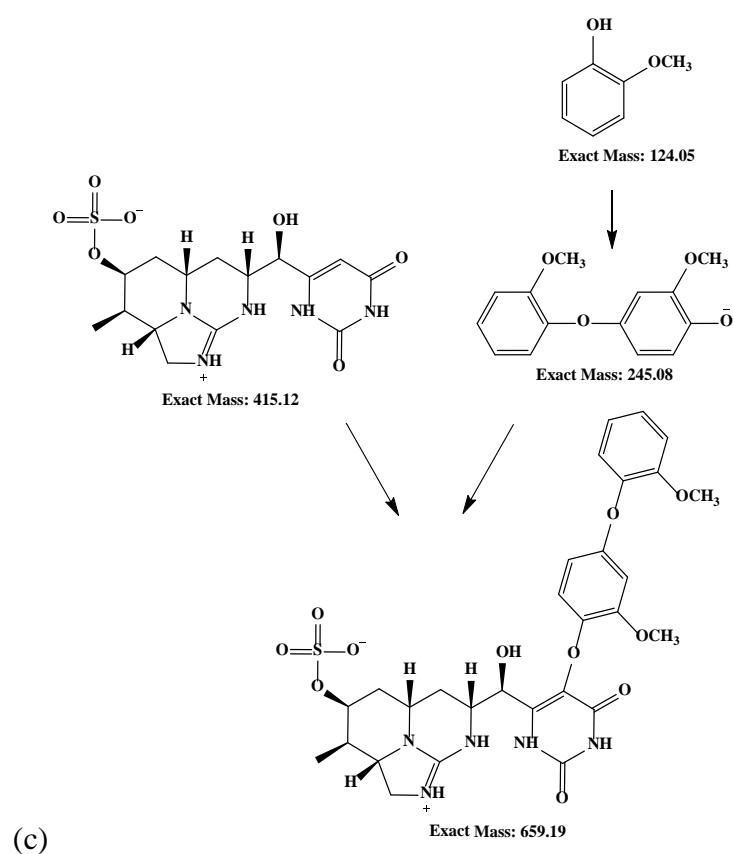
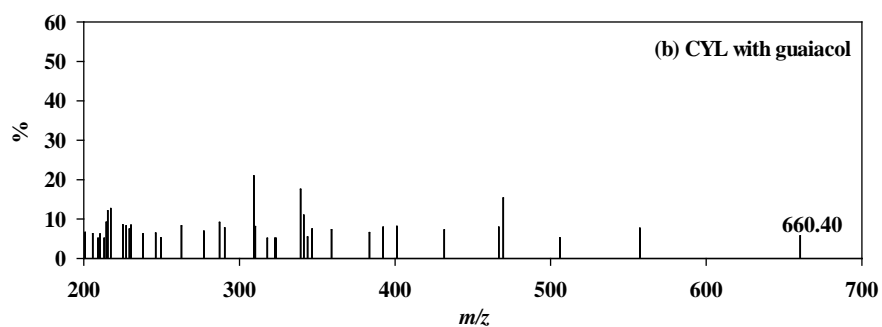
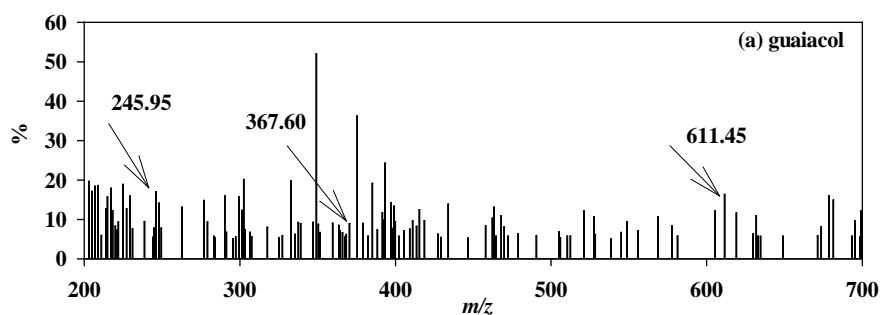


Figure 3. 11: High resolution ESI (+)-MS spectra from LC-Quadrupole-MS/MS for the cross-coupled product of CYL and guaiacol. (a) Guaiacol as control and (b) CYL treated with guaiacol as a NOM surrogate (SPE extract after 2 hrs reaction of compounds by Fe^{III}-B*/H₂O₂ (5 μM/ 5 mM) at pH 9.5); (c) proposed reaction pathway of CYL cross-coupling with guaiacol.

In the GC-MS spectrum of guaiacol mediated by Fe^{III}-B*/H₂O₂ (Figure 3.12a), the product ion *m/z* 124 was identified as guaiacol (Appendix Figure A3.3) and the product ion *m/z* 244 suggested as a guaiacol self-coupled product (J. Lu et al., 2009). The derivative ANA with *m/z* 223 was observed in the spectrum of the system with ANA (Figure 3.12b), and its corresponding derivatization pathway was proposed according to a method described in an earlier study (V. Rodríguez et al., 2006). Because it only appeared in Figure 3.12b, the product at mass 315 is suggested as the cross-coupled product of ANA and guaiacol. Based on the reported oxidation products dihydro-ANA (*m/z* 168) and epoxy-ANA (*m/z* 182) (Draisici et al., 2001; James et al., 2005; James et al., 1998), the double bond on the ring of ANA is assumed to be the primary site for oxidation. Accordingly, an initial cross-coupled product with molecular weight at 287 would be preferentially formed by a guaiacol radical attacking at the double bond. The subsequent derivatization of this cross-coupled product would result in a product with mass of *m/z* 345, which then transforms to the product with mass 315 by hydrolysis of the ester group. Figure 3.12c summarises the proposed derivatization of ANA and cross-coupling of ANA with guaiacol.

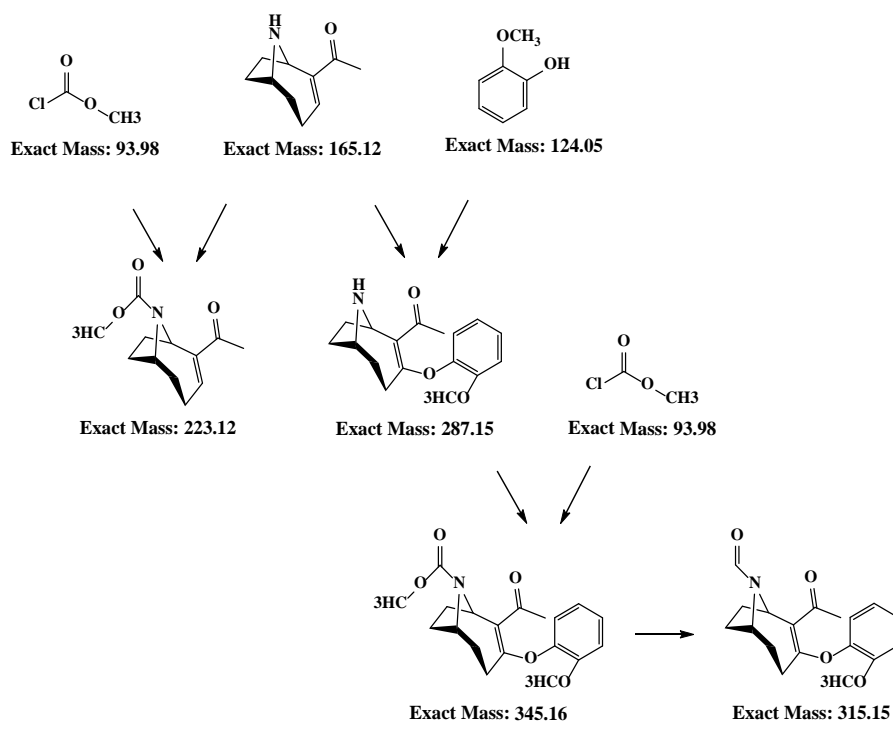
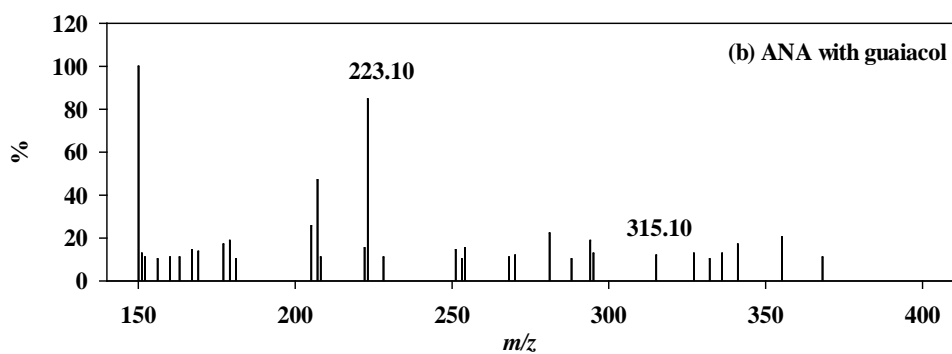
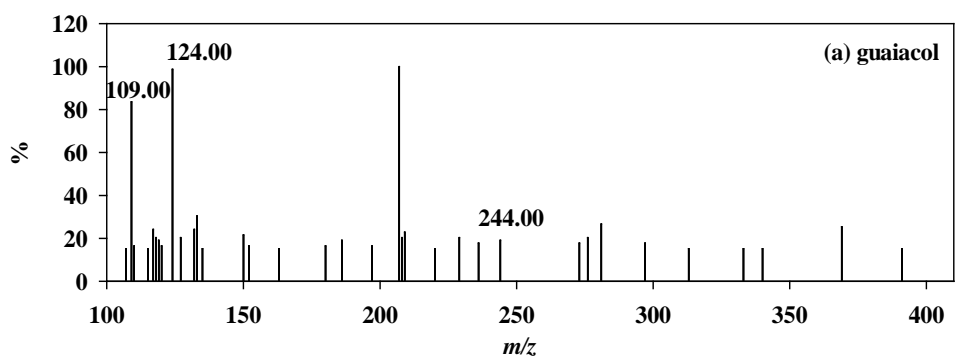


Figure 3. 12: GC-MS mass spectra for the cross-coupled product of ANA and guaiacol. (a) Guaiacol as control and (b) ANA treated with guaiacol as a NOM surrogate (SPE extract after 2 hrs reaction of compounds by $\text{Fe}^{\text{III}}\text{-B}^*/\text{H}_2\text{O}_2$ (5 μM / 5 mM) at pH 9.5); (c) proposed reaction pathway of ANA derivatization and ANA cross-coupling with guaiacol.

NOM components with phenolic functional groups are proposed as cross-coupling with CYL and ANA, leading to increased removal rates of the substrate. NOM components with carboxylate functionality can participate in cross-coupling with CYL. It should be noted that cross-coupled products proposed in the pathways are one of the possible structural isomers involving C-O-C bonding, and C-O-C formation may occur at other carbon atoms of the substrate and surrogates. Furthermore, it is possible to form C-N-C and/or C-C coupling (Kim et al., 1997; Sun, Huang, et al., 2016; Weber et al., 2005). The pathways described in Figure 3.10c, Figure 3.11c, and Figure 3.12c are shown for one possible configuration.

3.3.5 The effect of NOM on cyanotoxin degradation products

The uracil moiety is required for the toxicity of CYL, and compounds containing C5 and C6 substitution result in lower or non-toxic effects (Banker et al., 2001). With enzyme catalysis, CYL complexation with NOM may lower its toxicity when radical-mediated covalent interactions occur at the uracil ring. Enzyme-catalysed cross-coupling between CYL and NOM is likely to reduce the toxicity of CYL, due to C5 and C6 substitution (Banker et al., 2001), or conformational change of the uracil moiety by radical attack (Mailman, 2008). We previously identified a series of CYL products formed in the catalytic oxidative degradation mediated by $\text{Fe}^{\text{III}}\text{-B}^*/\text{H}_2\text{O}_2$ (Appendix Scheme A3.1). In the previous study (Chapter 2), degradation products were generally transformed from CYL via hydroxylation, sulphate elimination, tricyclic ring opening and uracil ring modification. Free radicals generated from CYL products containing secondary amines may covalently bond with NOM through cross-coupling during $\text{Fe}^{\text{III}}\text{-B}^*/\text{H}_2\text{O}_2$ catalysis (Bialk et al., 2007; Dec et al., 2000; Thorn et al., 1996). CYL products with carbonyl moieties were likely to promote addition reactions to NOM compounds with aromatic amines (Gulkowska et al., 2013). Apart from the reduced toxicity resulting from uracil ring modification, covalent bonding with NOM is also expected to suppress the toxicity of CYL products (e.g., m/z 448, 350, 336 and 318).

ANA conformational changes by covalent bonding with NOM mediated by $\text{Fe}^{\text{III}}\text{-B}^*/\text{H}_2\text{O}_2$ may affect its binding affinity to receptors (Swanson et al., 1986), resulting in reduced toxicity. ANA intermediate products were identified through high resolution mass spectrometry analysis, including the formation of nitrogen-containing products via ANA epoxidation and the formation of cyclised and linear products via ANA deamination (Appendix Scheme A3.2). Based on the known non-toxic epoxidized ANA (James et al., 1998), the ANA nitrogen-containing products transformed from epoxidized ANA are suggested to be non-toxic. In the presence of NOM, ANA products with primary amines (e.g., m/z 164, 122 and 146) and secondary amines (e.g., m/z 182, 138 and 140) likely engage in radical-radical covalent coupling reaction with NOM (Bialk et al., 2007; Dec et al., 2000; Thorn et al., 1996), which could result in reduced toxicity risk for the cyclised nitrogen-containing products as well.

3.4 Conclusions

According to cyanotoxin quantification in reactions, CYL and ANA removal by $\text{Fe}^{\text{III}}\text{-B}^*/\text{H}_2\text{O}_2$ were found to be affected by NOM, in that cyanotoxin removal increased as NOM was increased from 0 ppm to 30 ppm. The cyanotoxin reactions with NOM surrogates suggest cross-coupling of cyanotoxin with specific NOM components as one possibility to increase removal. Further, corresponding pathways of cross-coupled products formation are proposed via one-electron oxidation. Rather than a negative impact of NOM on physical and chemical treatments, NOM radical-mediated cross-coupling with cyanotoxin mediated by $\text{Fe}^{\text{III}}\text{-B}^*/\text{H}_2\text{O}_2$ was found to increase cyanotoxin transformation into compounds of lower toxicity.

Chapter 4: Estrogenic activity of cylindrospermopsin and anatoxin-a and their oxidative products by Fe^{III}-B*/H₂O₂

Manuscript published in Water Research journal (DOI: 10.1016/j.watres.2018.01.018)

Chapter abstract

The cyanotoxins released into waters during cyanobacterial blooms can pose serious hazards to humans and animals. Apart from their toxicological mechanisms, cyanotoxins have been shown to be involved in estrogenic activity by *in vivo* and *in vitro* assays; however, there is little information on the change in estrogenicity of cyanotoxins following chemical oxidation. In this study, the estrogenic activity of cylindrospermopsin (CYL) and anatoxin-a (ANA) at concentrations ranging from 2.4×10^{-7} M to 2.4×10^{-12} M (CYL) and 7.1×10^{-6} M to 7.1×10^{-11} M (ANA), and after treatment by the Fe^{III}-B*/H₂O₂ catalyst system, was investigated by the yeast estrogen screen (YES) assay. The results indicate that CYL and ANA acted as agonists in the YES assay (CYL logEC₅₀ = -8.901; ANA logEC₅₀ = -6.789), their binding affinity to estrogen receptors is associated with their intrinsic properties, including ring structures and toxicant properties. CYL and ANA were shown to simulate endocrine disrupting chemicals (EDCs) to modulate the 17β-estradiol-induced estrogenic activity, resulting in non-monotonic dose responses. The treated CYL showed a significantly altered estrogenicity compared to the untreated CYL (T₍₂₎ = 8.168, p ≤ 0.05), while the estrogenicity of the treated ANA was not significantly different to the untreated ANA (T₍₂₎ = 1.295, p > 0.05). Intermediate products generated from CYL and ANA oxidized by Fe^{III}-B*/H₂O₂ were identified using Q-Exactive Tandem Mass Spectrometry (LC-MS/MS). Treatment with Fe^{III}-B*/H₂O₂ yielded open-ring by-products which likely resulted in CYL's reduced binding affinity to estrogen receptors. The insignificant change in the estrogenicity of treated ANA was possibly a result of its multiple

ring structure products, which were likely able to bind to estrogen receptors. The comparisons for the estrogenicity of these cyanotoxins before and after $\text{Fe}^{\text{III}}\text{-B}^*/\text{H}_2\text{O}_2$ treatment suggest that the reductions in estrogenicity achieved by oxidation were dependent on the levels of cyanotoxins removed, as well as the estrogenicity of the degradation products. This is the first study on the change in the estrogenicity of CYL and ANA upon oxidation by $\text{Fe}^{\text{III}}\text{-B}^*/\text{H}_2\text{O}_2$, a high activity catalyst system.

4.1 Introduction

Cyanotoxins in the form of cyanobacterial secondary metabolites (W. W. Carmichael, 1992) have been the subject of many studies over recent decades due to their wide distribution (Pelaez et al., 2010) and high toxicity (Duy et al., 2000). They can be categorized into cyclic peptides including microcystins and nodularin, and alkaloids including cylindrospermopsin (CYL, Figure 4.1a) and anatoxin-a (ANA, Figure 4.1b) (Svrcek et al., 2004). The widespread CYL and ANA (de la Cruz et al., 2013; Duy et al., 2000; Kinnear, 2010; Osswald et al., 2007) in particular have been associated with cases of human poisoning and animal deaths reported in the USA (D. Stevens et al., 1988), Australia (Saker et al., 1999), Finland (Sivonen et al., 1990), Scotland (Edwards et al., 1992), Ireland (James et al., 1997), Brazil (Wayne W Carmichael et al., 2001), France (Gugger et al., 2005), New Zealand (Wood et al., 2007), and the Netherlands (Faassen et al., 2012), among others countries. In addition to the hepatotoxic, neurotoxic and cytotoxic effects of cyanotoxins (Funari et al., 2008), there are also indications of endocrine disrupting effects as well. Extracts of cyanobacteria have been shown to be estrogenic by human breast carcinoma cell line MVLN *in vitro* assay (Jonas et al., 2015; Štěpánková et al., 2011; Sychrová et al., 2012). Further, microcystin-LR and nodularin-R induced weak estrogenic potency in cultured mammalian cells (Oziol et al., 2010), and the endocrine disrupting effect of microcystin-LR has also been reported by *in vivo* assay (Rogers et al., 2011). However, information on the estrogenic potency by CYL and ANA is limited.

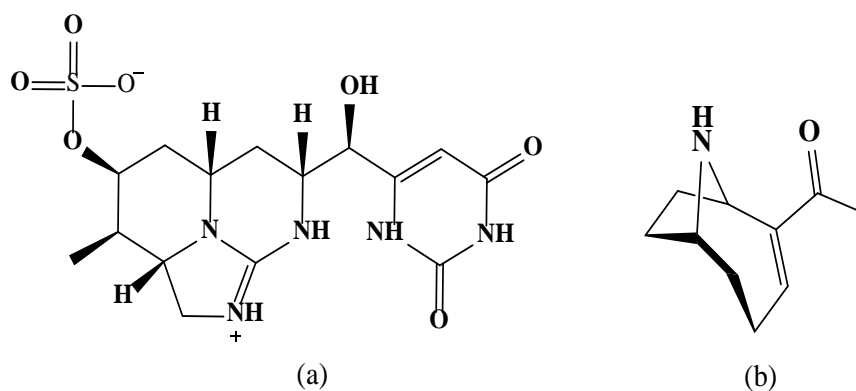


Figure 4. 1: The structure of (a) cylindrospermopsin and (b) anatoxin-a

CYL and ANA oxidative degradation have been conducted by chlorine, ozone and other oxidizing agents, resulting in varying degrees of efficiencies and shortcomings (E. Rodríguez, Onstad, et al., 2007; E. Rodríguez, Sordo, et al., 2007). In our study on the oxidative degradation of CYL and ANA, we attempted the catalytic oxidative degradation of CYL and ANA using a high activity catalyst system, the iron (III) tetra-amido-macrocyclic ligand (Fe^{III} -TAML, designated as Fe^{III} -B^{*})/ H_2O_2 catalyst system. CYL and ANA degradation were achieved by Fe^{III} -B^{*}/ H_2O_2 , however, the effect of oxidation by Fe^{III} -B^{*}/ H_2O_2 on the estrogenicity of the cyanotoxins was unclear.

In this study the yeast estrogen screen (YES) assay, one of the most robust and widely used *in vitro* assays (Balsiger et al., 2010; Leusch et al., 2010) was applied to measure the estrogenic potency of cyanotoxin samples. Yeast cell-based assay has been used previously to detect the estrogenicity of samples from wastewater, sewage and surface water (Aerni et al., 2004; Murk et al., 2002; Rutishauser et al., 2004). However, some issues have been raised about the YES assay (Beresford et al., 2000), especially in relation to the toxicity of samples to yeast cells (Citulski et al., 2012). The latter study investigated the toxicity of CYL and ANA to yeast cells by assessing yeast cell viability, while also establishing reliable estrogenic dose-response curves.

Our aim in this study was to investigate the potential estrogenic activity of CYL and ANA using the YES assay, explore the modulating effect of cyanotoxin on E2 induced estrogenic activity, and assess the Fe^{III}-B*/H₂O₂ catalyst system in remediating cyanotoxin induced estrogenicity.

4.2 Methodology

4.2.1 Reagents and materials

Cylindrospermopsin from Sapphire Bioscience (NZ) and (±)-anatoxin-a fumarate from Abcam were used as received. ZnCl₂ was purchased from BDH Chemicals, and 17β-estradiol (E2) was from Cayman Chemical. The University of Auckland's School of Chemical Sciences supplied Fe^{III}-B*. The HPLC grade solvents were from Merck Millipore. All operations with cyanotoxin were conducted in a chemical fume hood taking all appropriate safety measures for handling toxic compounds and SC-UW medium.

4.2.2 Yeast estrogen screen assay

A genetically modified strains of *Saccharomyces cerevisiae* (DSY 219) was employed in the YES assay, which is engineered with the human estrogen receptor gene and expression plasmids carrying an estrogen responsive element controlling the expression of the reporter gene *lac-Z* (encoding the enzyme β-galactosidase) (Routledge et al., 1996). The intensity of the colorimetric response induced by β-galactosidase quantifies the amount of β-galactosidase and so the level of estrogenic activity (Campbell et al., 2006).

The YES assay protocol used was modified from Balsiger et al. (2010). In brief, DSY219 was incubated overnight in SC-UW media at 30 °C. The following day the yeast cells were diluted with SC-UW media to an optical density at 600 nm (1 cm path length) (OD₆₀₀) of 0.08 and incubated at 30 °C to an OD₆₀₀ of 0.1. The yeast cells were then harvested by centrifugation

(4000 rpm/2 min) and re-suspended in 2.5×SC-UW media to obtain the yeast inoculum for the YES assay. Every 750 μL sample for estrogenicity testing (Table 1) was exposed to the yeast cell solution (250 μL) for 2 hrs, after which 100 μL of the mixture was transferred to a 96-well micro-plate containing Gal-Screen Reagent (100 μL) (Life Technologies NZ Ltd.) in each well. Finally, after incubating at 30 °C for 30 min, the chemiluminescent signal of the GAL-Screen was measured by a Victor™X luminescence plate reader.

Table 4. 1: Parameters in the YES assay

The YES assay	Initial concentration of cyanotoxin and E2
Individual cyanotoxin assay	CYL: 2.4×10^{-7} M to 2.4×10^{-12} M
	ANA: 7.1×10^{-6} M to 7.1×10^{-11} M
	ZnCl ₂ *: 1.0×10^{-6} M to 1.6×10^{-8} M
	E2: 4.0×10^{-7} M to 4.0×10^{-12} M
Competition assay CYL/ANA/ZnCl ₂ : E2 = 1: 1 (v/v)	CYL: 2.4×10^{-5} M to 2.4×10^{-8} M E2: 4.0×10^{-5} M to 4.0×10^{-9} M
	Blank: E2 = 1: 1 (v/v) as control ANA: 3.6×10^{-5} M to 3.6×10^{-8} M E2: 2.0×10^{-6} M to 2.0×10^{-11} M
Treated cyanotoxin	ZnCl ₂ : 8.0×10^{-8} M to 8.0×10^{-11} M E2: 4.0×10^{-5} M to 4.0×10^{-9} M
	CYL: 2.4×10^{-7} M to 2.4×10^{-12} M ANA: 7.1×10^{-6} M to 7.1×10^{-11} M
	CYL-treated: C _{treated} to C _{treated} ×10 ⁻⁶ ANA-treated: C _{treated} to C _{treated} ×10 ⁻⁶
	E2: 4.0×10^{-7} M to 4.0×10^{-12} M

Chemicals were subjected to a 10-fold serial dilution; or a 2-fold serial dilution*. C_{treated} indicated as the concentration of cyanotoxin treated by Fe^{III}-B*/H₂O₂.

4.2.3 Estrogenic response of cyanotoxin treated by Fe^{III}-B*/H₂O₂

The initial reaction conditions were: 2.4×10^{-7} M CYL or 7.1×10^{-6} M ANA in the pH 9.5 0.01 M Na₂CO₃/NaHCO₃ buffer and 5.0×10^{-6} M Fe^{III}-B*. Reactions were initialized by adding H₂O₂ 5.0×10^{-3} M. Sample was taken at intervals during the reaction and added with catalase to quench the residual H₂O₂. Samples were filtered through 0.2 μm RC syringe filters (Phenomenex NZ Ltd) and applied to LC-MS (Shimadzu Series model LC-MS 2020, Japan) for cyanotoxin quantification. After the catalytic oxidative degradation, the treated cyanotoxin and its related 10-fold serial dilutions were exposed to yeast cell solution, and the estrogenicity induced by the treated cyanotoxin was detected by the YES assay. The treated cyanotoxins were concentrated by the solid-phase extraction (SPE) for intermediate products identification. The LC-MS method and SPE procedure are provided in the appendix of Chapter 4.

4.2.4 Cytotoxicity of cyanotoxins on yeast cells

To measure the cytotoxic effect of cyanotoxin on yeast cells, 1 mL sample (Table 4.2) was incubated with the yeast inoculum (1 mL) at 30 °C for 24 hrs. The samples used for the flow cytometer (Model BDTM LSR II, 60 μL/min) were prepared following the guidelines for Cell Viability Kit (no. 349483), BD Bioscience.

Table 4. 2: Parameters in cytotoxicity test

Concentration of cyanotoxin and ZnCl ₂
CYL: 3.6×10^{-6} M, 1.8×10^{-6} M, 1.8×10^{-7} M, 1.8×10^{-8} M, 1.8×10^{-9} M
ANA: 9.1×10^{-5} M, 4.5×10^{-5} M, 4.5×10^{-6} M, 4.5×10^{-7} M, 4.5×10^{-8} M
ZnCl ₂ : 7.0×10^{-2} M, 7.0×10^{-3} M, 7.0×10^{-4} M, 7.0×10^{-5} M

4.2.5 Data calculation and statistical analysis

The signals obtained by the plate reader were used to indicate the estrogenicity of samples. A dose-response curve was plotted by GraphPad Prism version 5.0 (GraphPad Software, San Diego California USA), based on a four-parameter-log(agonist) vs response-curve equation (Balsiger et al., 2010):

$$Y = Bottom + \frac{Top - Bottom}{1 + 10^{((LogEC_{50} - X) * HillSlope)}} \quad \text{Eq. 4.1}$$

where Top and Bottom are the maximal and the basal response; EC₅₀ is the concentration of agonist that gives a response half way between the maximal (Top) response and the basal (Bottom) response; Y is the activity response of samples; X is the logarithm of E2 concentrations; HillSlope indicates the steepness of the curve. Bottom, Top, HillSlope, and EC₅₀ are generated automatically by the software.

EC_f was converted using the following equation (Eq.4.2), then a normalized dose-response curve was plotted using Prism of EC_f values and % β-galactosidase:

$$EC_f = \left[\left(\frac{f}{100-f} \right)^{\frac{1}{HillSlope}} \right] * EC_{50} \quad \text{Eq.4.2}$$

The ratio of live yeast cells was converted by the number of live cells measured in every 1×10⁵ event (Eq.4.3):

$$live\ yeast\ cells\ \% = \frac{live\ cells\ number}{1 \times 10^5} \times 100\ \% \quad \text{Eq.4.3}$$

The significance of the differences among the multiple samples was assessed by one-way ANOVA performed in GraphPad Prism version 5.0, with logEC₅₀ means and corresponding standard deviations; the significant difference between two samples was compared using T-test in GraphPad Prism version 5.0, with logEC₅₀ means and corresponding standard error of the mean.

4.3 Results and discussion

4.3.1 Cytotoxicity of cyanotoxins to yeast cells

The viability of yeast exposed to cyanotoxin was detected using flow cytometry (Figure 4.2) to determine the toxicity effect on the yeast cells. The viability of yeast cells incubated with CYL at concentrations ranging from 1.8×10^{-9} M to 3.6×10^{-6} M was not significantly different from yeast cells in the blank (Figure 4.2a) ($F_{(5, 12)} = 0.219$, $p > 0.05$), implying CYL is not significantly toxic to the yeast cells. There was an insignificant difference in the viability of yeast cells incubated with ANA at 9.1×10^{-5} M and ANA at 4.5×10^{-6} M or less compared to the blank, while yeast cells cultured with ANA at 4.5×10^{-5} M showed a reduced population (Figure 4.2b) ($F_{(5, 12)} = 9.332$, $p < 0.05$). The significant impact of ZnCl_2 at 7.0×10^{-2} M on cell viability (Figure 4.2c) can be associated with cytolysis due to the highly concentrated zinc salt (Hosiner et al., 2014) ($F_{(4, 10)} = 1.805 \times 10^2$, $p < 0.001$). The viability of cell exposing to decreased zinc salt concentration showed similar values to the blank, suggesting that zinc at 7.0×10^{-3} M or less had no toxicity to yeast cells over 24 hrs. Despite the very slight difference induced by ANA on yeast cells at 4.5×10^{-5} M, both ANA at 4.5×10^{-5} M and ZnCl_2 at 7.0×10^{-2} M were excluded in the YES assay to minimize the potential effect of these candidates at higher concentrations.

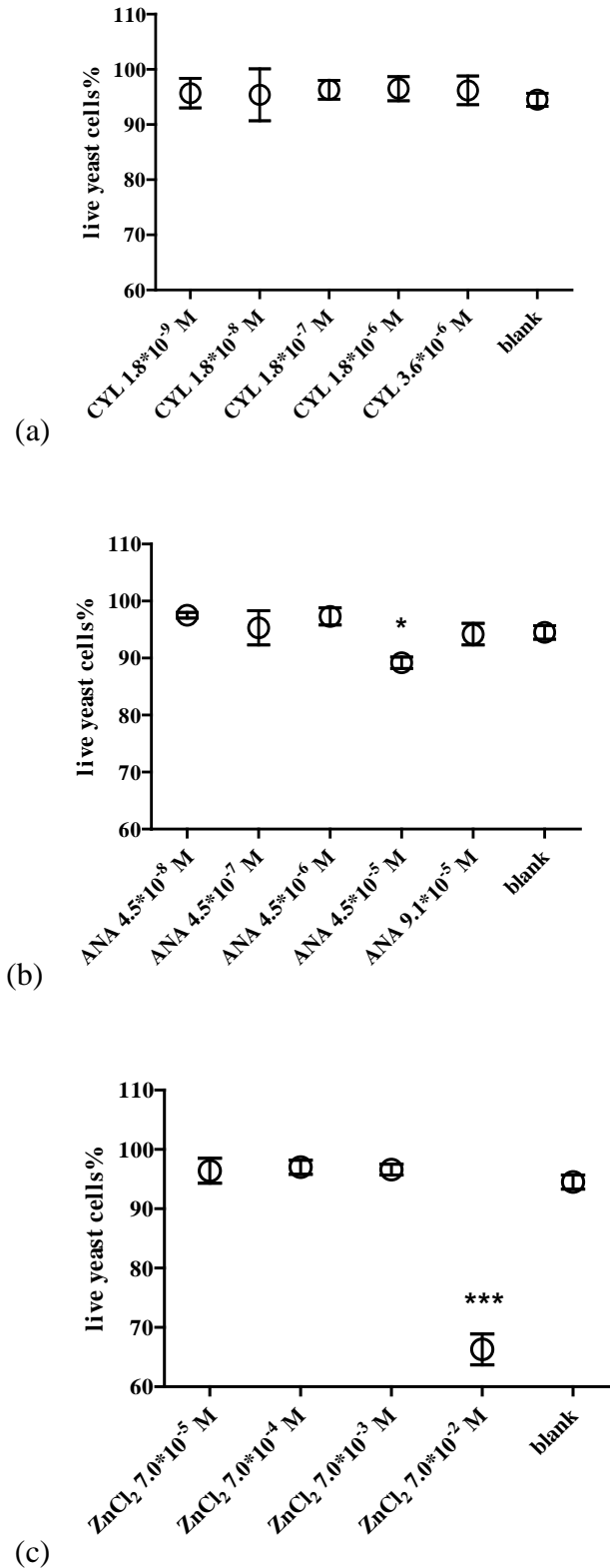


Figure 4. 2: Cytotoxicity of cyanotoxins on the yeast cells. The ratios of live yeast cells incubating with (a) CYL, (b) ANA and (c) ZnCl₂ for 24 hrs. All data points are averages of three independent runs with error bars representing standard deviation. * indicates a significant difference between sample and blank ($p < 0.05$), * indicates a significant difference between sample and blank ($p < 0.001$).**

4.3.2 Estrogenic activity of cyanotoxins

Figure 4.3a shows that the % β -galactosidase responses of cyanotoxins followed the same profile as for the E2 standard, but with differing slopes ($F_{(12, 40)} = 2.351 \times 10^{12}$, $p < 0.0001$).

Figure 4.3b indicates that the $\log EC_{50}$ induced by CYL was not significantly different to the $\log EC_{50}$ induced by E2, while the $\log EC_{50}$ values for ANA and $ZnCl_2$ were significantly different from the $\log EC_{50}$ induced by E2 ($F_{(3, 5)} = 74.830$, $p < 0.001$).

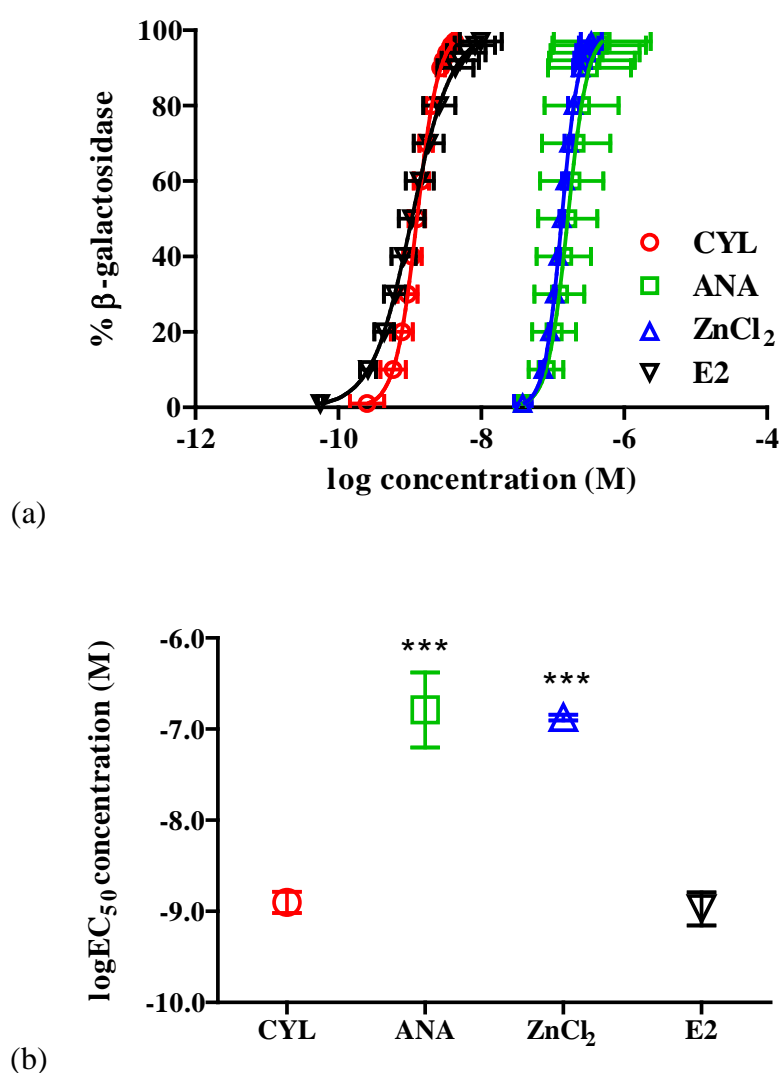


Figure 4. 3: Estrogenicity induced by cyanotoxins. Figure (a) shows normalized curves plotted by $\log EC_f$ values and % β -galactosidase; (b) shows the $\log EC_{50}$ values of each chemical. All data points are averages of two or three independent runs with error bars representing standard deviation. * indicates a significant difference between sample and E2 ($p < 0.001$).**

As shown previously (Denier et al., 2009), the results for E2 and ZnCl₂ indicate that the YES assay is reliable for assessing the estrogenicity of both endogenous hormone and endocrine disrupting chemicals. The signals identified from CYL and ANA suggest that both cyanotoxins can effectively bind to the estrogen receptors to form the complex that initiates the production of β -galactosidase. We associated the binding affinity of cyanotoxins to estrogen receptors and the actions of cyanotoxins as agonists with the intrinsic properties identified for CYL and ANA. Toxicants can interact with receptors and lead to agonist or antagonist mechanisms (Mailman, 2008), which is analogous to the way endocrine disrupters function in endocrine systems (Crisp et al., 1998; Mueller, 2004). CYL as a potent protein synthesis inhibitor *in vitro* (Suzanne M Frosio et al., 2003) is also suggested as a potential endocrine disruptor due to its binding affinity to progesterone receptors (F. M. Young et al., 2008). CYL's potential as an endocrine disruptor is also implied by its typical target organs (Hawkins et al., 1985) – organs commonly affected by known endocrine disrupting chemicals (Mueller, 2004). ANA can irreversibly bind to nicotinic acetylcholine receptors (Osswald et al., 2007). Although the agonist effect of ANA on estrogen receptors has not been elucidated in the literature, the affinity of ANA for estrogen receptors has been suggested based on its known binding to nicotinic acetylcholine receptors (Campos et al., 2006). Accordingly, ANA may function as a neuroendocrine disruptor through its action with both nicotinic acetylcholine receptors and estrogen receptors (Crisp et al., 1998; Kavlock et al., 1996).

When characterising their action as agonists in the YES assay, the ring structures of both cyanotoxins are key factors in their affinity to estrogen receptors. Their ring construction can favour estrogen receptor binding by increasing the rigidity of the structure, as well as the steric centre (Blair et al., 2000; Fang et al., 2001; Safe et al., 2001). Due to the high correlation between relative binding affinities and structural features (Blair et al., 2000; Nishihara et al., 2000), the lower logEC₅₀ value induced by CYL compared to ANA can be explained by CYL's

multiple rings. CYL (Figure 4.1a) has a tricyclic guanidine moiety and hydroxymethyl uracil (Ohtani et al., 1992), while ANA (Figure 4.1b), on the other hand, is a bicyclic secondary amine (W. W. Carmichael, 1992).

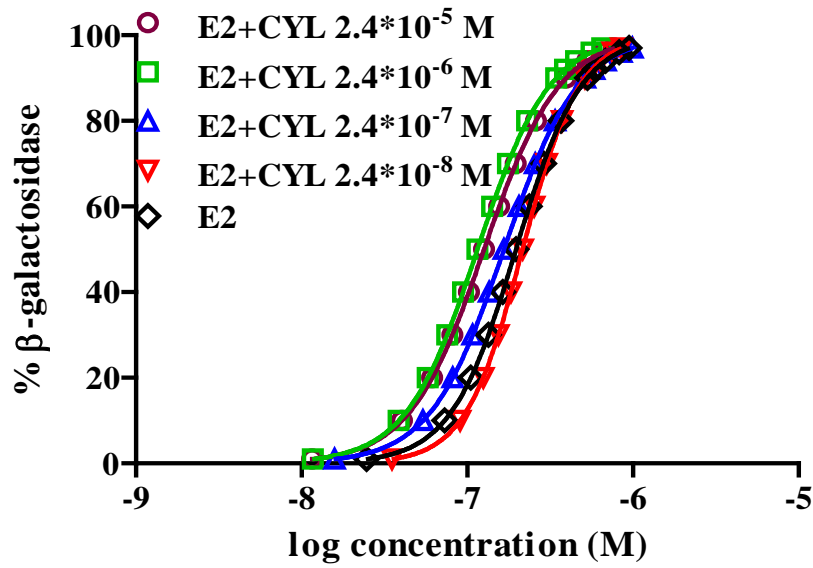
4.3.3 Modulation of E2 activity by cyanotoxins

To investigate the effect of CYL and ANA on the estrogenic activity of natural estrogen, E2 induced estrogenicity was measured when exposed to cyanotoxin. The competition assay demonstrated that the co-exposure of E2 to different concentrations of CYL resulted in variations in the % β -galactosidase slope shift (Figure 4.4a) ($F_{(16, 50)} = 2.309 \times 10^{12}$, $p < 0.0001$). Figures 4.4a and 4.4b show that CYL had a dose-dependent effect in the potency of E2-induced β -galactosidase in the YES assay. Contrary to the profile for the E2 control (Figure 4.4a), adding CYL at high concentrations (e.g., 2.4×10^{-5} M) to E2 resulted in a left slope shift, while CYL at low concentrations (e.g., 2.4×10^{-8} M) resulted in a right slope shift. The shift in slopes can also be seen in Figure 4.4b, which shows a significant difference between the half maximum effective concentration ($\log EC_{50}$) of E2 (E2 $\log EC_{50}$) and the half maximum effective concentration of E2 exposed to CYL (E2-CYL $\log EC_{50}$) ($F_{(4, 10)} = 8.031 \times 10^{12}$, $p < 0.0001$). These results show CYL can act either as an agonist or an antagonist – depending on its concentration.

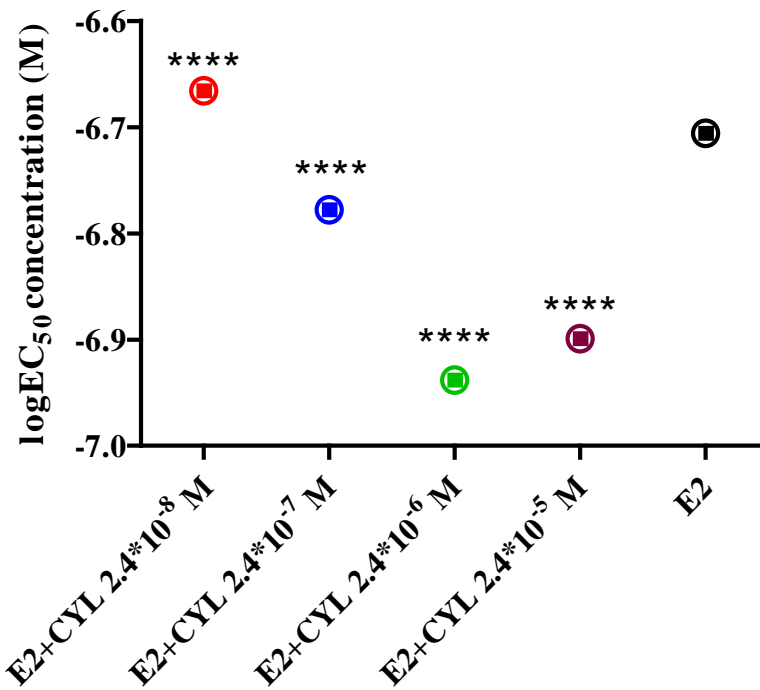
In the case of ANA, the competition assay (Figure 4.5a) showed that adding different concentrations of ANA to E2 (E2-ANA) resulted in differences in the % β -galactosidase-induced estrogenicity slope shift compared to the E2 positive control ($F_{(16, 50)} = 2.971 \times 10^{11}$, $p < 0.0001$). The right slope shift resulted from the reduced potency of the % β -galactosidase-induced estrogenicity following the co-exposure of E2 to ANA. Accordingly, ANA can be categorized as an E2 antagonist. These differences can be seen more clearly in Figure 4.5b ($F_{(4, 10)} = 5.411 \times 10^{11}$, $p < 0.0001$), where the co-exposure of E2 to different concentrations of

ANA resulted in a higher half maximum effective concentration (E2-ANA logEC₅₀) than the half maximum effective concentration (logEC₅₀) seen for E2 (E2 logEC₅₀). However, ANA did not behave as a classic antagonist in the YES assay because an inverse dose-response effect was observed by the antagonist effect of ANA on the E2 induced β -galactosidase in the YES assay.

The competition assay for ZnCl₂ added at different concentrations to E2 also resulted in differences in the % β -galactosidase-induced estrogenicity slope shift (Figure 4.6a) ($F_{(16, 50)} = 7.055 \times 10^{11}$, $p < 0.0001$). The half maximum effective concentration (logEC₅₀) for E2 (E2 logEC₅₀) was significantly different from the half maximum effective concentration of E2 exposed to ZnCl₂ (E2-ZnCl₂ logEC₅₀) (Figure 4.6b) ($F_{(4, 10)} = 1.632 \times 10^{12}$, $p < 0.0001$). The observations for ZnCl₂ are in agreement with results from the study by Denier et al. (2009), further validating the use of ZnCl₂ as an external control for this experiment.

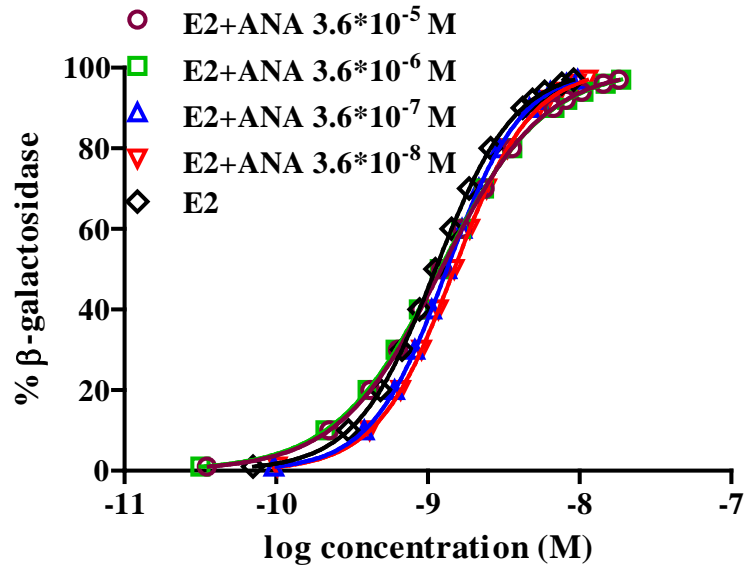


(a)

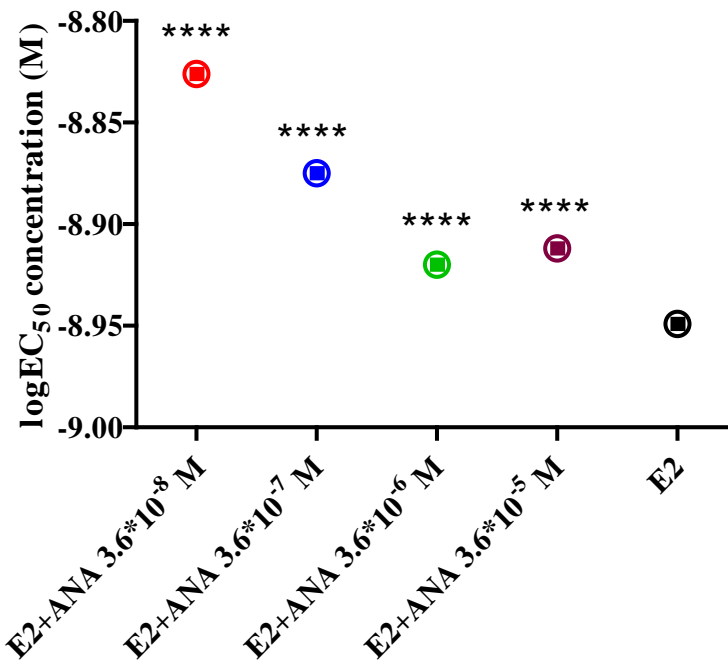


(b)

Figure 4. 4: Modification on E2 induced estrogenicity by CYL. Figure (a) shows dose-response curves by logEC_f values of E2 and % β -galactosidase in the presence of CYL; (b) shows the logEC₅₀ values of E2 in the presence of CYL. All data points are averages of three independent runs with error bars representing standard deviation. ** indicates a significant difference between sample and E2 ($p < 0.0001$). Small error bars are not visible in the graphs.**

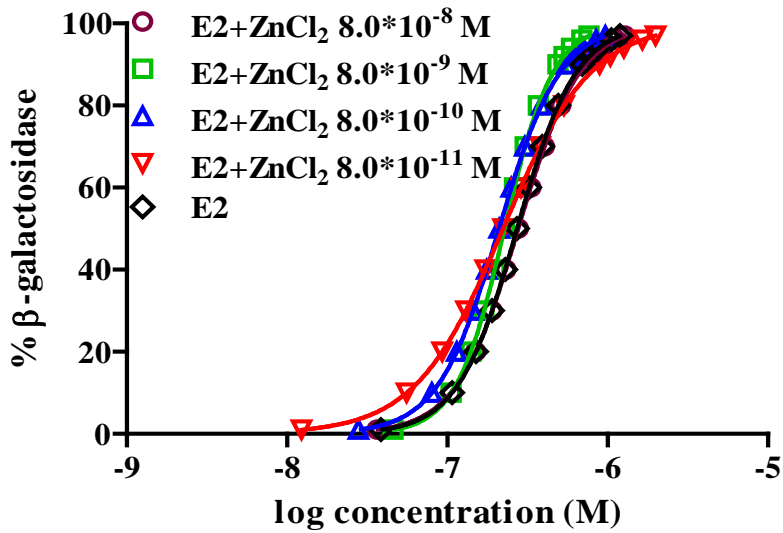


(a)

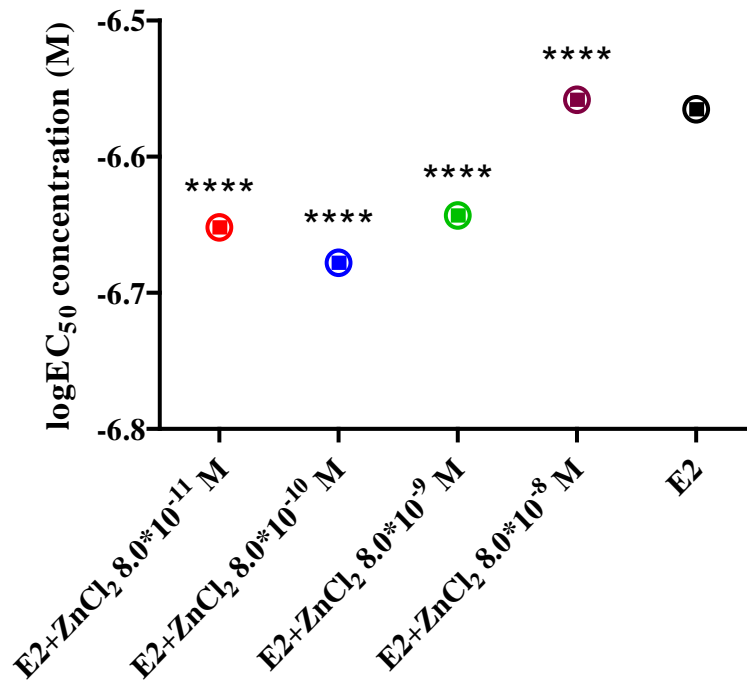


(b)

Figure 4. 5: Modification on E2 induced estrogenicity by ANA. Figure (a) shows dose-response curves by logEC_f values of E2 and % β -galactosidase in the presence of ANA; (b) shows the logEC₅₀ values of E2 in the presence of ANA. All data points are averages of three independent runs with error bars representing standard deviation. ** indicates a significant difference between sample and E2 ($p < 0.0001$). Small error bars are not visible in the graphs.**



(a)



(b)

Figure 4. 6: Modification on E2 induced estrogenicity by ZnCl₂. Figure (a) shows dose-response curves by logEC_f values of E2 and % β-galactosidase in the presence of ZnCl₂; (b) shows the logEC₅₀ values of E2 in the presence of ZnCl₂. All data points are averages of three independent runs with error bars representing standard deviation. ** indicates a significant difference between sample and E2 (p < 0.0001). Small error bars are not visible in the graphs.**

Overall, the dose-response experiments demonstrated that CYL and ANA induced non-monotonic dose responses in the YES assay. Such non-monotonic dose-response behaviours are common to chemicals or pollutants known as estrogen active chemicals (EACs), that have the ability to interfere with or disrupt the function of endogenous hormones (Almstrup et al., 2002; Li et al., 2007; Owen et al., 2014; Vandenberg et al., 2012). The causes of non-monotonic dose responses are not completely understood. Some equation-based computational models have proposed that the co-presence of an endogenous ligand and an exogenous ligand, such as EACs, and the concentration of each ligand can result in mixed-ligand dimers (Conolly et al., 2004; Kohn et al., 1993; Li et al., 2007). The relative abundance of endogenous ligand-receptor homodimers, exogenous ligand-receptor homodimers, and mixed-ligand heterodimers will influence the ratio of corepressor (CoR) and coactivator (CoA) in the cell, resulting in either agonist or antagonist effects (Conolly et al., 2004; Li et al., 2007).

These effects could explain the dose-dependent response for CYL observed in this work. The agonist response seen with high concentrations of CYL (i.e., 2.4×10^{-5} M and 2.4×10^{-6} M) is a result of CYL competing against E2. However when CYL concentrations are reduced to 2.4×10^{-7} M, the chances of CYL binding to receptor will be reduced by E2 competition, resulting in a cumulative reduction effect. The dose-response behaviours also show that CYL at low concentrations (i.e., 2.4×10^{-8} M) had an antagonist effect. The antagonist effect may be associated with the affinity changes of the receptors when exposed to very low CYL concentrations in the presence of E2. Future dose-response studies will be directed towards determining the lowest concentration of CYL that reduces estrogen-induced β -galactosidase assay.

The non-monotonic dose-response behaviours by EACs can also be explained by the phosphorylation status of the receptor (Atanaskova et al., 2002; Li et al., 2007; Rochette-Egly, 2003), as well as the auto-inhibitory effect of a high dose of the ligand on receptor expression

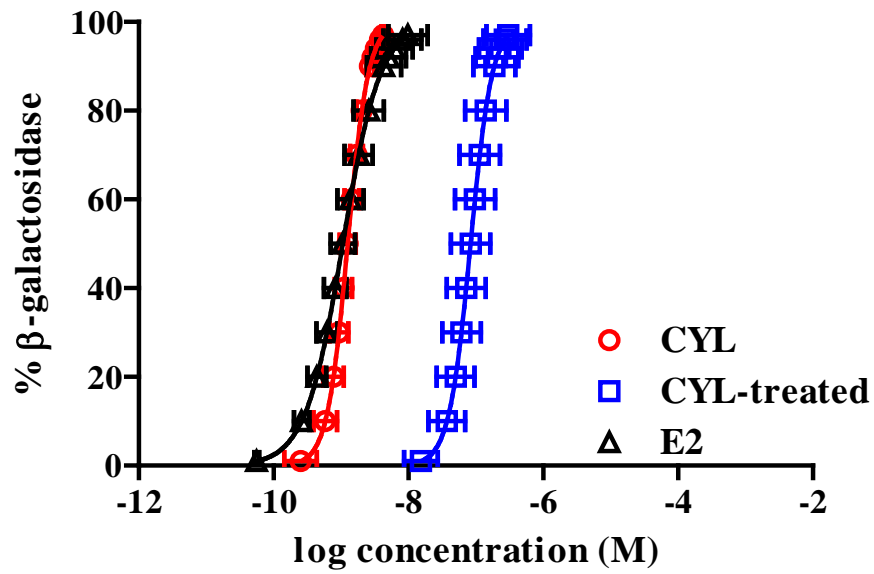
(Webb et al., 1992). In both cases, the presence of high concentration of cyanotoxins may lead to a regulation of the receptor. Further, ANA may affect protein kinases by acting as ion channels (Arias, 2006). The modulation of protein kinase by ANA combined with the auto-inhibitory effect on receptor expression with high concentrations of ANA may explain the inversely antagonist dose-response seen for ANA. Running this experiment for this paper, future dose-response studies will be directed towards determining the lowest concentration of ANA showing an agonistic effect.

Some earlier studies reported that estrogenicity of samples measured by the YES assay varied against the values predicted by the concentration addition model, or estrogenicity calculated by chemical analysis (Beck et al., 2006; Thorpe et al., 2006). There are a wide range of suggested causes of such deviations, including: chemicals disrupting the activation of estrogen response elements (Thorpe et al., 2006), anti-estrogenic compounds and/or unknown compounds with estrogenicity (Beck et al., 2006), estrogen receptor antagonists (Snyder et al., 2001), weak estrogens (Rajapakse et al., 2001), and non-estrogenic toxicants (Frische et al., 2009). The influence by cyanotoxins should also be considered when analysing the estrogenic activity of natural samples by YES assay. According to New Zealand Ministry of Health's 2016 guidelines, the concentrations of CYL and ANA in drinking water should not exceed 0.001 mg/L (2.4×10^{-9} M) and 0.006 mg/L (3.6×10^{-8} M), respectively. Epidemiological studies have demonstrated an association between environmental exposure to EDCs and human disease and disability (Vandenberg et al., 2012). The findings of this work suggest the possibility of chronic consequences for humans of CYL and ANA exposure at guideline values – or below.

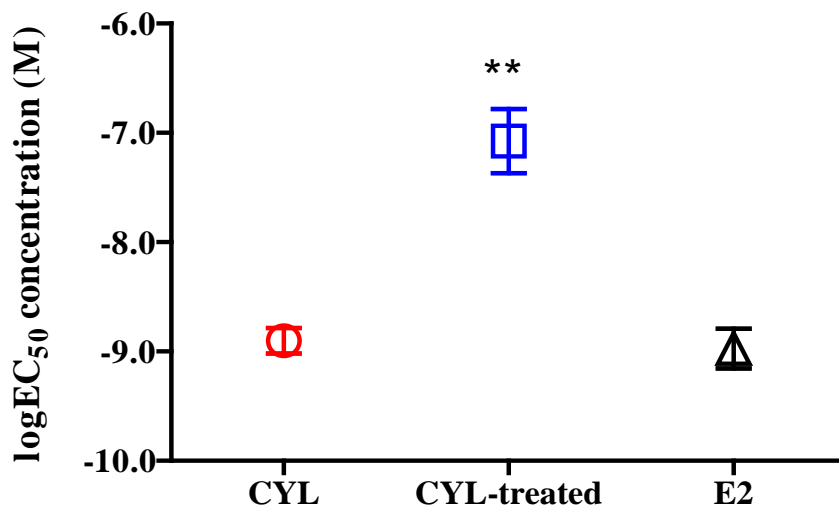
4.3.4 Estrogenicity of treated cyanotoxins by Fe^{III}-B*/H₂O₂

To evaluate the effect of Fe^{III}-B*/H₂O₂ on the estrogenicity of cyanotoxin, the estrogenicity of oxidized CYL and ANA was investigated by the YES assay. Figure 4.7a shows the difference between slopes for CYL and CYL treated by Fe^{III}-B*/H₂O₂ ($F_{(8, 30)} = 1.292 \times 10^{13}$, $p < 0.0001$). The difference is also evident when their logEC₅₀ values are compared in Figure 4.7b ($F_{(2, 3)} = 52.180$, $p < 0.01$). Figure 4.8a shows the different slopes for the β -galactosidase responses of untreated ANA, and then ANA treated by Fe^{III}-B*/H₂O₂ ($F_{(8, 30)} = 2.163 \times 10^{13}$, $p < 0.0001$). However, the comparison logEC₅₀ values in Figure 4.8b indicate no significant difference ($F_{(2, 3)} = 6.290$, $p > 0.05$). Similarly, the T-test result for the estrogenicity of treated CYL was significantly different from untreated CYL ($T_{(2)} = 8.168$, $p < 0.05$), while no significant difference was seen between the estrogenic activity of untreated ANA and treated ANA ($T_{(2)} = 1.295$, $p > 0.05$).

Fe^{III}-B* has been reported to produce non-estrogenic activity (W Chadwick Ellis et al., 2010). Further, the influence of the catalase on estrogenicity quantification can be excluded due to its rapid exhaustion by H₂O₂ by 1 min. Because of the negligible influence of Fe^{III}-B*/H₂O₂, and its evident oxidation efficiency (Appendix Figure A4.1), oxidized cyanotoxin was strongly associated with the measured estrogenicity, indicating that oxidized cyanotoxin may act as agonist or antagonist, and/or induce synergistic or antagonistic modulation of the parent cyanotoxin. For both mechanisms, the influence of oxidized cyanotoxin on the estrogenicity detected was related to its relative binding affinity to estrogen receptors, which can be highly dependent on constructional transformation by oxidation.

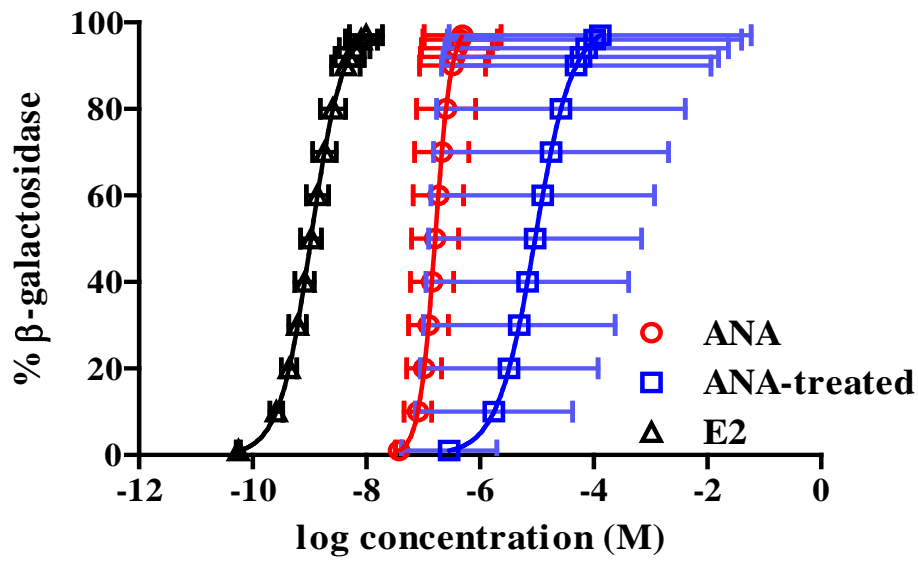


(a)

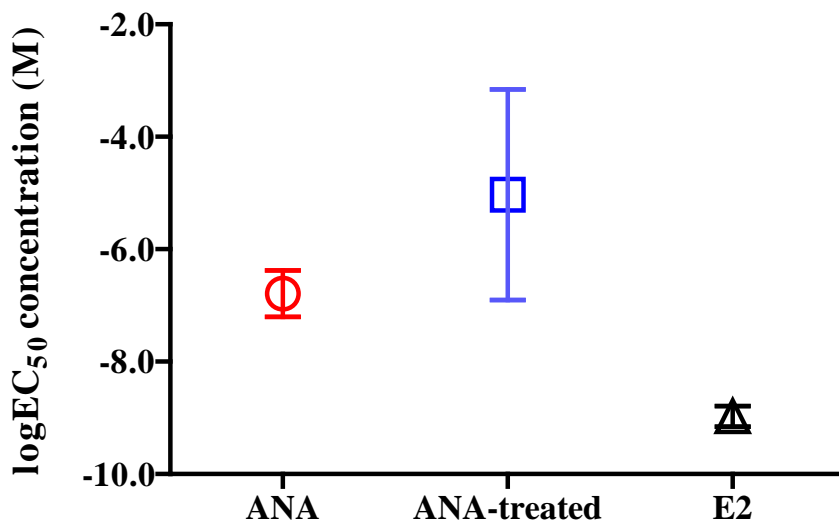


(b)

Figure 4. 7: Estrogenicity of CYL (2.4×10^{-7} M) treated by Fe^{III} -B*/ H_2O_2 (5.0×10^{-6} M/ 5.0×10^{-3} M). Figure (a) shows dose-response curves by $logEC_f$ values and % β -galactosidase; (b) shows the $logEC_{50}$ values of each sample with standard deviation from duplicates. ** indicates a significant difference between treated CYL and E2, as well as between treated CYL and CYL ($p < 0.01$).



(a)

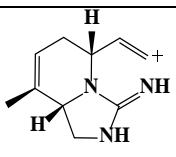
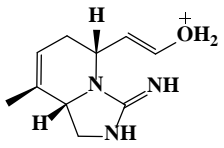
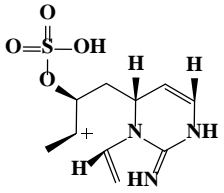
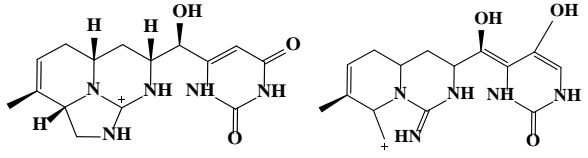
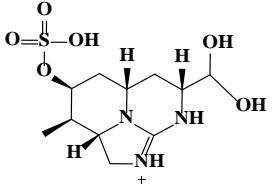
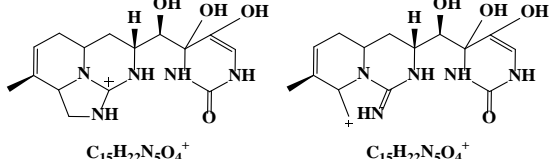
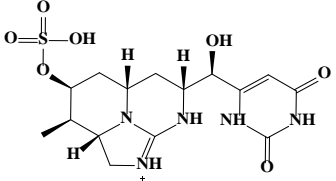


(b)

Figure 4. 8: Estrogenicity of ANA (7.1×10^{-6} M) treated by $\text{Fe}^{\text{III}}\text{-B}^*/\text{H}_2\text{O}_2$ (5.0×10^{-6} M/ 5.0×10^{-3} M). Figure (a) shows dose-response curves by logEC_f values and % β -galactosidase; (b) shows the logEC₅₀ values of each sample with standard deviation from duplicates. No significant difference is observed among logEC₅₀ by ANA, treated ANA and E2 ($p > 0.05$).

In Chapter 2, the intermediates of CYL and ANA mediated by $\text{Fe}^{\text{III}}\text{-B}^*/\text{H}_2\text{O}_2$ were identified by Q-Exactive tandem mass spectrometry (LC-MS/MS), and a series of cyanotoxin degradation products was proposed. CYL was generally transformed into products with destroyed tricyclic and uracil rings (Table 4.3), resulting in a decrease in its binding affinity to estrogen receptors. Furthermore, it appears that the majority of CYL by-products had destroyed rings, hence showed little or no binding affinity to estrogen receptors. Overall, a reduced estrogenic activity of CYL was achieved by $\text{Fe}^{\text{III}}\text{-B}^*/\text{H}_2\text{O}_2$ via catalytic oxidative degradation. ANA degradation was mainly conducted via unsaturated carbon bond oxidation and loss of ammonia, to produce a large number of ANA products with rings (Table 4.4). Although the estrogenicity induced by parent ANA decreased, ANA breakdown products with ring structures likely produced estrogenicity by binding to estrogen receptors, increasing the overall estrogenic level. A previous study of estrogenicity induced by EDC oxidation products reported that one EE_2 oxidation product may have higher estrogenicity than EE_2 itself (J. L. Chen et al., 2012). The resulting reduced estrogenicity of the parent ANA, but induced estrogenicity of ANA products likely explains the changed $\log\text{EC}_{50}$ value observed, while no significant corresponding difference in statistical values was found. When comparing the estrogenic activities of cyanotoxins before and after treatment, the reduction in levels of cyanotoxin estrogenicity should be correlated with removal level concentrations, and also related to its degradation by-products. Further, the daughter by-products of cyanotoxin may be significant when evaluating the removal efficiency of estrogenicity via oxidation.

Table 4. 3: Proposed structures and formula for the CID product ions from CYL mass spectra

Accurate mass (error, ppm)	RDB	Proposed product ion structure and molecular formula
176.1183 (0.43)	5.5	 $C_{10}H_{14}N_3^+$
194.1288 (0.06)	4.5	 $C_{10}H_{16}N_3O^+$
274.0855 (0.45)	4.5	 $C_{10}H_{16}N_3O_4S^+$
318.1564 (0.96)	8.5	 $C_{15}H_{20}N_5O_3^+$ $C_{15}H_{20}N_5O_3^+$
322.1072 (1.30)	3.5	 $C_{11}H_{20}N_3O_6S^+$
336.1668 (0.36)	7.5	 $C_{15}H_{22}N_5O_4^+$ $C_{15}H_{22}N_5O_4^+$
416.1235 (0.06)	7.5	 $C_{15}H_{22}N_5O_7S^+$

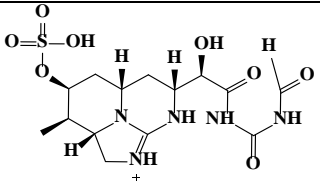
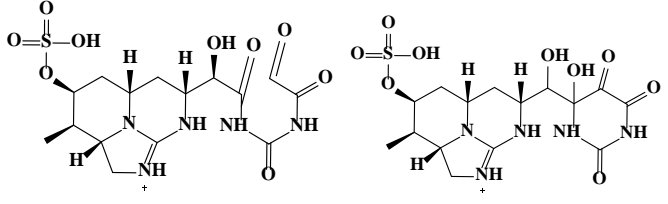
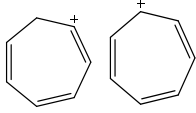
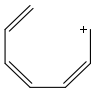
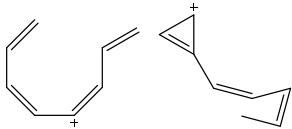
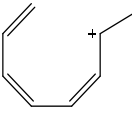
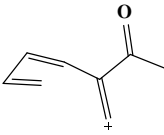
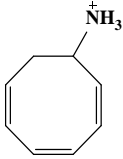
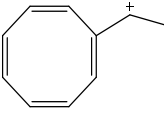
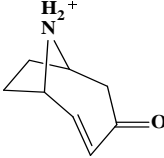
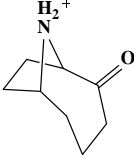
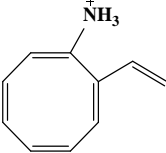
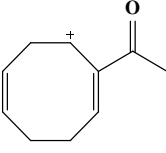
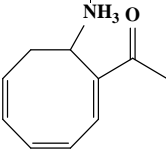
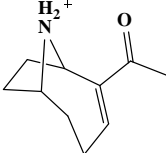
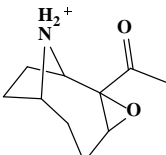
Accurate mass (error, ppm)	RDB	Proposed product ion structure and molecular formula
420.1182 (0.48)	6.5	 $C_{14}H_{22}N_5O_8S^+$
448.1133 (0.08)	7.5	 $C_{15}H_{22}N_5O_9S^+$ $C_{15}H_{22}N_5O_9S^+$

Table 4. 4: Proposed structures and formula for the CID product ions from ANA mass spectra

Accurate mass (error, ppm)	RDB	Proposed product ion structure and molecular formula
91.0546 (0.34)	4.5	 $C_7H_7^+$ $C_7H_7^+$
93.0704 (0.53)	3.5	 $C_7H_9^+$
105.0702 (0.28)	4.5	 $C_8H_9^+$ $C_8H_9^+$
107.0859 (0.40)	3.5	 $C_8H_{11}^+$
121.0652 (0.39)	4.5	 $C_8H_9O^+$
122.0967 (0.23)	3.5	 $C_8H_{12}N^+$
131.0857 (1.47)	5.5	 $C_{10}H_{11}^+$
138.0914 (0.060)	3.5	 $C_8H_{12}NO^+$

Accurate mass (error, ppm)	RDB	Proposed product ion structure and molecular formula
140.1071 (0.08)	2.5	 $C_8H_{14}NO^+$
146.0964 (0.01)	5.5	 $C_{10}H_{12}N^+$
149.0963 (1.20)	4.5	 $C_{10}H_{13}O^+$
164.1072 (0.20)	4.5	 $C_{10}H_{14}NO^+$
166.1228 (1.14)	3.5	 $C_{10}H_{16}NO^+$
182.1177 (0.14)	3.5	 $C_{10}H_{16}NO_2^+$

4.4 Conclusions

CYL and ANA were shown for the first time to induce estrogenic activity as agonists in the YES assay. Further, they can also be considered as potential endocrine disrupting chemicals due to their modulations on E2 activity. The non-monotonic dose responses by cyanotoxin were also discussed. The results found for the estrogenicity of cyanotoxin mediated by Fe^{III}-B*/H₂O₂ imply that reducing the estrogenic levels of EDCs depends on the level of reduction of the parent cyanotoxin – and the resulting degradation products. Due to the unexpected estrogenicity produced by the efficiency of the oxidation, bioassays used in combination with chromatographic quantification are recommended for an integrated assessment of EDCs estrogenic activity following their destruction. Consideration of the inter-relationship between the toxicity and endocrine disrupting nature of CYL and ANA is recommended for future pathological work and toxicological studies.

Chapter 5: Summary, Conclusions and Recommendations for Future Work

5.1 Summary

The efficiency of cylindrospermopsin (CYL) and anatoxin-a (ANA) degradation by the $\text{Fe}^{\text{III}}\text{-B}^*/\text{H}_2\text{O}_2$ catalyst system was investigated at different pH values to meet the first research objective of this thesis. The pK_a value for $\text{Fe}^{\text{III}}\text{-B}^*$ fell at pH in the range 9.3 to 10.5, with the highest reactivity of $\text{Fe}^{\text{III}}\text{-B}^*$ activators occurring around pH 10. Since $\text{Fe}^{\text{III}}\text{-B}^*/\text{H}_2\text{O}_2$ catalysis rates were shown to be significantly pH dependent, finding the optimal pH appears to be a challenge to the real-world application of the $\text{Fe}^{\text{III}}\text{-B}^*/\text{H}_2\text{O}_2$ catalyst system. To evaluate the efficiency of pH-dependent $\text{Fe}^{\text{III}}\text{-B}^*/\text{H}_2\text{O}_2$ catalysis on cyanotoxin degradation, $\text{Fe}^{\text{III}}\text{-B}^*/\text{H}_2\text{O}_2$ for cyanotoxin degradation was conducted at pH values ranging from 8.5 to 11.5. The first attempt at heterogeneous $\text{Fe}^{\text{III}}\text{-B}^*$ catalyst generation was made by anchoring dissolved $\text{Fe}^{\text{III}}\text{-B}^*$ onto functionalised silica gel. With the aim of minimizing $\text{Fe}^{\text{III}}\text{-B}^*$ diffusion in solution while at the same time maximizing coverage ratio, the repetitive sets of re-suspension and filtration were applied during the heterogeneous $\text{Fe}^{\text{III}}\text{-B}^*$ catalyst generation. Cyanotoxin removal by homogeneous formulation and heterogeneous formulation were compared. To understand the mechanism of cyanotoxin degradation mediated by $\text{Fe}^{\text{III}}\text{-B}^*/\text{H}_2\text{O}_2$, the degradation pathways for CYL and ANA were established. Cyanotoxin degradation products mediated by the $\text{Fe}^{\text{III}}\text{-B}^*/\text{H}_2\text{O}_2$ catalyst system were identified by Q-Exactive Tandem Mass Spectrometry, and the product ions were characterised by CID mass spectra with assistance from Mass Frontier.

Natural organic matter (NOM) is generally responsible for reduced treatment efficiency due to effects related to competition for active sites, radiation absorption and membrane fouling. So the influence by NOM is always a consideration when investigating removal rates for all water

treatment technologies. In recognition of the challenge posed by NOM in water treatment technologies, the influence of NOM on CYL and ANA removal by $\text{Fe}^{\text{III}}\text{-B}^*/\text{H}_2\text{O}_2$ was explored as the second task. CYL and ANA oxidative removal by $\text{Fe}^{\text{III}}\text{-B}^*/\text{H}_2\text{O}_2$ were conducted in the presence of NOM ranging from 0 to 30 ppm. To characterize the NOM constituents participating in the oxidative cross-coupling with cyanotoxin, NOM oxidized by $\text{Fe}^{\text{III}}\text{-B}^*/\text{H}_2\text{O}_2$ was monitored by EEM and UV/Vis in the absence of cyanotoxin. Further, two NOM surrogates with typical functional groups were selected with the aim of characterizing the interaction between humic/fulvic fractions and cyanotoxins. The effect of these two model NOM compounds on cyanotoxin degradation mediated by $\text{Fe}^{\text{III}}\text{-B}^*/\text{H}_2\text{O}_2$ was investigated. The high resolution mass spectrometry analysis by LC-MS/MS and GC-MS was used to demonstrate the enzyme-catalysed oxidative coupling between cyanotoxin and NOM surrogates, and the radical-mediated cross-coupling pathways were proposed based on $\text{Fe}^{\text{III}}\text{-B}^*$ mediated one-electron oxidation.

The potential for estrogenic activity induced by cyanotoxins CYL and ANA was studied in parallel, with an evaluation of the estrogenicity of cyanotoxins degraded by $\text{Fe}^{\text{III}}\text{-B}^*/\text{H}_2\text{O}_2$. To establish reliable estrogenic dose-response curves, the toxicity of cyanotoxin to yeast cells was investigated by assessing yeast cell viability using flow cytometry. Following the assessment of yeast cell viability, the estrogenic activity of CYL and ANA at concentrations ranging from 2.4×10^{-7} M to 2.4×10^{-12} M (CYL) and 7.1×10^{-6} M to 7.1×10^{-11} M (ANA) was quantified using the yeast estrogen screen (YES) assay. Further, the estrogenic activity of E2 exposed to cyanotoxin was measured to investigate the modulating effect of CYL and ANA on E2 induced estrogenicity. The estrogenicity of cyanotoxin treated by $\text{Fe}^{\text{III}}\text{-B}^*/\text{H}_2\text{O}_2$ was evaluated, and compared to the estrogenicity of untreated cyanotoxin. In the YES assay, ZnCl_2 and E2 were applied as controls, and their estrogenic responses were referred in the discussion. The $\log\text{EC}_{50}$

value of each chemical/sample was calculated using a four-parameter-log (agonist) vs response-curve equation.

5.2 Conclusions

5.2.1 Oxidative degradation of CYL and ANA by Fe^{III}-B*/H₂O₂

At pH 8.5 to 9.5, and a ratio of Fe^{III}-B* to substrate of 1: 0.048 (mole/mole), consistently high levels (87 % ~ 89 %) of CYL removal were achieved. This remarkably high and stable level of degradation was likely caused by the sufficient oxidized Fe^{III}-B* consumed by CYL. With a ratio of Fe^{III}-B* to the substrate of 1: 1.42 (mole/mole), Fe^{III}-B*/H₂O₂ applied at pH 8.5 achieved 75 % removal of ANA. As the pH was further increased to 9.5, the ANA removal rate increased to 96 %. For both cyanotoxins, rate constants increased with pH increasing from 8.5 to 11.5; a finding explained by the resulting enhanced formation of oxidized Fe^{III}-B*. The higher removal rates of CYL and ANA during the initial degradation phase (around 0 – 20 min) were consistent with the higher rate constants. As the reaction continued, however, cyanotoxin removal at pH 10.5 and 11.5 entered a plateau, resulting in a drop in the removal efficiency of cyanotoxin. The significant Fe^{III}-B* self-destruction at pH values above 10 most likely explained the increasing rate constants at the initial phase and the decreasing removal rates at the end of the reaction period. Following the assessment of coverage ratios by bleaching dye, heterogeneous Fe^{III}-B* catalyst was applied to remove the cyanotoxins. With an identical mole ratio of Fe^{III}-B* and H₂O₂ as used in the homogeneous formulation, heterogeneous Fe^{III}-B*/H₂O₂ contributed to a similar cyanotoxin removal efficiency to homogeneous Fe^{III}-B*/H₂O₂, resulting in 93 % CYL removal and 88 % ANA removal. Catalytic oxidative degradation of cyanotoxin by heterogeneous formulation was likely augmented with solid adsorption, using electrostatic interaction between charged molecules and the functionalised heterogeneous catalysts. Both homogeneous and heterogeneous Fe^{III}-B*/H₂O₂ catalyst system indicate

significant catalytic oxidative degradation of both cyanotoxins, compared with the selective oxidation by general oxidants (e.g., chlorine and permanganate). The efficient and effective removal of these cyanotoxins suggests the $\text{Fe}^{\text{III}}\text{-B}^*/\text{H}_2\text{O}_2$ catalyst system as an ideal alternative for the purification of cyanotoxin-contaminated water.

Besides this similar efficiency as homogeneous $\text{Fe}^{\text{III}}\text{-B}^*$, the heterogeneous $\text{Fe}^{\text{III}}\text{-B}^*$ formulation suggested possible application and utility of the catalyst system. According to one market report, “Industrial Catalyst Market by Type (Heterogeneous & Homogeneous), by Material (Metal, Chemical, Zeolites and Organometallic Materials), by Application and by Region - Global Trends and Forecasts to 2020”, a heterogeneous catalyst is considered to form the largest segment of its type in the industrial catalyst market, and heterogeneous catalysis is projected to be the fastest-growing form of industrial catalysis for the period between 2015 and 2020. There are future challenges for heterogeneous $\text{Fe}^{\text{III}}\text{-B}^*$, but expectations remain high. The finding from this part of work serves as a background for the desired application of other types and formulations of $\text{Fe}^{\text{III}}\text{-TAML}$ for contaminant removal. The catalytic reactions by immobilised $\text{Fe}^{\text{III}}\text{-B}^*$ described herein are a promising start for application of the larger geometric $\text{Fe}^{\text{III}}\text{-TAML}$. By taking advantage of powder catalysts, particle geometries with large accessible external surfaces and/or in various shapes could be developed. With full-scale commercial reactors, some typical catalyst geometries, including spheres, Raschig rings, hollow extrudates, and trilobes, are anticipated by granulating, pelleting and extruding from appropriate powders coated with $\text{Fe}^{\text{III}}\text{-TAML}$.

CYL degradation occurred mainly through hydroxylation, tricyclic guanidine ring opening, uracil moiety modification and sulphate group elimination. Accordingly, destruction of the uracil ring is expected to result in reduced toxicity of CYL. The degradation products of ANA were mainly transformed from ANA epoxidation and ANA deamination. Epoxidized ANA m/z 182 leads to a series of nitrogen-containing secondary by-products, whereas, deaminated ANA

m/z 149 further transforms into cyclised or linear products. Because epoxy-ANA is known to be non-toxic, the majority ANA degradation products are thought to have reduced toxicity. Consequently, $\text{Fe}^{\text{III}}\text{-B}^*/\text{H}_2\text{O}_2$ is proposed as reducing CYL and ANA toxicity by oxidizing toxic cyanotoxins to non-toxic or reduced-toxicity products.

5.2.2 Oxidative removal of CYL and ANA by $\text{Fe}^{\text{III}}\text{-B}^*/\text{H}_2\text{O}_2$ in the presence of NOM

Ninety-one percent of CYL was removed with the addition 0.5 ppm NOM, and nearly complete removal of ANA was observed with 0.6 ppm NOM within 120 min. Further, increasing the NOM dosage resulted in faster completion of removal, with no residual cyanotoxin available at 60 min in the presence of 30 ppm NOM. The results so far show enhanced CYL and ANA removal when NOM is present in concentrations as high as 30 ppm, indicating NOM as being beneficial to cyanotoxin removal in the ratios $\leq 1: 0.0033$ (NOM/CYL, mg/mg) and $\leq 1: 0.039$ (NOM/ANA, mg/mg). During the cyanotoxin treatment, NOM has a reduced negative impact on cyanotoxin removal as mediated by $\text{Fe}^{\text{III}}\text{-B}^*/\text{H}_2\text{O}_2$. The reduced negative influence of NOM suggests certain advantages of $\text{Fe}^{\text{III}}\text{-B}^*/\text{H}_2\text{O}_2$ over physical and chemical technologies (e.g., membrane filtration, photocatalysis, and chlorination) regarding the removal of cyanotoxins. This finding also suggests opportunities that exist for $\text{Fe}^{\text{III}}\text{-B}^*/\text{H}_2\text{O}_2$ to be employed at multiple stages of cyanotoxin treatment, where the impact of NOM concentration is not significant.

As illustrated in Chapter Three, $\text{Fe}^{\text{III}}\text{-B}^*/\text{H}_2\text{O}_2$ oxidized substrates via one-electron oxidation, whereby NOM and cyanotoxin radical species were generated. These radicals then proceeded to interact by self-coupling and cross-coupling, leading to the formation of intermediate products. Radical-mediated cross-coupling between the components of NOM and cyanotoxin molecules is highly suggested as one explanation for the enhanced removal efficiency. The transformed fluorophore signatures found by EEM and the changes in absorbance spectra identified in UV/Vis indicated that NOM components from humic-like and fulvic-like fractions,

especially the compounds with aromatic and carboxylate groups were oxidized by $\text{Fe}^{\text{III}}\text{-B}^*/\text{H}_2\text{O}_2$. Accordingly, NOM compounds with aromatic and carboxylate moieties were likely to cross-couple with cyanotoxins in the reaction mediated by $\text{Fe}^{\text{III}}\text{-B}^*/\text{H}_2\text{O}_2$. Guaiacol and glycolic acid were selected as NOM surrogates, which represent NOM with an aromatic moiety and NOM with a carboxylate moiety, respectively. When mediated by $\text{Fe}^{\text{III}}\text{-B}^*/\text{H}_2\text{O}_2$, guaiacol increased removal of both cyanotoxins, and glycolic acid increased CYL removal only. The radical-mediated cross-couplings between NOM components and cyanotoxins were characterized as CYL cross-coupling with NOM constituents with aromatic and carboxylate moieties, and ANA cross-coupling with NOM constituents with an aromatic moiety. Cross-coupling pathways between NOM surrogates and cyanotoxins were proposed based on an enzyme-catalysed one-electron oxidation. The cross-coupling of the parent cyanotoxins with NOM can result in a reduced toxicity due to inhibition of the CYL uracil ring and a conformational change in the ANA molecule, and the cross-coupling of degradation products with NOM may further lower their toxicity.

5.2.3 Estrogenic activity of CYL and ANA and their oxidative products by $\text{Fe}^{\text{III}}\text{-B}^*/\text{H}_2\text{O}_2$

When the estrogenic activity of cyanotoxins was investigated, cyanotoxins were found to bind to estrogen receptors by mimicking endogenous ligands; the complex formed was able to activate the production of enzyme β -galactosidase, leading to an agonist dose-response mechanism. The functionalisation of CYL and ANA in inducing estrogenic activity revealed that both cyanotoxins are potential agonists in the YES assay. The ring structures are proposed as one reason for the binding affinity of both CYL and ANA to estrogen receptors. The cyanotoxins also demonstrated alterations on E2 induced estrogenicity, where synergistic and antagonistic modulations were seen by CYL and antagonistic modulation was observed by ANA. These findings for cyanotoxin effects on E2 activity indicate the potential of both CYL and ANA to be endocrine disrupting chemicals (EDCs). As a result of their actions as agonists

in the YES assay and their modulations on endogenous estrogen (E2), deviations caused by cyanotoxins should be considered when determining the potential estrogenic activity of natural samples by the YES assay. The logEC₅₀ induced by E2 exposed to cyanotoxin revealed that CYL and ANA can display non-monotonic dose-response behaviours. Around 86 % removal of cyanotoxins was achieved by Fe^{III}-B*/H₂O₂ at pH 9.5 after a reaction time of 1 hr. Although significant removal was observed for both cyanotoxins, the changes in estrogenicity induced in the treated cyanotoxins differed. Comparing the logEC₅₀ values before and after treatment, the estrogenicity of treated CYL was significantly different to that for CYL, while the estrogenicity of treated ANA was not significantly different to the level for native ANA. The identification of corresponding products reveals that CYL degradation products with ring breakage structures are likely related to the significantly different logEC₅₀ value, while ANA oxidized products with intact ring structures may have contributed to the insignificant difference found.

5.3 Recommendations for Future Work

Overall, this thesis highlights the advantages of Fe^{III}-B*/H₂O₂ in terms of the removal efficiency and non-toxic product formation of cyanotoxins CYL and ANA from applying different formulations of Fe^{III}-B* and the modelled NOM system. The following recommendations are offered for related research on cyanotoxins CYL and ANA, and the Fe^{III}-B*/H₂O₂ catalyst system in future.

- 1) In order to evaluate the long-term effects of cyanotoxin by-products on health, further work on toxicity evaluation of oxidized cyanotoxins by Fe^{III}-B*/H₂O₂ is encouraged, via *in vitro* and *in vivo* assays.
- 2) Extensive research on heterogeneous Fe^{III}-TAML is recommended in regard to the types of support materials, and modes of functionalised immobilisation. In the interests of meeting

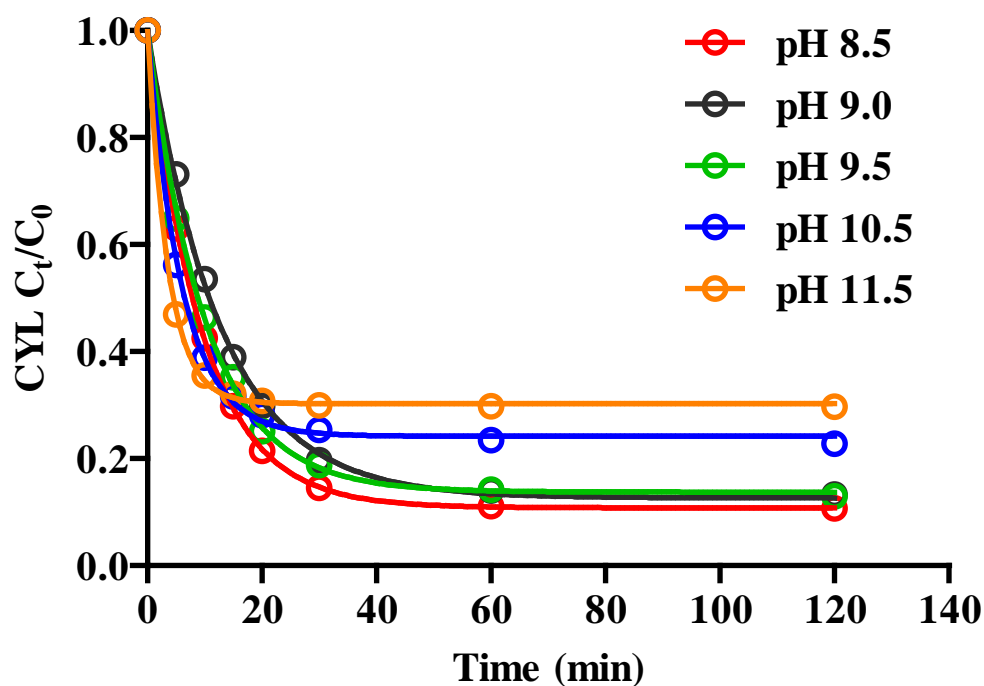
the increasing market demand and economical operations, it will be important to integrate engineering with catalysis to create optimal bulk processes for heterogeneous Fe^{III}-TAML.

- 3) Regarding NOM cross-coupled products, a further study applying density functional theory calculation (DFT) in collaboration with NMR analysis is recommended such that DFT could provide a more accurate identification of the reactive sites of each compound in relation to the cross-coupling process and product structures.
- 4) Due to the complexity of actual NOM constituents and the life-threatening properties of the cyanotoxins themselves, seeking a deeper insight into the toxicological properties of cross-coupling products is strongly encouraged.
- 5) Since *in vitro* assays may not always predict results *in vivo*, complementary *in vivo* assays are suggested for a comprehensive assessment of the estrogenic activity of CYL and ANA.
- 6) Considering the modulations of estrogenic CYL on E2, future CYL dose-response studies are recommended using CYL concentrations below 2.4×10^{-8} M, with the aim of assessing CYL antagonism in the YES assay.
- 7) Future investigation on ANA non-monotonic dose-response behaviours should be directed towards determining the lowest ANA concentration producing agonistic effects.
- 8) Due to the modulations of E2 induced estrogenicity seen at low cyanotoxin concentrations, priority should be given to developing guidelines for cyanotoxin exposure levels in relation to adverse health consequences.
- 9) Exploration on the inter-relationship between cyanotoxin toxicity mechanisms and their endocrine disrupting action is recommended through pathological work in conjunction with epidemiological studies.
- 10) Because of the detected estrogenicity levels of oxidized ANA, estrogenicity reduction of EDCs should not be simply predicted by their oxidized efficiency. The estrogenicity

induced by EDCs degradation products should be also considered in evaluating the estrogenicity of EDCs in the environment.

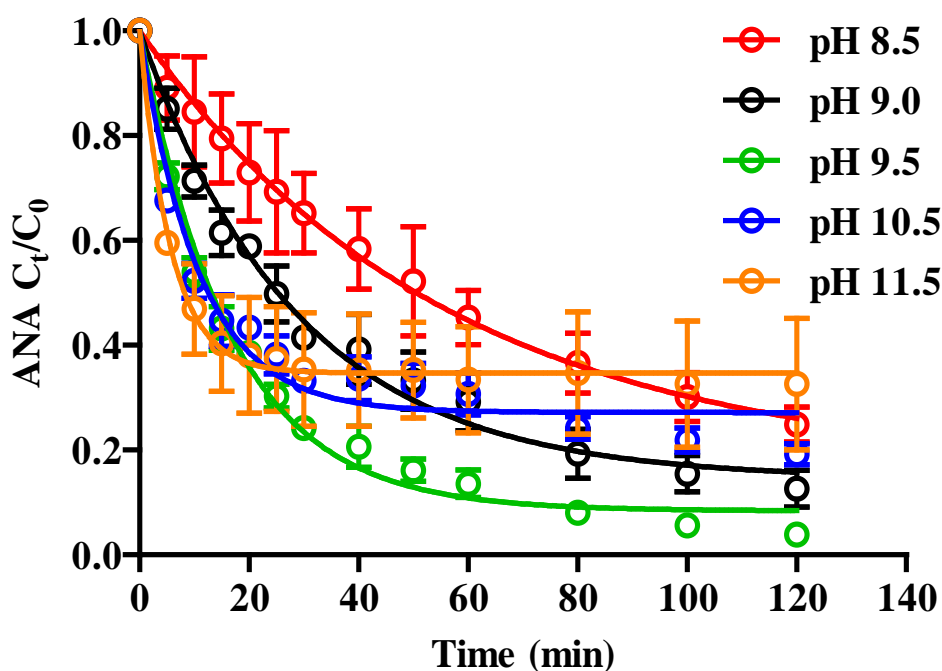
- 11) Due to the complex composition of ANA intermediate products, the application of surrogates or chemical extraction is recommended for identifying and eliminating ANA products with estrogenic activity.
- 12) Bioassays together with chromatographic quantification are recommended for an integrated assessment of EDCs estrogenic activity following their oxidative degradation.

Appendix - Chapter 2



(a)

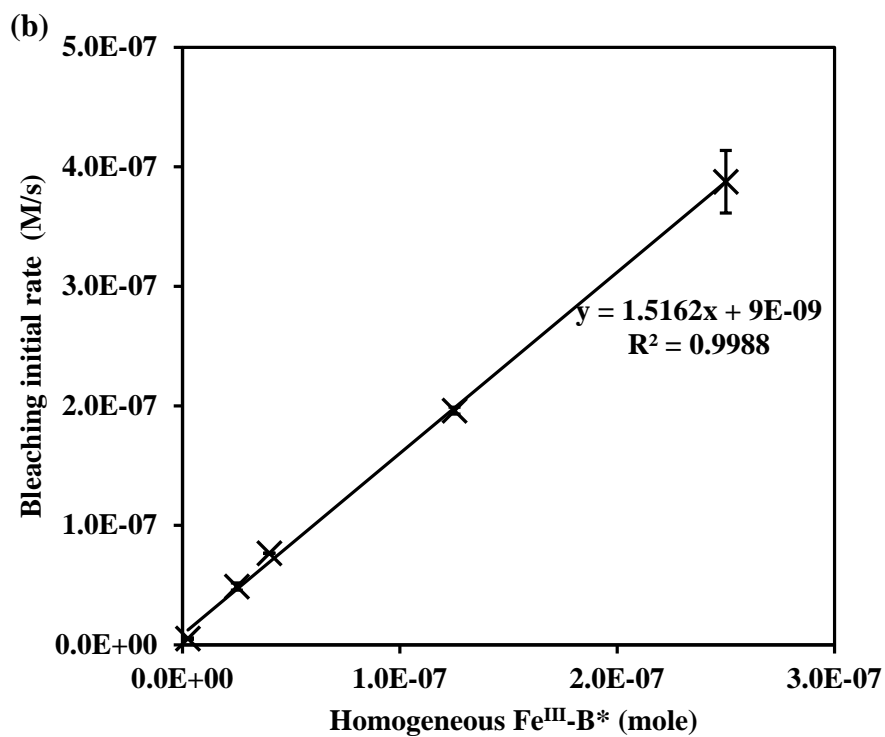
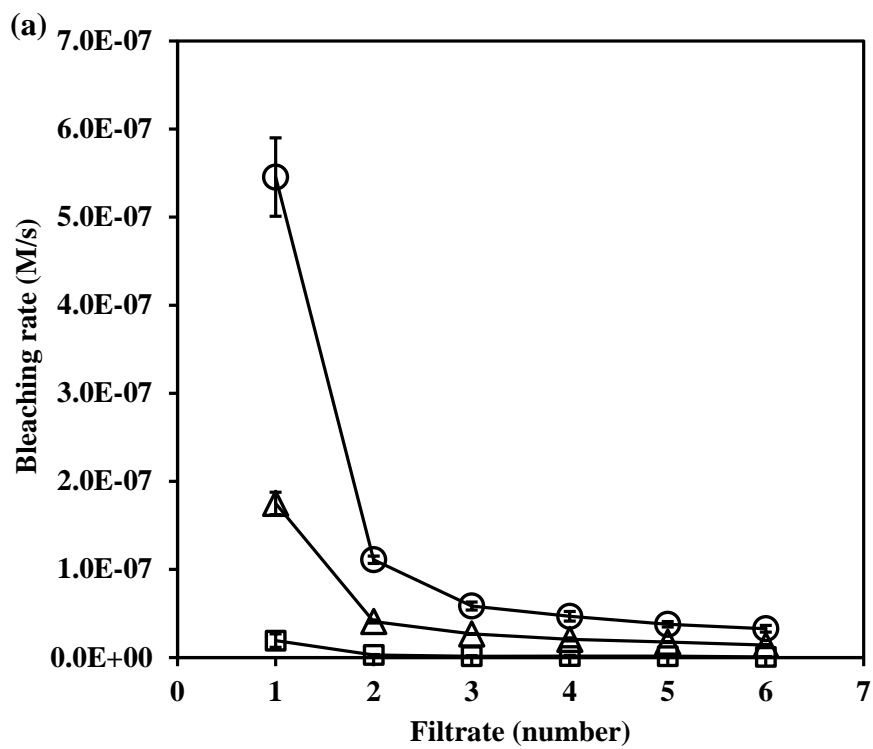
pH	k (min ⁻¹) with 95 % confidence intervals	C _{res} with 95 % confidence intervals	R ²
8.5	0.1047 [0.1032 - 0.1061]	0.1081 [0.1044 - 0.1118]	0.9998
9	0.07854 [0.07474 - 0.08235]	0.1266 [0.1124 - 0.1408]	0.9981
9.5	0.09798 [0.09326 - 0.1027]	0.1374 [0.1248 - 0.1500]	0.9981
10.5	0.1653 [0.1568 - 0.1738]	0.242 [0.2333 - 0.2508]	0.9983
11.5	0.2788 [0.2644 - 0.2933]	0.3029 [0.2973 - 0.3085]	0.9989



(b)

pH	k (min ⁻¹) with 95 % confidence intervals	C _{res} with 95 % confidence intervals	R ²
8.5	0.0181 [0.01590 - 0.02030]	0.1657 [0.1131 - 0.2184]	0.9959
9	0.03477 [0.02983 - 0.03970]	0.1445 [0.09800 - 0.1910]	0.9889
9.5	0.06025 [0.05233 - 0.06818]	0.08396 [0.04844 - 0.1195]	0.988
10.5	0.09244 [0.06956 - 0.1153]	0.2716 [0.2293 - 0.3140]	0.9591
11.5	0.1764 [0.1574 - 0.1954]	0.3467 [0.3355 - 0.3579]	0.9943

Figure A2.1: Cyanotoxin degradation data fitted by Eq.1. (a) CYL degradation at different pH by homogeneous Fe^{III}-B*/H₂O₂; (b) ANA degradation at different pH by homogeneous Fe^{III}-B*/H₂O₂.



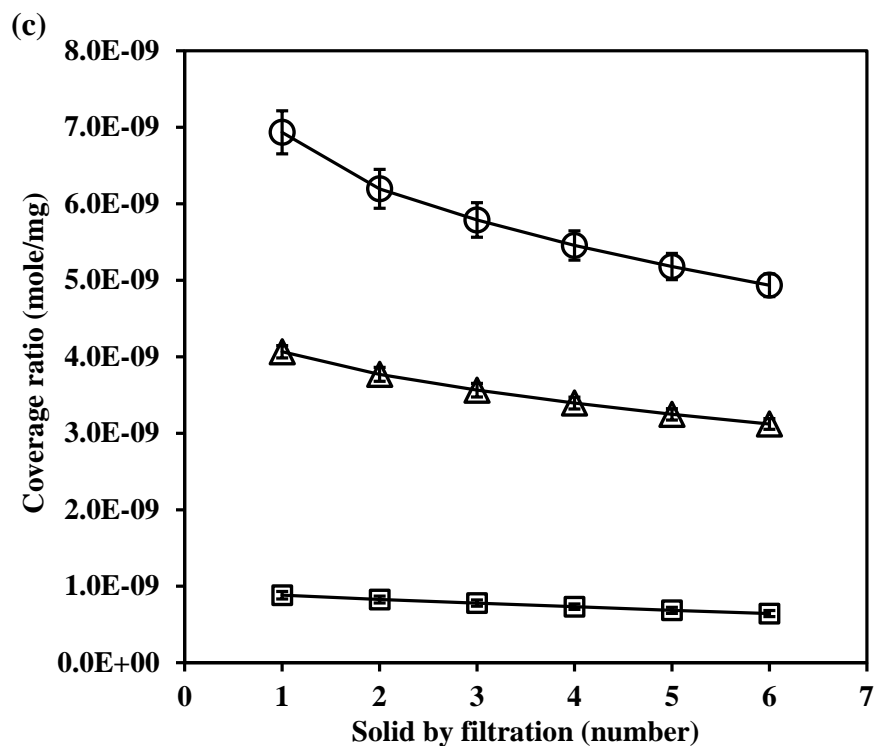
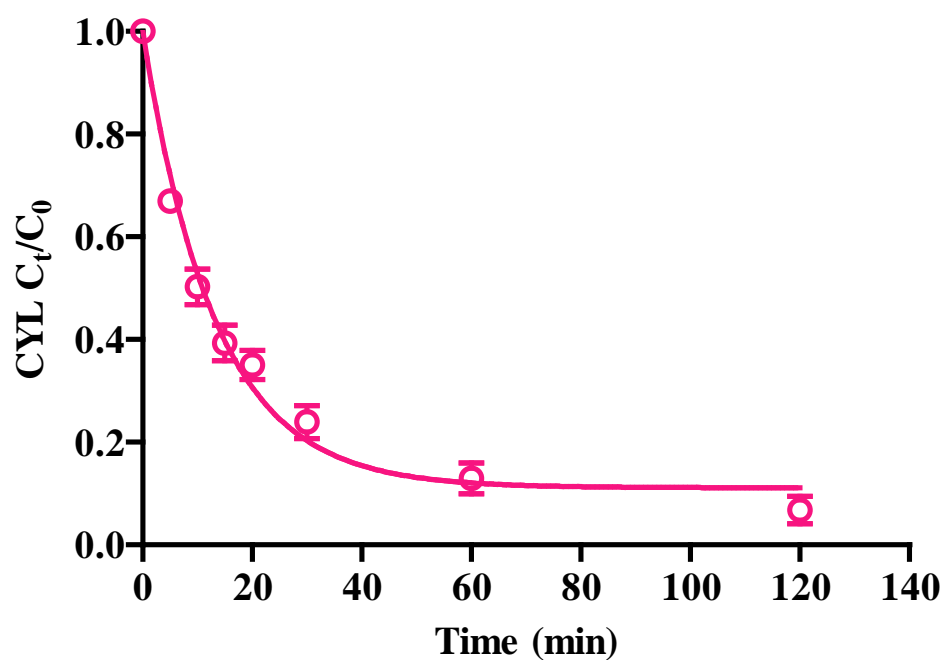
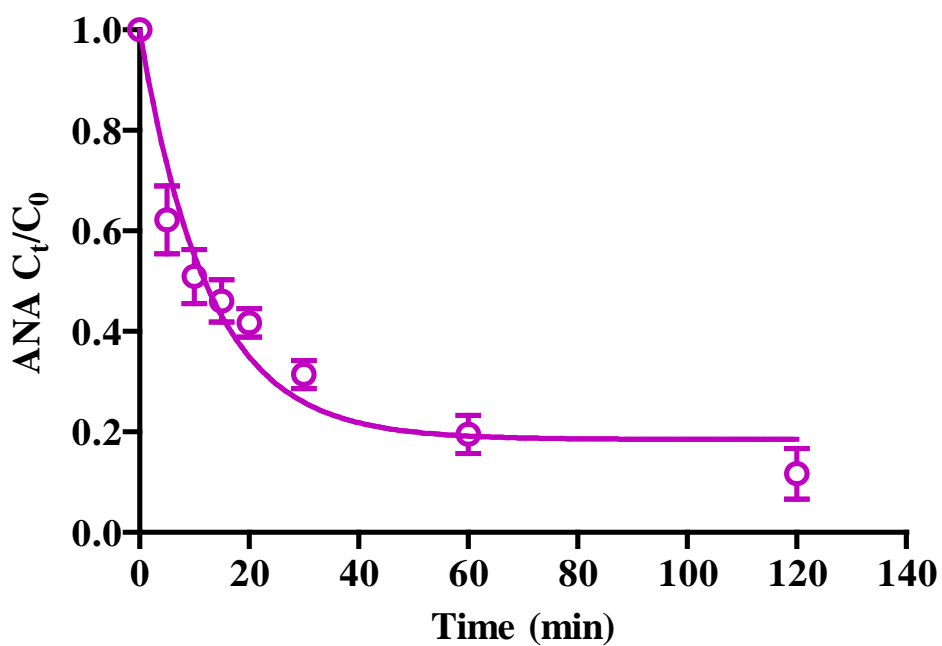


Figure A2.2: Coverage assessment of heterogeneous Fe^{III}-B*. (a) The initial rates of orange dye (45 μ M) bleaching by filtrate from heterogeneous Fe^{III}-B* generation (2.5×10^{-6} (○), 1.25×10^{-6} (△) and 2.5×10^{-7} (□) mole homogeneous Fe^{III}-B* and 240 mg MSG) and H₂O₂ (1 mM) at pH 9.5 (0.01 M); (b) the initial rates of orange dye (45 μ M) bleaching by homogeneous Fe^{III}-B* standards (2.5×10^{-9} , 2.5×10^{-8} , 4×10^{-8} , 1.25×10^{-7} and 2.5×10^{-7} mole) and H₂O₂ (1 mM) at pH 9.5 (0.01 M); (c) the coverage ratios of heterogeneous Fe^{III}-B* (mean \pm standard deviation of three independent runs).



(a)

pH	k (min ⁻¹) with 95 % confidence intervals	C _{res} with 95 % confidence intervals	R ²
9.5	0.07565 [0.06523 - 0.08608]	0.1113 [0.06939 - 0.1532]	0.9612

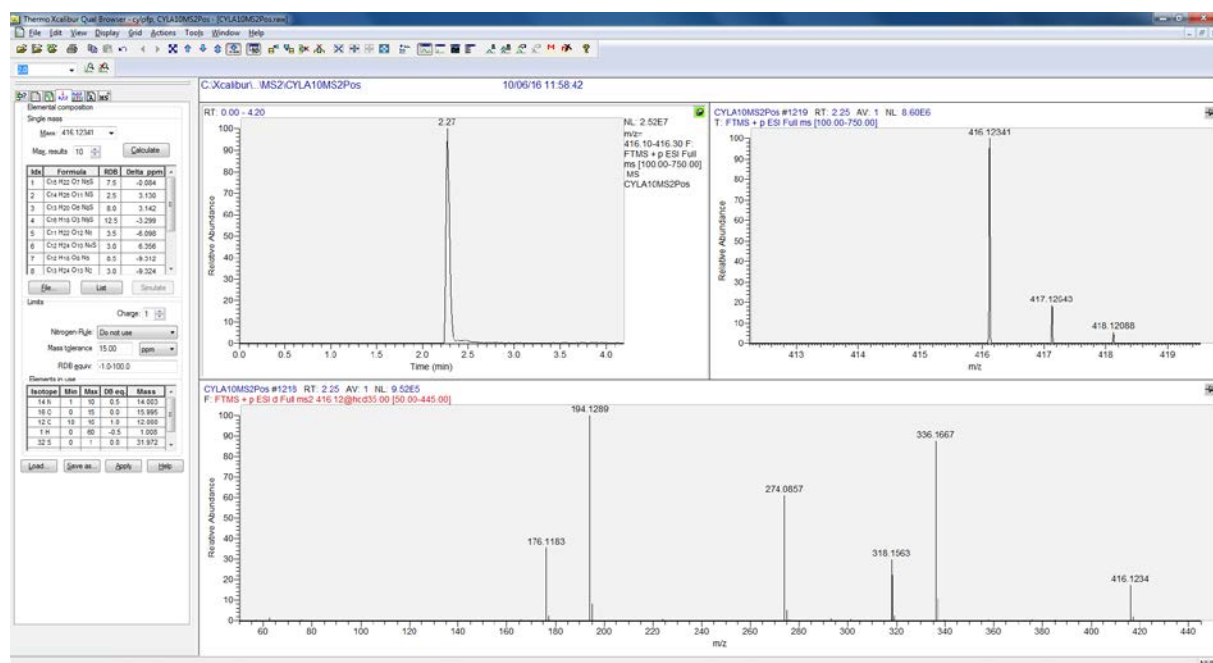


(b)

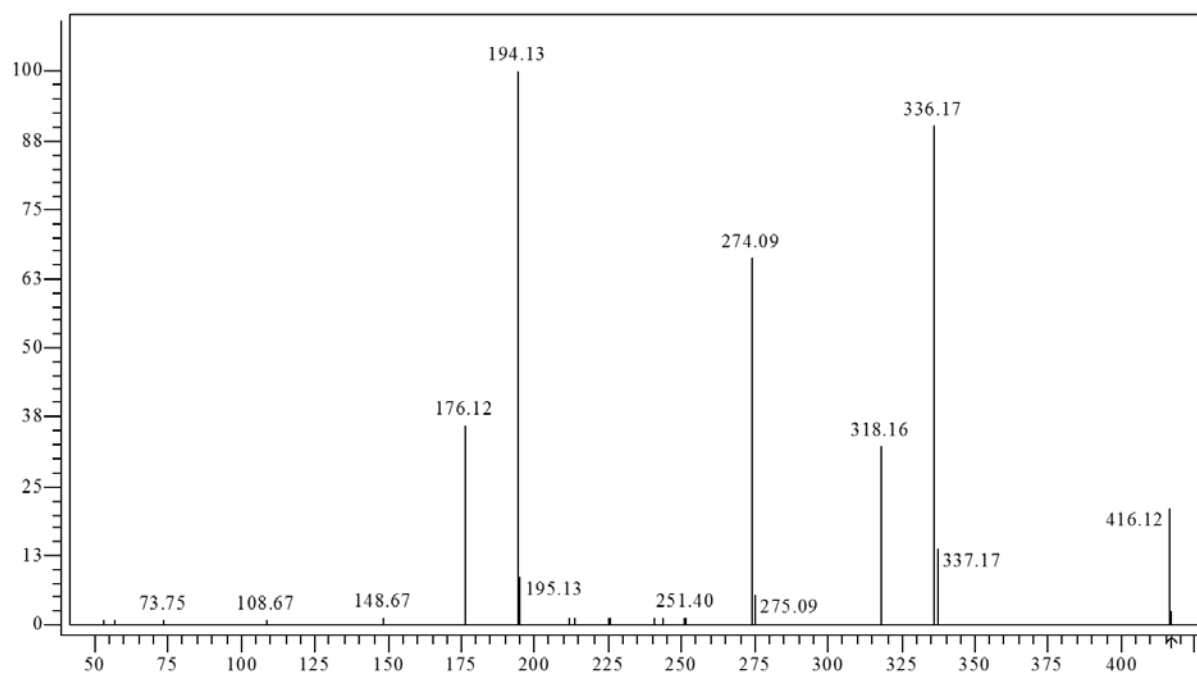
pH	k (min ⁻¹) with 95 % confidence intervals	C _{res} with 95 % confidence intervals	R ²
9.5	0.07994 [0.05998 - 0.09991]	0.1851 [0.1171 - 0.2531]	0.8762

Figure A2.3: Cyanotoxin degradation data fitted by Eq.1. (a) CYL degradation at pH 9.5 by heterogeneous Fe^{III}-B*/H₂O₂; (b) ANA degradation at pH 9.5 by heterogeneous Fe^{III}-B*/H₂O₂.

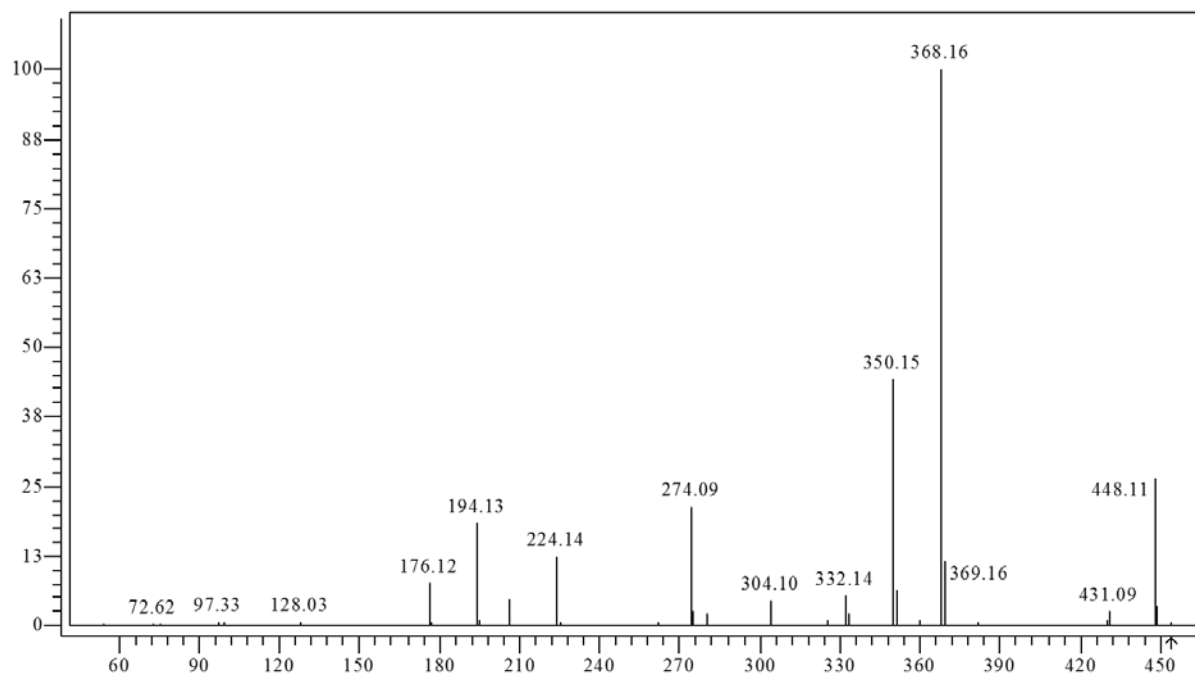
(a)



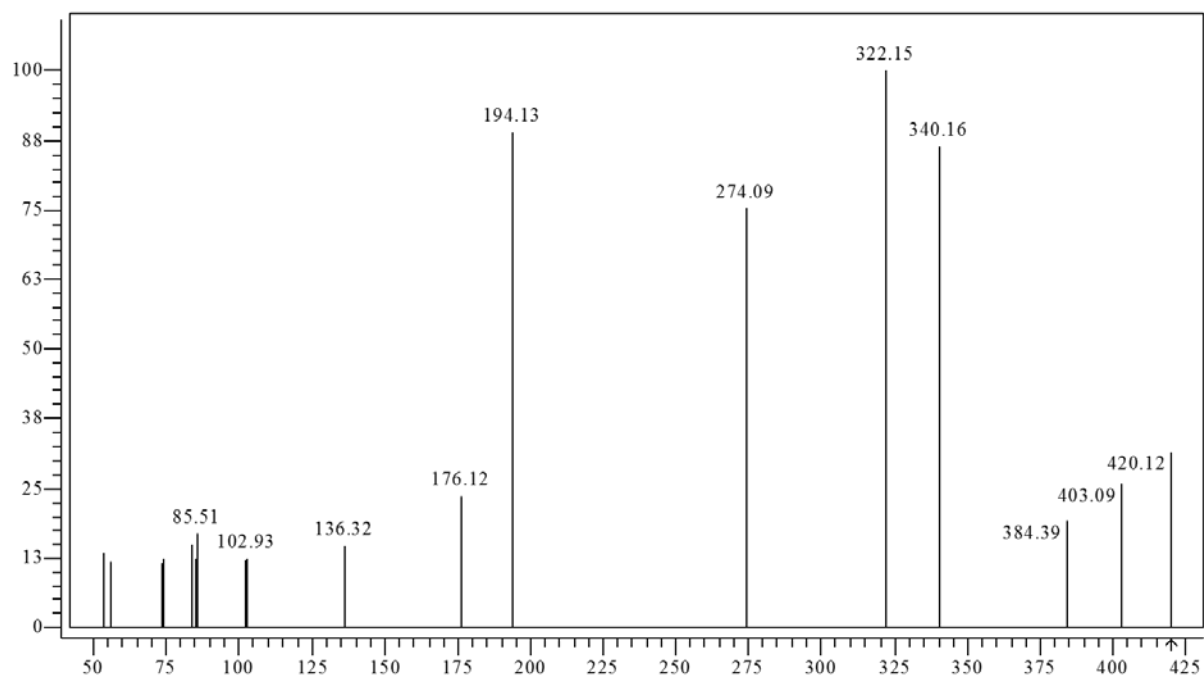
(b)



(c)



(d)



(e)

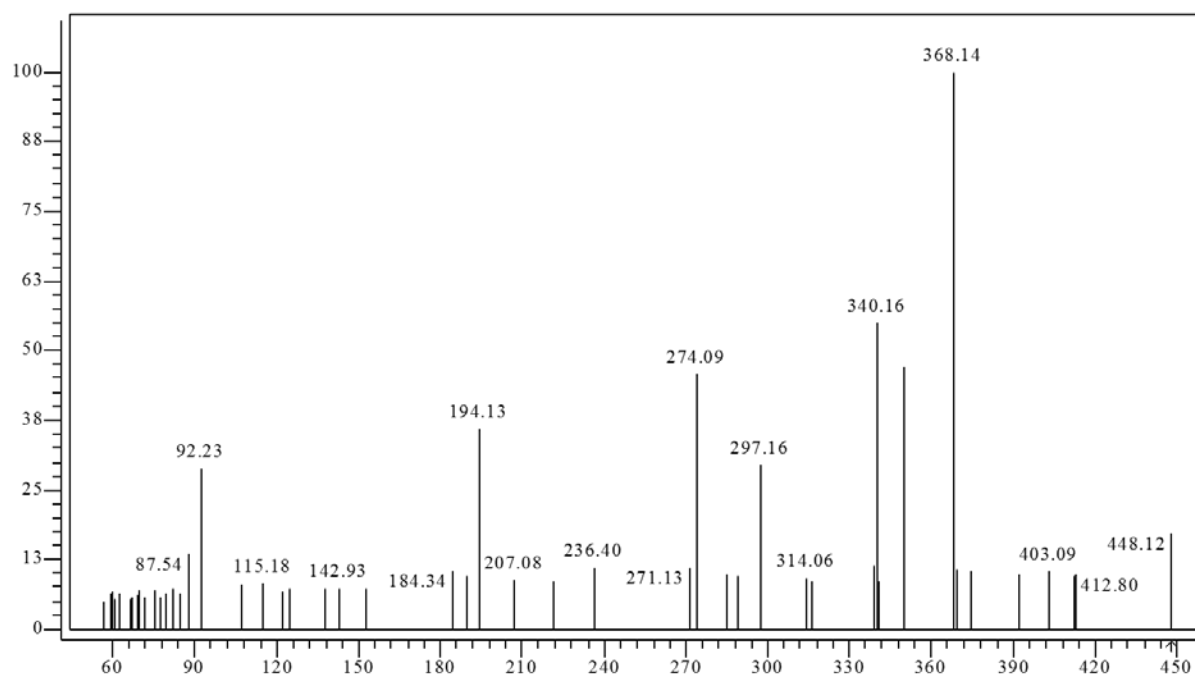
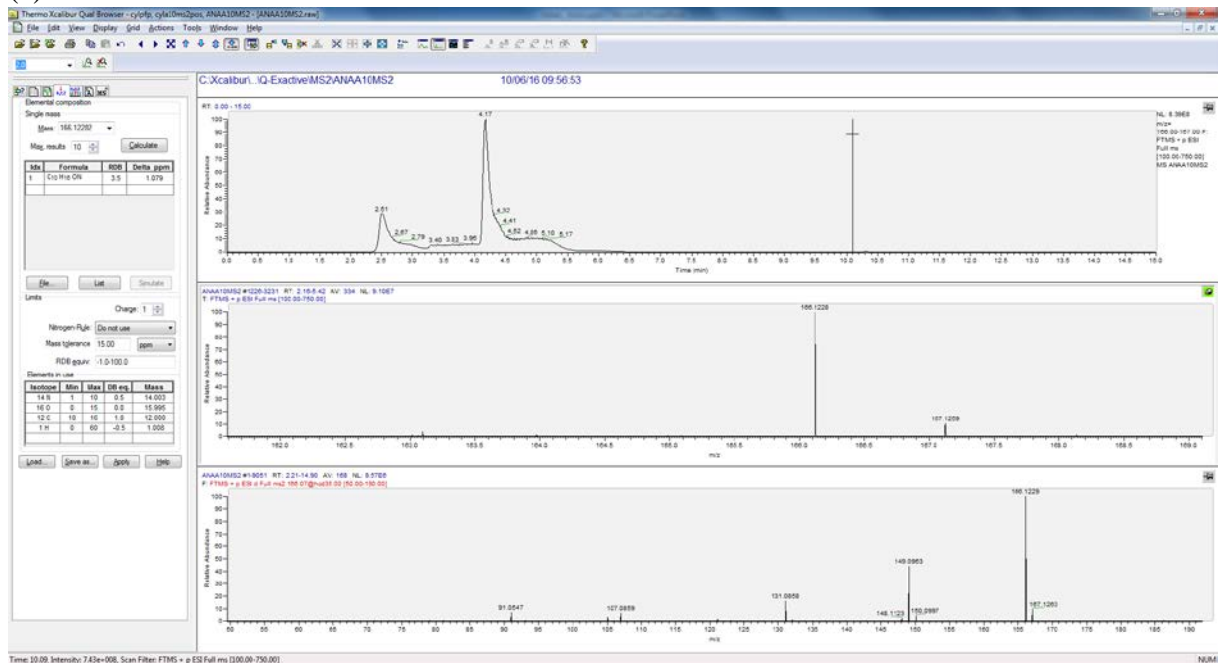
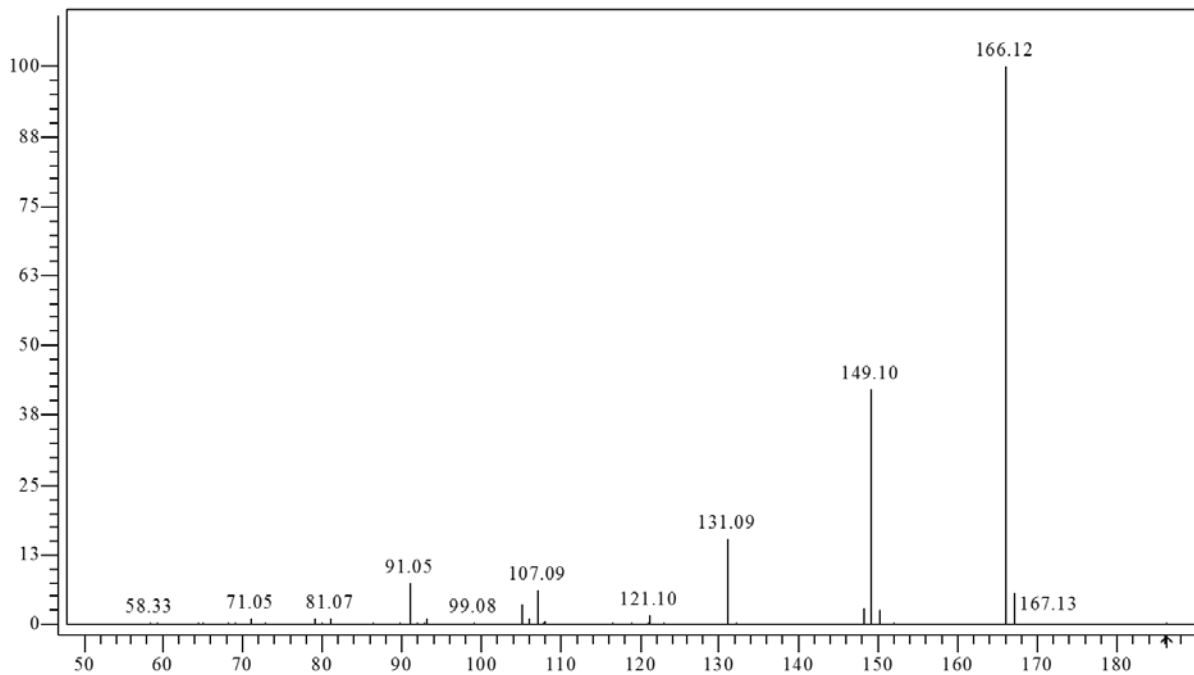


Figure A2.4: Positive mode Q-Exactive tandem mass spectra of CYL: (a) product ion spectrum MS^1 (targeting m/z 416); (b) product ion spectrum MS^2 (targeting m/z 416); (c) product ion spectrum MS^2 (targeting m/z 448); (d) product ion spectrum MS^2 (targeting m/z 420); (e) composite spectrum of m/z 416.

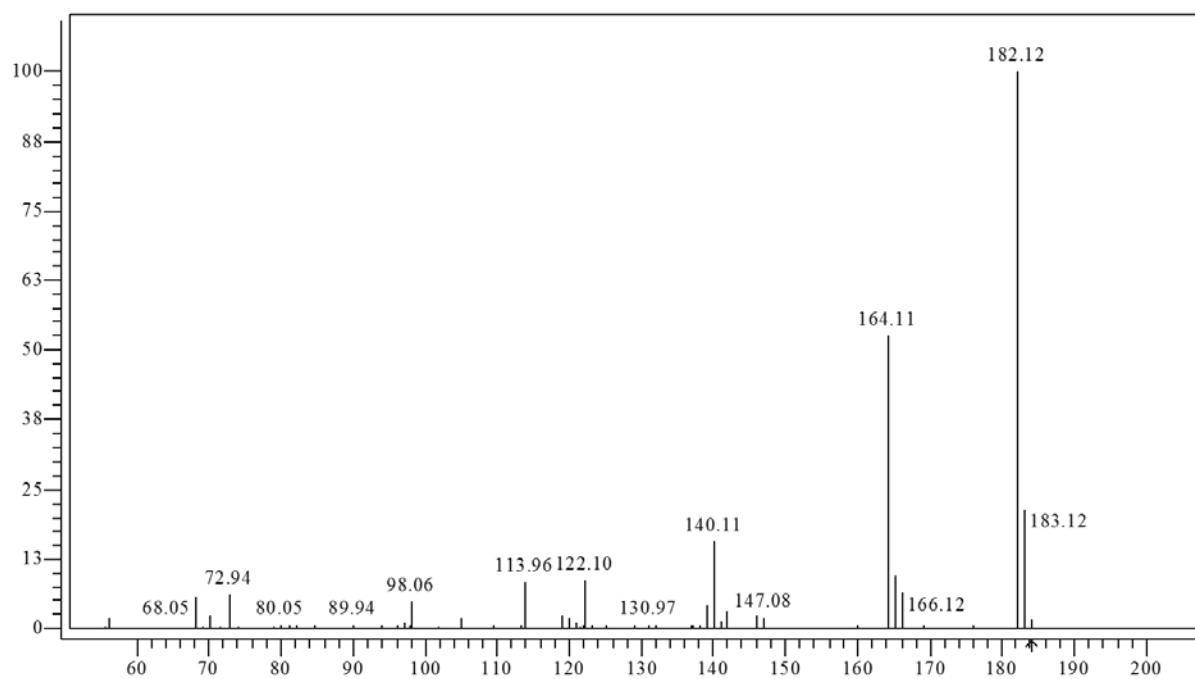
(a)



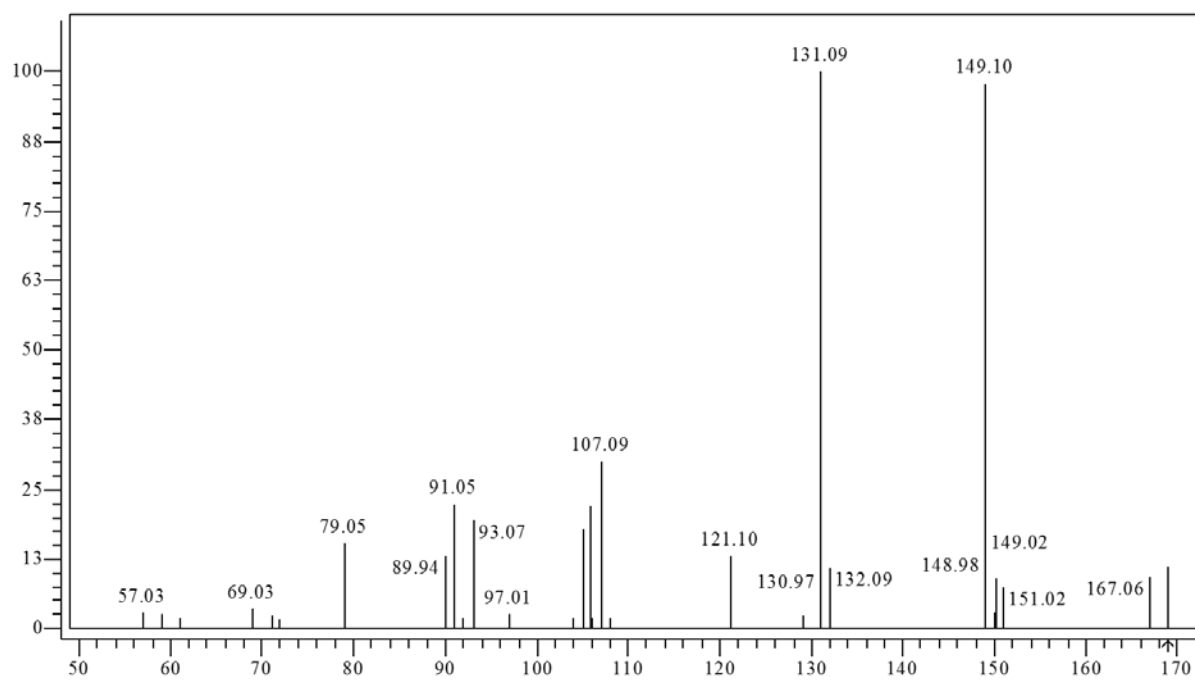
(b)



(c)



(d)



(e)

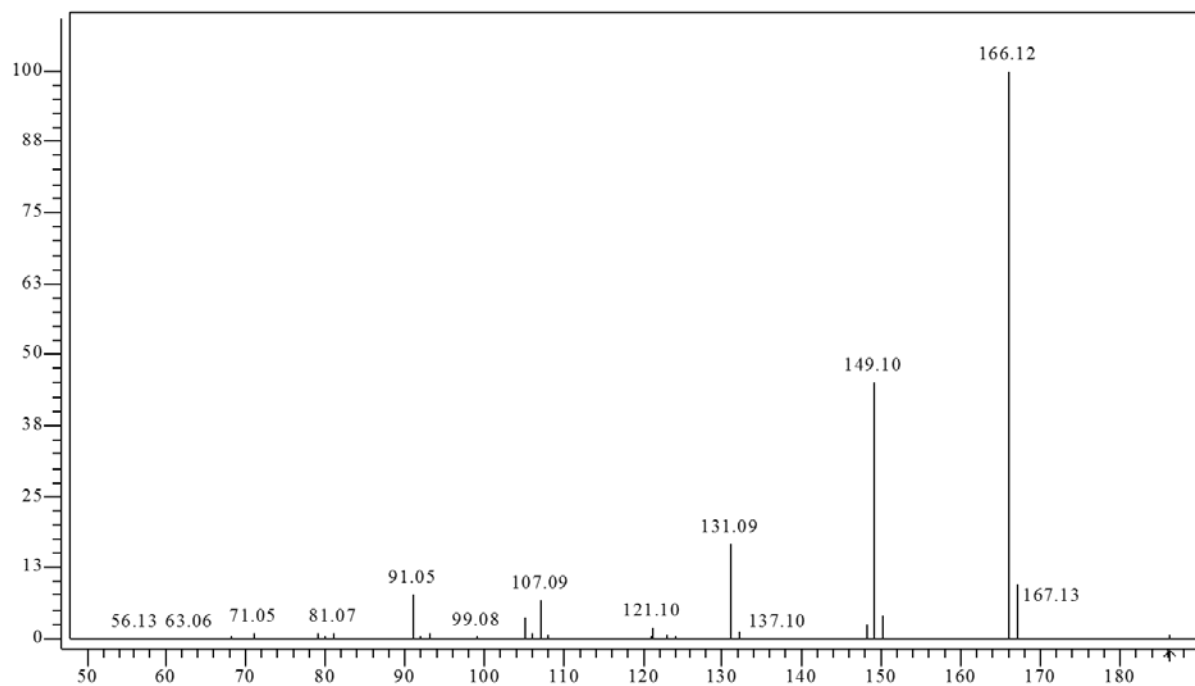
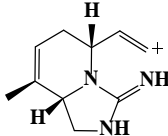
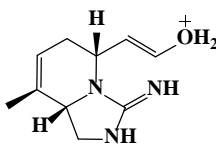
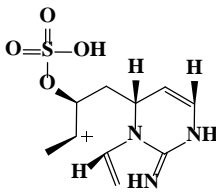
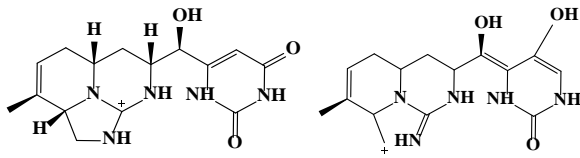
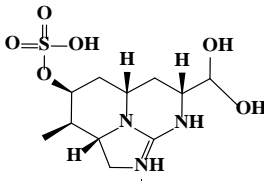
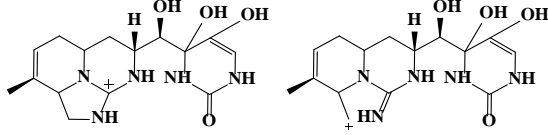
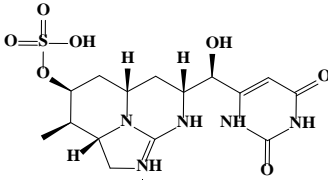


Figure A2.5: Positive mode Q-Exact tandem mass spectra of ANA: (a) product ion spectrum MS¹ (targeting *m/z* 166); (b) product ion spectrum MS² (targeting *m/z* 166); (c) product ion spectrum MS² (targeting *m/z* 182); (d) product ion spectrum MS² (targeting *m/z* 149); (e) composite spectrum of *m/z* 166.

Table A2.1: Proposed structures and formula for the CID product ions from CYL mass spectra

Accurate mass (error, ppm)	RDB	Proposed product ion structure and molecular formula
176.1183 (0.43)	5.5	 $C_{10}H_{14}N_3^+$
194.1288 (0.06)	4.5	 $C_{10}H_{16}N_3O^+$
274.0855 (0.45)	4.5	 $C_{10}H_{16}N_3O_4S^+$
318.1564 (0.96)	8.5	 $C_{15}H_{20}N_5O_3^+$
322.1072 (1.30)	3.5	 $C_{11}H_{20}N_3O_6S^+$
336.1668 (0.36)	7.5	 $C_{15}H_{22}N_5O_4^+$
416.1235 (0.06)	7.5	 $C_{15}H_{22}N_5O_7S^+$

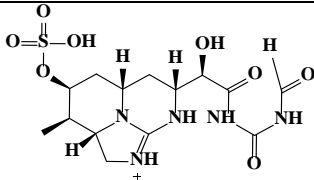
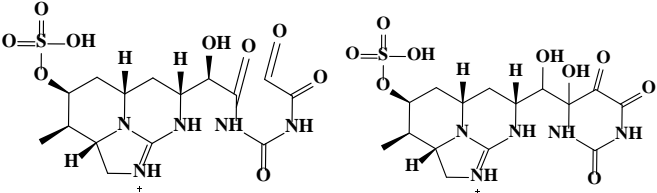
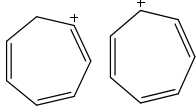
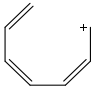
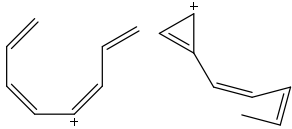
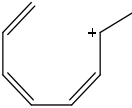
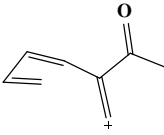
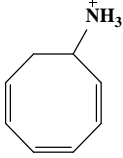
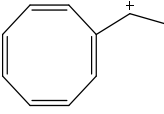
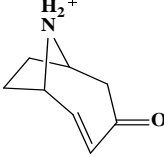
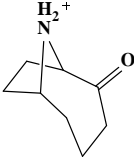
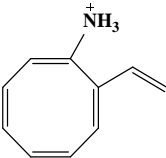
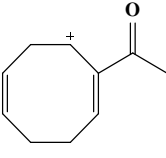
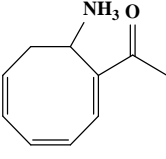
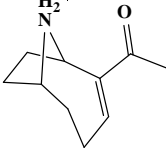
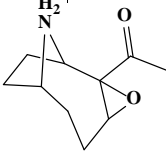
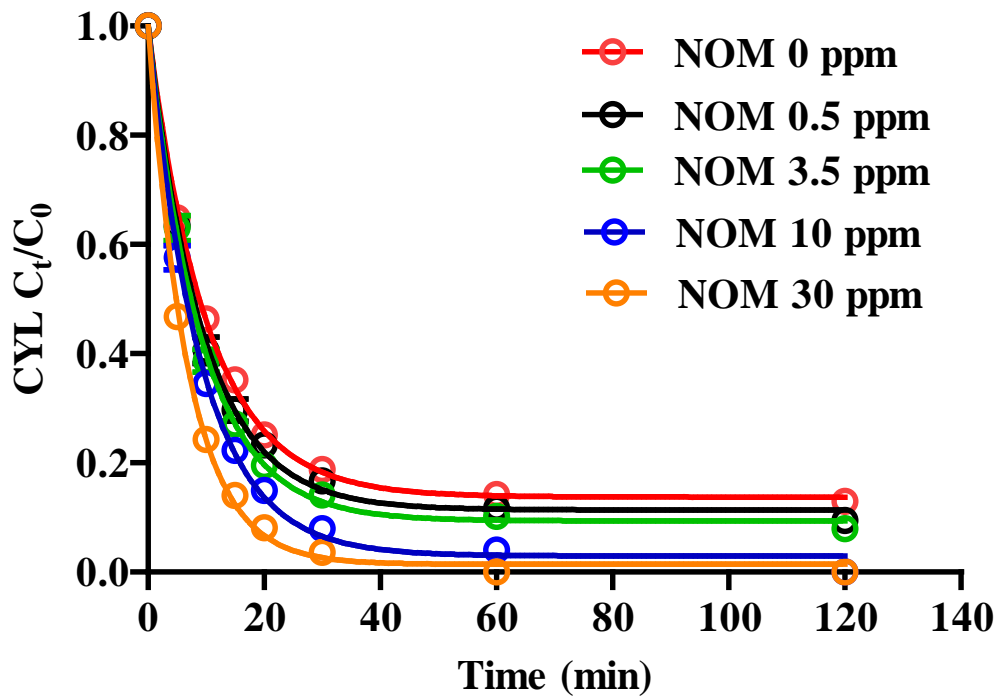
Accurate mass (error, ppm)	RDB	Proposed product ion structure and molecular formula
420.1182 (0.48)	6.5	 <p data-bbox="932 528 1054 562">$C_{14}H_{22}N_5O_8S^+$</p>
448.1133 (0.08)	7.5	 <p data-bbox="767 786 890 819">$C_{15}H_{22}N_5O_9S^+$</p> <p data-bbox="1107 786 1230 819">$C_{15}H_{22}N_5O_9S^+$</p>

Table A2.2: Proposed structures and formula for the CID product ions from ANA mass spectra

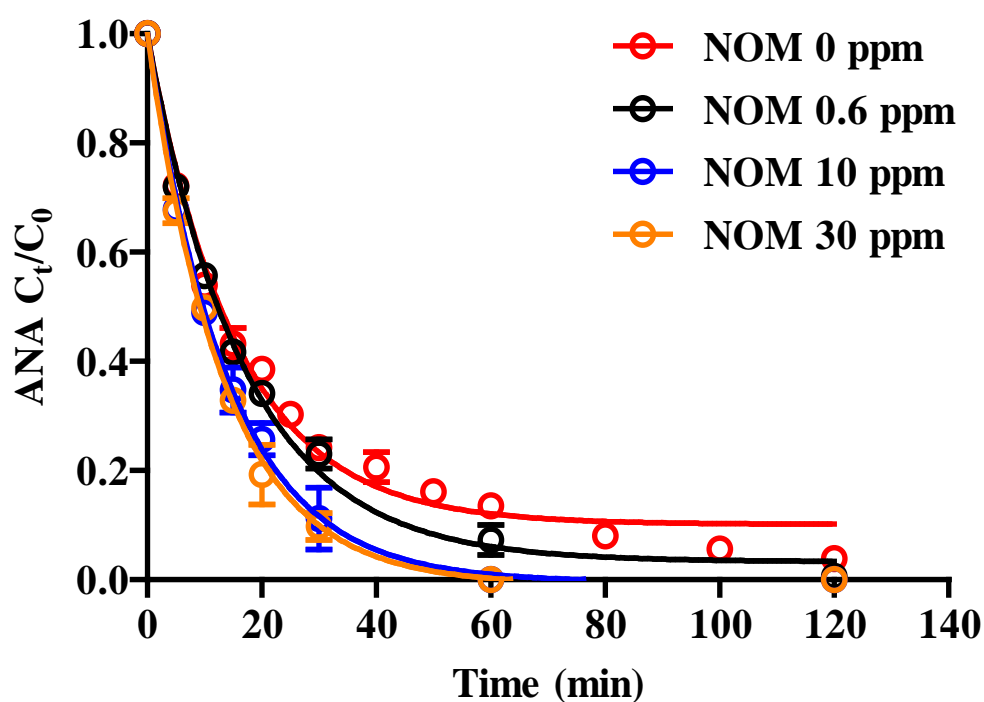
Accurate mass (error, ppm)	RDB	Proposed product ion structure and molecular formula
91.0546 (0.34)	4.5	 $C_7H_7^+$ $C_7H_7^+$
93.0704 (0.53)	3.5	 $C_7H_9^+$
105.0702 (0.28)	4.5	 $C_8H_9^+$ $C_8H_9^+$
107.0859 (0.40)	3.5	 $C_8H_{11}^+$
121.0652 (0.39)	4.5	 $C_8H_9O^+$
122.0967 (0.23)	3.5	 $C_8H_{12}N^+$
131.0857 (1.47)	5.5	 $C_{10}H_{11}^+$
138.0914 (0.060)	3.5	 $C_8H_{12}NO^+$

Accurate mass (error, ppm)	RDB	Proposed product ion structure and molecular formula
140.1071 (0.08)	2.5	 $C_8H_{14}NO^+$
146.0964 (0.01)	5.5	 $C_{10}H_{12}N^+$
149.0963 (1.20)	4.5	 $C_{10}H_{13}O^+$
164.1072 (0.20)	4.5	 $C_{10}H_{14}NO^+$
166.1228 (1.14)	3.5	 $C_{10}H_{16}NO^+$
182.1177 (0.14)	3.5	 $C_{10}H_{16}NO_2^+$

Appendix - Chapter 3



NOM	k (min ⁻¹) with 95 % confidence intervals	C _{res} with 95 % confidence intervals	R ²
0	0.09798 [0.09326 - 0.1027]	0.1374 [0.1248 - 0.1500]	0.9981
0.5	0.1058 [0.09817 - 0.1135]	0.1138 [0.09504 - 0.1326]	0.9959
3.5	0.1087 [0.1023 - 0.1151]	0.09376 [0.07839 - 0.1091]	0.9973
10	0.1099 [0.1031 - 0.1168]	0.02957 [0.01229 - 0.04685]	0.997
30	0.1464 [0.1387 - 0.1541]	0.01424 [0.001682 - 0.02679]	0.9981



(b)

NOM	k (min^{-1}) with 95 % confidence intervals	C_{res} with 95 % confidence intervals	R^2
0	0.06025 [0.05233 - 0.06818]	0.08396 [0.04844 - 0.1195]	0.988
0.6	0.05919 [0.05383 - 0.06454]	0.03301 [0.0002817 - 0.06574]	0.9928
10	0.07067 [0.06367 - 0.07768]	-0.00462 [-0.03958 - 0.03034]	0.9916
30	0.07439 [0.06757 - 0.08120]	-0.00902 [-0.04083 - 0.02279]	0.993

Figure A3.1: Cyanotoxin degradation data fitted by Eq.1. (a) CYL degradation by $\text{Fe}^{\text{III}}\text{-B}^*/\text{H}_2\text{O}_2$ with varying NOM; (b) ANA degradation by $\text{Fe}^{\text{III}}\text{-B}^*/\text{H}_2\text{O}_2$ with varying NOM.

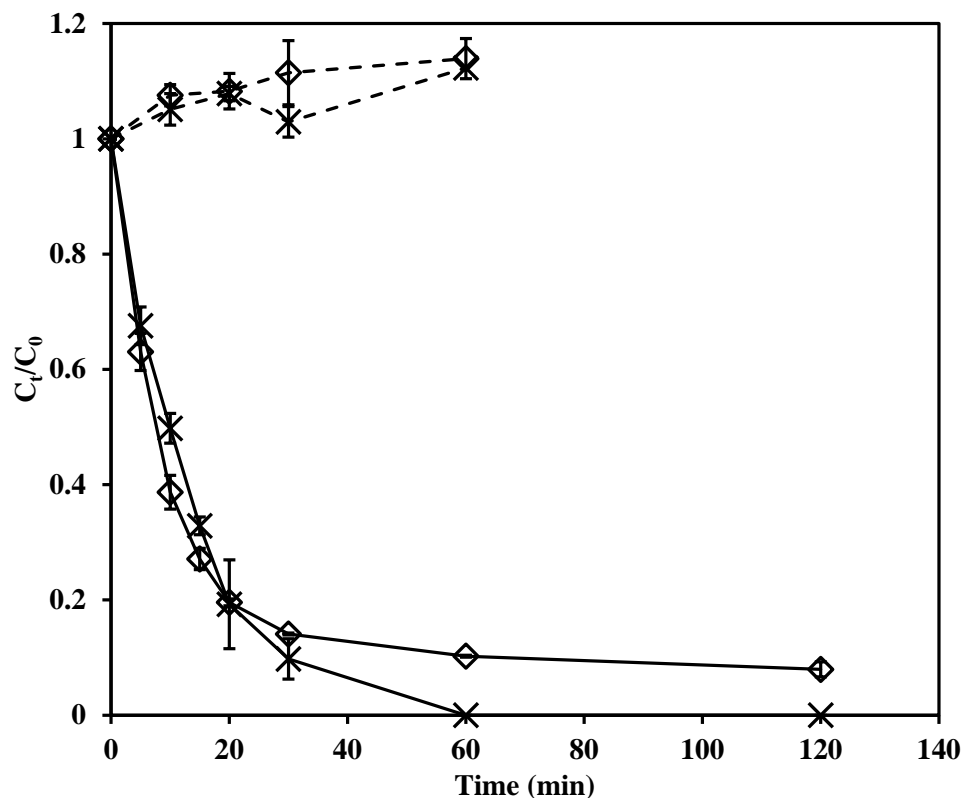


Figure A3.2: Cyanotoxin removal by Fe^{III}-B*/H₂O₂ with NOM or with oxidized NOM at pH 9.5 (0.01 M). —◇— represents sample of CYL (0.24 μM) with NOM (3.5 ppm) removal by Fe^{III}-B*/H₂O₂ (5 μM/ 5 mM), —x— represents sample of ANA (7.1 μM) with NOM (30 ppm) removal by Fe^{III}-B*/H₂O₂ (5 μM/ 5 mM), - -◇- - represents sample of CYL (0.24 μM) removal by oxidized NOM (3.5 ppm), - -x- - represents sample of ANA (7.1 μM) removal by oxidized NOM (30 ppm) (mean ± standard deviation of three independent runs).

Conditions: oxidized NOM was produced by NOM (3.5 ppm NOM designated for CYL, 30 ppm NOM designated for ANA) reacting with Fe^{III}-B*/H₂O₂ (5 μM/ 5 mM) at pH 9.5 0.01 M Na₂CO₃/NaHCO₃ buffer. Reacting NOM was taken at intervals and treated with catalase. The oxidized NOM was then mixed with CYL (0.24 μM) or ANA (7.1 μM) thoroughly. Cyanotoxin was quantified by LC-MS.

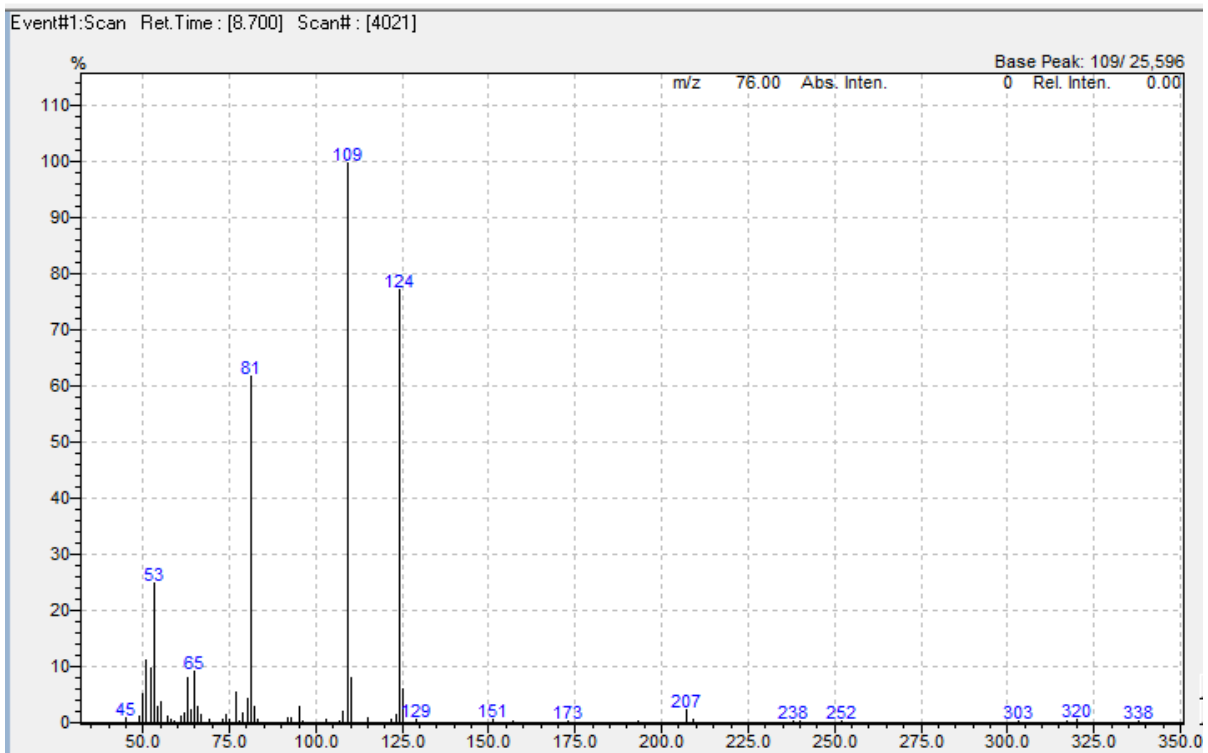
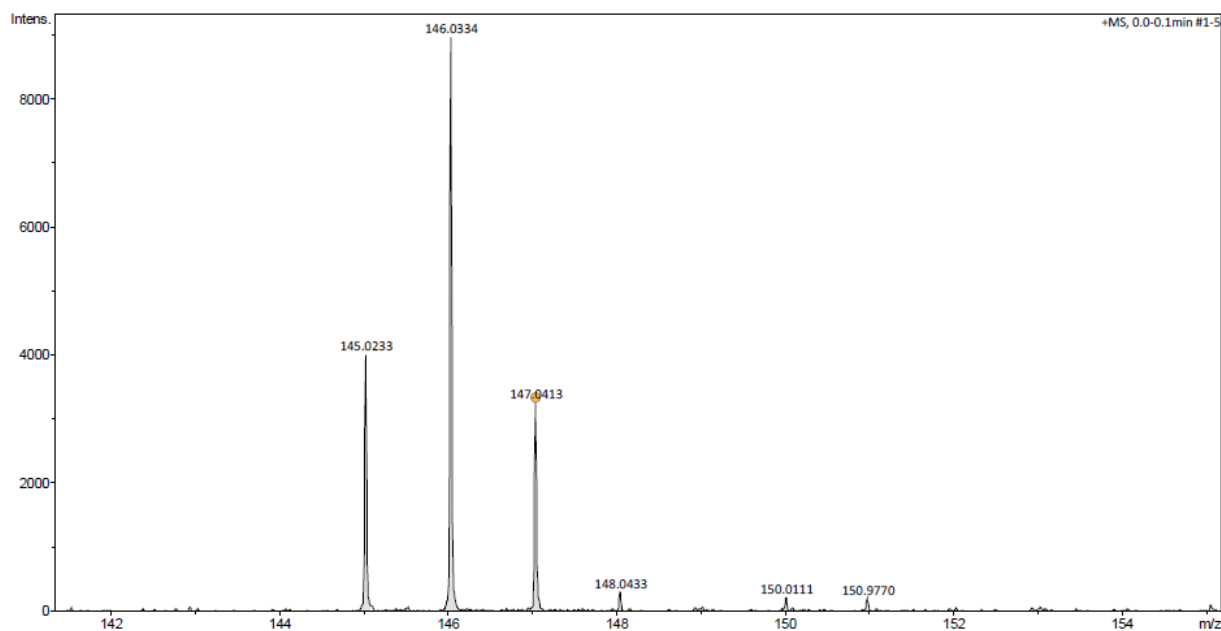


Figure A3.3: Gas chromatographic profile obtained by the analysis of guaiacol at 0.088 ppm.



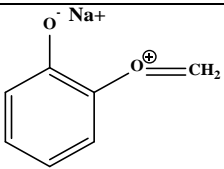
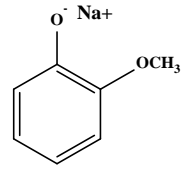
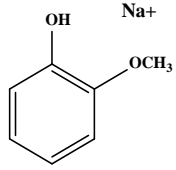
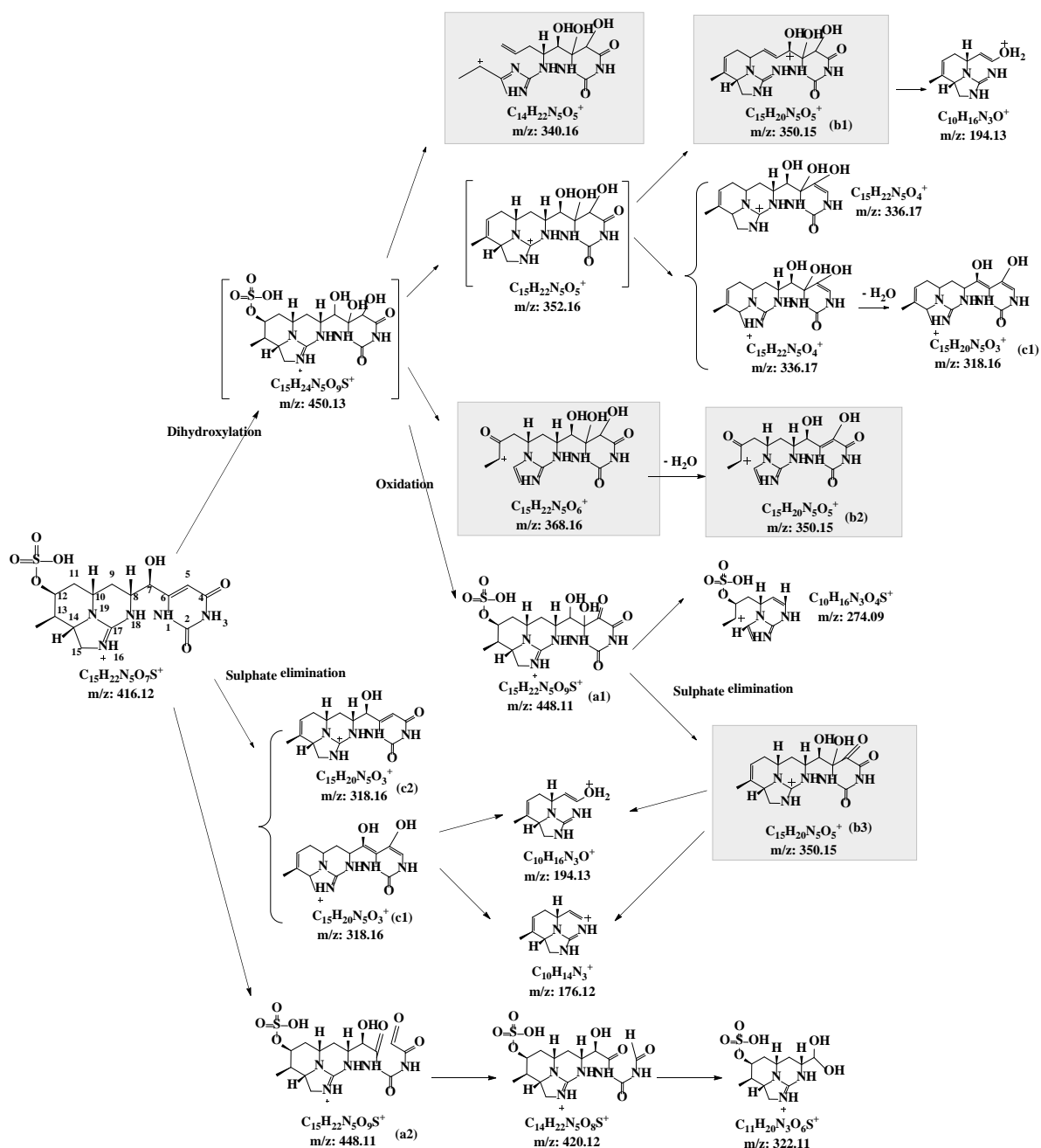
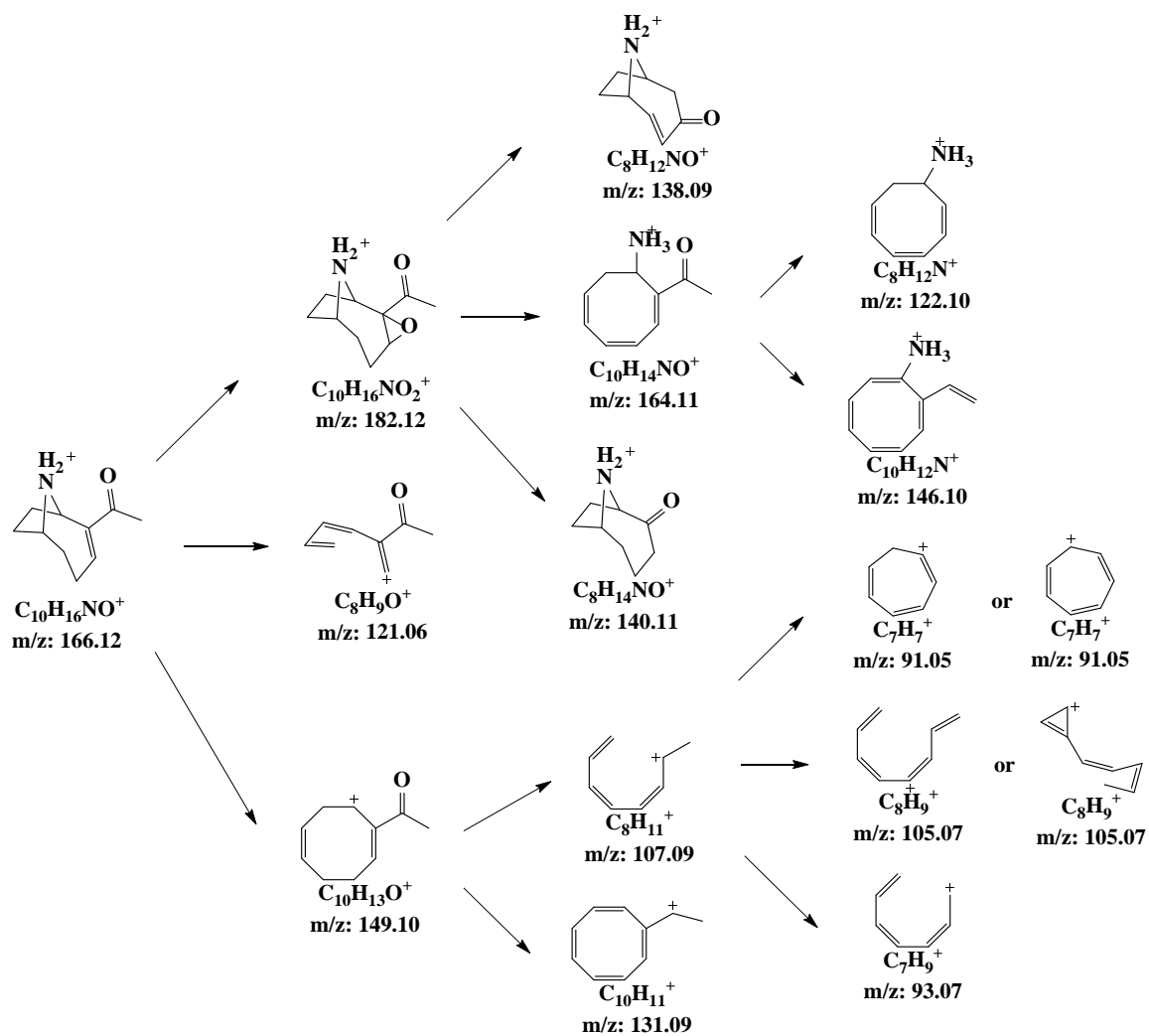
Accurate mass (error, ppm)	RDB	Proposed product ion structure and molecular formula
145.0260 (-18.62)	4.5	 $C_7H_6NaO_2^+$
146.0344 (-2.92)	4.0	 $C_7H_7NaO_2$
147.0417 (-2.39)	3.5	 $C_7H_8NaO_2^+$

Figure A3.4: High resolution ESI (+)-MS spectrum from LC-ToF-MS/MS for guaiacol (1 μ L of guaiacol at 1.129 g/mL in 1 mL methanol) in positive ion mode.



Scheme A3.1: Proposed pathway for CYL oxidation by $Fe^{III}\text{-B}^*/H_2O_2$. Ionic species were recovered from SPE eluate and observed in the MS^1 mass spectrum. Bracketed structures were not observed but were hypothesized to be present theoretically. Shaded composition were absent in MS^1 mass spectrum but seen in the tandem mass spectra as key ions, so were included in CID fragmentations analysis.



Scheme A3.2: Proposed pathway for ANA oxidation by $\text{Fe}^{\text{III}}\text{-B}^*/\text{H}_2\text{O}_2$. Ionic species were recovered from SPE eluate and observed in the MS^1 mass spectrum.

Appendix - Chapter 4

1. The LC-MS method for CYL and ANA:

Compounds were separated on a Waters Atlantis T3 column (3 μm , 3.0 \times 150 mm) at 0.2 mL/min flow rate (Temp. 30 $^{\circ}\text{C}$). Milli-Q water/0.1 % formic acid (v/v) as mobile phase A and methanol/0.1 % formic acid, (v/v) as mobile phase B were used for both cyanotoxins. The gradient elution program for CYL was 1 min: 5 % B, 8 – 12 min: 50 % B, and 16 min: 0 % B, with a linear increase between the isocratic periods. The gradient elution program for ANA was 0.01 min: 20 % B, 3 – 5 min: 90 % B, and 10 min: 20 % B, with a linear increase between the isocratic periods. CYL was monitored at m/z 416 and ANA was monitored at m/z 166 in positive ion mode (SIM). The concentration of cyanotoxin was determined based on a standard curve obtained by plotting pure cyanotoxin against the peak area of the LC-MS curve.

2. The solid-phase extraction (SPE) method for CYL and ANA:

The CYL-SPE method (Hypersep Hypercab SPE cartridges, Thermo Fisher Scientific, NZ Ltd.): 1) cartridges were conditioned with two column volumes of methanol and rinsed with two column volumes of water; 2) samples were loaded onto cartridges at a flow rate of 1 – 2 mL/min; 3) cartridges were washed with one column volume of water and fully air-dried prior to elution; and 4) CYL was eluted with 95 % methanol/ 5 % formic acid (v/v).

The ANA-SPE method (Strata-X-CW polymeric weak cation SPE cartridges, Phenomenex Australia Pty Ltd.): 1) one column volume of methanol followed by one column volume of water was applied to condition the cartridges; 2) samples were loaded after adjustment to pH 6 ~ 7; 3) one column volume of water followed by one column volume of methanol was used to wash the cartridges; and 4) samples were eluted with 5 % formic acid in methanol.

For both CYL and ANA SPE samples, the eluate was evaporated to dryness in a speed vacuum concentrator (Savant SPD131DDA, ThermoFisher) and then reconstituted in methanol for analysis.

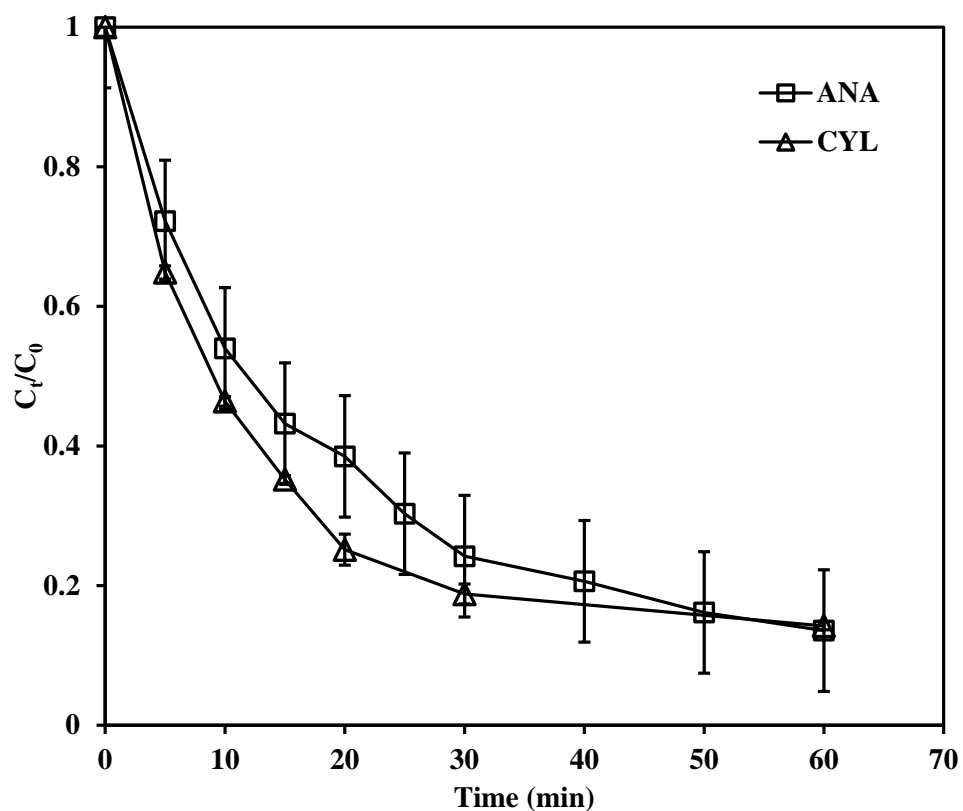
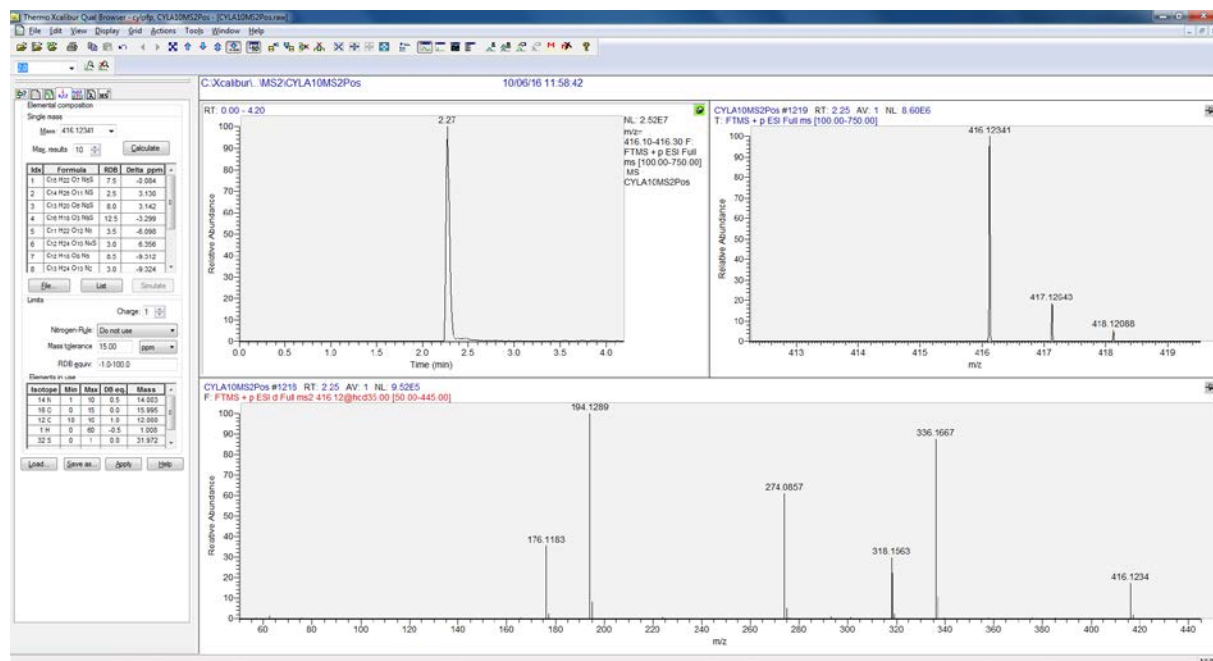
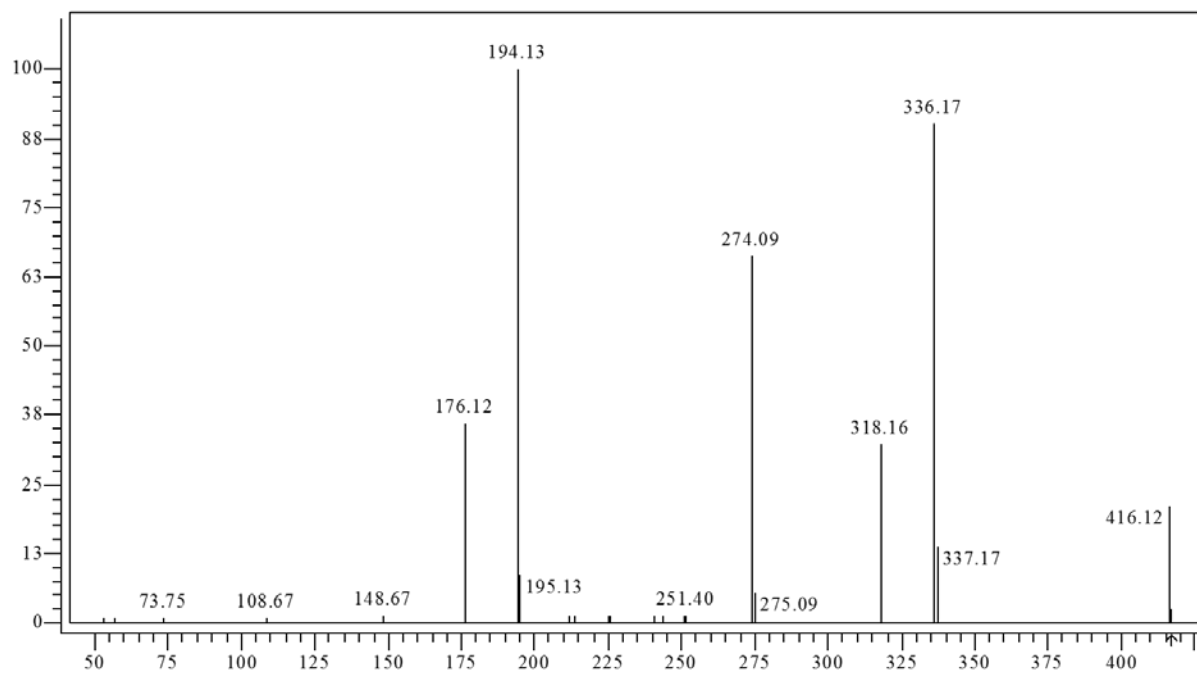


Figure A4.1: Cyanotoxins degradation by Fe^{III}-B*/H₂O₂. CYL (Δ) (2.4×10⁻⁷ M) or ANA (□) (7.1×10⁻⁶ M) treated by Fe^{III}-B*/H₂O₂ (5.0×10⁻⁶ M/ 5.0×10⁻³ M) at pH 9.5 (0.01 M Na₂CO₃/NaHCO₃ buffer).

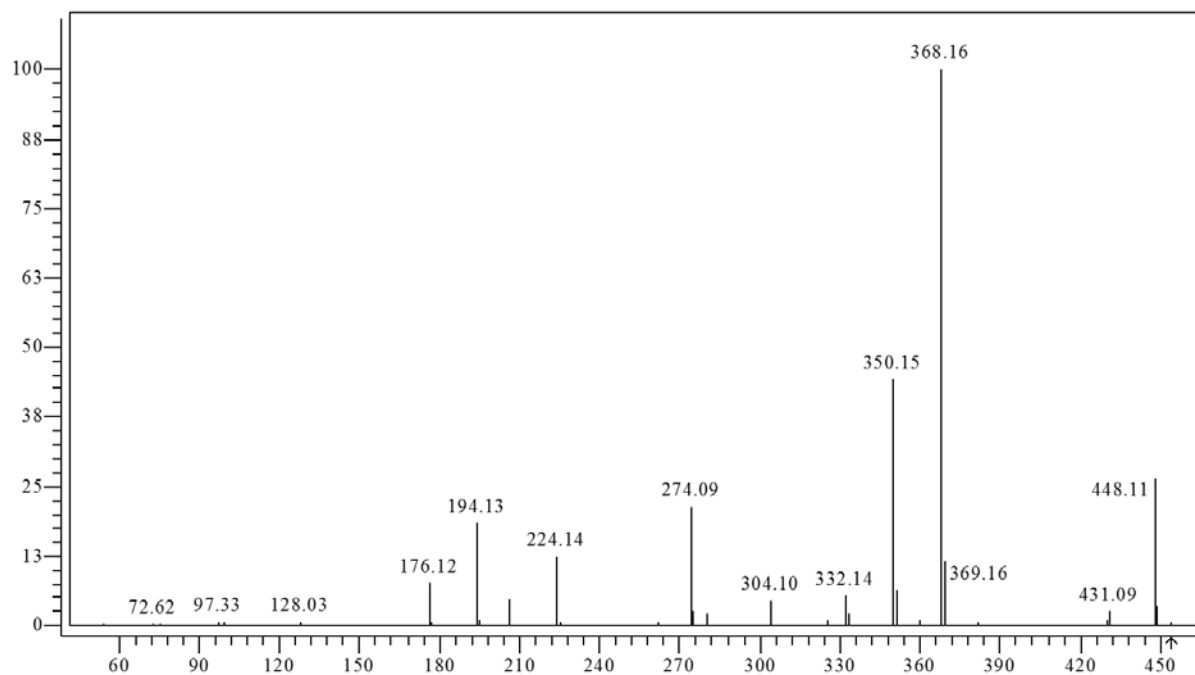
(a)



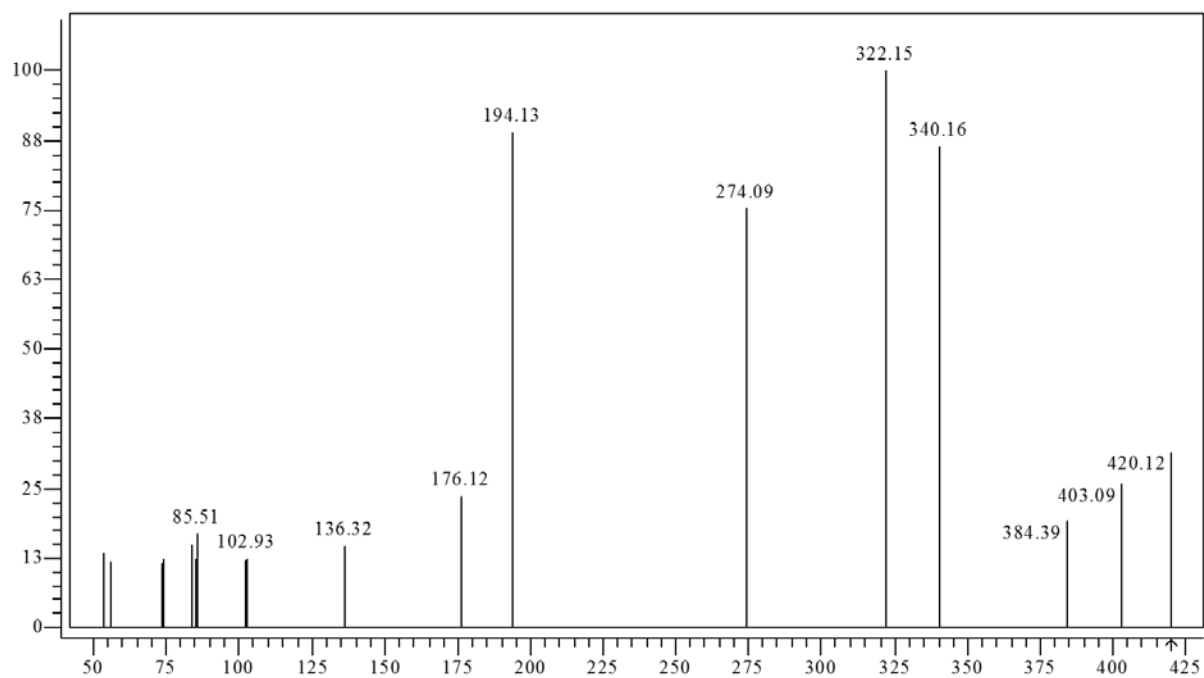
(b)



(c)



(d)



(e)

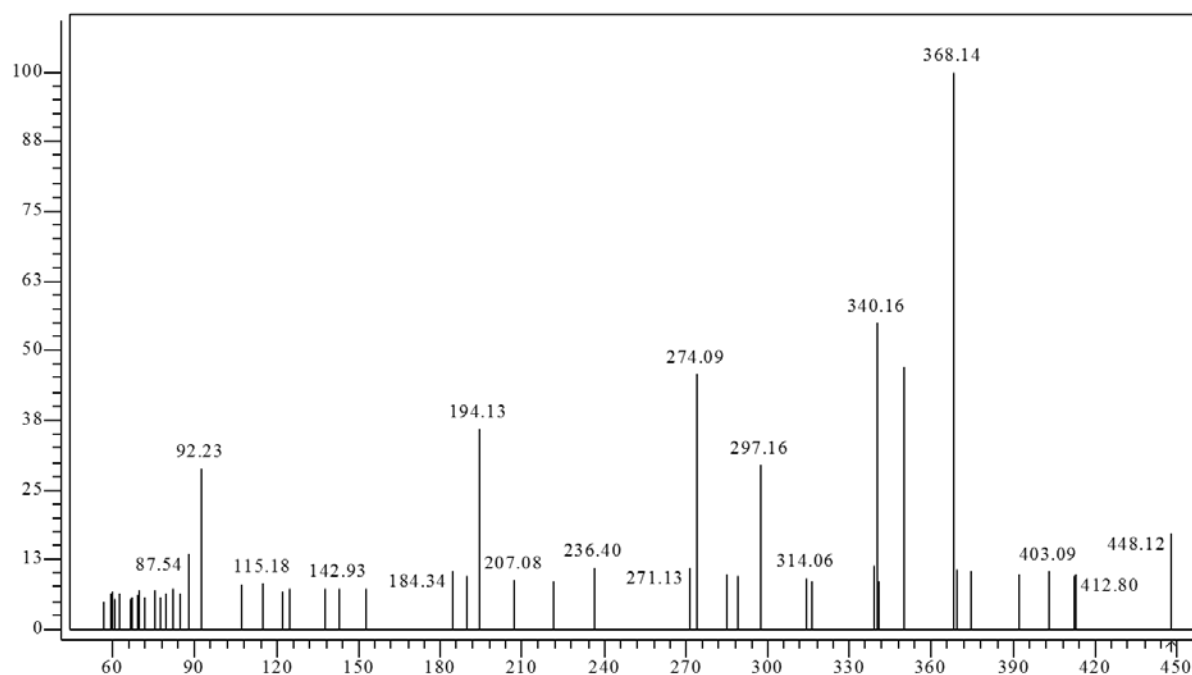
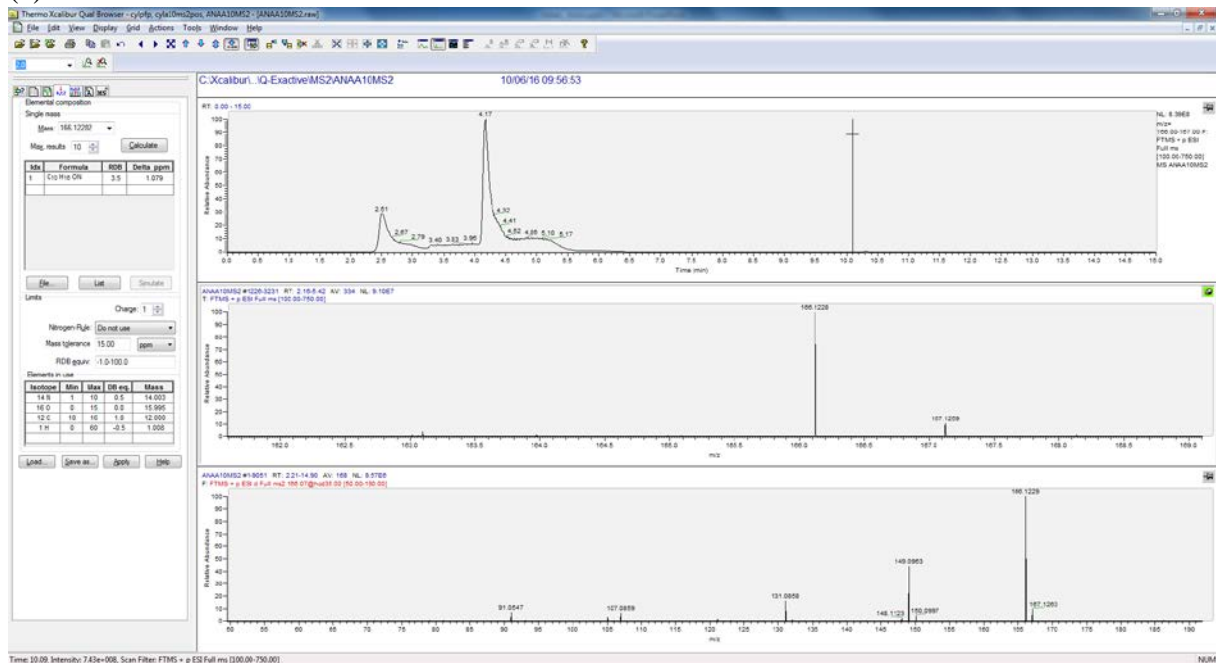
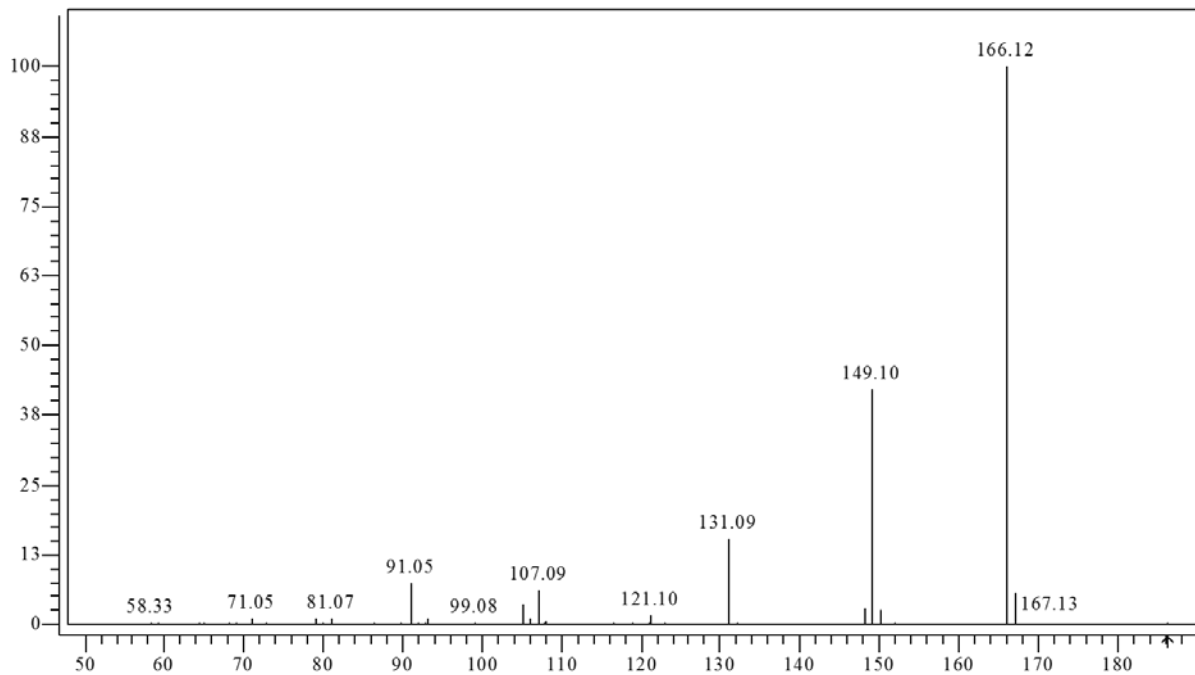


Figure A4.2: Positive mode Q-Exactive tandem mass spectra of CYL: (a) product ion spectrum MS^1 (targeting m/z 416); (b) product ion spectrum MS^2 (targeting m/z 416); (c) product ion spectrum MS^2 (targeting m/z 448); (d) product ion spectrum MS^2 (targeting m/z 420); (e) composite spectrum of m/z 416.

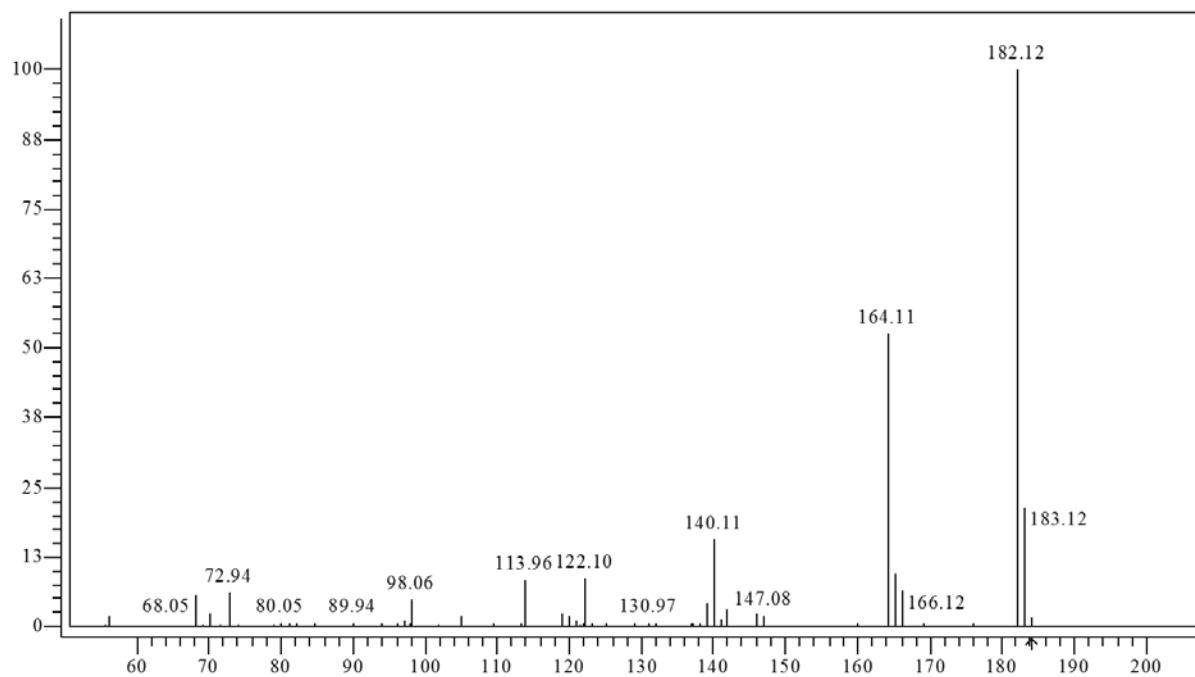
(a)



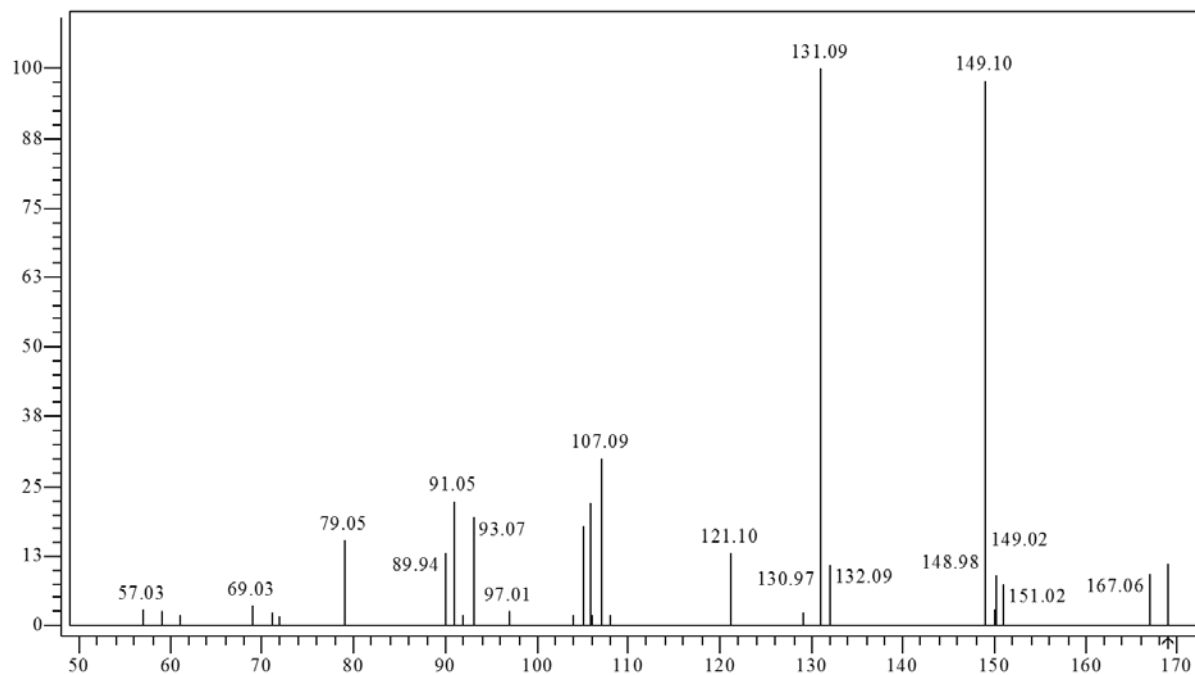
(b)



(c)



(d)



(e)

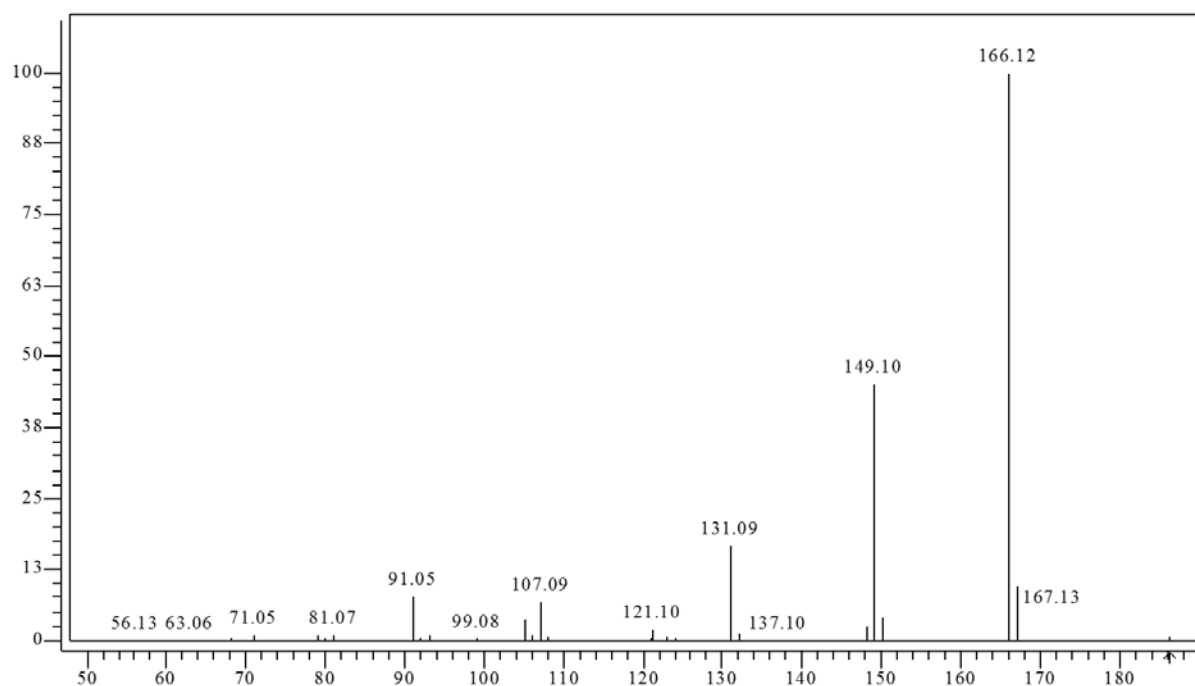


Figure A4.3: Positive mode Q-Exact tandem mass spectra of ANA: (a) product ion spectrum MS¹ (targeting m/z 166); (b) product ion spectrum MS² (targeting m/z 166); (c) product ion spectrum MS² (targeting m/z 182); (d) product ion spectrum MS² (targeting m/z 149); (e) composite spectrum of m/z 166.

References

- Aerni, H.-R., Kobler, B., Rutishauser, B. V., Wettstein, F. E., Fischer, R., Giger, W., . . . Schönenberger, R. (2004). Combined biological and chemical assessment of estrogenic activities in wastewater treatment plant effluents. *Analytical and Bioanalytical Chemistry*, 378(3), 688-696.
- Afzal, A., Oppenländer, T., Bolton, J. R., & El-Din, M. G. (2010). Anatoxin-a degradation by advanced oxidation processes: Vacuum-UV at 172 nm, photolysis using medium pressure UV and UV/H₂O₂. *Water Research*, 44(1), 278-286. <http://dx.doi.org/10.1016/j.watres.2009.09.021>
- Al-Sammak, M. A., Hoagland, K. D., Snow, D. D., & Cassada, D. (2013). Methods for simultaneous detection of the cyanotoxins BMAA, DABA, and anatoxin-a in environmental samples. *Toxicon*, 76, 316-325. <http://dx.doi.org/10.1016/j.toxicon.2013.10.015>
- Alaerts, L., Wahlen, J., Jacobs, P. A., & De Vos, D. E. (2008). Recent progress in the immobilization of catalysts for selective oxidation in the liquid phase. *Chemical Communications*(15), 1727-1737.
- Almstrup, K., Fernández, M. F., Petersen, J. H., Olea, N., Skakkebæk, N. E., & Leffers, H. (2002). Dual effects of phytoestrogens result in u-shaped dose-response curves. *Environmental Health Perspectives*, 110(8), 743.
- Amitai, G., Adani, R., Sod-Moriah, G., Rabinovitz, I., Vincze, A., Leader, H., . . . Hadar, Y. (1998). Oxidative biodegradation of phosphorothiolates by fungal laccase. *FEBS letters*, 438(3), 195-200.
- Arias, H. R. (2006). Marine toxins targeting ion channels. *Marine drugs*, 4(3), 37-69.
- Atanaskova, N., Keshamouni, V. G., Krueger, J. S., Schwartz, J. A., Miller, F., & Reddy, K. B. (2002). MAP kinase/estrogen receptor cross-talk enhances estrogen-mediated signaling and tumor growth but does not confer tamoxifen resistance. *Oncogene*, 21(25), 4000-4008.
- Ballot, A., Fastner, J., & Wiedner, C. (2010). Paralytic shellfish poisoning toxin-producing cyanobacterium *Aphanizomenon gracile* in northeast Germany. *Applied and environmental microbiology*, 76(4), 1173-1180.
- Balsiger, H. A., de la Torre, R., Lee, W.-Y., & Cox, M. B. (2010). A four-hour yeast bioassay for the direct measure of estrogenic activity in wastewater without sample extraction, concentration, or sterilization. *Science of The Total Environment*, 408(6), 1422-1429. <http://dx.doi.org/10.1016/j.scitotenv.2009.12.027>
- Banerjee, D., Apollo, F. M., Ryabov, A. D., & Collins, T. J. (2009). The impact of surfactants on FeIII - TAML - catalyzed oxidations by peroxides: Accelerations, decelerations, and loss of activity. *Chemistry-A European Journal*, 15(39), 10199-10209.
- Banerjee, D., Markley, A. L., Yano, T., Ghosh, A., Berget, P. B., Minkley, E. G., . . . Collins, T. J. (2006). "Green" oxidation catalysis for rapid deactivation of bacterial spores. *Angewandte Chemie International Edition*, 45(24), 3974-3977.
- Banker, R., Carmeli, S., Werman, M., Teltsch, B., Porat, R., & Sukenik, A. (2001). Uracil moiety is required for toxicity of the cyanobacterial hepatotoxin cylindrospermopsin. *Journal of Toxicology and Environmental Health, Part A*, 62(4), 281-288. 10.1080/009841001459432
- Barr, D. B., Bravo, R., Weerasekera, G., Caltabiano, L. M., Whitehead Jr, R. D., Olsson, A. O., . . . Sampson, E. J. (2004). Concentrations of dialkyl phosphate metabolites of organophosphorus pesticides in the US population. *Environmental Health Perspectives*, 112(2), 186.

- Beach, E. S., Duran, J. L., Horwitz, C. P., & Collins, T. J. (2009). Activation of hydrogen peroxide by an Fe-TAML complex in strongly alkaline aqueous solution: homogeneous oxidation catalysis with industrial significance. *Industrial & Engineering Chemistry Research*, 48(15), 7072-7076.
- Beck, I.-C., Bruhn, R., & Gandrass, J. (2006). Analysis of estrogenic activity in coastal surface waters of the Baltic Sea using the yeast estrogen screen. *Chemosphere*, 63(11), 1870-1878.
- Beresford, N., Routledge, E. J., Harris, C. A., & Sumpter, J. P. (2000). Issues arising when interpreting results from an in vitro Assay for estrogenic activity. *Toxicology and Applied Pharmacology*, 162(1), 22-33. <http://dx.doi.org/10.1006/taap.1999.8817>
- Berry, D. F., & Boyd, S. A. (1985). Reaction rates of phenolic humus constituents and anilines during cross-coupling. *Soil Biology and Biochemistry*, 17(5), 631-636. [http://dx.doi.org/10.1016/0038-0717\(85\)90039-2](http://dx.doi.org/10.1016/0038-0717(85)90039-2)
- Bialk, H. M., Hedman, C., Castillo, A., & Pedersen, J. A. (2007). Laccase-Mediated Michael Addition of 15N-Sulfapyridine to a Model Humic Constituent. *Environmental Science & Technology*, 41(10), 3593-3600. 10.1021/es0617338
- Bialk, H. M., Simpson, A. J., & Pedersen, J. A. (2005). Cross-coupling of sulfonamide antimicrobial agents with model humic constituents. *Environmental Science & Technology*, 39(12), 4463-4473. 10.1021/es0500916
- Bistan, M., Logar, R., & Tišler, T. (2011). Detection of estrogenic activity in Slovenian wastewaters by bioassay. *Open Life Sciences*, 6(5), 829-837.
- Bláha, L., Babica, P., & Maršálek, B. (2009). Toxins produced in cyanobacterial water blooms-toxicity and risks. *Interdisciplinary toxicology*, 2(2), 36-41.
- Blair, R. M., Fang, H., Branham, W. S., Hass, B. S., Dial, S. L., Moland, C. L., . . . Sheehan, D. M. (2000). The estrogen receptor relative binding affinities of 188 natural and xenochemicals: structural diversity of ligands. *Toxicological Sciences*, 54(1), 138-153.
- Bogialli, S., Bruno, M., Curini, R., Di Corcia, A., & Laganà, A. (2006). Simple and rapid determination of anatoxin-a in lake water and fish muscle tissue by liquid-chromatography–tandem mass spectrometry. *Journal of Chromatography A*, 1122(1–2), 180-185. <http://dx.doi.org/10.1016/j.chroma.2006.04.064>
- Bond, T., Goslan, E. H., Jefferson, B., Roddick, F., Fan, L., & Parsons, S. A. (2009). Chemical and biological oxidation of NOM surrogates and effect on HAA formation. *Water Research*, 43(10), 2615-2622. <http://dx.doi.org/10.1016/j.watres.2009.03.036>
- Campbell, C. G., Borglin, S. E., Green, F. B., Grayson, A., Wozni, E., & Stringfellow, W. T. (2006). Biologically directed environmental monitoring, fate, and transport of estrogenic endocrine disrupting compounds in water: A review. *Chemosphere*, 65(8), 1265-1280. <http://dx.doi.org/10.1016/j.chemosphere.2006.08.003>
- Campinas, M., & Rosa, M. J. (2006). The ionic strength effect on microcystin and natural organic matter surrogate adsorption onto PAC. *Journal of Colloid and Interface Science*, 299(2), 520-529. <http://dx.doi.org/10.1016/j.jcis.2006.02.042>
- Campos, F., Durán, R., Vidal, L., Faro, L. R. F., & Alfonso, M. (2006). In vivo Effects of the Anatoxin-a on Striatal Dopamine Release. *Neurochemical Research*, 31(4), 491-501. 10.1007/s11064-006-9042-x
- Carmichael, W. W. (1992). Cyanobacteria secondary metabolites—the cyanotoxins. *Journal of Applied Bacteriology*, 72(6), 445-459. 10.1111/j.1365-2672.1992.tb01858.x
- Carmichael, W. W., Azevedo, S., An, J. S., Molica, R., Jochimsen, E. M., Lau, S., . . . Eaglesham, G. K. (2001). Human fatalities from cyanobacteria: chemical and biological evidence for cyanotoxins. *Environmental Health Perspectives*, 109(7), 663.

- Carmichael, W. W., Biggs, D. F., & Peterson, M. A. (1979). Pharmacology of Anatoxin-a, produced by the freshwater cyanophyte *Anabaena flos-aquae* NRC-44-1. *Toxicon*, 17(3), 229-236. [http://dx.doi.org/10.1016/0041-0101\(79\)90212-5](http://dx.doi.org/10.1016/0041-0101(79)90212-5)
- Carneiro, C., Andreoli, C. V., da Nobrega Cunha, C. d. L., & Gobbi, E. F. (2014). *Reservoir eutrophication: preventive management: an applied example of integrated basin management interdisciplinary research*: IWA Publishing.
- Casida, J. E., & Quistad, G. B. (2004). Organophosphate toxicology: safety aspects of nonacetylcholinesterase secondary targets. *Chemical research in toxicology*, 17(8), 983-998.
- Catherine, Q., Susanna, W., Isidora, E.-S., Mark, H., Aurelie, V., & Jean-François, H. (2013). A review of current knowledge on toxic benthic freshwater cyanobacteria—ecology, toxin production and risk management. *Water Research*, 47(15), 5464-5479.
- Chahbane, N., Popescu, D.-L., Mitchell, D. A., Chanda, A., Lenoir, D., Ryabov, A. D., . . . Collins, T. J. (2007). Fe III–TAML-catalyzed green oxidative degradation of the azo dye Orange II by H₂O₂ and organic peroxides: products, toxicity, kinetics, and mechanisms. *Green Chemistry*, 9(1), 49-57.
- Chanda, A., Khetan, S. K., Banerjee, D., Ghosh, A., & Collins, T. J. (2006). Total degradation of fenitrothion and other organophosphorus pesticides by catalytic oxidation employing Fe-TAML peroxide activators. *Journal of the American Chemical Society*, 128(37), 12058-12059. 10.1021/ja064017e
- Chanda, A., Ryabov, A. D., Mondal, S., Alexandrova, L., Ghosh, A., Hangun-Balkir, Y., . . . Collins, T. J. (2006). Activity-stability parameterization of homogeneous green oxidation catalysts. *Chemistry – A European Journal*, 12(36), 9336-9345. 10.1002/chem.200600630
- Chanda, A., Shan, X., Chakrabarti, M., Ellis, W. C., Popescu, D. L., Tiago de Oliveira, F., . . . Bominaar, E. L. (2008). (TAML)FeIV=O complex in aqueous solution: Synthesis and spectroscopic and computational characterization. *Inorganic Chemistry*, 47(9), 3669-3678. 10.1021/ic7022902
- Chen, J. L., Ravindran, S., Swift, S., Wright, L. J., & Singhal, N. (2012). Catalytic oxidative degradation of 17 α -ethinylestradiol by FeIII-TAML/H₂O₂: Estrogenicities of the products of partial, and extensive oxidation. *Water Research*, 46(19), 6309-6318. <http://dx.doi.org/10.1016/j.watres.2012.09.012>
- Chen, L., Zhao, C., Dionysiou, D. D., & O'Shea, K. E. (2015). TiO₂ photocatalytic degradation and detoxification of cylindrospermopsin. *Journal of Photochemistry and Photobiology A: Chemistry*, 307, 115-122.
- Chiswell, R. K., Shaw, G. R., Eaglesham, G., Smith, M. J., Norris, R. L., Seawright, A. A., & Moore, M. R. (1999). Stability of cylindrospermopsin, the toxin from the cyanobacterium, *Cylindrospermopsis raciborskii*: Effect of pH, temperature, and sunlight on decomposition. *Environmental Toxicology*, 14(1), 155-161. 10.1002/(SICI)1522-7278(199902)14:1<155::AID-TOX20>3.0.CO;2-Z
- Chorus, I., & Bartram, J. (1999). Toxic cyanobacteria in water: a guide to their public health consequences, monitoring and management.
- Citulski, J., & Farahbakhsh, K. (2012). Overcoming the toxicity effects of municipal wastewater sludge and biosolid extracts in the Yeast Estrogen Screen (YES) assay. *Chemosphere*, 87(5), 498-503. <http://doi.org/10.1016/j.chemosphere.2011.12.043>
- Codd, G., Steffensen, D., Burch, M., & Baker, P. (1994). Toxic blooms of cyanobacteria in Lake Alexandrina, South Australia—learning from history. *Marine and Freshwater Research*, 45(5), 731-736.

- Codd, G. A. (2000). Cyanobacterial toxins, the perception of water quality, and the prioritisation of eutrophication control. *Ecological Engineering*, 16(1), 51-60. [http://dx.doi.org/10.1016/S0925-8574\(00\)00089-6](http://dx.doi.org/10.1016/S0925-8574(00)00089-6)
- Colborn, T., vom Saal, F. S., & Soto, A. M. (1993). Developmental effects of endocrine-disrupting chemicals in wildlife and humans. *Environmental Health Perspectives*, 101(5), 378-384.
- Collins, T. J. (2002). TAML oxidant activators: a new approach to the activation of hydrogen peroxide for environmentally significant problems. *Accounts of Chemical Research*, 35(9), 782-790. 10.1021/ar010079s
- Collins, T. J. (2011). TAML activators: green chemistry catalysts as effective small molecule mimics of the peroxidase enzymes. *Chem. New Zealand*, 72-77.
- Collins, T. J., & Gordon-Wylie, S. W. (1989). A manganese(V)-oxo complex. *Journal of the American Chemical Society*, 111(12), 4511-4513. 10.1021/ja00194a063
- Conley, D. J., Bonsdorff, E., Carstensen, J., Destouni, G., Gustafsson, B. G., Hansson, L.-A., . . . Zillén, L. (2009). Tackling hypoxia in the Baltic Sea: Is engineering a solution? *Environmental Science & Technology*, 43(10), 3407-3411. 10.1021/es8027633
- Conley, D. J., Paerl, H. W., Howarth, R. W., Boesch, D. F., Seitzinger, S. P., Karl, E., . . . Gene, E. (2009). Controlling eutrophication: nitrogen and phosphorus. *Science*, 123, 1014-1015.
- Conolly, R. B., & Lutz, W. K. (2004). Nonmonotonic dose-response relationships: mechanistic basis, kinetic modeling, and implications for risk assessment. *Toxicological Sciences*, 77(1), 151-157. 10.1093/toxsci/kfh007
- Cozzi, F. (2006). Immobilization of organic catalysts: when, why, and how. *Advanced Synthesis & Catalysis*, 348(12 - 13), 1367-1390.
- Cozzolino, A., & Piccolo, A. (2002). Polymerization of dissolved humic substances catalyzed by peroxidase. Effects of pH and humic composition. *Organic Geochemistry*, 33(3), 281-294. [http://dx.doi.org/10.1016/S0146-6380\(01\)00160-7](http://dx.doi.org/10.1016/S0146-6380(01)00160-7)
- Crisp, T. M., Clegg, E. D., Cooper, R. L., Wood, W. P., Anderson, D. G., Baetcke, K. P., . . . Patel, Y. M. (1998). Environmental endocrine disruption: an effects assessment and analysis. *Environmental Health Perspectives*, 106(Suppl 1), 11-56.
- Dagnino, D., & Schripsema, J. (2005). ¹H NMR quantification in very dilute toxin solutions: application to anatoxin-a analysis. *Toxicon*, 46(2), 236-240. <http://dx.doi.org/10.1016/j.toxicon.2005.04.014>
- De Boever, P., Demaré, W., Vanderperren, E., Cooreman, K., Bossier, P., & Verstraete, W. (2001). Optimization of a yeast estrogen screen and its applicability to study the release of estrogenic isoflavones from a soygerm powder. *Environmental Health Perspectives*, 109(7), 691-697.
- De Coster, S., & van Larebeke, N. (2012). Endocrine-disrupting chemicals: associated disorders and mechanisms of action. *Journal of environmental and public health*, 2012
- de la Cruz, A. A., Hiskia, A., Kaloudis, T., Chernoff, N., Hill, D., Antoniou, M. G., . . . Dionysiou, D. D. (2013). A review on cylindrospermopsin: the global occurrence, detection, toxicity and degradation of a potent cyanotoxin. *Environmental Science: Processes & Impacts*, 15(11), 1979-2003. 10.1039/C3EM00353A
- Dec, J., & Bollag, J.-M. (2000). Phenoloxidase-mediated interactions of phenols and anilines with humic materials. *Journal of Environmental Quality*, 29(3), 665-676.
- del Pozo, C., Corma, A., Iglesias, M., & Sánchez, F. (2011). Recyclable mesoporous silica-supported chiral ruthenium-(NHC) NN-pincer catalysts for asymmetric reactions. *Green Chemistry*, 13(9), 2471-2481.
- Delgado, L. F., Charles, P., Glucina, K., & Morlay, C. (2012). The removal of endocrine disrupting compounds, pharmaceutically activated compounds and cyanobacterial

- toxins during drinking water preparation using activated carbon—A review. *Science of The Total Environment*, 435–436, 509-525.
<http://dx.doi.org/10.1016/j.scitotenv.2012.07.046>
- Denier, X., Hill, E. M., Rotchell, J., & Minier, C. (2009). Estrogenic activity of cadmium, copper and zinc in the yeast estrogen screen. *Toxicology in Vitro*, 23(4), 569-573.
- Devitt, E. C., & Wiesner, M. R. (1998). Dialysis investigations of atrazine-organic matter interactions and the role of a divalent metal. *Environmental Science & Technology*, 32(2), 232-237. 10.1021/es970179m
- Devlin, J. P., Edwards, O. E., Gorham, P. R., Hunter, N. R., Pike, R. K., & Stavric, B. (1977). Anatoxin-a, a toxic alkaloid from *Anabaena flos-aquae* NRC-44h. *Canadian Journal of Chemistry*, 55(8), 1367-1371. 10.1139/v77-189
- Dixon, M., Falconet, C., Ho, L., Chow, C., O'Neill, B., & Newcombe, G. (2010). Nanofiltration for the removal of algal metabolites and the effects of fouling. *Water Science and Technology*, 61(5), 1189-1199.
- Dodds, W. K., Bouska, W. W., Eitzmann, J. L., Pilger, T. J., Pitts, K. L., Riley, A. J., . . . Thornbrugh, D. J. (2009). Eutrophication of U.S. freshwaters: analysis of potential economic damages. *Environmental Science & Technology*, 43(1), 12-19. 10.1021/es801217q
- Draisci, R., Ferretti, E., Palleschi, L., & Marchiafava, C. (2001). Identification of anatoxins in blue-green algae food supplements using liquid chromatography-tandem mass spectrometry. *Food Additives & Contaminants*, 18(6), 525-531.
- Duesterberg, C. K., Mylon, S. E., & Waite, T. D. (2008). pH Effects on Iron-Catalyzed Oxidation using Fenton's Reagent. *Environmental Science & Technology*, 42(22), 8522-8527. 10.1021/es801720d
- Duy, T. N., Lam, P. K., Shaw, G. R., & Connell, D. W. (2000). Toxicology and risk assessment of freshwater cyanobacterial (blue-green algal) toxins in water *Reviews of Environmental Contamination and Toxicology* (pp. 113-185): Springer.
- Easton, J. (1995). The dye maker's view. *Colour in dyehouse effluent*, 11
- Edwards, C., Beattie, K. A., Scrimgeour, C. M., & Codd, G. A. (1992). Identification of anatoxin-A in benthic cyanobacteria (blue-green algae) and in associated dog poisonings at Loch Insh, Scotland. *Toxicon*, 30(10), 1165-1175.
[http://dx.doi.org/10.1016/0041-0101\(92\)90432-5](http://dx.doi.org/10.1016/0041-0101(92)90432-5)
- Ellis, W. C., Tran, C. T., Denardo, M. A., Fischer, A., Ryabov, A. D., & Collins, T. J. (2009). Design of more powerful iron-TAML peroxidase enzyme mimics. *Journal of the American Chemical Society*, 131(50), 18052-18053. 10.1021/ja9086837
- Ellis, W. C., Tran, C. T., Roy, R., Rusten, M., Fischer, A., Ryabov, A. D., . . . Collins, T. J. (2010). Designing green oxidation catalysts for purifying environmental waters. *Journal of the American Chemical Society*, 132(28), 9774-9781.
- EPA. (2008). Drinking water contaminant candidate list and regulatory determinations CCL 3. Retrieved January 28, 2009,
- Faassen, E. J., Harkema, L., Begeman, L., & Lurling, M. (2012). First report of (homo)anatoxin-a and dog neurotoxicosis after ingestion of benthic cyanobacteria in The Netherlands. *Toxicon*, 60(3), 378-384.
<http://dx.doi.org/10.1016/j.toxicon.2012.04.335>
- Falconer, I. R. (1999). An overview of problems caused by toxic blue-green algae (cyanobacteria) in drinking and recreational water. *Environmental Toxicology*, 14(1), 5-12.
- Falconer, I. R., Hardy, S. J., Humpage, A. R., Froschio, S. M., Tozer, G. J., & Hawkins, P. R. (1999). Hepatic and renal toxicity of the blue-green alga (cyanobacterium) *Cylindrospermopsis raciborskii* in male Swiss albino mice. *Environmental Toxicology*,

- 14(1), 143-150. 10.1002/(SICI)1522-7278(199902)14:1<143::AID-TOX18>3.0.CO;2-H
- Falconer, I. R., & Humpage, A. R. (2006). Cyanobacterial (blue-green algal) toxins in water supplies: Cylindrospermopsins. *Environmental Toxicology*, 21(4), 299-304. 10.1002/tox.20194
- Fang, H., Tong, W., Shi, L. M., Blair, R., Perkins, R., Branham, W., . . . Sheehan, D. M. (2001). Structure–activity relationships for a large diverse set of natural, synthetic, and environmental estrogens. *Chemical research in toxicology*, 14(3), 280-294. 10.1021/tx000208y
- Feng, Y., Colosi, L. M., Gao, S., Huang, Q., & Mao, L. (2013). Transformation and removal of tetrabromobisphenol a from water in the presence of natural organic matter via laccase-catalyzed reactions: reaction rates, products, and pathways. *Environmental Science & Technology*, 47(2), 1001-1008. 10.1021/es302680c
- Fenton, S. E. (2006). Endocrine-disrupting compounds and mammary gland development: early exposure and later life consequences. *Endocrinology*, 147(6), s18-s24.
- Fitzgeorge, R., Clark, S., & Keevil, C. (1994). Routes of intoxication. *Special Publications of the Royal Society of Chemistry*, 149, 69-74.
- Forgacs, E., Cserháti, T., & Oros, G. (2004). Removal of synthetic dyes from wastewaters: a review. *Environment International*, 30(7), 953-971. <http://dx.doi.org/10.1016/j.envint.2004.02.001>
- Foss, A. J., & Aabel, M. T. (2013). The extraction and analysis of cylindrospermopsin from human serum and urine. *Toxicon*, 70, 54-61.
- Fotiou, T., Triantis, T., Kaloudis, T., & Hiskia, A. (2015). Photocatalytic degradation of cylindrospermopsin under UV-A, solar and visible light using TiO₂. Mineralization and intermediate products. *Chemosphere*, 119, S89-S94.
- Fowler, P. A., Bellingham, M., Sinclair, K. D., Evans, N. P., Pocar, P., Fischer, B., . . . O'Shaughnessy, P. J. (2012). Impact of endocrine-disrupting compounds (EDCs) on female reproductive health. *Molecular and Cellular Endocrinology*, 355(2), 231-239. <http://dx.doi.org/10.1016/j.mce.2011.10.021>
- Francis, G. (1878). Poisonous Australian Lake. *Nature*, 18, 11. 10.1038/018011d0
- Frische, T., Faust, M., Meyer, W., & Backhaus, T. (2009). Toxic masking and synergistic modulation of the estrogenic activity of chemical mixtures in a yeast estrogen screen (YES). *Environmental Science and Pollution Research*, 16(5), 593-603. 10.1007/s11356-009-0184-7
- Fristachi, A., Sinclair, J., Hall, S., Hambrook Berkman, J., Boyer, G., Burkholder, J., . . . Frazier, W. (2008). Cyanobacterial harmful algal blooms: Chapter 3: occurrence of cyanobacterial harmful algal blooms workgroup report. *US Environmental Protection Agency Papers*, 40.
- Froschio, S. M., Humpage, A. R., Burcham, P. C., & Falconer, I. R. (2003). Cylindrospermopsin - induced protein synthesis inhibition and its dissociation from acute toxicity in mouse hepatocytes. *Environmental Toxicology*, 18(4), 243-251.
- Froschio, S. M., Humpage, A. R., Wickramasinghe, W., Shaw, G., & Falconer, I. R. (2008). Interaction of the cyanobacterial toxin cylindrospermopsin with the eukaryotic protein synthesis system. *Toxicon*, 51(2), 191-198. <http://dx.doi.org/10.1016/j.toxicon.2007.09.001>
- Funari, E., & Testai, E. (2008). Human health risk assessment related to cyanotoxins exposure. *Critical Reviews in Toxicology*, 38(2), 97-125. doi:10.1080/10408440701749454
- Furey, A., Crowley, J., Lehane, M., & James, K. J. (2003). Liquid chromatography with electrospray ion-trap mass spectrometry for the determination of anatoxins in

- cyanobacteria and drinking water. *Rapid Communications in Mass Spectrometry*, 17(6), 583-588. 10.1002/rcm.932
- Furuta, C., Suzuki, A. K., Taneda, S., Kamata, K., Hayashi, H., Mori, Y., . . . Taya, K. (2004). Estrogenic activities of nitrophenols in diesel exhaust particles. *Biology of reproduction*, 70(5), 1527-1533.
- Gallard, H., & De Laat, J. (2000). Kinetic modelling of Fe(III)/H₂O₂ oxidation reactions in dilute aqueous solution using atrazine as a model organic compound. *Water Research*, 34(12), 3107-3116. [https://doi.org/10.1016/S0043-1354\(00\)00074-9](https://doi.org/10.1016/S0043-1354(00)00074-9)
- Gallo, P., Fabbrocino, S., Cerulo, M. G., Ferranti, P., Bruno, M., & Serpe, L. (2009). Determination of cylindrospermopsin in freshwaters and fish tissue by liquid chromatography coupled to electrospray ion trap mass spectrometry. *Rapid Communications in Mass Spectrometry*, 23(20), 3279-3284. 10.1002/rcm.4243
- Gao, J., Niklason, L., & Langer, R. (1998). Surface hydrolysis of poly (glycolic acid) meshes increases the seeding density of vascular smooth muscle cells. *Journal of biomedical materials research*, 42(3), 417-424.
- Ghassempour, A., Najafi, N. M., Mehdinia, A., Davarani, S. S. H., Fallahi, M., & Nakhshab, M. (2005). Analysis of anatoxin-a using polyaniline as a sorbent in solid-phase microextraction coupled to gas chromatography–mass spectrometry. *Journal of Chromatography A*, 1078(1–2), 120-127. <http://dx.doi.org/10.1016/j.chroma.2005.04.053>
- Ghosh, A., Mitchell, D. A., Chanda, A., Ryabov, A. D., Popescu, D. L., Upham, E. C., . . . Collins, T. J. (2008). Catalase– peroxidase activity of Iron (III)– TAML activators of hydrogen peroxide. *Journal of the American Chemical Society*, 130(45), 15116-15126.
- Ghosh, A., Ryabov, A. D., Mayer, S. M., Horner, D. C., Prasuhn, D. E., Sen Gupta, S., . . . Collins, T. J. (2003). Understanding the mechanism of H⁺-induced demetalation as a design strategy for robust iron(III) peroxide-activating catalysts. *Journal of the American Chemical Society*, 125(41), 12378-12379. 10.1021/ja0367344
- Giesy, J. P., Hilscherova, K., Jones, P. D., Kannan, K., & Machala, M. (2002). Cell bioassays for detection of aryl hydrocarbon (AhR) and estrogen receptor (ER) mediated activity in environmental samples. *Marine Pollution Bulletin*, 45(1–12), 3-16. [http://dx.doi.org/10.1016/S0025-326X\(02\)00097-8](http://dx.doi.org/10.1016/S0025-326X(02)00097-8)
- Gillesby, B. E., & Zacharewski, T. R. (1998). Exoestrogens: mechanisms of action and strategies for identification and assessment. *Environmental Toxicology and Chemistry*, 17(1), 3-14.
- Gottlieb, A., Shaw, C., Smith, A., Wheatley, A., & Forsythe, S. (2003). The toxicity of textile reactive azo dyes after hydrolysis and decolourisation. *Journal of Biotechnology*, 101(1), 49-56.
- Graham, J. L., Loftin, K. A., Meyer, M. T., & Ziegler, A. C. (2010). Cyanotoxin mixtures and taste-and-odor compounds in cyanobacterial blooms from the midwestern United States. *Environmental Science & Technology*, 44(19), 7361-7368. 10.1021/es1008938
- Griffiths, D. J., & Saker, M. L. (2003). The Palm Island mystery disease 20 years on: a review of research on the cyanotoxin cylindrospermopsin. *Environmental Toxicology*, 18(2), 78-93.
- Gugger, M., Lenoir, S., Berger, C., Ledreux, A., Druart, J.-C., Humbert, J.-F., . . . Bernard, C. (2005). First report in a river in France of the benthic cyanobacterium *Phormidium favosum* producing anatoxin-a associated with dog neurotoxicosis. *Toxicon*, 45(7), 919-928. <http://dx.doi.org/10.1016/j.toxicon.2005.02.031>
- Gulkowska, A., Sander, M., Hollender, J., & Krauss, M. (2013). Covalent Binding of Sulfamethazine to Natural and Synthetic Humic Acids: Assessing Laccase Catalysis

- and Covalent Bond Stability. *Environmental Science & Technology*, 47(13), 6916-6924. 10.1021/es3044592
- Gupta, S. S., Stadler, M., Noser, C. A., Ghosh, A., Steinhoff, B., Lenoir, D., . . . Collins, T. J. (2002). Rapid total destruction of chlorophenols by activated hydrogen peroxide. *Science*, 296(5566), 326-328.
- Gutiérrez-Praena, D., Pichardo, S., Jos, Á., Moreno, F. J., & Cameán, A. M. (2012). Biochemical and pathological toxic effects induced by the cyanotoxin Cylindrospermopsin on the human cell line Caco-2. *Water Research*, 46(5), 1566-1575. <http://dx.doi.org/10.1016/j.watres.2011.12.044>
- Guzmán-Guillén, R., Moreno, I., Prieto Ortega, A. I., Eugenia Soria-Díaz, M., Vasconcelos, V., & Cameán, A. M. (2015). CYN determination in tissues from freshwater fish by LC-MS/MS: Validation and application in tissues from subchronically exposed tilapia (*Oreochromis niloticus*). *Talanta*, 131(0), 452-459. <http://dx.doi.org/10.1016/j.talanta.2014.07.091>
- Hashimoto, T., Onda, K., Nakamura, Y., Tada, K., Miya, A., & Murakami, T. (2007). Comparison of natural estrogen removal efficiency in the conventional activated sludge process and the oxidation ditch process. *Water Research*, 41(10), 2117-2126. <http://dx.doi.org/10.1016/j.watres.2007.02.029>
- Havens, K. E. (2008). Cyanobacteria blooms: effects on aquatic ecosystems *Cyanobacterial harmful algal blooms: state of the science and research needs* (pp. 733-747): Springer.
- Havens, K. E., Fukushima, T., Xie, P., Iwakuma, T., James, R. T., Takamura, N., . . . Yamamoto, T. (2001). Nutrient dynamics and the eutrophication of shallow lakes Kasumigaura (Japan), Donghu (PR China), and Okeechobee (USA). *Environmental Pollution*, 111(2), 263-272. [http://dx.doi.org/10.1016/S0269-7491\(00\)00074-9](http://dx.doi.org/10.1016/S0269-7491(00)00074-9)
- Hawkins, P. R., Runnegar, M. T., Jackson, A., & Falconer, I. (1985). Severe hepatotoxicity caused by the tropical cyanobacterium (blue-green alga) *Cylindrospermopsis raciborskii* (Woloszynska) Seenaya and Subba Raju isolated from a domestic water supply reservoir. *Applied and environmental microbiology*, 50(5), 1292-1295.
- He, X., de la Cruz, A. A., O'Shea, K. E., & Dionysiou, D. D. (2014). Kinetics and mechanisms of cylindrospermopsin destruction by sulfate radical-based advanced oxidation processes. *Water Research*, 63(0), 168-178. <http://dx.doi.org/10.1016/j.watres.2014.06.004>
- He, X., Zhang, G., de la Cruz, A. A., O'Shea, K. E., & Dionysiou, D. D. (2014). Degradation mechanism of cyanobacterial toxin Cylindrospermopsin by hydroxyl radicals in homogeneous UV/H₂O₂ process. *Environmental Science & Technology*, 48(8), 4495-4504. 10.1021/es403732s
- Her, N., Amy, G., Chung, J., Yoon, J., & Yoon, Y. (2008). Characterizing dissolved organic matter and evaluating associated nanofiltration membrane fouling. *Chemosphere*, 70(3), 495-502. <http://dx.doi.org/10.1016/j.chemosphere.2007.06.025>
- Hitzfeld, B. C., Höger, S. J., & Dietrich, D. R. (2000). Cyanobacterial toxins: removal during drinking water treatment, and human risk assessment. *Environmental Health Perspectives*, 108(Suppl 1), 113.
- Ho, L., Dreyfus, J., Boyer, J., Lowe, T., Bustamante, H., Duker, P., . . . Newcombe, G. (2012). Fate of cyanobacteria and their metabolites during water treatment sludge management processes. *Science of The Total Environment*, 424, 232-238.
- Ho, L., Lambling, P., Bustamante, H., Duker, P., & Newcombe, G. (2011). Application of powdered activated carbon for the adsorption of cylindrospermopsin and microcystin toxins from drinking water supplies. *Water Research*, 45(9), 2954-2964.
- Hosiner, D., Gerber, S., Lichtenberg-Frate, H., Glaser, W., Schüller, C., & Klipp, E. (2014). Impact of acute metal stress in *Saccharomyces cerevisiae*. *PloS one*, 9(1), e83330.

- Hu, A., Yee, G. T., & Lin, W. (2005). Magnetically recoverable chiral catalysts immobilized on magnetite nanoparticles for asymmetric hydrogenation of aromatic ketones. *Journal of the American Chemical Society*, 127(36), 12486-12487. 10.1021/ja053881o
- Hudnell, H. K. (2008). *Cyanobacterial harmful algal blooms: state of the science and research needs* (Vol. 619): Springer Science & Business Media.
- Hudnell, H. K. (2010). The state of US freshwater harmful algal blooms assessments, policy and legislation. *Toxicon*, 55(5), 1024-1034.
- Humpage, A. (2008). Toxin types, toxicokinetics and toxicodynamics *Cyanobacterial harmful algal blooms: State of the science and research needs* (pp. 383-415): Springer.
- Humpage, A. R., Fontaine, F., Frosco, S., Burcham, P., & Falconer, I. R. (2005). Cylindrospermopsin genotoxicity and cytotoxicity: role of cytochrome P-450 and oxidative stress. *Journal of Toxicology and Environmental Health, Part A*, 68(9), 739-753.
- Hunger, K. (2005). Toxicology and toxicological testing of colorants. *Review of Progress in Coloration and Related Topics*, 35(1), 76-89.
- Isquith, A., Abbott, E., & Walters, P. (1972). Surface-bonded antimicrobial activity of an organosilicon quaternary ammonium chloride. *Applied microbiology*, 24(6), 859-863.
- Jal, P., Patel, S., & Mishra, B. (2004). Chemical modification of silica surface by immobilization of functional groups for extractive concentration of metal ions. *Talanta*, 62(5), 1005-1028.
- James, K. J., Crowley, J., Hamilton, B., Lehane, M., Skulberg, O., & Furey, A. (2005). Anatoxins and degradation products, determined using hybrid quadrupole time-of-flight and quadrupole ion-trap mass spectrometry: forensic investigations of cyanobacterial neurotoxin poisoning. *Rapid Communications in Mass Spectrometry*, 19(9), 1167-1175. 10.1002/rcm.1894
- James, K. J., Furey, A., Sherlock, I. R., Stack, M. A., Twohig, M., Caudwell, F. B., & Skulberg, O. M. (1998). Sensitive determination of anatoxin-a, homoanatoxin-a and their degradation products by liquid chromatography with fluorimetric detection. *Journal of Chromatography A*, 798(1-2), 147-157. [http://dx.doi.org/10.1016/S0021-9673\(97\)01207-7](http://dx.doi.org/10.1016/S0021-9673(97)01207-7)
- James, K. J., Sherlock, I. R., & Stack, M. A. (1997). Anatoxin-a in Irish freshwater and cyanobacteria, determined using a new fluorimetric liquid chromatographic method. *Toxicon*, 35(6), 963-971. [http://dx.doi.org/10.1016/S0041-0101\(96\)00201-2](http://dx.doi.org/10.1016/S0041-0101(96)00201-2)
- Jarusutthirak, C., Mattaraj, S., & Jiratananon, R. (2007). Factors affecting nanofiltration performances in natural organic matter rejection and flux decline. *Separation and Purification Technology*, 58(1), 68-75. <http://dx.doi.org/10.1016/j.seppur.2007.07.010>
- Jho, E., Singhal, N., & Turner, S. (2012). Tetrachloroethylene and hexachloroethane degradation in Fe (III) and Fe (III)-citrate catalyzed Fenton systems. *Journal of Chemical Technology and Biotechnology*, 87(8), 1179-1186.
- Jonas, A., Scholz, S., Fetter, E., Sychrova, E., Novakova, K., Ortmann, J., . . . Hilscherova, K. (2015). Endocrine, teratogenic and neurotoxic effects of cyanobacteria detected by cellular in vitro and zebrafish embryos assays. *Chemosphere*, 120, 321-327. <http://dx.doi.org/10.1016/j.chemosphere.2014.07.074>
- Jones, C. W. (1999). *Applications of hydrogen peroxide and derivatives* (Vol. 2): Royal Society of Chemistry.
- Juday, R. E., Keller, E. J., Horpestad, A., Bahls, L. L., & Glasser, S. (1981). A toxic bloom of *Anabaena flos-aquae* in Hebgen reservoir Montana in 1977 *The Water Environment* (pp. 103-112): Springer.

- Kase, R., Hansen, P.-D., Fischer, B., Manz, W., Heininger, P., & Reifferscheid, G. (2008). Integral assessment of estrogenic potentials of sediment-associated samples. *Environmental Science and Pollution Research*, 15(1), 75-83.
- Katchalski-Katzir, E. (1993). Immobilized enzymes — learning from past successes and failures. *Trends in Biotechnology*, 11(11), 471-478. [http://dx.doi.org/10.1016/0167-7799\(93\)90080-S](http://dx.doi.org/10.1016/0167-7799(93)90080-S)
- Katchalski-Katzir, E., & Kraemer, D. M. (2000). Eupergit® C, a carrier for immobilization of enzymes of industrial potential. *Journal of Molecular Catalysis B: Enzymatic*, 10(1-3), 157-176. [http://dx.doi.org/10.1016/S1381-1177\(00\)00124-7](http://dx.doi.org/10.1016/S1381-1177(00)00124-7)
- Kavlock, R. J., Daston, G. P., DeRosa, C., Fenner-Crisp, P., Gray, L. E., Kaattari, S., . . . Maczka, C. (1996). Research needs for the risk assessment of health and environmental effects of endocrine disruptors: a report of the US EPA-sponsored workshop. *Environmental Health Perspectives*, 104(Suppl 4), 715.
- Kazankov, G. M., Sergeeva, V. S., Efremenko, E. N., Alexandrova, L., Varfolomeev, S. D., & Ryabov, A. D. (2000). Highly efficient degradation of thiophosphate pesticides catalyzed by platinum and palladium aryl oxime metallacycles. *Angewandte Chemie*, 39(17), 3117-3119.
- Kim, J.-E., Fernandes, E., & Bollag, J.-M. (1997). Enzymatic coupling of the herbicide bentazon with humus monomers and characterization of reaction products. *Environmental Science & Technology*, 31(8), 2392-2398. 10.1021/es961016l
- Kinnear, S. (2010). Cylindrospermopsin: a decade of progress on bioaccumulation research. *Marine drugs*, 8(3), 542-564.
- Kohn, M. C., & Portier, C. J. (1993). Effects of the mechanism of receptor - mediated gene expression on the shape of the dose - response curve. *Risk Analysis*, 13(5), 565-572.
- Korshin, G., Chow, C. W. K., Fabris, R., & Drikas, M. (2009). Absorbance spectroscopy-based examination of effects of coagulation on the reactivity of fractions of natural organic matter with varying apparent molecular weights. *Water Research*, 43(6), 1541-1548. <http://dx.doi.org/10.1016/j.watres.2008.12.041>
- Kubicki, J. D., & Aplitz, S. E. (1999). Models of natural organic matter and interactions with organic contaminants. *Organic Geochemistry*, 30(8), 911-927. [http://dx.doi.org/10.1016/S0146-6380\(99\)00075-3](http://dx.doi.org/10.1016/S0146-6380(99)00075-3)
- Kundu, S., Chanda, A., Thompson, J. V. K., Diabes, G., Khetan, S. K., Ryabov, A. D., & Collins, T. J. (2015). Rapid degradation of oxidation resistant nitrophenols by TAML activator and H₂O₂. *Catalysis Science & Technology*, 5(3), 1775-1782. 10.1039/C4CY01426J
- Kuo, L. Y., & Perera, N. M. (2000). Paraoxon and parathion hydrolysis by aqueous molybdenocene dichloride (Cp₂MoCl₂): first reported pesticide hydrolysis by an organometallic complex. *Inorganic Chemistry*, 39(10), 2103-2106.
- Lahti, K., Ahtiainen, J., Rapala, J., Sivonen, K., & Niemelä, S. (1995). Assessment of rapid bioassays for detecting cyanobacterial toxicity. *Letters in applied microbiology*, 21(2), 109-114.
- Lamsal, R., Walsh, M. E., & Gagnon, G. A. (2011). Comparison of advanced oxidation processes for the removal of natural organic matter. *Water Research*, 45(10), 3263-3269.
- Leusch, F. D., De Jager, C., Levi, Y., Lim, R., Puijker, L., Sacher, F., . . . Chapman, H. F. (2010). Comparison of five in vitro bioassays to measure estrogenic activity in environmental waters. *Environmental Science & Technology*, 44(10), 3853-3860.
- Li, L., Andersen, M. E., Heber, S., & Zhang, Q. (2007). Non-monotonic dose-response relationship in steroid hormone receptor-mediated gene expression. *Journal of molecular endocrinology*, 38(5), 569-585.

- Liu, S., Lim, M., Fabris, R., Chow, C. W., Drikas, M., Korshin, G., & Amal, R. (2010). Multi-wavelength spectroscopic and chromatography study on the photocatalytic oxidation of natural organic matter. *Water Research*, 44(8), 2525-2532.
- Liu, Y., Liang, P., & Guo, L. (2005). Nanometer titanium dioxide immobilized on silica gel as sorbent for preconcentration of metal ions prior to their determination by inductively coupled plasma atomic emission spectrometry. *Talanta*, 68(1), 25-30.
- Lu, G., & Zhao, X. S. (2004). *Nanoporous materials: science and engineering* (Vol. 4): World Scientific.
- Lu, J., & Huang, Q. (2009). Removal of acetaminophen using enzyme-mediated oxidative coupling processes: II. Cross-coupling with natural organic matter. *Environmental Science & Technology*, 43(18), 7068-7073.
- Mailman, R. B. (2008). Toxicant-receptor interactions: fundamental principles. *Molecular and Biochemical Toxicology. 4th Edition*. Chichester: John Wiley & Sons, Inc, 359-390.
- Mao, L., Lu, J., Habteselassie, M., Luo, Q., Gao, S., Cabrera, M., & Huang, Q. (2010). Ligninase-mediated removal of natural and synthetic estrogens from water: II. reactions of 17 β -estradiol. *Environmental Science & Technology*, 44(7), 2599-2604. 10.1021/es903058k
- Marques, H. M. (2007). Insights into porphyrin chemistry provided by the microperoxidases, the haempeptides derived from cytochrome c. *Dalton Transactions*(39), 4371-4385. 10.1039/B710940G
- Matilainen, A., Gjessing, E. T., Lahtinen, T., Hed, L., Bhatnagar, A., & Sillanpää, M. (2011). An overview of the methods used in the characterisation of natural organic matter (NOM) in relation to drinking water treatment. *Chemosphere*, 83(11), 1431-1442. <http://dx.doi.org/10.1016/j.chemosphere.2011.01.018>
- Matilainen, A., & Sillanpää, M. (2010). Removal of natural organic matter from drinking water by advanced oxidation processes. *Chemosphere*, 80(4), 351-365. <http://dx.doi.org/10.1016/j.chemosphere.2010.04.067>
- Matsumoto, T., Ueno, M., Wang, N., & Kobayashi, S. (2008). Recent advances in immobilized metal catalysts for environmentally benign oxidation of alcohols. *Chemistry—An Asian Journal*, 3(2), 196-214.
- McLachlan, J. A., & Arnold, S. F. (1996). Environmental estrogens. *American Scientist*, 84(5), 452-461.
- McMorn, P., & Hutchings, G. J. (2004). Heterogeneous enantioselective catalysts: strategies for the immobilisation of homogeneous catalysts. *Chemical Society Reviews*, 33(2), 108-122.
- Merel, S., Walker, D., Chicana, R., Snyder, S., Baurès, E., & Thomas, O. (2013). State of knowledge and concerns on cyanobacterial blooms and cyanotoxins. *Environment International*, 59, 303-327. <http://dx.doi.org/10.1016/j.envint.2013.06.013>
- Meriluoto, J. A., & Spoof, L. E. (2008). Cyanotoxins: sampling, sample processing and toxin uptake *Cyanobacterial harmful algal blooms: State of the science and research needs* (pp. 483-499): Springer.
- Metcalf, J., Beattie, K., Saker, M., & Codd, G. (2002). Effects of organic solvents on the high performance liquid chromatographic analysis of the cyanobacterial toxin cylindrospermopsin and its recovery from environmental eutrophic waters by solid phase extraction. *FEMS microbiology letters*, 216(2), 159-164.
- Meunier, B. (2000a). *Biomimetic oxidations catalyzed by transition metal complexes*: World Scientific.
- Meunier, B. (2000b). *Models of heme peroxidases and catalases*: Imperial College Press: UK.
- Mitchell, D. A., Ryabov, A. D., Kundu, S., Chanda, A., & Collins, T. J. (2010). Oxidation of pinacyanol chloride by H₂O₂ catalyzed by Fe^{III} complexed to tetraamidomacrocyclic

- ligand: unusual kinetics and product identification. *Journal of Coordination Chemistry*, 63(14-16), 2605-2618. 10.1080/00958972.2010.492426
- Mohamed, Z. A. (2008). Toxic cyanobacteria and cyanotoxins in public hot springs in Saudi Arabia. *Toxicon*, 51(1), 17-27. <http://dx.doi.org/10.1016/j.toxicon.2007.07.007>
- Molloy, L., Wonnacott, S., Gallagher, T., Brough, P. A., & Livett, B. G. (1995). Anatoxin-a is a potent agonist of the nicotinic acetylcholine receptor of bovine adrenal chromaffin cells. *European Journal of Pharmacology: Molecular Pharmacology*, 289(3), 447-453. [http://dx.doi.org/10.1016/0922-4106\(95\)90153-1](http://dx.doi.org/10.1016/0922-4106(95)90153-1)
- Mondal, S., Hangun-Balkir, Y., Alexandrova, L., Link, D., Howard, B., Zandhuis, P., . . . Collins, T. J. (2006). Oxidation of sulfur components in diesel fuel using Fe-TAML® catalysts and hydrogen peroxide. *Catalysis Today*, 116(4), 554-561. <http://dx.doi.org/10.1016/j.cattod.2006.06.025>
- Moore, R. E. (1996). Cyanobacterial secondary metabolites *Microbial Growth on C1 Compounds* (pp. 245-252): Springer.
- Moreira, C., Azevedo, J., Antunes, A., & Vasconcelos, V. (2013). Cyindrospermopsin: Occurrence, methods of detection and toxicology. *Journal of applied microbiology*, 114(3), 605-620.
- Moreno-Castilla, C. (2004). Adsorption of organic molecules from aqueous solutions on carbon materials. *Carbon*, 42(1), 83-94.
- Mueller, S. O. (2004). Xenoestrogens: mechanisms of action and detection methods. *Analytical and Bioanalytical Chemistry*, 378(3), 582-587. 10.1007/s00216-003-2238-x
- Munter, R. (2001). Advanced oxidation processes—current status and prospects. *Proc. Estonian Acad. Sci. Chem*, 50(2), 59-80.
- Murk, A. J., Legler, J., van Lipzig, M. M. H., Meerman, J. H. N., Belfroid, A. C., Spenkelink, A., . . . Vethaak, D. (2002). Detection of estrogenic potency in wastewater and surface water with three in vitro bioassays. *Environmental Toxicology and Chemistry*, 21(1), 16-23. 10.1002/etc.5620210103
- Nakada, N., Nyunoya, H., Nakamura, M., Hara, A., Iguchi, T., & Takada, H. (2004). Identification of estrogenic compounds in wastewater effluent. *Environmental Toxicology and Chemistry*, 23(12), 2807-2815. 10.1897/03-699.1
- Nash, J. P., Kime, D. E., Van der Ven, L. T., Wester, P. W., Brion, F., Maack, G., . . . Tyler, C. R. (2004). Long-term exposure to environmental concentrations of the pharmaceutical ethynylestradiol causes reproductive failure in fish. *Environmental Health Perspectives*, 1725-1733.
- Neverov, A. A., & Brown, R. S. (2004). Cu (II)-Mediated decomposition of phosphorothionate P=S pesticides. Billion-fold acceleration of the methanolysis of fenitrothion promoted by a simple Cu (II)-ligand system. *Organic & biomolecular chemistry*, 2(15), 2245-2248.
- Newcombe, G., Drikas, M., & Hayes, R. (1997). Influence of characterised natural organic material on activated carbon adsorption: II. Effect on pore volume distribution and adsorption of 2-methylisoborneol. *Water Research*, 31(5), 1065-1073. [http://dx.doi.org/10.1016/S0043-1354\(96\)00325-9](http://dx.doi.org/10.1016/S0043-1354(96)00325-9)
- Newcombe, G., & Nicholson, B. (2004). Water treatment options for dissolved cyanotoxins. *Aqua*, 53, 227-239.
- NIKAWA, H., ISHIDA, K., HAMADA, T., SATODA, T., MURAYAMA, T., TAKEMOTO, T., . . . FUJIMOTO, H. (2005). Immobilization of octadecyl ammonium chloride on the surface of titanium and its effect on microbial colonization in vitro. *Dental materials journal*, 24(4), 570-582.

- Nishihara, T., Nishikawa, J.-i., Kanayama, T., Dakeyama, F., Saito, K., Imagawa, M., . . . Utsumi, H. (2000). Estrogenic activities of 517 chemicals by yeast two-hybrid assay. *Journal of health science*, *46*(4), 282-298.
- Nkambule, T., Krause, R., Mamba, B., & Haarhoff, J. (2009). Characterisation of natural organic matter (NOM) and its removal using cyclodextrin polyurethanes. *Water SA*, *35*(2), 200-203.
- Noyori, R., Aoki, M., & Sato, K. (2003). Green oxidation with aqueous hydrogen peroxide. *Chemical Communications*(16), 1977-1986.
- Ohtani, I., Moore, R. E., & Runnegar, M. T. C. (1992). Cylindrospermopsin: a potent hepatotoxin from the blue-green alga *Cylindrospermopsis raciborskii*. *Journal of the American Chemical Society*, *114*(20), 7941-7942. 10.1021/ja00046a067
- Onstad, G. D., Strauch, S., Meriluoto, J., Codd, G. A., & von Gunten, U. (2007). Selective oxidation of key functional groups in cyanotoxins during drinking water ozonation. *Environmental Science & Technology*, *41*(12), 4397-4404. 10.1021/es0625327
- Onundi, Y. B. (2015). Oxidation of Bisphenol A, Triclosan and 4-Nonylphenol by Fe-B* activated peroxide.
- Osswald, J., Rellán, S., Gago, A., & Vasconcelos, V. (2007). Toxicology and detection methods of the alkaloid neurotoxin produced by cyanobacteria, anatoxin-a. *Environment International*, *33*(8), 1070-1089. <http://dx.doi.org/10.1016/j.envint.2007.06.003>
- Owen, S. C., Doak, A. K., Ganesh, A. N., Nedyalkova, L., McLaughlin, C. K., Shoichet, B. K., & Shoichet, M. S. (2014). Colloidal drug formulations can explain “bell-shaped” concentration–response curves. *ACS chemical biology*, *9*(3), 777-784.
- Oziol, L., & Bouaïcha, N. (2010). First evidence of estrogenic potential of the cyanobacterial heptotoxins the nodularin-R and the microcystin-LR in cultured mammalian cells. *Journal of Hazardous Materials*, *174*(1–3), 610-615. <http://dx.doi.org/10.1016/j.jhazmat.2009.09.095>
- Paerl, H. W., Hall, N. S., & Calandrino, E. S. (2011). Controlling harmful cyanobacterial blooms in a world experiencing anthropogenic and climatic-induced change. *Science of The Total Environment*, *409*(10), 1739-1745. <http://dx.doi.org/10.1016/j.scitotenv.2011.02.001>
- Paerl, H. W., & Huisman, J. (2008). Blooms like it hot. *SCIENCE-NEW YORK THEN WASHINGTON-*, *320*(5872), 57.
- Palace, V. P., Evans, R. E., Wautier, K., Baron, C., Vandenbyllardt, L., Vandersteen, W., & Kidd, K. (2002). Induction of vitellogenin and histological effects in wild fathead minnows from a lake experimentally treated with the synthetic estrogen, ethynylestradiol. *Water Quality Research Journal of Canada*, *37*(3), 637-650.
- Pauwels, B., Noppe, H., De Brabander, H., & Verstraete, W. (2008). Comparison of steroid hormone concentrations in domestic and hospital wastewater treatment plants. *Journal of environmental engineering*, *134*(11), 933-936.
- Peck, M., Gibson, R. W., Kortenkamp, A., & Hill, E. M. (2004). Sediments are major sinks of steroidal estrogens in two United Kingdom rivers. *Environmental Toxicology and Chemistry*, *23*(4), 945-952.
- Pelaez, M., Antoniou, M., He, X., Dionysiou, D., de la Cruz, A., Tsimeli, K., . . . Westrick, J. (2010). Sources and occurrence of cyanotoxins worldwide. In D. Fatta-Kassinou, K. Bester & K. Kümmerer (Eds.), *Xenobiotics in the Urban Water Cycle* (Vol. 16, pp. 101-127): Springer Netherlands.
- Pelekani, C., & Snoeyink, V. L. (1999). Competitive adsorption in natural water: role of activated carbon pore size. *Water Research*, *33*(5), 1209-1219. [http://dx.doi.org/10.1016/S0043-1354\(98\)00329-7](http://dx.doi.org/10.1016/S0043-1354(98)00329-7)

- Piccolo, A., Cozzolino, A., Conte, P., & Spaccini, R. (2000). Polymerization of humic substances by an enzyme-catalyzed oxidative coupling. *Naturwissenschaften*, 87(9), 391-394. 10.1007/s001140050747
- Popescu, D.-L., Chanda, A., Stadler, M. J., Mondal, S., Tehrani, J., Ryabov, A. D., & Collins, T. J. (2008). Mechanistically inspired design of FeIII–TAML peroxide-activating catalysts. *Journal of the American Chemical Society*, 130(37), 12260-12261. 10.1021/ja805099e
- Popescu, D.-L., Vrabel, M., Brausam, A., Madsen, P., Lente, G., Fabian, I., . . . Collins, T. J. (2010). Thermodynamic, electrochemical, high-pressure kinetic, and mechanistic studies of the formation of oxo FeIV–TAML species in water. *Inorganic Chemistry*, 49(24), 11439-11448. 10.1021/ic1015109
- Price, P. M., Clark, J. H., & Macquarrie, D. J. (2000). Modified silicas for clean technology. *Journal of the Chemical Society, Dalton Transactions*(2), 101-110.
- Prociv, P. (2004). Algal toxins or copper poisoning-revisiting the Palm Island" epidemic". *Medical Journal of Australia*, 181(6), 344-344.
- Puma, G. L., Bono, A., Krishnaiah, D., & Collin, J. G. (2008). Preparation of titanium dioxide photocatalyst loaded onto activated carbon support using chemical vapor deposition: A review paper. *Journal of Hazardous Materials*, 157(2), 209-219.
- Puschner, B., Hoff, B., & Tor, E. R. (2008). Diagnosis of anatoxin-a poisoning in dogs from North America. *Journal of Veterinary Diagnostic Investigation*, 20(1), 89-92.
- Qin, B., Zhu, G., Gao, G., Zhang, Y., Li, W., Paerl, H. W., & Carmichael, W. W. (2010). A drinking water crisis in Lake Taihu, China: Linkage to climatic variability and lake management. *Environmental Management*, 45(1), 105-112. 10.1007/s00267-009-9393-6
- Rajapakse, N., Ong, D., & Kortenkamp, A. (2001). Defining the impact of weakly estrogenic chemicals on the action of steroidal estrogens. *Toxicological Sciences*, 60(2), 296-304.
- Rochette-Egly, C. (2003). Nuclear receptors: integration of multiple signalling pathways through phosphorylation. *Cellular Signalling*, 15(4), 355-366. [http://dx.doi.org/10.1016/S0898-6568\(02\)00115-8](http://dx.doi.org/10.1016/S0898-6568(02)00115-8)
- Rodríguez, E., Onstad, G. D., Kull, T. P. J., Metcalf, J. S., Acero, J. L., & von Gunten, U. (2007). Oxidative elimination of cyanotoxins: Comparison of ozone, chlorine, chlorine dioxide and permanganate. *Water Research*, 41(15), 3381-3393. <http://dx.doi.org/10.1016/j.watres.2007.03.033>
- Rodríguez, E., Sordo, A., Metcalf, J. S., & Acero, J. L. (2007). Kinetics of the oxidation of cylindrospermopsin and anatoxin-a with chlorine, monochloramine and permanganate. *Water Research*, 41(9), 2048-2056. <http://dx.doi.org/10.1016/j.watres.2007.01.033>
- Rodríguez, V., Yonamine, M., & Pinto, E. (2006). Determination of anatoxin - a in environmental water samples by solid - phase microextraction and gas chromatography - mass spectrometry. *Journal of separation science*, 29(13), 2085-2090.
- Rogers, E. D., Henry, T. B., Twiner, M. J., Gouffon, J. S., McPherson, J. T., Boyer, G. L., . . . Wilhelm, S. W. (2011). Global gene expression profiling in larval zebrafish exposed to microcystin-LR and microcystis reveals endocrine disrupting effects of cyanobacteria. *Environmental Science & Technology*, 45(5), 1962-1969. 10.1021/es103538b
- Rose, J., Holbech, H., Lindholst, C., Nørum, U., Povlsen, A., Korsgaard, B., & Bjerregaard, P. (2002). Vitellogenin induction by 17 β -estradiol and 17 α -ethinylestradiol in male zebrafish (*Danio rerio*). *Comparative Biochemistry and Physiology Part C: Toxicology & Pharmacology*, 131(4), 531-539. [http://dx.doi.org/10.1016/S1532-0456\(02\)00035-2](http://dx.doi.org/10.1016/S1532-0456(02)00035-2)

- Rositano, J., Newcombe, G., Nicholson, B., & Sztajn bok, P. (2001). Ozonation of nom and algal toxins in four treated waters. *Water Research*, 35(1), 23-32. [http://dx.doi.org/10.1016/S0043-1354\(00\)00252-9](http://dx.doi.org/10.1016/S0043-1354(00)00252-9)
- Ross, J. R. (2011). *Heterogeneous catalysis: fundamentals and applications*: Elsevier.
- Routledge, E. J., & Sumpter, J. P. (1996). Estrogenic activity of surfactants and some of their degradation products assessed using a recombinant yeast screen. *Environmental Toxicology and Chemistry*, 15(3), 241-248.
- Runnegar, M. T., Kong, S.-M., Zhong, Y.-Z., & Lu, S. C. (1995). Inhibition of reduced glutathione synthesis by cyanobacterial alkaloid cylindrospermopsin in cultured rat hepatocytes. *Biochemical Pharmacology*, 49(2), 219-225. [http://dx.doi.org/10.1016/S0006-2952\(94\)00466-8](http://dx.doi.org/10.1016/S0006-2952(94)00466-8)
- Rutishauser, B. V., Pesonen, M., Escher, B. I., Ackermann, G. E., Aerni, H. R., Suter, M. J. F., & Eggen, R. I. (2004). Comparative analysis of estrogenic activity in sewage treatment plant effluents involving three in vitro assays and chemical analysis of steroids. *Environmental Toxicology and Chemistry*, 23(4), 857-864.
- Ryabov, A. D., & Collins, T. J. (2009). Mechanistic considerations on the reactivity of green FeIII-TAML activators of peroxides. In E. Rudi van & D. H. Colin (Eds.), *Advances in inorganic chemistry* (Vol. Volume 61, pp. 471-521): Academic Press.
- Sabater, S., Mata, J. A., & Peris, E. (2014). Catalyst enhancement and recyclability by immobilization of metal complexes onto graphene surface by noncovalent interactions. *ACS Catalysis*, 4(6), 2038-2047. 10.1021/cs5003959
- Sadiq, R., & Rodriguez, M. J. (2004). Disinfection by-products (DBPs) in drinking water and predictive models for their occurrence: a review. *Science of The Total Environment*, 321(1), 21-46.
- Safe, S. H., Pallaroni, L., Yoon, K., Gaido, K., Ross, S., Saville, B., & McDonnell, D. (2001). Toxicology of environmental estrogens. *Reproduction, Fertility and Development*, 13(4), 307-315.
- Saker, M. L., Thomas, A. D., & Norton, J. H. (1999). Cattle mortality attributed to the toxic cyanobacterium *Cylindrospermopsis raciborskii* in an outback region of North Queensland. *Environmental Toxicology*, 14(1), 179-182. 10.1002/(sici)1522-7278(199902)14:1<179::aid-tox23>3.0.co;2-g
- Sakpal, T., Kumar, A., Kamble, S., & Kumar, R. (2012). Carbon dioxide capture using amine functionalized silica gel. *Indian Journal of Chemistry-Part A InorganicPhysical Theoretical and Analytical*, 51(9), 1214.
- Sarathy, S., & Mohseni, M. (2010). Effects of UV/H₂O₂ advanced oxidation on chemical characteristics and chlorine reactivity of surface water natural organic matter. *Water Research*, 44(14), 4087-4096. <http://dx.doi.org/10.1016/j.watres.2010.05.025>
- Schnitzer, M. (1978). Chapter 1 Humic substances: chemistry and reactions. In M. Schnitzer & S. U. Khan (Eds.), *Developments in Soil Science* (Vol. Volume 8, pp. 1-64): Elsevier.
- Seawright, A. A., Nolan, C. C., Shaw, G. R., Chiswell, R. K., Norris, R. L., Moore, M. R., & Smith, M. J. (1999). The oral toxicity for mice of the tropical cyanobacterium *Cylindrospermopsis raciborskii* (Woloszynska). *Environmental Toxicology*, 14(1), 135-142. 10.1002/(SICI)1522-7278(199902)14:1<135::AID-TOX17>3.0.CO;2-L
- Segner, H., Navas, J. M., Schäfers, C., & Wenzel, A. (2003). Potencies of estrogenic compounds in in vitro screening assays and in life cycle tests with zebrafish in vivo. *Ecotoxicology and Environmental Safety*, 54(3), 315-322. [http://dx.doi.org/10.1016/S0147-6513\(02\)00040-4](http://dx.doi.org/10.1016/S0147-6513(02)00040-4)
- Senogles, P.-J., Scott, J. A., & Shaw, G. (2000). Efficiency of UV treatment with and without the photocatalyst titanium dioxide for the degradation of the cyanotoxin cylindrospermopsin. *Resource and environmental biotechnology*, 3(2-3), 111-125.

- Senogles, P., Shaw, G., Smith, M., Norris, R., Chiswell, R., Mueller, J., . . . Eaglesham, G. (2000). Degradation of the cyanobacterial toxin cylindrospermopsin, from *Cylindrospermopsis raciborskii*, by chlorination. *Toxicon*, 38(9), 1203-1213. [http://dx.doi.org/10.1016/S0041-0101\(99\)00210-X](http://dx.doi.org/10.1016/S0041-0101(99)00210-X)
- Senogles, P. J., Scott, J. A., Shaw, G., & Stratton, H. (2001). Photocatalytic degradation of the cyanotoxin cylindrospermopsin, using titanium dioxide and UV irradiation. *Water Research*, 35(5), 1245-1255. [http://dx.doi.org/10.1016/S0043-1354\(00\)00372-9](http://dx.doi.org/10.1016/S0043-1354(00)00372-9)
- Severeys, A., De Vos, D. E., Fiermans, L., Verpoort, F., Grobet, P. J., & Jacobs, P. A. (2001). A heterogeneous cis - dihydroxylation catalyst with stable, site - isolated osmium - diolate reaction centers. *Angewandte Chemie International Edition*, 40(3), 586-589.
- Shah, N. S., He, X., Khan, H. M., Khan, J. A., O'Shea, K. E., Boccelli, D. L., & Dionysiou, D. D. (2013). Efficient removal of endosulfan from aqueous solution by UV-C/peroxides: a comparative study. *Journal of Hazardous Materials*, 263, 584-592.
- Shappell, N. W., Vrabel, M. A., Madsen, P. J., Harrington, G., Billey, L. O., Hakk, H., . . . Ro, K. (2008). Destruction of estrogens using Fe-TAML/peroxide catalysis. *Environmental Science & Technology*, 42(4), 1296-1300.
- Shephard, G. S., Stockenström, S., de Villiers, D., Engelbrecht, W. J., & Wessels, G. F. (2002). Degradation of microcystin toxins in a falling film photocatalytic reactor with immobilized titanium dioxide catalyst. *Water Research*, 36(1), 140-146.
- Shimizu, I., Yoshino, A., Okabayashi, H., Nishio, E., & J. O'Connor, C. (1997). Kinetics of interaction of 3-aminopropyltriethoxysilane on a silica gel surface using elemental analysis and diffuse reflectance infrared Fourier transform spectra. *Journal of the Chemical Society, Faraday Transactions*, 93(10), 1971-1979. 10.1039/A608121E
- Simmons, K. E., Minard, R. D., & Bollag, J. M. (1989). Oxidative co-oligomerization of guaiacol and 4-chloroaniline. *Environmental Science & Technology*, 23(1), 115-121. 10.1021/es00178a016
- Sivonen, K., Niemelä, S. I., Niemi, R. M., Lepistö, L., Luoma, T. H., & Räsänen, L. A. (1990). Toxic cyanobacteria (blue-green algae) in Finnish fresh and coastal waters. *Hydrobiologia*, 190(3), 267-275. 10.1007/bf00008195
- Smith, V. (2003). Eutrophication of freshwater and coastal marine ecosystems a global problem. *Environmental Science and Pollution Research*, 10(2), 126-139. 10.1065/espr2002.12.142
- Snyder, S. A., Villeneuve, D. L., Snyder, E. M., & Giesy, J. P. (2001). Identification and quantification of estrogen receptor agonists in wastewater effluents. *Environmental Science & Technology*, 35(18), 3620-3625. 10.1021/es001254n
- Söffker, M., & Tyler, C. R. (2012). Endocrine disrupting chemicals and sexual behaviors in fish—a critical review on effects and possible consequences. *Critical Reviews in Toxicology*, 42(8), 653-668.
- Song, W., Yan, S., Cooper, W. J., Dionysiou, D. D., & O'Shea, K. E. (2012). Hydroxyl radical oxidation of Cylindrospermopsin (Cyanobacterial Toxin) and its role in the photochemical transformation. *Environmental Science & Technology*, 46(22), 12608-12615. 10.1021/es302458h
- Sotiriou-Leventis, C., Wang, X., Mulik, S., Thangavel, A., & Leventis, N. (2008). Immobilization of Pd catalysts on mesoporous silica for amine-and copper-free Sonogashira coupling reactions. *Synthetic Communications*®, 38(14), 2285-2298.
- Štěpánková, T., Ambrožová, L., Bláha, L., Giesy, J. P., & Hilscherová, K. (2011). In vitro modulation of intracellular receptor signaling and cytotoxicity induced by extracts of cyanobacteria, complex water blooms and their fractions. *Aquatic Toxicology*, 105(3), 497-507. <http://dx.doi.org/10.1016/j.aquatox.2011.08.002>

- Stevens, D., & Krieger, R. (1988). Analysis of Anatoxin-a by GCIECD. *Journal of analytical toxicology*, 12(3), 126-131.
- Stevens, D. K., & Krieger, R. I. (1991). Stability studies on the cyanobacterial nicotinic alkaloid snatoxin-A. *Toxicon*, 29(2), 167-179. [http://dx.doi.org/10.1016/0041-0101\(91\)90101-V](http://dx.doi.org/10.1016/0041-0101(91)90101-V)
- Sun, K., Huang, Q., & Gao, Y. (2016). Laccase-catalyzed oxidative coupling reaction of Triclosan in aqueous solution. *Water, Air, & Soil Pollution*, 227(10), 358. 10.1007/s11270-016-3064-z
- Sun, K., Luo, Q., Gao, Y., & Huang, Q. (2016). Laccase-catalyzed reactions of 17 β -estradiol in the presence of humic acid: Resolved by high-resolution mass spectrometry in combination with ¹³C labeling. *Chemosphere*, 145, 394-401. <http://dx.doi.org/10.1016/j.chemosphere.2015.11.117>
- Svrcek, C., & Smith, D. W. (2004). Cyanobacteria toxins and the current state of knowledge on water treatment options: a review. *Journal of Environmental Engineering and Science*, 3(3), 155-185.
- Swanson, K., Allen, C., Aronstam, R., Rapoport, H., & Albuquerque, E. (1986). Molecular mechanisms of the potent and stereospecific nicotinic receptor agonist (+)-anatoxin-a. *Molecular pharmacology*, 29(3), 250-257.
- Świetlik, J., Dąbrowska, A., Raczyk-Stanisławiak, U., & Nawrocki, J. (2004). Reactivity of natural organic matter fractions with chlorine dioxide and ozone. *Water Research*, 38(3), 547-558. <http://dx.doi.org/10.1016/j.watres.2003.10.034>
- Sychrová, E., Štěpánková, T., Nováková, K., Bláha, L., Giesy, J. P., & Hilscherová, K. (2012). Estrogenic activity in extracts and exudates of cyanobacteria and green algae. *Environment International*, 39(1), 134-140. <http://dx.doi.org/10.1016/j.envint.2011.10.004>
- Tamura, H., Maness, S. C., Reischmann, K., Dorman, D. C., Gray, L. E., & Gaido, K. W. (2001). Androgen receptor antagonism by the organophosphate insecticide fenitrothion. *Toxicological Sciences*, 60(1), 56-62.
- Tanabe, K., Misono, M., Hattori, H., & Ono, Y. (1990). *New solid acids and bases: their catalytic properties* (Vol. 51): Elsevier.
- Teixeira, M. R., & Sousa, V. S. (2013). Fouling of nanofiltration membrane: Effects of NOM molecular weight and microcystins. *Desalination*, 315, 149-155. <http://dx.doi.org/10.1016/j.desal.2012.03.012>
- Terao, K., Ohmori, S., Igarashi, K., Ohtani, I., Watanabe, M. F., Harada, K. I., . . . Watanabe, M. (1994). Electron microscopic studies on experimental poisoning in mice induced by cylindrospermopsin isolated from blue-green alga Umezakia natans. *Toxicon*, 32(7), 833-843. [http://dx.doi.org/10.1016/0041-0101\(94\)90008-6](http://dx.doi.org/10.1016/0041-0101(94)90008-6)
- Thomas, J. M. (1988). Uniform heterogeneous catalysts: The role of solid - state chemistry in their development and design. *Angewandte Chemie International Edition in English*, 27(12), 1673-1691.
- Thomas, J. M., Maschmeyer, T., Johnson, B. F. G., & Shephard, D. S. (1999). Constrained chiral catalysts. *Journal of Molecular Catalysis A: Chemical*, 141(1-3), 139-144. [http://dx.doi.org/10.1016/S1381-1169\(98\)00257-X](http://dx.doi.org/10.1016/S1381-1169(98)00257-X)
- Thomas, P., Stephens, M., Wilkie, G., Amar, M., Lunt, G. G., Whiting, P., . . . Wonnacott, S. (1993). (+)-Anatoxin-a is a potent agonist at neuronal nicotinic acetylcholine receptors. *Journal of Neurochemistry*, 60(6), 2308-2311. 10.1111/j.1471-4159.1993.tb03519.x
- Thorn, K. A., Goldenberg, W. S., Younger, S. J., & Weber, E. J. (1996). Covalent binding of aniline to humic substances *Humic and Fulvic Acids* (Vol. 651, pp. 299-326): American Chemical Society.

- Thorpe, K. L., Gross-Sorokin, M., Johnson, I., Brighty, G., & Tyler, C. R. (2006). An assessment of the model of concentration addition for predicting the estrogenic activity of chemical mixtures in wastewater treatment works effluents. *Environmental Health Perspectives*, 114, 90.
- Tischer, W., & Wedekind, F. (1999). Immobilized enzymes: methods and applications *Biocatalysis-from discovery to application* (pp. 95-126): Springer.
- Van Apeldoorn, M. E., Van Egmond, H. P., Speijers, G. J., & Bakker, G. J. (2007). Toxins of cyanobacteria. *Molecular nutrition & food research*, 51(1), 7-60.
- Vandenberg, L. N., Colborn, T., Hayes, T. B., Heindel, J. J., Jacobs Jr, D. R., Lee, D.-H., . . . Welshons, W. V. (2012). Hormones and endocrine-disrupting chemicals: Low-dose effects and nonmonotonic dose responses. *Endocrine reviews*, 33(3), 378-455.
- Verma, S., & Sillanpää, M. (2015). Degradation of anatoxin-a by UV-C LED and UV-C LED/H₂O₂ advanced oxidation processes. *Chemical Engineering Journal*, 274, 274-281.
- Vlad, S., Anderson, W. B., Peldszus, S., & Huck, P. M. (2014). Removal of the cyanotoxin anatoxin-a by drinking water treatment processes: a review. *Journal of water and health*, 12(4), 601-617.
- von Gunten, U., & Hoigne, J. (1994). Bromate formation during ozonation of bromide-containing waters: Interaction of ozone and hydroxyl radical reactions. *Environmental Science & Technology*, 28(7), 1234-1242. 10.1021/es00056a009
- Walker, H. W. (2014). *Harmful algae blooms in drinking water: Removal of cyanobacterial cells and toxins*: CRC Press.
- Walters, P., Abbott, E., & Isquith, A. (1973). Algicidal activity of a surface-bonded organosilicon quaternary ammonium chloride. *Applied microbiology*, 25(2), 253-256.
- Webb, P., Lopez, G. N., Greene, G. L., Baxter, J. D., & Kushner, P. J. (1992). The limits of the cellular capacity to mediate an estrogen response. *Molecular Endocrinology*, 6(2), 157-167.
- Weber, W. J., Huang, Q., & Pinto, R. A. (2005). Reduction of disinfection byproduct formation by molecular reconfiguration of the fulvic constituents of natural background organic matter. *Environmental Science & Technology*, 39(17), 6446-6452. 10.1021/es050220i
- Westrick, J., Szlag, D., Southwell, B., & Sinclair, J. (2010). A review of cyanobacteria and cyanotoxins removal/inactivation in drinking water treatment. *Analytical and Bioanalytical Chemistry*, 397(5), 1705-1714. 10.1007/s00216-010-3709-5
- Westrick, J. A. (2008). Cyanobacterial toxin removal in drinking water treatment processes and recreational waters *Cyanobacterial Harmful Algal Blooms: State of the Science and Research Needs* (pp. 275-290): Springer.
- Wiegand, C., & Pflugmacher, S. (2005). Ecotoxicological effects of selected cyanobacterial secondary metabolites a short review. *Toxicology and Applied Pharmacology*, 203(3), 201-218. <http://dx.doi.org/10.1016/j.taap.2004.11.002>
- Wolfe, R. L. (1990). Ultraviolet disinfection of potable water. *Environmental Science & Technology*, 24(6), 768-773. 10.1021/es00076a001
- Wood, S. A., Selwood, A. I., Rueckert, A., Holland, P. T., Milne, J. R., Smith, K. F., . . . Cary, C. S. (2007). First report of homoanatoxin-a and associated dog neurotoxicosis in New Zealand. *Toxicon*, 50(2), 292-301. <http://dx.doi.org/10.1016/j.toxicon.2007.03.025>
- Würtele, M. A., Kolbe, T., Lipsz, M., Külberg, A., Weyers, M., Kneissl, M., & Jekel, M. (2011). Application of GaN-based ultraviolet-C light emitting diodes – UV LEDs – for water disinfection. *Water Research*, 45(3), 1481-1489. <http://dx.doi.org/10.1016/j.watres.2010.11.015>
- Ying, G.-G., Kookana, R. S., & Ru, Y.-J. (2002). Occurrence and fate of hormone steroids in the environment. *Environment International*, 28(6), 545-551.

- Young, F. M., Micklem, J., & Humpage, A. R. (2008). Effects of blue-green algal toxin cylindrospermopsin (CYN) on human granulosa cells in vitro. *Reproductive Toxicology*, 25(3), 374-380. <http://dx.doi.org/10.1016/j.reprotox.2008.02.006>
- Young, W., Whitehouse, P., & Johnson, I. (2002). *Proposed predicted-no-effect-concentrations (PNECs) for natural and synthetic steroid oestrogens in surface waters*: Environment Agency.
- Zamyadi, A., Ho, L., Newcombe, G., Bustamante, H., & Prévost, M. (2012). Fate of toxic cyanobacterial cells and disinfection by-products formation after chlorination. *Water Research*, 46(5), 1524-1535. <http://dx.doi.org/10.1016/j.watres.2011.06.029>
- Zhang, G., Nadagouda, M. N., O'Shea, K., El-Sheikh, S. M., Ismail, A. A., Likodimos, V., . . . Dionysiou, D. D. (2014). Degradation of cylindrospermopsin by using polymorphic titanium dioxide under UV-Vis irradiation. *Catalysis Today*, 224(0), 49-55. <http://dx.doi.org/10.1016/j.cattod.2013.10.072>
- Zhang, G., Wurtzler, E. M., He, X., Nadagouda, M. N., O'Shea, K., El-Sheikh, S. M., . . . Dionysiou, D. D. (2015). Identification of TiO₂ photocatalytic destruction byproducts and reaction pathway of cylindrospermopsin. *Applied Catalysis B: Environmental*, 163(0), 591-598. <http://dx.doi.org/10.1016/j.apcatb.2014.08.034>
- Zhao, C., Pelaez, M., Dionysiou, D. D., Pillai, S. C., Byrne, J. A., & O'Shea, K. E. (2014). UV and visible light activated TiO₂ photocatalysis of 6-hydroxymethyl uracil, a model compound for the potent cyanotoxin cylindrospermopsin. *Catalysis Today*, 224(0), 70-76. <http://dx.doi.org/10.1016/j.cattod.2013.09.042>
- Zhao, X. S., Bao, X. Y., Guo, W., & Lee, F. Y. (2006). Immobilizing catalysts on porous materials. *Materials Today*, 9(3), 32-39. [http://dx.doi.org/10.1016/S1369-7021\(06\)71388-8](http://dx.doi.org/10.1016/S1369-7021(06)71388-8)
- Zularisam, A. W., Ahmad, A., Sakinah, M., Ismail, A. F., & Matsuura, T. (2011). Role of natural organic matter (NOM), colloidal particles, and solution chemistry on ultrafiltration performance. *Separation and Purification Technology*, 78(2), 189-200. <http://dx.doi.org/10.1016/j.seppur.2011.02.001>